

DISSERTATION

SIMPLIFIED MEMBRANE-LIKE SYSTEMS DESCRIBING THE PHYSICAL BEHAVIORS  
OF CHOLESTEROL AND ANTI-DIABETIC DRUGS

Submitted by:

Alejandro M. Trujillo

Graduate Degree Program in Cell and Molecular Biology

In partial fulfillment of the requirements

For the Degree of Doctorate of Philosophy

Colorado State University

Fort Collins, Colorado

Fall 2013

Doctoral Committee:

Advisor: Debbie C. Crans

Deborah A. Roess

Melinda A. Frye

Alan K. Van Orden

Copyright by Alejandro M. Trujillo

All Rights Reserved

## ABSTRACT

### SIMPLIFIED MEMBRANE-LIKE SYSTEMS DESCRIBING THE PHYSICAL BEHAVIORS OF CHOLESTEROL AND ANTI-DIABETIC DRUGS

This work evaluates the properties contributing to natural membrane permeability by using simplified systems. Absorption mechanisms are a critical step in evaluating the action of orally active drugs. Reverse micelles (RMs) were used as a membrane-like model to analyze the permeation through spectroscopy. The properties exerted by the ligand and ligand substituents were evaluated in the context of membrane permeation. The polydentate ligand of anti-diabetic dipicolinatooxvanadium(V)  $[\text{VO}_2\text{dipic}]^-$ , 2,6-pyridinedicarboxylate ( $\text{dipic}^{2-}$ ) was observed for permeability in sodium bis(2-ethylhexyl)sulfosuccinate (AOT) RMs. Measurements using proton nuclear magnetic resonance ( $^1\text{H}$  NMR) spectroscopy revealed the permeation and hydrophobic stability at physiological pH for  $\text{dipic}^{2-}$ . Substituents,  $\text{NH}_2$ ,  $\text{OH}$ ,  $\text{H}$ ,  $\text{Cl}$ ,  $\text{NO}_2$  were evaluated for influencing the stability and permeability of  $[\text{VO}_2(\text{dipic})]^-$  in AOT RMs. Using infrared spectroscopy (IR), substituent changes significantly influenced the permeation of the vanadium complex series. Properties contributing to the membrane permeation of drugs may also be altered by membrane composition. Cholesterol is present in intestinal membranes and is known to possess properties reducing permeability. A system composed of cetyltrimethylammonium bromide (CTAB), 1-pentanol, cholesterol, and an aqueous phase formed RMs characterized by NMR and dynamic light scattering (DLS). Cholesterol altered the RM structure and proton transfer rates between the water and 1-pentanol of the system. Combined, this work illustrates that ligands, substituents, and membrane components influence the uptake of orally administered drugs.

## TABLE OF CONTENTS

ABSTRACT .....	ii
INTRODUCTION .....	1
CHAPTER 1: <i>Cholesterol Affects Proton Transfer in CTAB Reverse Micelles</i> .....	24
CHAPTER 2: <i>Penetration of Negatively Charged Lipid Interfaces by the Doubly Deprotonated Dipicolinate</i> .....	58
CHAPTER 3: <i>Correlating Insulin Enhancing Properties with Physical Chemical Properties of Vanadium Dipicolinate Complexes</i> .....	86
CONCLUSIONS .....	117
APPENDIX.....	122
APPENDIX ARTICLE 1: <i>Coexisting Aggregates in Mixed Aerosol-OT and Cholesterol Microemulsions</i> .....	123
APPENDIX ARTICLE 2: <i>Effects of Vanadium-Containing Compounds on Membrane Lipids and on Microdomains Used in Receptor-Mediated Signaling</i> .....	130
APPENDIX ARTICLE 3: <i>Do Vanadium compounds Drive Reorganization of the Plasma Membrane and Activation of Insulin Receptors with Lipid Rafts?</i> .....	143
APPENDIX ARTICLE 4: <i>How Environments Affects Drug Activity: Localization, Compartmentalization and Reactions of a Vanadium Insulin-Enhancing Compound Dipicolinatooxovanadium(V)</i> .....	157

APPENDIX ARTICLE 5: *Anti-diabetic Effects of a Series of Vanadium Dipicolinate Complexes*  
*in Rats with Streptozotocin-Induced Diabetes* .....172

## INTRODUCTION

Over 25 million individuals in the U.S. have diabetes, 90 - 95% are classified as type 2<sup>1</sup>. Oral administration of vanadium containing compounds normalizes diabetic symptomology<sup>2-4</sup>. Many vanadium compounds are orally active; however, their absorption is poor and the mechanism is not clearly defined<sup>5-7</sup>. One possible mechanism of absorption occurs passively, permeating membranes<sup>8,9</sup>. This work uses artificial membrane mimics to observe the molecular properties contributing to passive permeation. Analyses of the organic ligand and substituent effects were performed to reveal the physical properties that contribute to the anti-diabetic response to dipicolinatooxovanadium(V) [VO<sub>2</sub>(dipic)] *in vivo*. The influence of membrane composition on permeation and absorption led to the development of an artificial membrane system containing cholesterol.

### *Type 2 diabetes mellitus and vanadium*

Type 2 diabetes mellitus (T2DM) is a complex metabolic disorder involving insulin production from pancreatic  $\beta$  cells and insulin resistance<sup>10</sup>. Insulin binding insulin receptors (IRs) initiates the signaling pathway that results in the absorption of glucose in insulin sensitive cells such as myocytes and adipocytes. Increased glucose absorption in the gastrointestinal (GI) tract and excessive glucose release from the liver results in elevated blood glucose levels, termed hyperglycemia. Signal transduction and glucose metabolism changes are targets for T2DM treatment.

Impaired signal transduction in muscle and adipose cells is a proposed mechanism of T2DM<sup>11</sup>. Defects in receptor mediated tyrosine phosphorylation, protein kinase B (PKB or Akt) activation, elevated lipid levels and phosphorylation on insulin receptor substrates (IRS-1)<sup>12</sup>

have been identified as contributors. However, the insulin-signaling pathway itself has yet to be fully resolved. Full activation requires two distinct insulin receptor (IR) signaling events activating the phosphoinositide-3-kinase (PI3K) and TC10 pathways,<sup>13</sup> summarized in figure I.1. The pathway continues to the translocation of glucose transporter type 4 (Glut4) containing vesicles to the plasma membrane, which remains unclear. Recent findings identify protein kinase C (atypical  $\zeta/\lambda$ ) (PKC $\zeta/\lambda$ ), Akt substrate of 160 kDa AS160<sup>11</sup> and microdomain compartmentalization of Akt and PI3K<sup>14</sup> as updates to the signaling pathway with functioning in the translocation of Glut4 vesicles. The unresolved mechanistic features of GLUT4 translocation leave some effects of anti-diabetic treatments debated.

Recent findings show significant improvements in diabetic symptoms through Roux-en-Y gastric bypass surgery (RYGB)<sup>15,16</sup>. Improved glucose utilization through up-regulation of glucose transporter 1 (Glut-1) and intestinal remodeling has been proposed as mechanisms.<sup>15</sup> The link between the restoration of glucose metabolism in the GI tract and clinical improvement in type 2 diabetes illustrates the critical nature of the small intestine. However, the mechanism creating the observed improvements is yet unknown. Intestinal brush boarder membrane (BBM) changes such as fluidity reductions<sup>17</sup>, total lipid reduction and phospholipid: cholesterol ratio changes<sup>18</sup> have been observed in diabetic patients receiving RYGB. In type 2 diabetes, membrane changes show that cholesterol content increased in the GI membranes, reducing fluidity, which was normalized with insulin<sup>19</sup>. Gene expression changes similar to non diabetics are also reported in T2DM patients after gastric bypass surgery<sup>15</sup>. However, RYGB surgery is not available for patients who do not meet obesity criteria<sup>16</sup>. Alternative means are required to assist these patients.

Vanadium exerts properties that mimic insulin, such as normalization of diabetic hyperglycemia, yet few vanadium compounds have progressed past phase I and II level clinical trials<sup>3,20</sup>. Interactions with many insulin pathway proteins including IRSs,<sup>21</sup> protein tyrosine kinases (PTKs)<sup>22,23</sup>, PI3K,<sup>21</sup> PKB or Akt,<sup>24,25</sup> and regulatory protein tyrosine phosphatase-1B (PTP-1B)<sup>3,26,27</sup> and alkaline phosphatase<sup>28</sup> have been reported, among others. Numerous vanadium-containing compounds exhibit properties contributing to diabetes treatment, however the mechanism of absorption is not clearly defined.

In membranes, vanadium interactions resulting in fluidity changes similar to insulin have been observed *in vitro*<sup>29,30</sup>. BBM microvilli remodeling,<sup>31,32</sup> cytoskeleton and actin interactions<sup>33,34</sup> have also been observed. Impaired glucose absorption and transport has been reported in intestinal tissues<sup>35,36</sup>. Also, increased glucose uptake has been observed in target cells<sup>37</sup> concomitantly with reduced circulating glucose concentrations. Gene expression changes resembling non-diabetics<sup>6</sup> have been documented as a result of oral vanadium administration. However, the active form remains uncertain and the array of vanadium properties contribute to the ambiguity. Additionally, environment can affect vanadium chemistry,<sup>38</sup> so determination of the active species is not intuitive and has not yet been determined. Yet, some vanadium compounds are more effective at treating T2DM than others *in vivo*<sup>6</sup>. Therefore, the properties contributing their activity must differ. Absorption is a critical property that is not clearly defined.

#### *Absorption of dipicolinatooxovanadium(V) [VO<sub>2</sub>(dipic)]*

Absorption, distribution, metabolism, excretion and toxicity (ADME/T) properties are used to investigate orally administered drugs<sup>39</sup>. ADME/T reports indicate vanadium is poorly absorbed in the GI tract<sup>5,6,40</sup>; less than 5% is absorbed, with 95% excreted in feces<sup>5</sup>. In general, ~33% of new drugs fail due to poor oral bioavailability<sup>41</sup>. Absorption is a limitation for diabetes

treatment using vanadium <sup>5</sup>. However, many vanadium-containing compounds perform well *in vivo*, indicating that little vanadium is needed to create an antidiabetic response <sup>6,42,43</sup>.

[VO<sub>2</sub>(dipic)]<sup>-</sup> is among the most effective at alleviating diabetic symptoms while exhibiting reduced toxicity <sup>6,31</sup>. The absorption mechanism has not been defined, but could occur through either passive or protein-assisted mechanisms.

Absorption through anion transport proteins is a possible protein-assisted mechanism for vanadium. To evaluate this mechanism, inhibition using 4,4'-diisothiocyano-2,2'-stilbenedisulfonic acid (DIDS) was performed on Madin-Darby Canine Kidney (MDCK), Caco-2 and human erythrocyte cells <sup>31,40,44</sup>. (VO<sub>2</sub>[dipic])<sup>-</sup> permeated by an alternative mechanism, while sodium metavanadate (NaVO<sub>3</sub>) (vanadate (VO<sub>2</sub><sup>+</sup> or H<sub>2</sub>VO<sub>4</sub><sup>-</sup>) in solution) was blocked <sup>40,45</sup>. Vanadate is formed when [VO<sub>2</sub>(dipic)]<sup>-</sup> dissociates, becoming the predominant species at ~ pH 6.5 <sup>46</sup>. In membrane model systems [VO<sub>2</sub>(dipic)]<sup>-</sup> permeated an anionic interface and interacted with a cationic interface, modulated by hydrophobic and Coulombic effects <sup>47,48</sup>. The findings deviated from established drug permeability rules, yet illustrated the potential for a passive mechanism. Determining the factors that contribute to the passive uptake of [VO<sub>2</sub>(dipic)]<sup>-</sup> is the goal of this work.

Drug stability as a function of pH is a critical factor with implications relevant to absorption. In animals, vanadium was administered through drinking water (~ pH 6.0) <sup>49</sup>. Orally administered drugs move through the esophagus to the stomach and are typically absorbed by the cells lining the small intestine called enterocytes <sup>50</sup>. The pH gradient for the differing compartments ranges from 1.0 - 3.0 in the stomach to 7.4 in the cytosol of enterocytes <sup>51-53</sup>. The pH change from 2.0 to 6.0 occurs over only a few centimeters of tissue. Focusing on [VO<sub>2</sub>(dipic)]<sup>-</sup>, stability is > 70 % until ~ pH 6.0 where dissociation to VO<sub>2</sub><sup>+</sup> (H<sub>2</sub>VO<sub>4</sub><sup>-</sup>) and dipic<sup>2-</sup>

occurs<sup>6,46</sup>. The structures of  $[\text{VO}_2(\text{dipic})]^-$ ,  $\text{dipic}^{2-}$  and  $(\text{H}_2\text{VO}_4)^-$  are illustrated in figure I.2. The dissociated products would be the dominant species at the cytosolic pH of 7.4. If the complex diffuses from the small intestine to the cytosol it will dissociate in the aqueous phase. However,  $[\text{VO}_2(\text{dipic})]^-$  is a more effective anti-diabetic agent than vanadate. Therefore, a significant difference in ADME/T between  $[\text{VO}_2(\text{dipic})]^-$  and vanadate must exist, presumably contributed by the ligand.

Membrane targeting may be key to explaining the observed increase in efficacy of  $[\text{VO}_2(\text{dipic})]^-$ . 2,6-pyridinediacarboxylate ( $\text{dipic}^{2-}$ ) may play a significant role in increasing the absorption of  $[\text{VO}_2(\text{dipic})]^-$ . Lipophilicity contributes to passive drug absorption by increasing membrane solubility<sup>54</sup>. Organic ligands increase the lipophilicity and efficacy of vanadium compounds, resulting in increased absorption and reduced toxicity<sup>31,55</sup>; however, pharmacokinetic guides indicate charged molecules and carboxyl ( $\text{COO}^-$ ) groups should possess poor permeability<sup>56,57</sup>.  $\text{Dipic}^{2-}$  has both in the form present near neutral pHs and therefore should not be lipophilic<sup>58</sup>. Evaluation of the membrane solubility of  $\text{dipic}^{2-}$  was performed in a membrane-like system in chapter 2<sup>59</sup>.

$[\text{VO}_2(\text{dipic})]^-$  dissociates in aqueous bulk at neutral pH, yet remains intact in surfactant interfaces<sup>47</sup>. Thus, since  $[\text{VO}_2(\text{dipic})]^-$  is stable in hydrophobic media, determining the properties contributing to permeation are of critical importance. Hydrophobic media in biological structures applies to hydrocarbon tails of lipid bilayers and protein folds. Hydrophobic media opens  $[\text{VO}_2(\text{dipic})]^-$  to chemistry not present in aqueous bulk, forming ternary complexes and catalyzing reactions<sup>38</sup>. The concept of pH is also skewed in confined hydrophobic environments<sup>60</sup>. So membrane interaction may play a more critical role in the action of  $[\text{VO}_2(\text{dipic})]^-$  than simply passing into the cytosol.

Ligand substituents have been used to increase the lipophilicity of drugs by increasing their permeability<sup>61</sup>. Accordingly, substituents on [VO<sub>2</sub>(dipic)]<sup>-</sup> may increase the stability of the complex in hydrophobic media. Stability data indicates substituents NH<sub>2</sub>, OH, Cl, and NO<sub>2</sub> reduced the aqueous stability and efficacy *in vivo* compared to H<sup>6</sup>. However, how these findings correlate with membrane permeability is yet unknown. The reduced stability in aqueous may increase solubility and stability in hydrophobic media, improving permeability. Analysis of substituent effects contributing to permeation was the focus of chapter 3.

#### *Cholesterol in membranes affecting absorption*

To evaluate passive permeability, the composition of the absorbing membrane is a critical element. One membrane component regulating permeability is cholesterol<sup>62</sup>. Abundant in animals, cholesterol is critical a precursor to steroid hormones<sup>64</sup>. In cells, the highest concentrations of cholesterol are observed in plasma membranes<sup>63</sup>. Cholesterol is present in the membranes of the enterocytes lining the small intestine<sup>18</sup>. The lipid ratio of the BBM of enterocytes is ~1.5 – 2.0 phospholipid: cholesterol<sup>51,65</sup>. Interestingly, elevated cholesterol was observed in the BBMs of diabetic rates, indicating a potential for disrupted passive drug absorption<sup>18</sup>. Examining the properties of cholesterol is needed to model a passive uptake mechanism of orally active compounds.

The most well studied property of cholesterol is altering membrane fluidity<sup>66,67</sup>. Cholesterol decreases fluidity<sup>67</sup>, producing phase changes in membranes<sup>68,69</sup>. In liposomes, cholesterol reduced the partition coefficient (permeability) of chlorpromazine<sup>70</sup>. Tight lipid packing may be the source of the decreased permeability<sup>68,71</sup>. Cholesterol increased elastic stiffness and viscosity in phospholipid multibilayers<sup>67</sup>. Forming heterogeneities in monolayers relates cholesterol to microdomain formation,<sup>72,73</sup> while inducing membrane curvature during

endocytosis links cholesterol to more sophisticated cellular processes<sup>74</sup>. Impacting cellular processes through the chemical activities of membrane-associated proteins also occurs with cholesterol<sup>75</sup>. Cholesterol altered charge transfer in bacterial reaction centers<sup>76,77</sup> and dipole potentials of lipid membranes<sup>78</sup>.

Although studies have documented the effects of cholesterol on membrane characteristics and protein activities, the location and orientation of cholesterol is debated. Cholesterol is presumed to stack longitudinally in membranes<sup>8</sup>; while this is accepted, experimental confirmation is limited. Definitive evidence of the orientation of cholesterol in the liquid state is lacking<sup>79</sup>. Theoretical modeling shows cholesterol H-bonding with phosphodiester groups of phosphatidylcholine<sup>80</sup>. Computer simulation indicates cholesterol intercalates between hydrocarbon tails of phospholipids<sup>81</sup>. Liquid state characterization of cholesterol was attempted as a part of this work. The characterization was not completed due to solvent insolubility driving self-aggregation.

In model systems cholesterol is reported in differing orientations<sup>82-84</sup>. Nuclear magnetic resonance (NMR) studies show cholesterol intercalated in phospholipid bilayers in the liquid-crystalline state<sup>82</sup>. In anionic RMs, cholesterol formed coexisting aggregates by DLS<sup>85</sup> but intercalated by NMR relaxation ( $T_1$ )<sup>86</sup>. However, cationic micelles show cholesterol analog sodium deoxycholate (NaDC) stacking longitudinally<sup>84</sup>. The many changes to membranes containing cholesterol may significantly change the absorption and activity of drugs including vanadium. The study of chapter 1 evaluates cholesterol in a reverse micelle (RM) system at a 1.5: 1 surfactant to cholesterol ratio. Specifically, the effect of cholesterol on RM structure and the interfacial water was examined.

### *Evaluating absorption using model systems*

Partition coefficients like  $\log P$  have been used to determine drug permeability comparing water to 1-octanol solubility<sup>87</sup>. Lipinski's law of five (Lo5) uses molecular predictors to guide drug development by increasing permeability<sup>54</sup>. Partition coefficients and molecular descriptors do not model the membrane interactions or pH changes encountered with oral administration of drugs. As a result, there are many exceptions to the  $\log P$  and Lo5 screening methods. Absorption mechanisms are difficult to model in biological systems. Artificial membrane models create simplified systems, allowing these critical observations to be made.

Absorption of vanadium has been studied using cell models, including MDCK, Caco-2 and human erythrocytes. Cell models have the advantage of evaluating downstream processes and cytotoxicity<sup>30,31</sup>. Limitations include alternative protein-assisted mechanisms, transport through junctions, and paracellular diffusion<sup>88,89</sup>. High growth times, consumed resources and detection limitations also apply to cell studies. The aim of isolating passive mechanisms has led to the development and use of artificial membranes.

Bilayers, vesicles, monolayers, micelles and reverse micelles are examples of artificial membranes. The amphiphilic environment of the aggregated surfactants models the microenvironments present in biological membranes. Amphiphilic compounds have a polar segment and a nonpolar segment as illustrated in figure I.3, and aggregate based on London Dispersion forces and H-bonding<sup>90</sup>. Bilayers can be formed in hours to minutes and may be characterized using X-ray scattering<sup>91</sup>. Natural lipids are common surfactants in bilayer systems such as parallel-artificial membrane permeation assay (PAMPAs)<sup>56,92</sup>. Vesicles, also termed liposomes, are bilayer suspensions present in biological processes and are useful in drug delivery and targeting<sup>93</sup>. Proteins can be incorporated in these systems, allowing for experiments probing

their functionality<sup>94</sup>. Limitations for vesicles are primarily through characterization methodologies. Electron microscopy techniques can be used but are time consuming<sup>95</sup>. Langmuir-Blodgett systems are monolayer systems formed in troughs where surface tension measurements investigate membrane perturbation<sup>73,96</sup>.

Micelles (Ms) and reverse micelles (RMs) are solution-state monolayer systems<sup>97</sup>. Formation occurs above the critical micelle concentration (cmc) and critical temperature (Krafft temperature)<sup>97,98</sup>. Interplay between aqueous, nonpolar and surfactant phases dictate M and RM formation. RMs are isotropic and can form with cationic, anionic or nonionic amphiphilic surfactant molecules<sup>99</sup>. RMs are thought to be spherical, although computational modeling suggests ellipsoid shapes are more likely<sup>100,101</sup>. RM systems are not as accepted by biology as phospholipid membranes however, they provide a defined gradient from the aqueous core to the nonpolar bulk. RMs have been used to study water and molecular behavior in confinement,<sup>102-105</sup> determine probe localization<sup>85,106,107</sup> and evaluate simple reactions<sup>108</sup>.

Cetyltrimethylammonium bromide (CTAB) and sodium bis(2-ethylhexyl)sulfosuccinate (AOT) RMs are illustrated in figure I.4 and were used as the model systems for this work. CTAB is cationic with a trimethylammonium head group while AOT is anionic with a sulfur trioxide head group and two carboxylate esters. A comparison between AOT, CTAB and dipalmitoylphosphatidylcholine (DPPC) is provided in figure I.5. The increased simplicity of these systems allows for characterization through solution state spectroscopy. CTAB and AOT RMs are evaluated herein using <sup>1</sup>H and <sup>51</sup>V NMR, DLS and IR spectroscopies.

FIGURES AND CAPTIONS

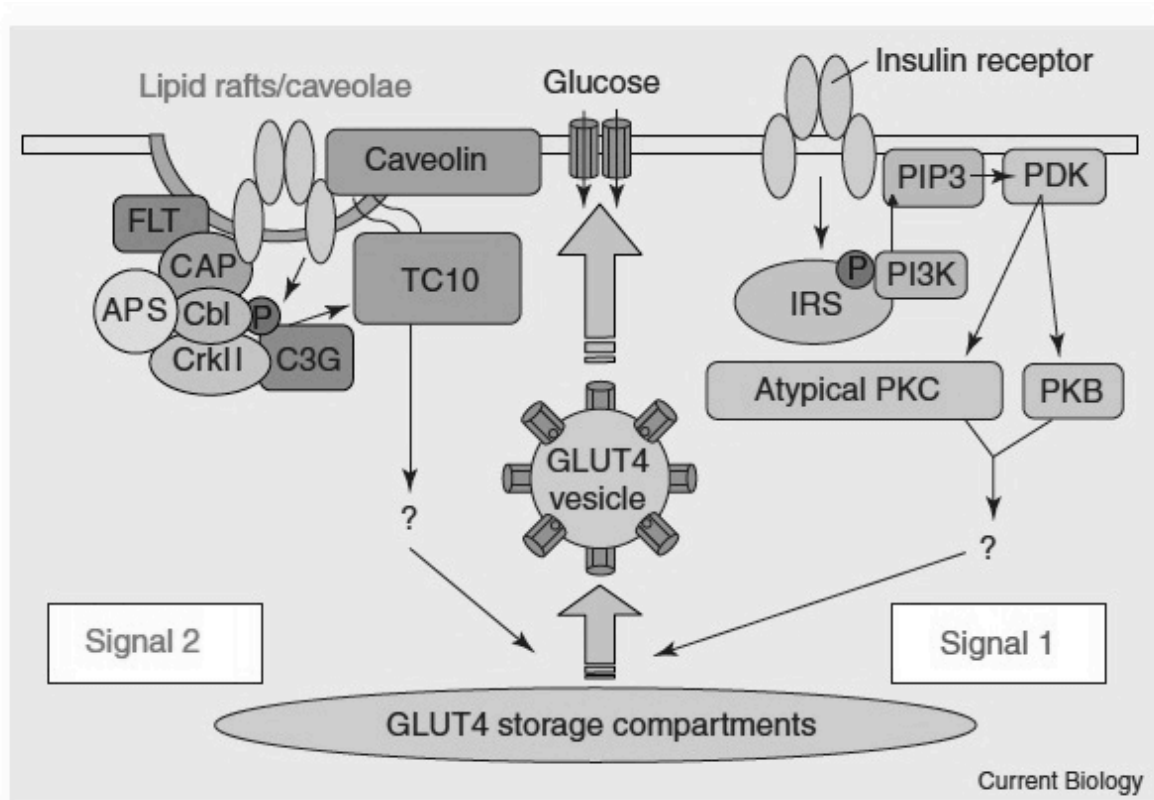


Figure I.1. Insulin-induced GLUT4 translocation from intracellular storage compartments to the plasma membrane requires two independent signaling pathways; one is dependent on the IRS/PI 3-kinase pathway (signal 1) and the other is dependent on the CAP/Cbl/TC10 pathway (signal 2). Signal 1 involves the phosphorylation of IRS proteins and recruitment of PI3-kinase, resulting in the generation of PI-3,4,5-P(3) which subsequently activates 3'-phosphoinoside-dependent kinase 1 (PDK1). Signal 2 involves the phosphorylation of Cbl and the recruitment of CrkII-C3G complex. Once Cbl is phosphorylated, the Cbl-CAP-CrkII-C3G complex translocates to the lipid raft microdomain where TC10 exists. The recruited C3G functions as a guanine nucleotide exchange factor for the TC10, resulting in the exchange of GDP for GTP. These two distinct insulin-induced signal transduction pathways act together to elicit the translocation of GLUT4 protein mediating via membrane trafficking systems. IRS, insulin receptor substrate;

PKB, protein kinase B (Akt); FLT, flotillin; PKC, protein kinase C; APS, Adaptor protein containing PH and SH2 domains.

*Reprinted from: Current Biology, 13 / 14, Kanzaki, M., Pessin, J. E., Insulin Signaling: GLUT4 Vesicles Exit via the Exocyst, R574-R576, 2003, with permission from Elsevier.*

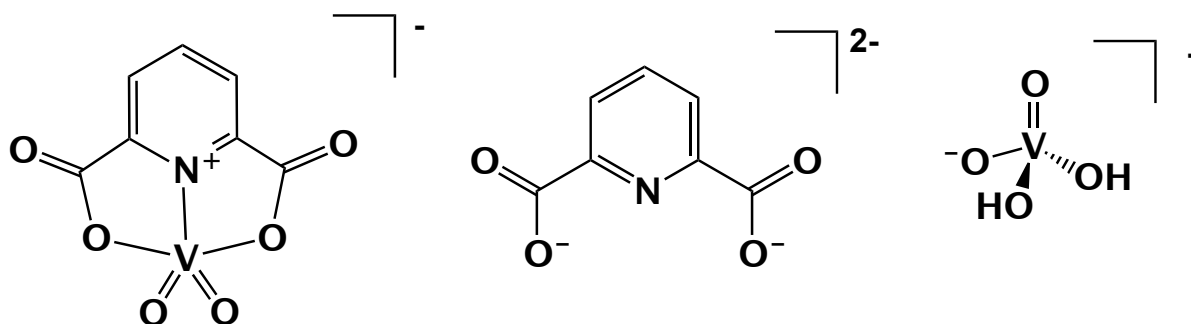


Figure I.2. Structural representations of dipicolinatooxovanadium(V) ( $VO_2[dipic]^-$ ), 2,6-pyridinedicarboxylate ( $dipic^{2-}$ ) and vanadate ( $H_2VO_4^-$ ).

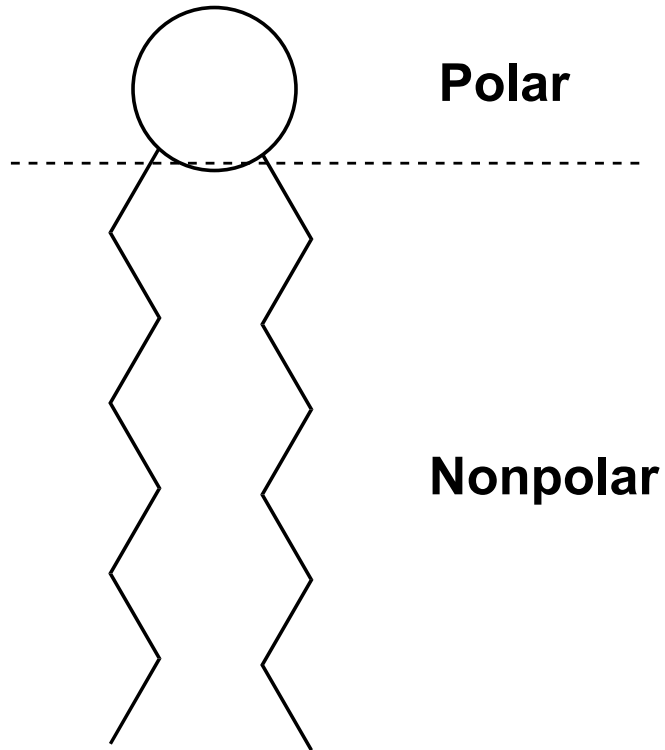


Figure I.3. Illustration of an amphiphile consisting of a polar and a nonpolar region. Polar ends can contain head groups that are charged (cationic, anionic), zwitterionic (both cationic and anionic) or nonionic. Nonpolar ends are typically aliphatic tails.

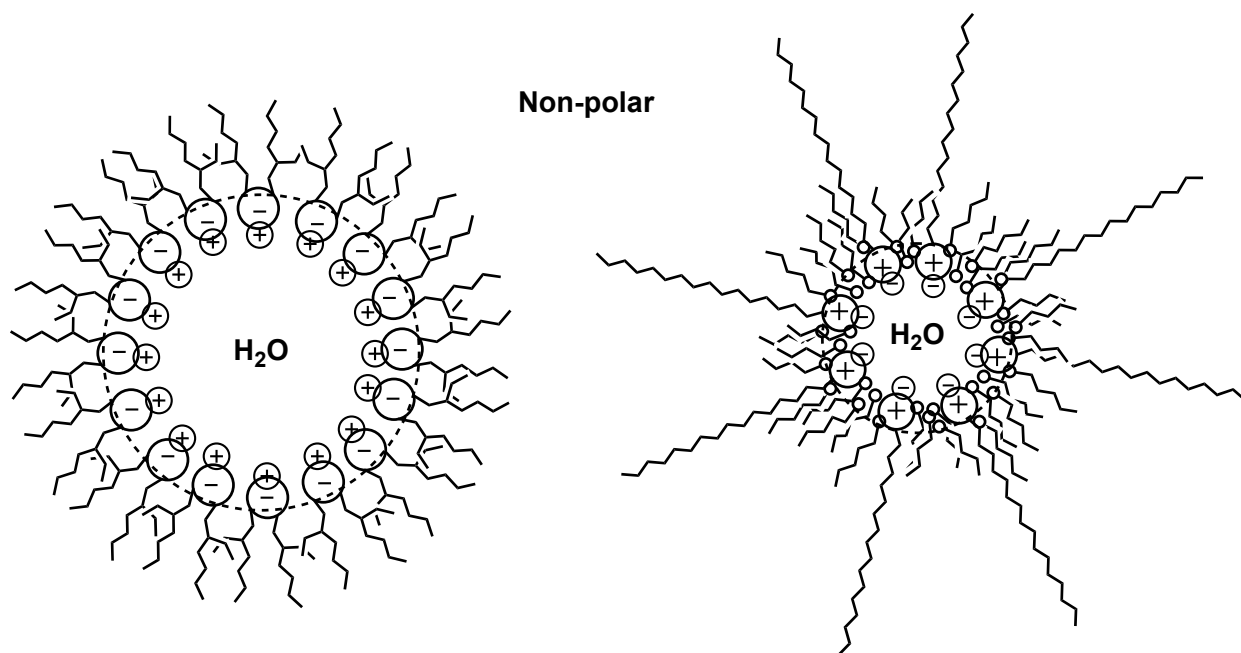


Figure I.4. An idealized representation of a spherical reverse micelle (RM) of sodium bis(2-ethylhexyl)sulfosuccinate (AOT) and an RM structure of cetyltrimethylammonium bromide (CTAB) with 1-pentanol as the co-surfactant.

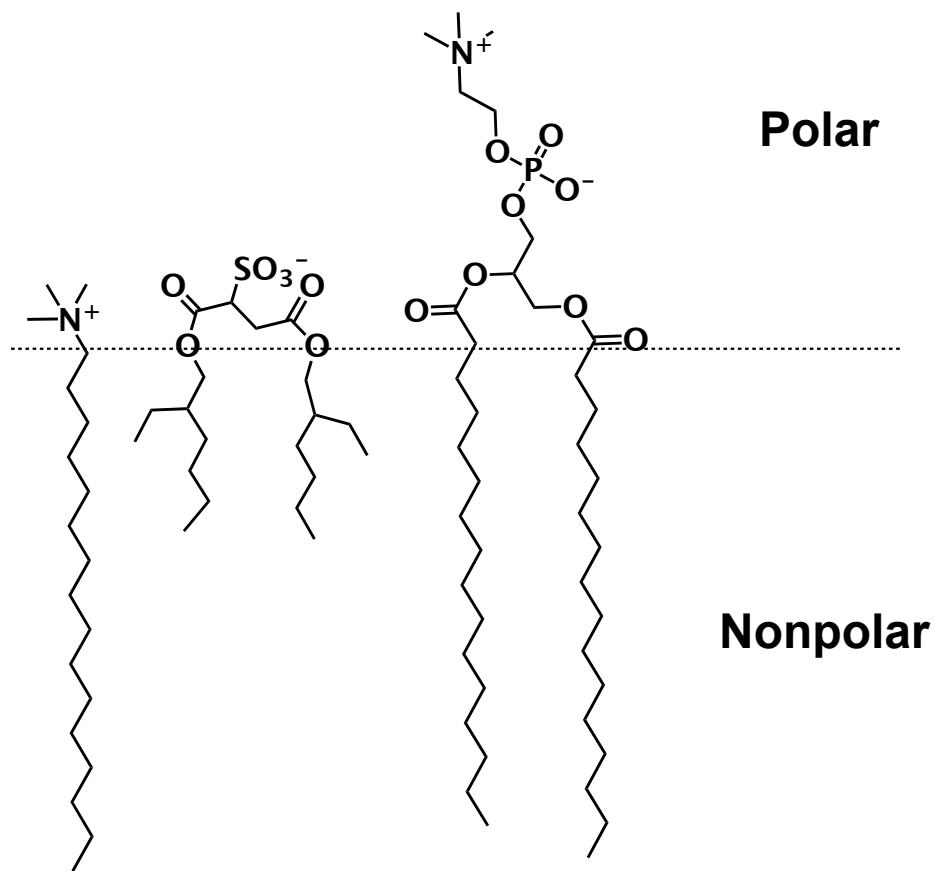


Figure I.5. Structural representations of, from left to right, CTAB, AOT, and dipalmitoylphosphatidylcholine (DPPC) comparing the polar and nonpolar regions of common surfactants to natural lipids.

## REFERENCES

- (1) The Expert Committee on the Diagnosis and Classification of Diabetes, *Diabetes Care* **2011**, *34*, S62-S69.
- (2) Willsky, G. R.; Goldfine, A. B.; Kostyniak, P. J.; McNeill, J. H.; Yang, L. Q.; Khan, H. R.; Crans, D. C. *Journal of Inorganic Biochemistry* **2001**, *85*, 33-42.
- (3) Thompson, K. H.; Lichter, J.; LeBel, C.; Scaife, M. C.; McNeill, J. H.; Orvig, C. *Journal of Inorganic Biochemistry* **2009**, *103*, 554-558.
- (4) Crans, D. C.; Smee, J. J.; Gaidamauskas, E.; Yang, L. Q. *Chemical Reviews* **2004**, *104*, 849-902.
- (5) Scior, T.; Guevara-Garcia, A.; Bernard, P.; Do, Q.-T.; Domeyer, D.; Laufer, S. *Mini-Reviews in Medicinal Chemistry* **2005**, *5*, 1-14.
- (6) Willsky, G. R.; Chi, L.; Godzala III, M.; Kostyniak, P. J.; Smee, J. J.; Trujillo, A. M.; Alfano, J. A.; Ding, W.; Hu, Z.; Crans, D. C. *Coordination Chemistry Reviews* **2011**, *255*, 2258-2262.
- (7) Cohen, N.; Halberstam, M.; Shlimovich, P.; Chang, C. J.; Shmoon, H.; Rossetti, L. *Journal of Clinical Investigation* **1995**, *95*, 2501-2509.
- (8) Alberts, B.; Johnson, A.; Lewis, J.; M., R.; Roberts, K.; Walter, P. *Molecular Biology of The Cell*; Garland Science, Taylor & Francis Group LLC.: New York, 2008.
- (9) Palm, K.; Stenberg, P.; Luthman, K.; Artursson, P. *Pharmaceutical Research* **1997**, *14*, 568-571.
- (10) Mayfield, J. *American Family Physician* **1998**, *58*, 1355-1362.
- (11) Choi, K.; Kin, Y.-B. *The Korean Journal of Internal Medicine* **2010**, *25*, 119-129.

- (12) Schmitz-Peiffer, C. *Cellular Signalling* **2000**, *12*, 583-594.
- (13) Kanzaki, M. *Endocrine Journal* **2006**, *53*, 267-293.
- (14) Gao, X.; Lowry, P. R.; Zhou, X.; Depry, C.; Wei, Z.; Wong, G. W.; Zhang, J. *Proceedings of the National Academy of Sciences* **2011**, *108*, 14509-14514.
- (15) Saeidi, N.; Meoli, L.; Nestoridi, E.; Gupta, N. K.; Kvas, S.; Kucharczyk, J.; Bonab, A. A.; Fischman, A. J.; Yarmush, M. L.; Stylopoulos, N. *Science* **2013**, *341*, 406-410.
- (16) Parikh, M.; Issa, R.; Vieira, D.; McMacken, M.; Saunders, J. K.; Ude-Welcome, A.; Schubart, U.; Ogedegbe, G.; Pachter, H. L. *Journal of the American College of Surgeons* **2013**, *217*, 527-532.
- (17) Bhor, V. M.; Sivakami, S. *Molecular and Cellular Biochemistry* **2003**, *252*, 125-132.
- (18) Keelan, M.; Walker, K.; Thomson, A. B. R. *Comp. Biochem. Physiol.* **1985**, *82A*, 83-89.
- (19) Brastius, T. A.; Dubeja, P. K. *The Journal of Biological Chemistry* **1985**, *260*, 12405-12409.
- (20) Thompson, K. H.; Orvig, C. *Journal of Inorganic Biochemistry* **2006**, *100*, 1925-1935.
- (21) Goldfine, A. B.; Patti, M. E.; Zuberi, L.; Goldstein, B. J.; LeBlanc, R.; Landaker, E. J.; Jiang, Z. Y.; Willsky, G. R.; Kahn, C. R. *Metabolism-Clinical and Experimental* **2000**, *49*, 400-410.
- (22) Sekar, N.; Li, J. P.; Shechter, Y. *Critical Reviews in Biochemistry and Molecular Biology* **1996**, *31*, 339-359.
- (23) Chasteen, N. D. *Vanadium-Protein Interactions*; Marcel Dekker: New York, 1995; Vol. 31.
- (24) Mehdi, M. Z.; Srivastava, A. K. *Archives of Biochemistry and Biophysics* **2005**, *440*, 158-164.

- (25) Shioda, N.; Ishigami, T.; Han, F.; Moriguchi, S.; Shibuya, M.; Iwabuchi, Y.; Fukunag, K. *Neuroscience* **2007**, *148*, 221-229.
- (26) Cornman, C. R.; Zovinka, E. P.; Meixner, M. H. *Inorganic Chemistry* **1995**, *34*, 5099-&.
- (27) Huyer, G.; Liu, S.; Kelly, J.; Moffat, J.; Payette, P.; Kennedy, B.; Tsaprailis, G.; Gresser, M. J.; Ramachandran, C. *Journal of Biological Chemistry* **1997**, *272*, 843-851.
- (28) Crans, D. C.; Keramidas, A. D.; Drouza, C. *Phosphorous, Sulfur, and Silicon* **1996**, *109-110*, 245-248.
- (29) Winter, P. W.; Al-Qatati, A.; Wolf-Ringwall, A. L.; Schoeberl, S.; Chatterjee, P. B.; Barisas, B. G.; Roess, D. A.; Crans, D. C. *Dalton Transactions* **2012**, *41*, 6419-6430.
- (30) Roess, D. A.; Smith, S. M. L.; Winter, P.; Zhou, J.; Dou, P.; Baruah, B.; Trujillo, A. M.; Levinger, N. E.; Yang, X. D.; Barisas, B. G.; Crans, D. C. *Chemistry & Biodiversity* **2008**, *5*, 1558-1570.
- (31) Zhang, Y.; Yang, X. D.; Wang, K.; Crans, D. C. *Journal of Inorganic Biochemistry* **2006**, *100*, 80-87.
- (32) Yang, X. G.; Wang, K.; Lu, J. F.; Crans, D. C. *Coordination Chemistry Reviews* **2003**, *237*, 103-111.
- (33) Chintala, S. K.; Kyritsis, A. P.; Mohan, P. M.; Mohanam, S.; Sawaya, R.; Gokslan, Z.; Yung, W. K. A.; Steck, P.; Uhm, J. H.; Aggarwal, B. B.; Rao, J. S. *Molecular Carcinogenesis* **1999**, *26*, 274-285.
- (34) Ramos, S.; Moura, J. J. G.; Aureliano, M. *Metallomics* **2012**, *4*, 16-22.
- (35) Tolman, E. L.; Barris, E.; Burns, M.; Pansini, A.; Partridge, R. *Life Sciences* **1979**, *25*, 1159-1164.
- (36) Tsiani, E.; Fantus, I. G. *Trends in Endocrinology and Metabolism* **1997**, *8*, 51-58.

- (37) Pereira, M. J.; Carvalho, E.; Eriksson, J. W.; Crans, D. C.; Aureliano, M. *Journal of Inorganic Biochemistry* **2009**, *103*, 1687-1692.
- (38) Crans, D. C.; Trujillo, A. M.; Pharazyn, P. S.; Cohen, M. D. *Coordination Chemistry Reviews* **2011**, *255*, 2178-2192.
- (39) Meena, A.; Yadav, D. K.; Srivastava, A.; Khan, F.; Chanda, D.; Chattopadhyay, S. K. *Chemical Biology & Drug Design* **2011**, *78*, 567-579.
- (40) Zhang, Y.; Yang, X.; Wang, K. *Chinese Science Bulletin* **2005**, *50*, 1854-1859.
- (41) Prentis, R. A.; Lis, Y.; Walker, S. R. *British Journal of Clinical Pharmacology* **1988**, *25*, 387-396.
- (42) McNeill, J. H.; Yuen, V. G.; Dai, S. T.; Orvig, C. *Molecular and Cellular Biochemistry* **1995**, *153*, 175-180.
- (43) Willsky, G. R.; Godzalla, M. E.; Kostyniak, P. J.; Chi, L. H.; Gupta, R.; Yuen, V. G.; McNeill, J. H.; Mahroof-Tahir, M.; Smee, J. J.; Yang, L. Q.; Lobernick, A.; Watson, S.; Crans, D. C. In *Vanadium: The Versatile Metal*; Kustin, K., Pessoa, J. C., Crans, D. C., Eds.; American Chemical Soc: Washington, 2007; Vol. 974, p 93-109.
- (44) Yang, X.; Wang, K.; Lu, J.; Crans, D. C. *Coordination Chemistry Reviews* **2003**, *237*, 103-111.
- (45) Yang, X. G.; Yang, X. D.; Yuan, L.; Wang, K.; Crans, D. C. *Pharmaceutical Research* **2004**, *21*, 1026-1033.
- (46) Crans, D. C.; Yang, L. Q.; Jakusch, T.; Kiss, T. *Inorganic Chemistry* **2000**, *39*, 4409-4416.
- (47) Crans, D. C.; Rithner, C. D.; Baruah, B.; Gourley, B. L.; Levinger, N. E. *Journal of the American Chemical Society* **2006**, *128*, 4437-4445.

- (48) Stover, J.; Rithner, C. D.; Inafuku, R. A.; Crans, D. C.; Levinger, N. E. *Langmuir* **2005**, *21*, 6250-6258.
- (49) Buglyo, P.; Crans, D. C.; Nagy, E. M.; Lindo, R. L.; Yang, L. Q.; Smee, J. J.; Jin, W. Z.; Chi, L. H.; Godzala, M. E.; Willsky, G. R. *Inorganic Chemistry* **2005**, *44*, 5416-5427.
- (50) Amidon, G. L.; Lennernas, H.; Shah, V. P.; Crison, J. R. *Pharmaceutical Research* **1995**, *12*, 413-420.
- (51) Kararli, T. T. *Biopharmaceutics and Drug Disposition* **1995**, *16*, 351-380.
- (52) Rune, S. J.; Viskum, K. *Gut* **1969**, *10*, 569-571.
- (53) Stewart, A. K.; Boyd, C. A. R.; Vaughan-Jones, R. D. *Journal of Physiology* **1999**, *516*, 209-217.
- (54) Lipinski, C. L., F; Dominy, BW; Feeney, PJ; *Advanced Drug Delivery Reviews* **1997**, *23*, 3-25.
- (55) Reul, B. A.; Amin, S. S.; Buchet, J.-P.; N., O. L.; Crans, D. C.; Brichard, S. M. *British Journal of Pharamcology* **1999**, *126*, 467-477.
- (56) Leung, S. S. F.; Mijalkovic, J.; Borrelli, K.; Jacobson, M. P. *Journal of Chemical Information and Modeling* **2012**, *52*, 1621-1636.
- (57) Abraham, M. H. *Journal of Pharmaceutical Sciences* **2011**, *100*, 1690-1701.
- (58) Peral, F.; Gallego, E. *Spectrochimica Acta Part A: Molecular and Biomolecular Spectroscopy* **2000**, *56*, 2149-2155.
- (59) Crans, D. C.; Trujillo, A. M.; Bonetti, S.; Rithner, C. D.; Baruah, B.; Levinger, N. E. *Journal of Organic Chemistry* **2008**, *73*, 9633-9640.
- (60) Crans, D. C.; Levinger, N. E. *Accounts of Chemical Research* **2011**, *45*, 1637-1645.

- (61) Kitagawa, S.; Hosokai, A.; Kaseda, Y.; Yamamoto, N.; Kaneko, Y.; Matsuoka, E. *International Journal of Pharmaceutics* **1998**, *161*, 115-122.
- (62) Szabo, G. *Nature* **1974**, *252*, 47-49.
- (63) Radhakrishnan, A.; McCommell, H. M. *Biochemistry* **2000**, *39*, 8119-8124.
- (64) Hanukoglu, I. *Journal of Steroid Biochemistry and Molecular Biology* **1992**, *43*, 779-804.
- (65) Lopez-Pedrosa, J. M.; Torres, M. I.; Fernandez, M. I.; Rios, A.; Gil, A. *The Journal of Nutrition* **1998**, *128*, 224-233.
- (66) Nishimura, S. Y.; Vrljic, M.; Klein, L. O.; McConnell, H. M.; Moerner, W. E. *Biophysical Journal* **2006**, *90*, 927-938.
- (67) El-Sayed, M. Y.; Guion, T. A.; Fayer, M. D. *Biochemistry* **1986**, *25*, 4825-4832.
- (68) Radhakrishnan, A.; Anderson, T. G.; McConnell, H. M. *Proceedings of the National Academy of Science* **2000**, *97*, 12422-12427.
- (69) Quinn, P. J.; Wolf, C. *Febs Journal* **2010**, *277*, 4685-4698.
- (70) Luxnat, M.; Galla, H. J. *Biochimica et Biophysica Acta* **1986**, *856*, 274-282.
- (71) Kaiser, H. J.; Lingwood, D.; Levental, I.; Sampaio, J. L.; Kalvodoca, L.; Rejendran, L.; Simons, K. *Proceedings of the National Academy of Sciences* **2009**, *106*, 16645-16650.
- (72) McQuaw, C. M.; Sostarecz, A. G.; Zheng, L. L.; Ewing, A. G.; Winograd, N. *Langmuir* **2005**, *21*, 807-813.
- (73) Sostarecz, A. G.; McQuaw, C. M.; Ewing, A. G.; Winograd, N. *Journal of the American Chemical Society* **2004**, *126*, 13882-13883.
- (74) Ivankin, A.; Kuzmenko, I.; Gidalevitz, D. *Physical Review Letters* **2012**, *108*, 238103 (238101-238105).

- (75) de Meyer, F. J. M.; Rodgers, J. M.; Willems, T. F.; Smit, B. *Biophysical Journal* **2010**, *99*, 3629-3638.
- (76) Pilotelle-Bunner, A.; Beaunier, P.; Tandori, J.; Maroti, P.; Clarke, R. J.; Sebban, P. *Biochemica et Biophysica Acta* **2009**, *1787*, 1039-1049.
- (77) Okamura, M. Y.; Paddock, M. L.; Graige, M. S.; Feher, G. *Biochemica et Biophysica Acta* **2000**, *1458*, 148-163.
- (78) Starke-Peterkovic, T.; Turner, N.; Vitha, M. F.; Waller, M. P.; Hibbs, D. E.; Clarke, R. J. *Biophysical Journal* **2006**, *90*, 4060-4070.
- (79) Huster, D.; Arnold, K.; Gawrisch, K. *Journal of Physical Chemistry B* **1999**, *103*, 243-251.
- (80) Soubias, O.; Jolibois, F.; Reat, V.; Milon, A. *Chemistry - A European Journal* **2004**, *10*, 6005-6014.
- (81) Dai, J.; Alwarawrah, M.; Huang, J. Y. *Journal of Physical Chemistry B* **2010**, *114*, 840-848.
- (82) Villalain, J. *European Journal of Biochemistry* **1996**, *241*, 586-593.
- (83) Segwick, M. A.; Trujillo, A. M.; Hendricks, N.; Levinger, N. E.; Crans, D. C. *Langmuir* **2010**, *27*, 948-954.
- (84) Liu, A. H.; Mao, S. Z.; Liu, M. L.; Du, Y. R. *Colloid and Polymer Science* **2008**, *286*, 1629-1636.
- (85) Sedgwick, M.; Cole, R. L.; Rithner, C. D.; Crans, D. C.; Levinger, N. E. *Journal of the American Chemical Society* **2012**, *134*, 11904-11907.
- (86) Maitra, A.; Patanjali, P. K. *Colloids and Surfaces* **1987**, *27*, 271-276.

- (87) Seydel, J. K.; Coats, E. A.; Cordes, H. P.; Wiese, M. *Archiv der Pharmazie* **1994**, *327*, 601-610.
- (88) Cheong, J. H.; Bannon, D.; Olivi, L.; Kim, Y.; Bressler, J. *Toxicological Sciences* **2004**, *77*, 334-340.
- (89) Adson, A.; Raub, T. J.; Burton, P. S.; Barsuhn, C. L.; Hilgers, A. R.; Ho, N. F. H.; Audus, K. L. *Journal of Pharmaceutical Sciences* **1994**, *83*, 1529-1536.
- (90) Prince, L. M. *Microemulsions theory and practice*; Academic Press Inc.: New York, 1977.
- (91) Pereira-Leite, C.; Carneiro, C.; Soares, J. X.; Afonso, C.; Nunes, C.; Lucio, M.; Reis, S. *European Journal of Pharmaceutics and Biopharmaceutics* **2013**, *84*, 183-191.
- (92) Nirasay, S.; Mouget, Y.; Marcotte, I.; Claverie, J. P. *International Journal of Pharmaceutics* **2011**, *421*, 170-175.
- (93) Arouri, A.; Hansen, A. H.; Rasmussen, T. E.; Mouritsen, O. G. *Current Opinion in Colloid & Interface Science* **2013**, *18*, 419-431.
- (94) Ojemyr, L. N.; Von Ballmoos, C.; Faxen, K.; Svahn, E. *Biochemistry* **2012**, *51*, 1092-1100.
- (95) Bouwstra, J. A.; Gooris, G. S.; Bras, W.; Talsma, H. *Chemistry and Physics of Lipids* **1993**, *64*, 83-98.
- (96) Al-Qatati, A.; Fontes, F. F.; Barisas, B. G.; Zhang, D.; Roess, D. A.; Crans, D. C. *Dalton Transactions* **2013**, *42*, 11912-11920.
- (97) Lawrence, M. J.; Rees, G. D. *Advanced Drug Delivery Reviews* **2000**, *45*, 89-121.
- (98) Fisher, L. R.; Oakenfull, D. G. *Chemical Society Reviews* **1977**, *6*, 25-42.
- (99) Uskokovic, V.; Drogenk, M. *Surface Review and Letters* **2005**, *12*, 239-277.

- (100) Vasquez, V. R.; Williams, B. C.; Graeve, O. A. *The Journal of Physical Chemistry B* **2011**, *115*, 2979-2987.
- (101) Abel, S.; Sterpone, F.; Bandyopadhyay, S.; Marchi, M. *Journal of Physical Chemistry B* **2004**, *108*, 19458-19466.
- (102) Moilanen, D. E.; Fenn, E. E.; Wong, D.; Fayer, M. D. *The Journal of Chemical Physics* **2009**, *131*, 1-9.
- (103) Halliday, N. A.; Peet, A. C.; Britton, M. M. *Journal of Physical Chemistry B* **2010**, *114*, 13745-13751.
- (104) McPhee, J. T.; Scott, E.; Levinger, N. E.; Van Orden, A. *The Journal of Physical Chemistry B* **2011**, *115*, 9585-9592.
- (105) Baruah, B.; Roden, J. M.; Sedgwick, M.; Correa, N. M.; Crans, D. C.; Levinger, N. E. *Journal of the American Chemical Society* **2006**, *128*, 12758-12765.
- (106) Vermathen, M.; Louie, E. A.; Chodosh, A. B.; Reid, S.; Simonis, U. *Langmuir* **1999**, *12*, 16(11).
- (107) Piletic, I. R.; Moilanen, D. E.; Spry, D. B.; Levinger, N. E.; Fayer, M. D. *Journal of Physical Chemistry A* **2006**, *110*, 4985-4999.
- (108) Johnson, M. D.; Lorenz, B. B.; Wilkins, P. C.; Lemons, B. G.; Baruah, B.; Lamborn, N.; Stahla, M.; Chatterjee, P. B.; Richens, D. T.; Crans, D. C. *Inorganic Chemistry* **2012**, *51*, 2757-2765.

## CHAPTER 1:<sup>1</sup>Cholesterol Affects Proton Transfer in CTAB Reverse Micelles

### *SUMMARY*

Cholesterol is known to have profound impacts on biological membranes. The work presented here shows that cholesterol changes the transfer of protons along the interface of a simplified membrane-like system. By affecting the local water pool of reverse micelles, cholesterol can affect properties of the local aqueous region. A change in the proton exchange rate was observed with the inclusion of cholesterol detected by <sup>1</sup>H NMR. By changing the pH of the aqueous phase, exchange rates slowed and the individual components separated into distinct signals. The signals were identified as hydrogen exchanged deuterium oxide and the hydroxyl group of 1-pentanol. This condition was reversed as pH became basic where elevated concentrations of <sup>-</sup>OH increased the rate producing one <sup>1</sup>H NMR signal. Interestingly, the pH “window” where the exchange rates decreased was a narrower range with cholesterol. Without cholesterol, exchange rates were reduced in specific ranges. Rate differences were quantified to ~10<sup>5</sup>s<sup>-1</sup> in the pH ranges of 2.0 – 3.0 and 11.6 – 12.0. These studies provide experimental evidence that natural membrane components like cholesterol impact reactions at the interface. Such interactions may contribute to previous observations indicating that membrane interfaces surrounding protein channels serve as proton-collecting antennae, significantly altering proton availability.

---

<sup>1</sup> By: Alejandro M. Trujillo, Bharat Baruah and Debbie C. Crans\*  
Alejandro M. Trujillo performed all experiments except figure 1.3  
*Manuscript prepared for submission to Nature Chemistry*

## INTRODUCTION

Chemical reactions occurring near plasma membranes regulate many activities associated with cellular processes<sup>1-7</sup>. Many factors contribute to these reactions, one being the membrane structure itself<sup>1,8-13</sup>. Properties that affect reaction rates include the behavior of water along membrane interfaces<sup>14</sup>. The behavior of water can be a defining factor for reaction rates in these complex biochemical environments<sup>14,15</sup>. The specific composition of compounds composing cellular membranes influence changes in the reactivity along these interfaces<sup>4-6,12,13,16-23</sup>. Cellular plasma membranes are composed of a variety of lipids, proteins and cholesterol, each with their own influence on membrane properties<sup>11</sup>. The heterogeneities within plasma membrane creates a conundrum for researchers aiming to define specific membrane properties<sup>24</sup>. These experimental complications have required the usage of simplified membrane mimics to model the structure and gain experimental accessibility<sup>5,6,16-18,25-29</sup>. By removing the heterogeneities of biological membranes, clearer definition of membrane properties can be achieved<sup>24</sup>. Previous studies in simplified systems have illustrated an effect of water in confinement<sup>30-33</sup>. Studies have used a variety of model systems including vesicles and bilayers to simpler aggregated structures like monolayers, micelles and reverse micelles<sup>34-37</sup>. The properties of water in confinement are critical to understanding chemical and biochemical events occurring along interfaces<sup>38</sup>.

A critical and extensively studied reaction in life sciences is proton ( $H^+$ ) transfer and how the process varies with the behavior of water and how it changes with its environment<sup>1,9,39,40</sup>. Fundamentally, the presence of a membrane-like surface creates a polarized region of water where  $H^+$  transfer is sensitive to perturbations. The importance of  $H^+$  transfer has most commonly been experimentally examined in acid-base catalyzed reactions in water<sup>41</sup>.  $H^+$  transfer rates in aqueous solution are generally diffusion limited ( $10^{-9} \text{ m}^2 \text{ s}^{-1}$ )<sup>41</sup>. Rates change based on

the environmental presence of acceptors <sup>41</sup>. Altered H<sup>+</sup> transfer rates along interfaces have been observed leading and characterized as, H<sup>+</sup> wire, H<sup>+</sup> collecting antenna, and the core / shell water models <sup>41,42</sup>. In a simplified membrane-like model system, cytochrome c oxidase attached to a pH sensitive probe, observed increased proton transfer rates by 400 fold compared to when *cytochrome c oxidase* was unincorporated <sup>1</sup>. However the complex mechanism of water oxidation catalyzed by *cytochrome c oxidase* requires the combination of theoretical modeling and experimental data <sup>2</sup>. Significant alterations in H<sup>+</sup> flow along interfaces have resulted in the suggestion that membrane-like interfaces act as a H<sup>+</sup> collecting antennae <sup>9</sup>. Experimental evidence supports the movement of H<sup>+</sup>s along membrane interfaces on a H<sup>+</sup> wire with significant increases in H<sup>+</sup> transfer rates observed <sup>41</sup>. The core / shell model used with reverse micelles describes different types of water and as a result significant differences in their properties should be accessible for measurement <sup>43</sup>. Cai, et al. have shown in lipid-conjugated nanoparticles, chemical exchange saturation transfer agents indicate a reduced exchange between metal coordinated water and bulk water <sup>44</sup>. These examples indicate a change in the chemical properties of water along interfaces resulting in the profound effects H<sup>+</sup> transfer rates.

Cholesterol is a critical component for biology, and specifically in membrane structures <sup>12,19,21,45</sup>. By removing the cholesterol typically present in living systems, it has been shown that profound effects occur, which result in ultimately killing the cell <sup>7</sup>. Cholesterol is known to have an influence on membrane physical characteristics and dynamics <sup>12,17</sup>. The physical properties that cholesterol exhibits when present in membranes contributes to the stability of the membrane structure by inducing an increase in rigidity creating a liquid ordered ( $L_o$ ) phase by tightly packing with other membrane components <sup>46</sup>. Tai, et al. has provided evidence that cholesterol reduces membrane fluidity under oxidative attack <sup>47</sup>. Cholesterol has been shown to alter the

structure of membranes also by inducing curvature<sup>48</sup>. Altering the structure of a membrane interface can have profound effects on the activity of the reactions taking place along these interfaces<sup>13,49,50</sup>. In membrane microdomains, which have an increased concentration of cholesterol, these structural changes affect the progression of biological pathways<sup>50</sup>. Emerging evidence has also indicated that there may be some effects on reactivity changes that occur near the interfaces associated with cholesterol<sup>19-21,51</sup>. It has been shown by Pilotelle-Bunner, et al. the presence of cholesterol in phospholipid membranes alters charge transfer reactions in *Rhodobacter sphaeroides* and other bacterial reaction centers<sup>10,52</sup>. The chemical activity of a bacterial reaction center is tied to the transfer of H<sup>+</sup>s in water<sup>41</sup>. In the present study it was aimed to directly evaluate the effect of cholesterol on the movement of a protons from water to a near by acceptor within a confined space.

Simplified model systems such as micelles and reversed micelles (RMs) have proved to be useful tools for exploring confined media by spectroscopy methods<sup>29,53,54</sup>. Specifically, for biology and biochemistry, simplified models have provided researchers with a tool to observe chemical events with fewer variables that are possible in cells. Such opportunities include the ability to define chemical reactions, such as H<sup>+</sup> transfer, at a level not accessible to cellular membranes<sup>5,6,9,16,25,26,55</sup>. RM systems have the advantages of being very simple, and amenable for spectroscopic studies probing the reactions occurring within them<sup>38,53,54,56</sup>. Here, the cationic cetyltrimethylammonium bromide (CTAB) RM system with will be explored as shown in figure 1.1. Previously, Halliday, et al. used the CTAB RM system and NMR to measure the pH of the samples created noting that signals for H<sub>2</sub>O and the hydroxyl group of 1-hexanol, split<sup>54</sup>. Liu, et al. has indicated through ROESY NMR experiments that a cholesterol analog, sodium deoxycholate, aligns with CTAB molecules in a membrane-like bilayer structure<sup>57</sup>. With a

mixed CTAB / 1-pentanol system, it is aimed to observe the change in structure and reactivity with the inclusion of cholesterol. Specifically, this work views changes to the structure of CTAB RMs formed with cholesterol and the rate of H<sup>+</sup> exchange of the aqueous region by pH manipulation.

## *MATERIALS AND METHODS*

### *Materials.*

Cetyltrimethylammonium bromide (95% purity), cyclohexane (99%), cholesterol (95%), 1-pentanol (95%), deuterium oxide (95% purity and 99.9% deuterium), NaOD (99% purity and 99% deuterium) and DCl (99% purity and 99% deuterium) were purchased from Aldrich and used as received. Purity of solvents and materials were examined by <sup>1</sup>H NMR spectroscopy.

### *Sample Preparation.*

Reverse micelle solutions were prepared by mixing 60 mM CTAB solid, 40 mM cholesterol solid (in cholesterol containing samples) and 300 mM 1-pentanol dispersed in cyclohexane organic solvent which is then vortexed creating a suspension that is then combined with the appropriate amount of aqueous to achieve the desired  $w_o$ , creating a transparent solution. The aqueous stock consists of pH adjusted D<sub>2</sub>O from 1.4 – 12.0 by adding DCl and/or NaOD to the solution and were stored in glass sample vials. The pH was measured on an Orion 420A pH meter with solutions at ambient temperature (25°C) and pressure (14.7 psi). The aliquots of aqueous the were then added to sample vials containing the other components of the RM system in accordance with  $w_o$  calculations defined by equation 1 and range here from 4 - 30. All concentrations of the compounds used in this manuscript are held constant. The components altered here include, volume of the aqueous stock, which were added to sample vials using

Eppendorff micropipettes and the volume of the cyclohexane solvent, which were added using glass syringes. The resulting mixtures of water-in-oil solutions were vortexed until homogenous, optically transparent solutions were observed. All samples were stored at room temperature in glass sample vials with Teflon lined tops.

#### *NMR Experiments.*

NMR experiments were performed on multiple spectrometers. Preliminary studies and the data in figures 1.2 and 1.3 were performed on a 400 MHz Varian NMR spectrometer and were acquired using the Varian provided pulse sequence with a spectral window of 5 kHz at a 90° pulse angle. The spectra in figure 1.3 were acquired on a 750 MHz Varian spectrometer at Pacific Northwest National Lab (PNNL). The data uses the <sup>1</sup>H Varian supplied pulse sequence with a spectral window of 5kHz at a 90° pulse angle. Samples were referenced to the most prevalent solvent peaks within the samples (7.26 ppm for CDCl<sub>3</sub> samples, 1.38 ppm for cyclohexane / RM samples). All spectra were acquired a minimum of 16 scans. The resulting spectra were transferred and worked up using either MestRec or MestRec Nova software, then plotted using Origin.

#### *NMR linewidth analysis.*

To quantify the changes observed in the rates of exchange observed by <sup>1</sup>H NMR the quantification of  $k_{eq}$  was achieved using unequally populated, two-site exchange equations based on the McConnell - Bloch equations<sup>58</sup>. At acidic pHs the fast exchange rate was observed by a single peak for the OHs from HOD and OH<sub>p</sub>. Where fast exchange occurred a rate constant in s<sup>-1</sup> was achieved using equation 1 and is displayed in table 1. When the signal shows a pattern that was broadened, indicating an intermediate rate of exchange, equation 2 was used. Where two individual peaks for the contributing compounds was observed equation 3 was used.

$$(1) k = \pi \Delta v_o^2 / 2 (4 \pi p_A p_B \Delta v_o^2 / (\pi (h_e - h_o)_A + \pi (h_e - h_o)_B)) - \text{Fast}$$

$$(2) k = p \Delta v_o / 2^{1/2} - \text{Intermediate}$$

$$(3) k = \pi (4 \pi p_A p_B \Delta v_o^2 / (\pi (h_e - h_o)_A + \pi (h_e - h_o)_B)) - \text{Slow}$$

Where  $k$  is the rate of exchange in  $s^{-1}$ ,  $p_A$  is the population in mole fraction of contributor A,  $p_B$  is the mole fraction of contributor B and  $\Delta v_o$  is the difference between the two exchanging peaks in Hz. The term  $h_e$  is the peak width at half height with exchange,  $h_o$  is the peak width at half height without exchange for contributors A and B.

### *DLS Experiments.*

Prior to light scattering experiments, attempts were made to filter the experimental samples using 2mm screw on filters (25 mm surfactant-free) from Thermo scientific. It was found that the filtration procedure caused the samples to be disturbed creating suspensions that were deemed unusable for spectroscopic analyses for unknown reasons. The samples used were unfiltered and were transferred into quartz cuvettes using glass syringes. The cuvettes used were Wyatt Technology Corp. 12 (2ml) quartz cell (P/N 161125) with a 8.5mm center height. Preliminary DLS experiments were conducted on a Wyatt Technology Corp. DynaPro Titan dynamic light scattering spectrometer. The data presented in figure 1.4 was acquired on Brookhaven ZetaPALS DLS instrument from Brookhaven Instruments Corporation using Brookhaven Instruments – ZetaPALS Particle Sizing Software with a 658.0 nm laser. Prior to acquiring data, the refractive index ( $n_i$ ) and viscosity ( $h$ ) parameters of the neat solvent (cyclohexane  $n_i$  1.421, and  $h$  0.899cP) were input into the program. Samples were allowed to equilibrate to 25°C and ran a minimum of 10 scans with the data fitted assuming spherical particles in solution at a 90° angle. Data was processed on DynaPro Dynamic version 6.7.3 software and plotted using Microsoft Excel.

## RESULTS

The influence of pH affecting the aqueous region of cetyltrimethylammonium bromide (CTAB) RMs was first reported by Halliday, et al. where pH approximations were made by observing the NMR signals for H<sub>2</sub>O and OH<sub>p</sub><sup>54</sup>. Our aim is to specifically evaluate the influence of cholesterol on changes occurring in H<sup>+</sup> transfer in the system, component structures were defined in figure 1.1. The chemical structures represented in figure 1.1a) and 1.1b) allow for the formation of the RM structure, with the chemical structure of cholesterol is illustrated in figure 1.1c). An idealized model defining the CTAB / 1-pentanol RM structure is illustrated in figure 1.1d). The RM structure shown in figure 1.1d) is a spherical micro emulsion where the polar head groups of CTAB and 1-pentanol aggregate, surrounding the water core. In this system, the size of the water core is determined and controlled by utilizing the equation;  $w_o = [\text{H}_2\text{O}]/[\text{surfactant}]$ . In CTAB RMs, the critical micelle concentration (cmc) for CTAB was discovered to be 40 mM, and RM formation was not dependent on water content<sup>59</sup>. It has been shown by Giustini et. al., that not all of the 1-pentanol molecules within the system exist along the interface<sup>60</sup>. Upon vortexing the resulting solutions, the samples appeared optically transparent and contained RMs dispersed in cyclohexane confirmed by conductivity measurements. Within RM systems it is known that there are two distinct types of water, where the interior core exhibits properties similar to those of bulk water, while the water layer located along the interfacial region is significantly different<sup>43</sup>. The difference is considered to be due to the local charges of the surfactant and the resulting alterations they have on the H-bonding network<sup>38,43</sup>. By using the relatively small RM size of  $w_o = 4$ , we aim to make the interfacial water more prominent in the system for spectroscopic observation of the behavior of this water

layer. Thus, the effect of pH on the aqueous phase of this system was a parameter of particular interest.

The control study of figure 1.2 shows the  $^1\text{H}$  NMR measurements as a stacked plot illustrating the chemical shift spectra for the compounds in this study. CTAB, cholesterol and 1-pentanol are shown in figure 1.2 with their chemical shifts recorded for the individual components. The data was recorded on a 400 MHz Varian NMR and the spectra for the individual samples contained, 300 mM 1-pentanol, 60 mM CTAB, and 40 mM cholesterol in chloroform ( $\text{CDCl}_3$ ) are shown. This study was performed to establish a baseline to determine the accuracy of the spectrometers used and the purity of the compounds. This work allowed for the appropriate peak assignments to be determined for each compound and resulted in the numbered labeling sequence shown on the structures in figure 1.1. The top spectrum in figure 1.2 illustrates the resonance signals for the CTAB / 1-pentanol RM system with cholesterol. This sample served as a control for the determination of the spectroscopic compatibility of the sample series to be evaluated. Additionally, figure 1.2 illustrates the chemical shift region containing the signals of interest (3 – 6 ppm), as well as the regions that are difficult to define (0 - ~2.5 ppm). The OH containing signals were found to be present the region of 3 – 6 ppm and this region will be the chemical shift range of focus for the proceeding figures. The chemical shift signals in figure 1.2 are assigned to the best of our knowledge yielding the assignments within the observations in this study<sup>54,59,61</sup>.

To examine any alterations to the structure of the RMs created with addition of cholesterol, we first analyzed the effect of increased water content on the system by  $^1\text{H}$  NMR. Cholesterol is known to alter the phase of cellular membranes, modulating between liquid ordered ( $L_o$ ) and liquid disordered ( $L_d$ ) and the amount of water in the system shifts this continuum

<sup>21</sup>. In a previous study using a cholesterol analog, sodium deoxycholate (NaDC) it was shown that NaDC was compatible with CTAB, indicating the potential for the compatibility between CTAB and compounds structurally similar to cholesterol <sup>57</sup>. Previously, it was found by Klicova, et al. that the concentration of water did not effect the RM formation of CTAB in chloroform above the 40 mM cmc <sup>59</sup>. Figure 1.3 describes the effect of altering the amounts of water within the system. The samples contain CTAB / cholesterol / 1-pentanol / cyclohexane and D<sub>2</sub>O. Deuterium oxide (D<sub>2</sub>O) was used to allow the spectrometer to maintain a lock on the deuterium resonance in these complex systems, increasing the accuracy of the NMR spectra acquired. The samples used in figure 1.3 contained 60 mM CTAB and used the co-surfactant 1-pentanol to encourage RM formation <sup>55,62</sup>. The  $w_o$  values relate to the water nano-droplet size within the micro emulsions and were assessed using the equation described previously. The surfactant concentration remained constant as the concentration of the aqueous phase increased. The increase in aqueous content was observable by the downfield change in chemical shift of the HOD (hydrogen exchanged D<sub>2</sub>O) signal in accordance to previous studies <sup>59,63</sup>. The lowest  $w_o$  value ( $w_o = 4$ ) showed chemical shift changes that were not seen in higher  $w_o$  values. These changes were observed in the signals assigned to the H<sup>+</sup>s; OH<sub>oi</sub> (OH - cholesterol), OH<sub>p</sub> (OH - 1-pentanol) and H1<sub>C</sub> (H1 - CTAB) and indicated a potential for a change to the RM structure. A similar chemical shift change was not observed in the H1<sub>p</sub> signal indicating no change in the local environment around this H<sup>+</sup>. The OH<sub>p</sub> and OH<sub>oi</sub> signals show up field changes in chemical shift when observed from large  $w_o$ s to small, changing from 4.20 to 4.05 ppm for OH<sub>p</sub>, and 4.70 to 4.55 ppm for OH<sub>oi</sub>. The H1<sub>C</sub> signal of CTAB showed a differing behavior, shifting downfield from 3.20 to 3.30 ppm. The movements of these particular signals are of interest due to their interfacial location and indicate an alteration in the local environment based on the water content

of the system. In samples with water content forming a RM size greater than  $w_o = 4$ , the signals stabilized and remained consistent throughout the remainder of the  $w_o$  range ( $w_o = 10 - 30$ ). The changes in  $H^+$  chemical shifts in the  $w_o = 4$  samples required the analysis of the micro emulsion structure<sup>37</sup>.

Dynamic Light Scattering (DLS) was used to define the size and shape of the particles present within samples containing cholesterol. Assuming Brownian movement for the particles within the sample, the diffusion coefficient is related to particle size by application of the Stokes-Einstein equation<sup>64</sup>. Previously, researchers have used DLS to provide data investigating the presence of RMs by calculating the hydrodynamic radius ( $R_h$ ) of a RM sample<sup>29,59,60</sup>. Interestingly, comparable literature findings for the  $R_h$  of CTAB RMs were few and were found to vary<sup>62,60,61</sup>. The data shown in figure 1.4 was acquired on a Brookhaven light scattering device using ZetaPALS (Brookhaven) particle sizing software program. The experimental data was applied to the spherical fit option within the Brookhaven program. The properties of viscosity ( $\eta$ ) and refractive index ( $n_i$ ) for the solvent (cyclohexane  $n_i$  1.421 and  $\eta$  0.899 cP) were set as parameters for the acquisition. The instrument was set up to acquire 10 scans per run, which were then averaged resulting in the final  $R_h$  of the samples in nanometers (nm). To establish a control for the RM measurements a sample of cyclohexane was ran prior to the experimental samples. The longest side of cyclohexane is  $\sim 0.58$  nm while our measurements found an  $R_h = 0.515$  nm ( $\pm 0.05$  nm) for cyclohexane experimentally. The average of these runs is illustrated as a circle at pH = 0 in figure 1.4. The remainder of the data points in figure 1.4 illustrates samples that contained 60 mM CTAB, 300 mM 1-pentanol, cyclohexane and  $H_2O$  at  $w_o = 4$  with 40 mM of cholesterol. The plot is the summation of 6 runs and the data shows an  $R_h$  for samples with aqueous phases at pH 2.5, 5.2, 7.8 and 10.0. The  $R_h$  for the samples across the pH range were

found to be 4 nm ( $\pm 1$  nm). By evaluating the correlation coefficient and the multimodal distributions of the samples, it was determined that the samples contained particles fitting a spherical RM shape. With the samples confirmed to contain spherical RMs the evaluation of the effect of cholesterol on the rate of  $H^+$  exchange in the system occurred.

To evaluate the flow of  $H^+$ s with the CTAB / 1-pentanol RM system the rate of exchange was observed by  $^1H$  NMR spectroscopy. The left side of figure 1.5 illustrates the behavior of the  $^1H$  signals as a function of pH in samples without cholesterol. The data in figure 1.5 were acquired on a 750 MHz Varian NMR and the samples used were set at  $w_o = 4$  to enhance the observability of the interfacial water in the system. At pH 1.4 the  $^1H$  NMR signals assigned to HOD (hydrogen exchanged  $D_2O$ ) and the OH signal from 1-pentanol ( $OH_p$ ) were observed as one signal. The observation of a singlet suggested a rate of exchange between the two  $H^+$ s to be occurring at a rate too high to be observed on the standard experimental timescale of  $\sim 1$  s. The exchange rate for this sample was defined by using an adaptation of the Bloch-McConnell equations<sup>58,65</sup>. When calculated using equation 1, the rate of  $H^+$  transfer between HOD and  $OH_p$ , was found to be on the order of  $10^7 s^{-1}$  and is shown in table 1. A high rate of  $H^+$  exchange within samples at acidic pHs was an expected result due the relatively high concentration of  $H_3O^+$  present within the aqueous phase of the system. However, the rate of proton exchange in bulk water has been found to be on the order of 1 ps<sup>41</sup>. The rate observed was found to be significantly faster in the RM systems than in bulk water suggesting a rate enhancement for the confined water.

As the pH of the aqueous phase approached a pH level of  $\sim 2$  (1.8), there was significant broadening observed in the signal that contained HOD and  $OH_p$  in the CTAB RM samples of figure 1.5. This observation is unique to CTAB / 1-pentanol RMs and indicates a significant

alteration in the chemistry of the aqueous environment. Observing pH 2.2 from figure 1.5, it was found that the signal was then split into two distinct signals where one signal was found to be HOD while the other was  $\text{OH}_p$ . The HOD signal was shifted downfield to 4.25 ppm, compared to the  $\text{OH}_p$ , which was shifted to 3.90 ppm. Signal assignments for the peaks described were achieved using comparative signal integration. The differences in the NMR spectra from pH 1.4 - 2.2 suggest an alteration in the exchange rate between  $\text{OH}_p$  and HOD. When equations 2 and 3 were applied to the spectra to pH 1.8 (equation 2) and 2.2 (equation 3) the resulting exchange rates were found to be on the order of  $10^2 \text{ s}^{-1}$ . The separated signals observed in figure 1.5 indicate the rate of  $\text{H}^+$  exchange in the samples is slow enough to be observed by NMR<sup>66</sup>. Within the pH range where multiple peaks were observed, we interpret this range as having reached an equilibrium, where the relative concentrations of  $\text{H}^+$  and  $\text{OH}^-$  are such that neither is in high demand, as a result, the transfer rate of the charges can reduce. By continuing through the pH range investigated, at a pH level of 11.6, the separated peaks were observed to be deviating from the equilibrium. An increase the rate of  $\text{H}^+$  transfer was observed as the signals for HOD and  $\text{OH}_p$  began coalescing, reverting back to a single signal, similar to the pattern observed at acidic pHs where the rate was high. At pH 12.0 the signals for HOD and  $\text{OH}_p$  returned to one signal. Throughout the pH series defined here, the remaining signals within the plot ( $\text{H1}_p$ ,  $\text{H2}_c$  and  $\text{H1}_c$ ) do not move as a function of pH. This data illustrated a reversible pH “window” where the rate of exchange was altered in a particular pH range. The deviation from the equilibrium was due to the altered relationship between concentrations of  $\text{H}^+$  and  $\text{OH}^-$ , where at basic conditions there was a increase in  $\text{OH}^-$  present within the samples resulting in an increased exchange rate.

To examine if cholesterol altered the rate of chemical exchange by perturbing the rate of  $\text{H}^+$  exchange between HOD and  $\text{OH}_p$  we mirrored the conditions of the samples on the left of

figure 1.5. The samples yielding the data on the right of figure 1.5 differed from those on the left by the presence of 40 mM cholesterol. The samples used contained 60 mM CTAB / 40 mM Cholesterol / 300 mM 1-pentanol / cyclohexane and D<sub>2</sub>O at  $w_o = 4$ . The chemical shift range from 3.0 to 6.0 ppm and a pH range from pH 1.4 – 12.0 were used and are consistent with the samples on the left side of figure 1.5. The signals (H1<sub>p</sub>, H2<sub>C</sub>, H6<sub>oi</sub> and H1<sub>C</sub>) exhibit no change in chemical shift as a function of pH, consistent with a stable system. By including cholesterol and using a small  $w_o$  size we created a system to evaluate cholesterol's effect on the H<sup>+</sup> transfer rates of the interfacial water region.

At pH 1.4, it was shown that the signals assigned to HOD, OH<sub>p</sub> and OH<sub>oi</sub> produced a single signal at 4.25 ppm. The three components (HOD, OH<sub>p</sub>, OH<sub>oi</sub>) were also found to exchanging at a high rate within these samples at 10<sup>7</sup> s<sup>-1</sup> using equation 1. The cholesterol containing samples remained consistent at 10<sup>7</sup> s<sup>-1</sup> for both pH 1.8 and 2.4. In contrasting this data with samples without cholesterol where exchange was reduced to 10<sup>2</sup> s<sup>-1</sup> at pH ~2, it was found that cholesterol influenced the rate of H<sup>+</sup> exchange resulting in a 10<sup>5</sup> s<sup>-1</sup> increase. This result supports observations that there are significant changes in the chemistry of interfaces with the inclusion of cholesterol<sup>20</sup>. By altering the chemical environment of the local water, support was also provided for cholesterol being integrated into the RM interface to influence the changes in H<sup>+</sup> transfer along the aqueous region observed. As the pH of the aqueous phase became increasingly basic, it was observed that at pH 2.4 – 2.7 that significant broadening occurred within this signal. At pH 3.0, the signals split into three distinct peaks. The HOD signal became a characteristically sharp singlet, distinct from OH<sub>p</sub>, and OH<sub>oi</sub> and was identified by signal integration. In addition to the observed HOD singlet, existed two signals in the nearby chemical shift region (4.0 – 4.5 ppm). The more intense up field signal at 4.13 ppm was assigned to the

OH signal that emanated from 1-pentanol ( $\text{OH}_p$ ). The less intense signal that was observed downfield of the HOD peak at 4.45 ppm was shown through signal integration to be present in a ~1:1 ratio to the  $\text{H}_{6_{ol}}$  signal of cholesterol. The signal was identified as the OH from cholesterol ( $\text{OH}_{ol}$ ). When the calculations illustrated in table 1 are applied to the spectra, confirmation of the decreased rate of exchange between  $\text{OH}_p$  and HOD to  $10^2 \text{ s}^{-1}$  was discovered. From pH 3.0 to 10.5 the exchange rate was found to be on the order of  $10^2 \text{ s}^{-1}$  in samples with cholesterol when applying equation 3, and was consistent for samples with multiple peaks for  $\text{OH}_p$  and HOD. The three distinct signals continued through pH 10.5 where there was an observable reversal of the separation. This range pH values where multiple signals were observed are described here as the “window,” where an equilibrium reduced the propensity for  $\text{H}^+$  exchange. The window was found to differ, being over a reduced range of pHs in samples containing cholesterol, indicating cholesterol had a modulating effect on the system. By observing pH 11.6 the cholesterol containing samples contain one broadened peak for  $\text{OH}_p$  and HOD. This broadened signal became increasingly sharpened as the pH value approached 12.0 at the top of plot.

This study illustrates that the pH window where  $\text{H}^+$  exchange was slowed differed in samples containing cholesterol. The presence of cholesterol within the system significantly altered the rate of  $\text{H}^+$  transfer as a function of pH in the regions of 1.8 – 3.0 and 11.6. For CTAB RMs in this range, there are multiple signals indicating a  $\text{H}^+$  exchange rate of  $10^2 \text{ s}^{-1}$  when compared to pH 1.4 where a rate of  $10^7 \text{ s}^{-1}$ . In cholesterol containing samples, there was one signal through pH 2.4, indicating a maintenance of a rate on the order of  $10^7 \text{ s}^{-1}$ . These results showed a  $10^5 \text{ s}^{-1}$  difference between the samples with cholesterol.

## *DISCUSSION AND CONCLUSIONS*

The studies presented here provide experimental evidence of cholesterol impacting reactions at the interface of a membrane-like structure. These observations are similar to those found in biology where cholesterol is known to have a critical role in membrane dynamics and chemical processes occurring along membranes<sup>6,7,17,19,21,22,26,51</sup>. Previously, cholesterol has been shown to alter charge transfer reactions in bacterial reaction centers<sup>10,52</sup>. The work of Yamashita, et al. and Branden, et al. showed that membrane-like interfaces act as H<sup>+</sup> collecting antennae where H<sup>+</sup>s gather along the aqueous side of the interface<sup>25,67</sup>. The researchers indicated that interfaces have effects on the H-bonding network of water along membrane-like structures. Here, the enhancement of H<sup>+</sup> transfer reactions by cholesterol assists in describing the effects of cell membrane components on their local environment. Cholesterol was found to increase the rate of H<sup>+</sup> transfer by 10<sup>5</sup> s<sup>-1</sup> at specific pH values observed as changes in <sup>1</sup>H NMR chemical shifts. The activation threshold of the reaction modulates the rate of a H<sup>+</sup> transfer event where a H<sup>+</sup> located on a donor is transferred to the site of an acceptor<sup>14</sup>. Specifically, we traced the effect of cholesterol on the energy needed to take one hydronium ion H<sub>3</sub>O<sup>+</sup> or H<sub>2</sub>O-H<sup>+</sup> (from HOD), to form H<sup>+</sup>-OH<sub>p</sub>. This transfer occurs when the energy required for movement is met. Cholesterol was shown to decrease the amount of energy needed to move the H<sup>+</sup>s in CTAB RMs, increasing the rate. The behavior of the <sup>1</sup>H NMR signals throughout the pH range showed a narrowed range where the rate of H<sup>+</sup> exchange was slow (10<sup>2</sup> s<sup>-1</sup>) in samples containing cholesterol. This narrowed pH range supports the interpretation of rate enhancement with the inclusion of cholesterol. By quantifying the changes in H<sup>+</sup> transfer rates in CTAB RMs, we have found that cholesterol plays a key role in contributing to the H<sup>+</sup> antenna theory.

Within the system used, cholesterol and 1-pentanol OH groups were available to participate in the observed transfer and rearrangement reactions with water. The associations between water and the OH groups created a thermodynamically stable aggregate system where the H-bonding network forms a “H<sup>+</sup> wire” where fast transport of H<sup>+</sup>s can occur similar to those found in other systems <sup>41</sup>. Here we observed charge rearrangement occurring along the interface of the RM as H<sup>+</sup> exchange between the OH head groups (OH<sub>p</sub> and OH<sub>o</sub>) and water molecules <sup>41</sup>. Within the aqueous phase of RM systems there are two types of water present with differing chemical properties between them as a result of charge localization <sup>38</sup>. The localization of perturbing charge tends to aggregate along the interfacial region, and not be transferred into the aqueous core <sup>41</sup>. Crans et al. showed in anionic surfactants H<sup>+</sup>s aggregate along the interface of RMs displacing the surfactant counter ions <sup>53</sup>. The aggregation of charges results in a pH gradient associated with the interface, contributing to the altered aqueous phase chemistry observed in RMs. This gradient can greatly affect the behavior of molecules along the interfacial region and contribute to rate changes in the reactions taking place in this environment. The acid present within the water phase is found in the form of either the Eigen cation, H<sub>3</sub>O<sub>4</sub><sup>+</sup> ((H<sub>2</sub>O)<sub>3</sub>H<sub>3</sub>O<sup>+</sup>) and/or the Zundel cation, H<sub>5</sub>O<sub>2</sub><sup>+</sup> (H<sub>2</sub>O-H<sup>+</sup>-OH<sub>2</sub>) and is reported to be highly sensitive to perturbations <sup>68,69</sup>. By including cholesterol, the OH group of the sterol altered the chemistry by perturbing the interface, lowering the energy barrier, resulting in rate enhancement of H<sup>+</sup> transfer.

In a previous study, cholesterol was not be compatible with the AOT RM system and created separate aggregations in solution <sup>29</sup>. However, cholesterol has been found to be very soluble in long chain alcohols <sup>70</sup>. By including 1-pentanol as a co-surfactant in the CTAB RM system, we have created a system where cholesterol was able to intercalate into the interfacial region impacting the rate of H<sup>+</sup> transfer. Previously, in CTAB, sodium deoxycholate (NaDC) was

found to interact with the CTAB surfactant when added in ratios corresponding to micelle formations<sup>57</sup>. By changing the rate of H<sup>+</sup> transfer we have shown that cholesterol is allocated in a position where the chemical effects of cholesterol can impact the water pool. Using DLS RM structures were found, supporting the findings with NaDC. However the potential for separate aggregations of cholesterol within the samples are possible. Giordani, et al. showed cholesterol self-aggregates in cyclohexane with a size of 0.6 - 0.7 nm in the concentration range which we used<sup>70</sup>. The analysis of the multimodal size distribution of the DLS data may have allowed for the identification of these aggregates. However, if the particles formed by cholesterol were of similar size, they would not be distinguishable as separate aggregates by DLS. The alteration of the OH chemical shift patterns by NMR should also have indicated that there are two distinct trends, which were not observed.

Another alternative explanation to the chemical shift changes that were observed is alteration in the viscosity of the samples. Spin-spin ( $T_2$ ) relaxation times are directly affected by changes in the viscosity of the solution being examined<sup>71</sup>. If these relaxation times were altered, the differing patterns observed in the NMR data are possible. However the changes are typically limited to alterations in line width<sup>72</sup>. Modulation of the pH in aqueous solutions are known to alter the viscosity in certain polymers<sup>73</sup>. Through studies using biological lipids, it has been shown that cholesterol plays a critical role in the phase transitions of cellular membranes<sup>35</sup>. Specifically, cholesterol has been known to increase the viscosity of solutions used to dissolve gallstones<sup>74</sup>. The data shown here could also be the result of phase alterations. By changing the viscosities of the samples, cholesterol in cooperation pH could certainly have an impact on NMR spectra. In cells, the measurement of the viscosity of the cytoplasm near the plasma membrane was compared to the viscosity away from the membrane and showed that the membrane had

little effect on viscosity <sup>75</sup>. However, this type of effect is difficult to quantify and account for by experimental means accessible to us. To the best of our knowledge, no studies have been performed on the viscosity of the interface of RMs and the effect this has on  $T_2$ . Halliday, et al. indicated that  $T_2$  in CTAB / hexanol RMs reached a minimum when the  $^1\text{H}$  NMR signal pattern changed ( $\text{OH}_p$  and HOD broadened) due to  $\text{H}^+$  exchange <sup>54</sup>. However, this correlation was not consistent in TX-100 RMs. Indeed, an inverse relationship between  $T_1$  and  $T_2$  is known to exist with increasing the viscosity of the system referred to as the inverse law of relaxation times with viscosity <sup>71</sup>. There is no doubt a potential contribution to the trends observed may be due to changes in viscosity. However, the work presented here indicates a reversible change, requiring either a reverse in the viscosity of the solution or chemical exchange. Neither the viscosity changes by pH or cholesterol would be reversible under the experimental conditions used, yet the changes observed exhibit this characteristic. By observing the work of Aramini, et. al. on a quadrupolar nucleus ( $^{27}\text{Al}$ ) there was a notable improvement in resolution with increasing viscosity, yet no change in chemical shift occurred <sup>72</sup>. Yet here significant changes in chemical shifts for the effected  $\text{H}^+$ s was observed, indicating a reversible change in the rate of  $\text{H}^+$  transfer as a function of pH by as much as  $10^5 \text{ s}^{-1}$  with the inclusion of cholesterol.

FIGURES AND TABLES

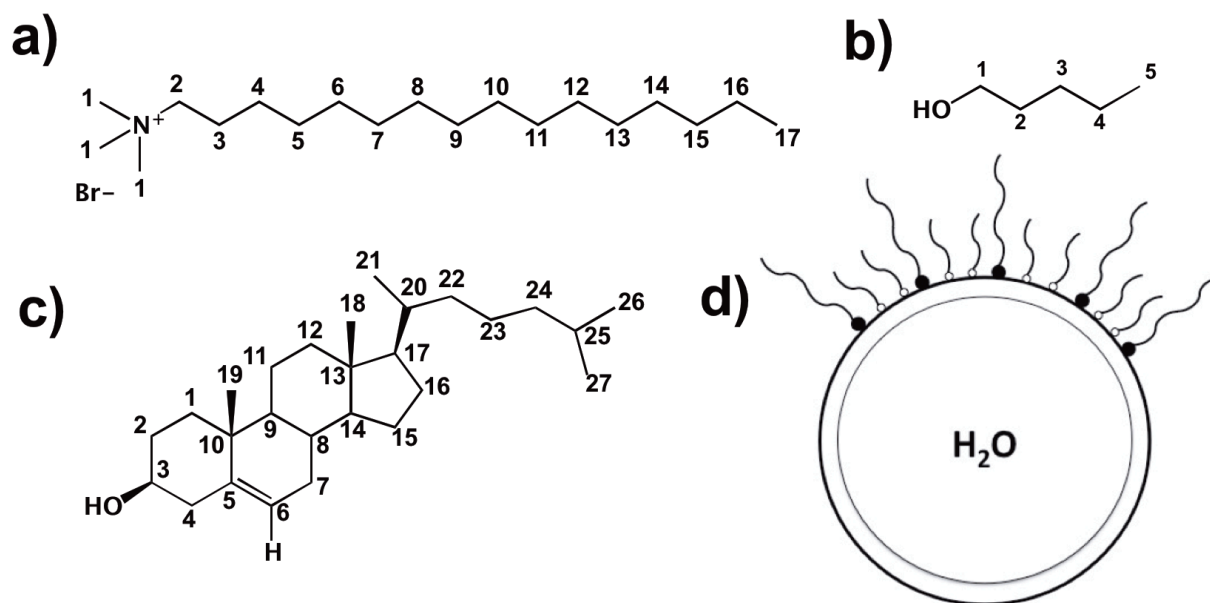


Figure 1.1. Structural representations referred to in this manuscript, (a) cetyltrimethylammonium bromide (CTAB), (b) 1-pentanol (pent), (c) cholesterol (chol), and (d) cartoon illustration of a CTAB / 1-pentanol RM structure. All chemical structures with carbon atoms attached to protons are numbered and correspond to the labeling in the NMR spectra in subsequent figures.

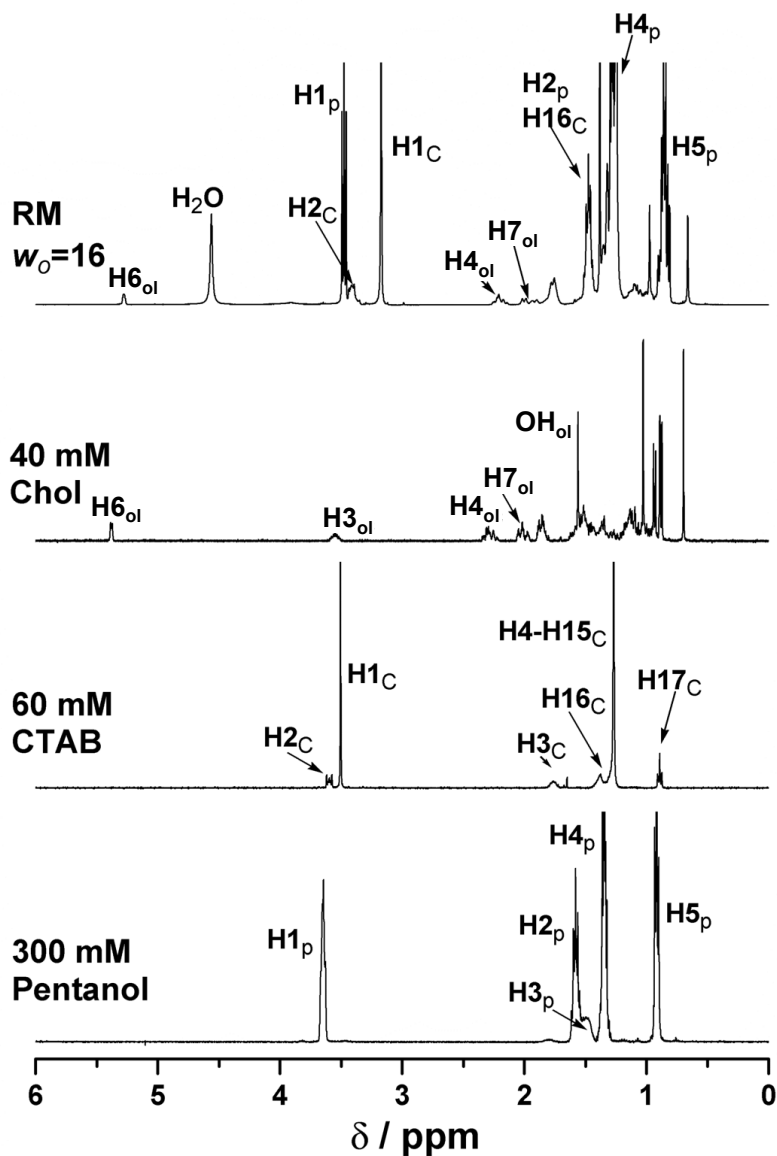


Figure 1.2. A  $^1\text{H}$  NMR stacked plot for 300 mM 1-pentanol ( $\text{HX}_p$ ), 60 mM CTAB ( $\text{HX}_c$ ), and 40 mM Chol ( $\text{HX}_{ol}$ ) in chloroform ( $\text{CDCl}_3$ ). The top spectrum shows an RM sample composed of 60 mM CTAB / 300 mM 1-pentanol / cyclohexane- $\text{d}_{12}$  /  $\text{D}_2\text{O}$  RM system with 40 mM added cholesterol. The spectra illustrate the full chemical shift range for the samples and the chloroform containing samples were internally referenced to the chloroform resonance (7.27 ppm). The RM sample of the top spectrum was referenced internally to cyclohexane resonance (1.44 ppm).

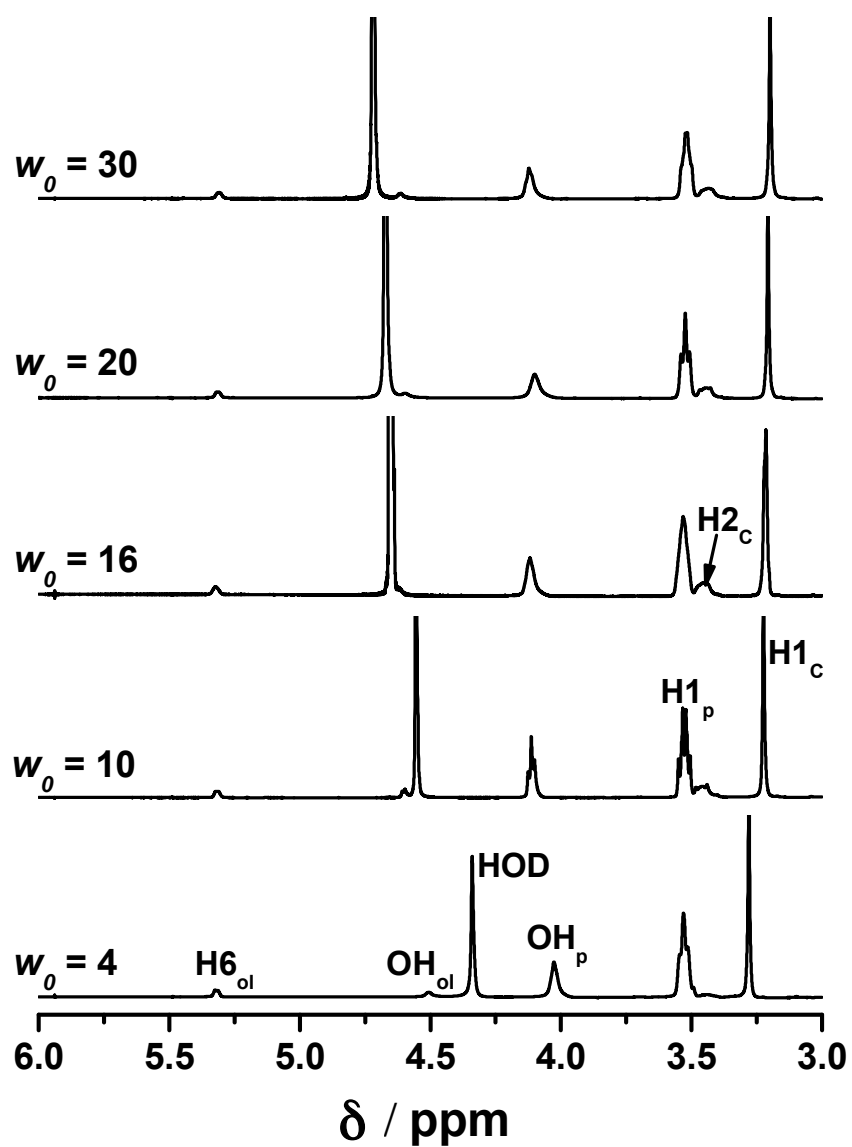


Figure 1.3. A  $^1\text{H}$  NMR stacked plot focused on the chemical shift range of 3 – 6 ppm. The samples consist of RMs composed of 60 mM CTAB / cyclohexane / 300 mM 1-pentanol /  $\text{D}_2\text{O}$  at varying  $w_0$  sizes ranging from 4 – 30. The samples were referenced internally to the cyclohexane resonance (1.44 ppm).

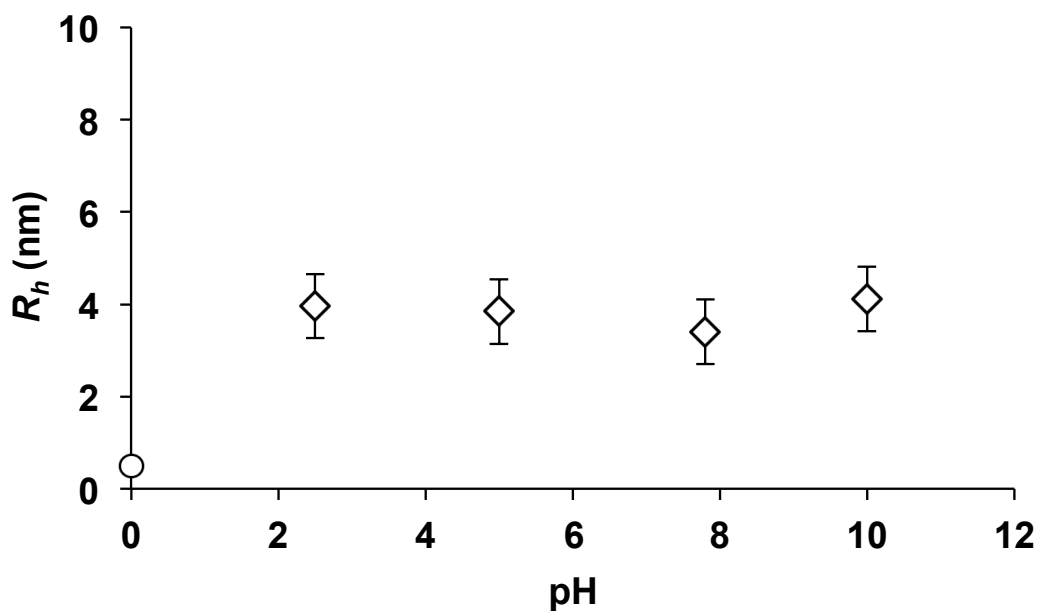


Figure 1.4. Hydrodynamic radii ( $R_h$ ) measurements by DLS illustrating RM size for samples at  $w_o = 4$  containing cholesterol. The plot shows samples of varying pH values (2.5, 5, 7.8 and 10.0) that contain 40 mM Cholesterol/ 60 mM CTAB/ 300 mM 1-pentanol/ cyclohexane/ D<sub>2</sub>O. Plotted at pH 0 is the cyclohexane control sample ( $0.515 \pm 0.05$  nm).

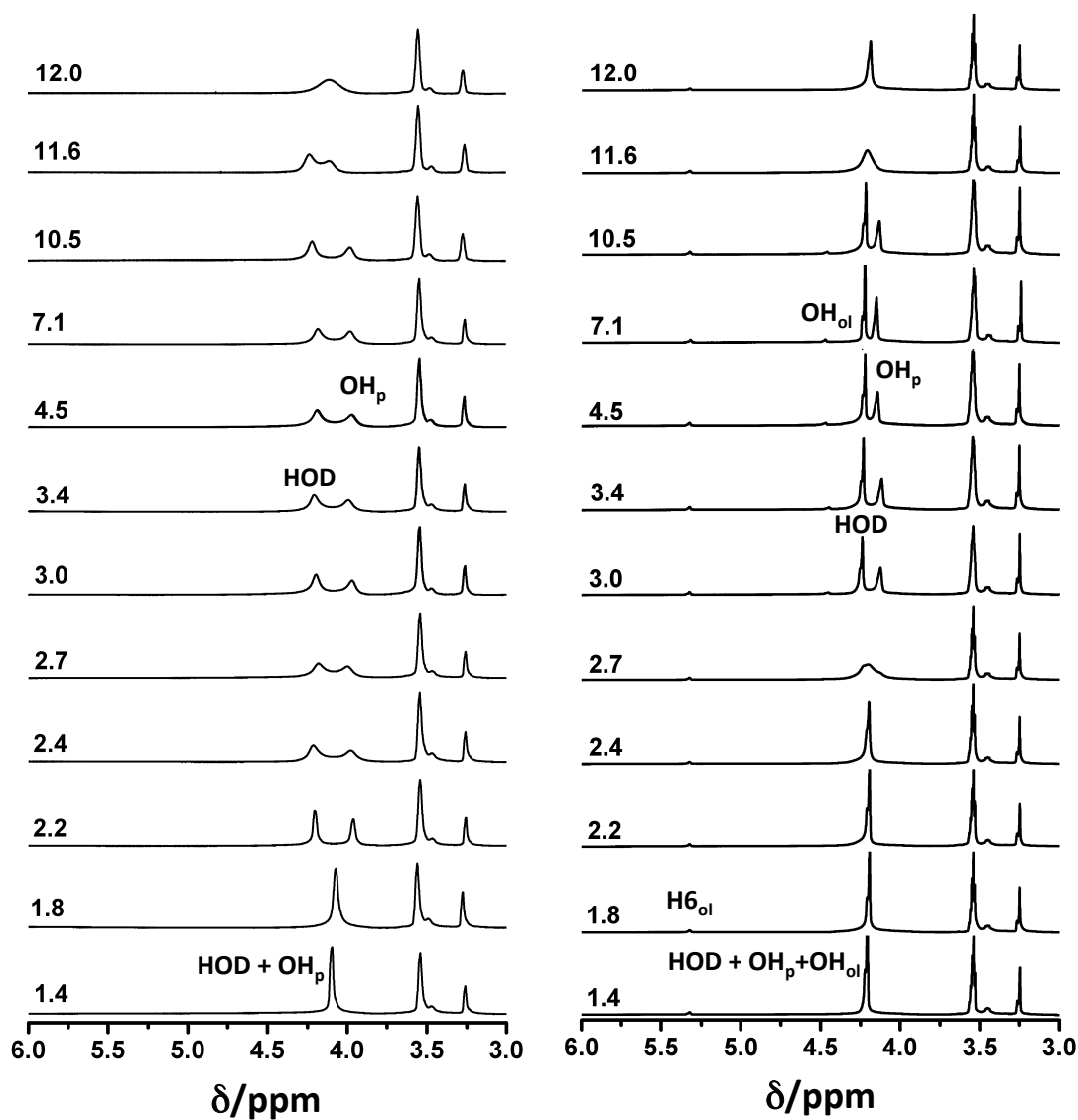


Figure 1.5. (left) A <sup>1</sup>H NMR stacked plot of the chemical shift range of 3 – 6 ppm for RM samples consisting of 60 mM CTAB / cyclohexane / 300 mM 1-pentanol / D<sub>2</sub>O at a  $w_o = 4$ . The series illustrates the pH range from 1.4 to 12. (right) A <sup>1</sup>H NMR stacked plot of RM samples consisting of 60 mM CTAB / cyclohexane / 300 mM 1-pentanol / D<sub>2</sub>O at  $w_o = 4$  with 40 mM cholesterol. The series shows varying pH of the aqueous phase ranging from 1.4 to 12. The samples were referenced internally to the cyclohexane resonance (1.44 ppm).

Table 1.1. Asymmetric two-site exchange rates describing the exchange for protons OH<sub>p</sub> and HOD based on <sup>1</sup>H NMR spectra of varying pH from figure 1.5.

pH range	CTAB RM Cholesterol content	
	0 mM	40 mM
1.4 – 1.8	$3.94 \times 10^7 \text{ s}^{-1}$ (a)	$2.98 \times 10^7 \text{ s}^{-1}$ (a)
1.8 – 2.2	$4.17 \times 10^2 \text{ s}^{-1}$ (b, c)	$2.98 \times 10^7 \text{ s}^{-1}$ (a)
2.2 – 2.7	$4.54 \times 10^2 \text{ s}^{-1}$ (c)	$2.98 \times 10^7 \text{ s}^{-1}$ (a)
2.7 – 3.0	$4.54 \times 10^2 \text{ s}^{-1}$ (c)	$5.50 \times 10^2 \text{ s}^{-1}$ (b)
3.0 – 10.5	$4.54 \times 10^2 \text{ s}^{-1}$ (c)	$9.79 \times 10^2 \text{ s}^{-1}$ (c)
10.5 – 11.6	$4.54 \times 10^2 \text{ s}^{-1}$ (c)	$5.50 \times 10^2 \text{ s}^{-1}$ (b)
11.6 – 12.0	$4.17 \times 10^2 \text{ s}^{-1}$ (b)	$2.98 \times 10^7 \text{ s}^{-1}$ (a)

(a) HOD and OH<sub>p</sub> are one sharp signal

(b) HOD and OH<sub>p</sub> are one broadened signal

(c) HOD and OH<sub>p</sub> are two sharp signals

SUPPLEMENTAL INFORMATION

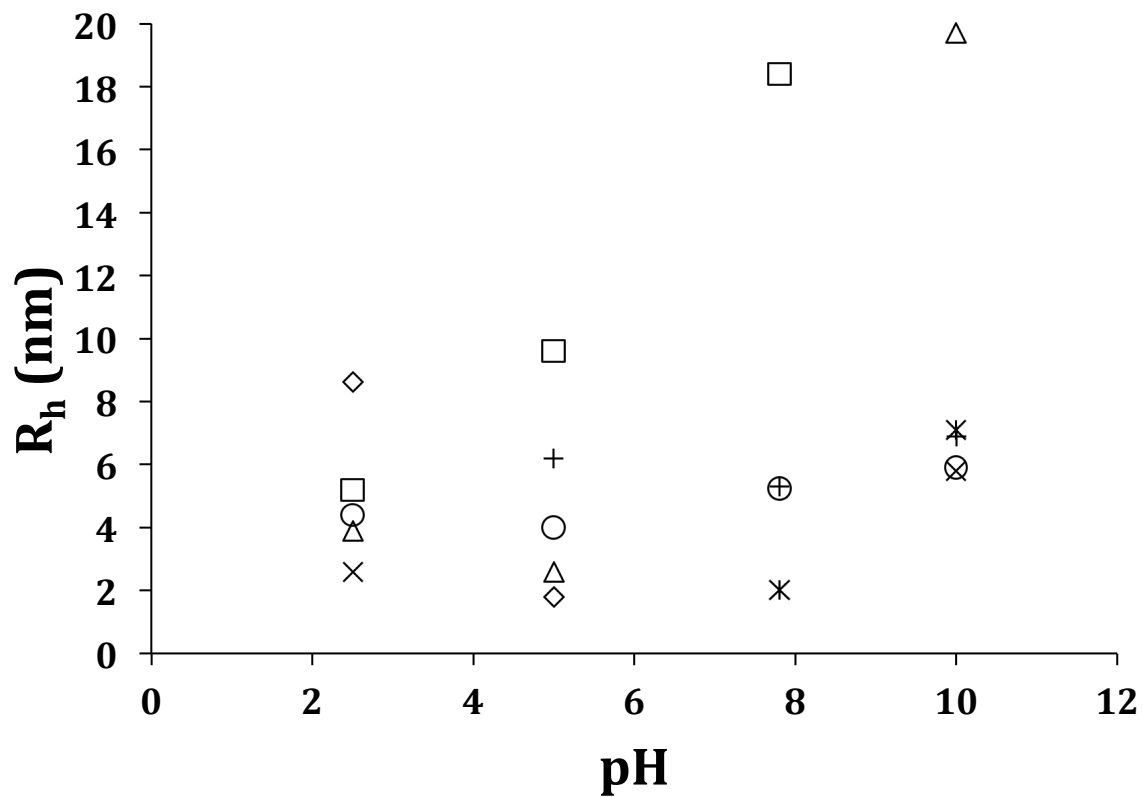


Figure S1.1. A scattered data plot illustrating the hydrodynamic radii  $R_h$  (nm) of RMs composed of 60 mM CTAB / 300 mM 1-pentanol at a  $w_o = 4$  as a function of pH. The different data points indicate the different runs performed on the same samples.

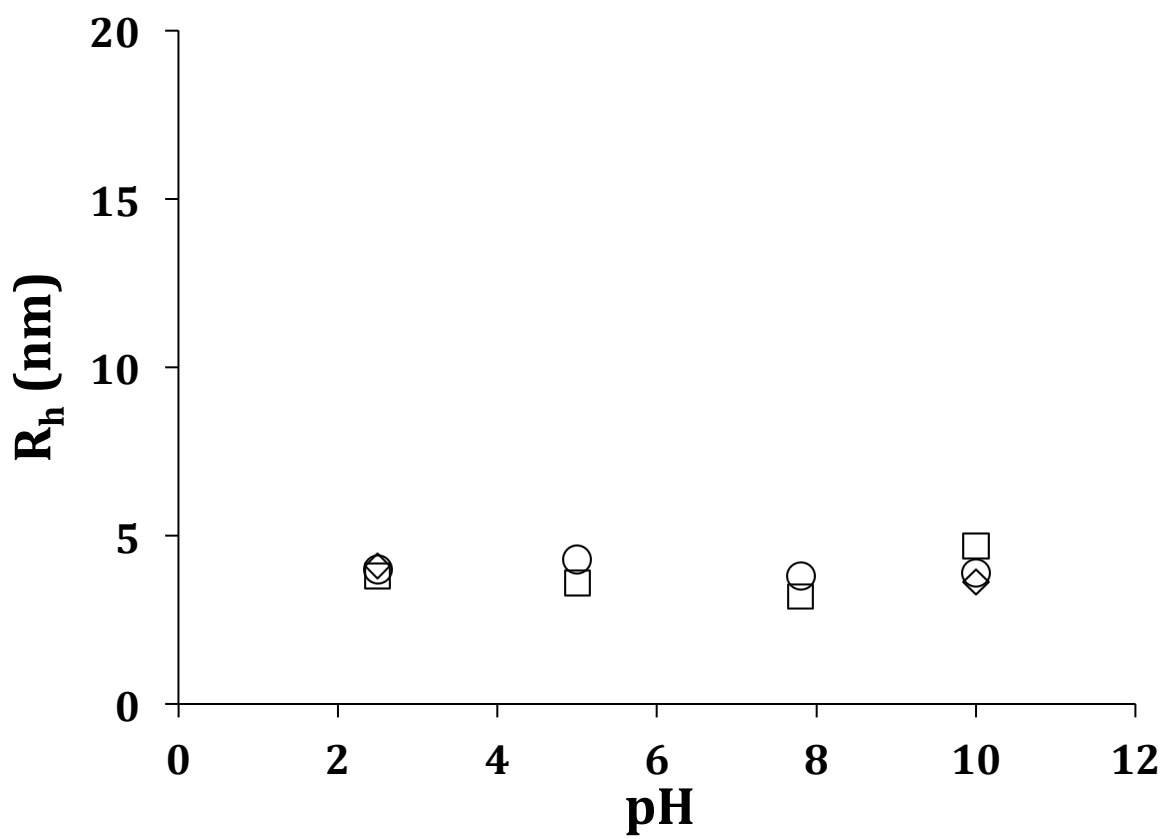


Figure S1.2. A plot of the hydrodynamic radii,  $R_h$  (nm) for RMs composed of 60 mM CTAB / 300 mM 1-pentanol with 40 mM of added cholesterol as a function of pH. The data points represent different runs performed on the same samples.

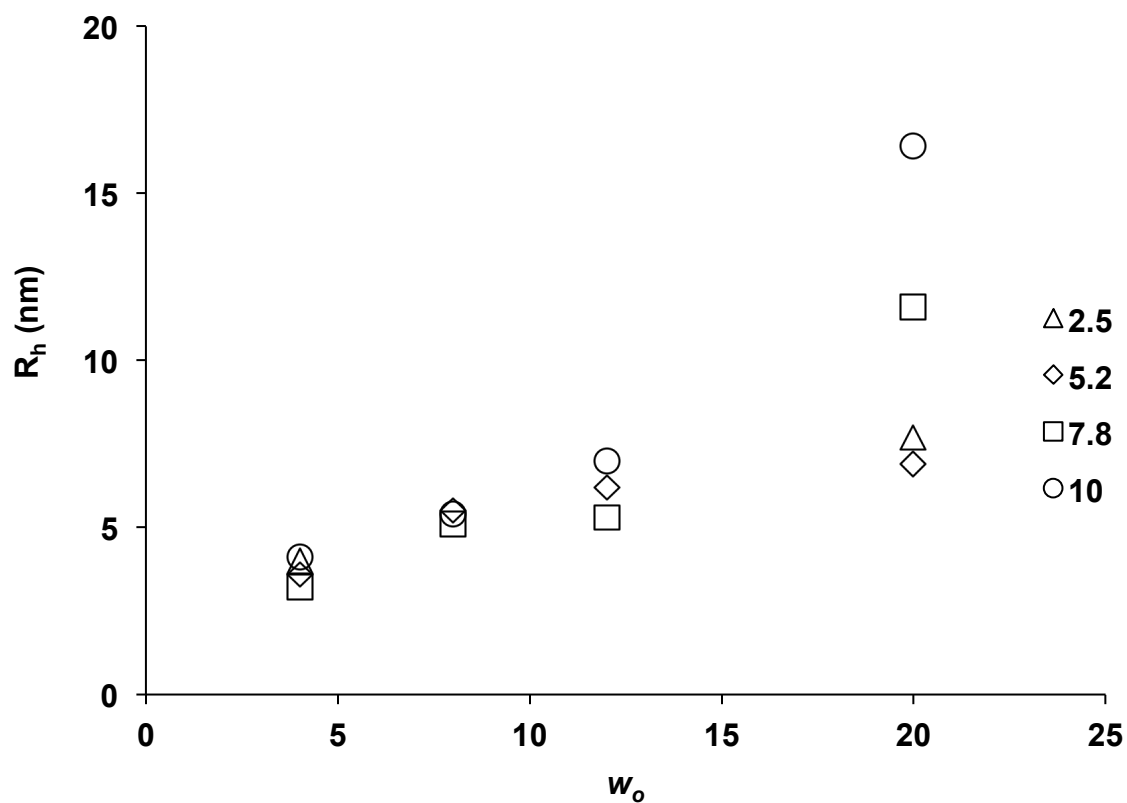


Figure S1.3. Plot representing the RM samples composed of 60 mM CTAB / 300 mM 1-pentanol with 40 mM cholesterol added. The plot illustrates the hydrodynamic radii,  $R_h$  (nm), of the samples as a function of water content ( $w_0$  size). The different data points represent the differing pH values of the aqueous phase for the samples.

## REFERENCES

- (1) Ojemyr, L.; Sanden, T.; J., W.; Brzezinski, P. *Biochemistry* **2009**, *48*, 2173-2179.
- (2) Siegbahn, P. E. M.; Blomberg, M. R. A. *Dalton Transactions* **2009**, 5832-5840.
- (3) Winter, P.; Van Orden, A. K.; Roess, D. A.; Barisas, B. G. *Biochemica et Biophysica Acta* **2012**, *1818*, 467-473.
- (4) Bukiya, A. N.; Belani, J. D.; Rychnovsky, S.; Dopico, A. M. *Journal of General Physiology* **2011**, *137*, 93-110.
- (5) Tai, W. Y.; Yang, Y. C.; Lin, H. J.; Huang, C. P.; Cheng, Y. L.; Chen, M. F.; Yen, H. L.; Liao, I. *Journal of Physical Chemistry B* **2010**, *114*, 15642-15649.
- (6) de Meyer, F. J. M.; Rodgers, J. M.; Willems, T. F.; Smit, B. *Biophysical Journal* **2010**, *99*, 3629-3638.
- (7) Mahammad, S.; Dinic, J.; Alder, J.; Parmryd, I. *Biochemica et Biophysica Acta* **2010**, *1801*, 625-634.
- (8) Groves, J. T.; Boxer, S. G.; McConnell, H. M. *Journal of Physical Chemistry B* **2000**, *104*, 11409-11415.
- (9) Nichols, J. W.; Abercrombie, R. F. *Journal of Membrane Biology* **2010**, *237*, 21-30.
- (10) Pilotelle-Bunner, A.; Beaunier, P.; Tandori, J.; Maroti, P.; Clarke, R. J.; Sebban, P. *Biochemica et Biophysica Acta* **2009**, *1787*, 1039-1049.
- (11) Simons, K.; Sampaio, J. L. *Cold Spring Harbor Perspectives in Biology* **2011**, 1-17.
- (12) Szabo, G. *Nature* **1974**, *252*, 47-49.
- (13) Al-Qatati, A.; Winter, P. W.; Wolf-Ringwall, A. L.; Chatterjee, P. B.; Van Orden, A. K.; Crans, D. C.; Roess, D. A.; Barisas, B. G. *Cell Biochemistry and Biophysics* **2011**.

- (14) Heberle, J. *Biophysical Journal* **2005**, *87*, 2105-2106.
- (15) Mulkidjanian, A. Y.; Heberle, J.; Cherepanov, D. A. *Biochemica et Biophysica Acta* **2006**, *1757*, 913-930.
- (16) Quinn, P. J. *Progress in Lipid Research* **2010**, *49*, 390-406.
- (17) McConnell, H. *Journal of Chemical Physics* **2009**, *130*.
- (18) Huster, D.; Arnold, K.; Gawrisch, K. *Journal of Physical Chemistry B* **1999**, *103*, 243-251.
- (19) Radhakrishnan, A.; McCommell, H. M. *Biochemistry* **2000**, *39*, 8119-8124.
- (20) Radhakrishnan, A.; McConnell, H. M. *The Journal of Chemical Physics* **2007**, *126*, 185101-185101-185111.
- (21) Radhakrishnan, A.; Anderson, T. G.; McConnell, H. M. *Proceedings of the National Academy of Science* **2000**, *97*, 12422-12427.
- (22) Nishimura, S. Y.; Vrljic, M.; Klein, L. O.; McConnell, H. M.; Moerner, W. E. *Biophysical Journal* **2006**, *90*, 927-938.
- (23) Starke-Peterkovic, T.; Turner, N.; Vitha, M. F.; Waller, M. P.; Hibbs, D. E.; Clarke, R. J. *Biophysical Journal* **2006**, *90*, 4060-4070.
- (24) Warschawski, D. E.; Arnold, A. A.; Beaugrand, M.; Gracel, A.; Chartrand, E.; Marcotte, I. *Biochemica et Biophysica Acta* **2011**, *1808*, 1957-1974.
- (25) Babayco, C. B.; Turgut, S.; Smith, A. M.; Sanii, B.; Land, D.; Parikh, A. N. *Soft Matter* **2010**, *6*, 5877-5881.
- (26) Quinn, P. J.; Wolf, C. *Febs Journal* **2010**, *277*, 4685-4698.
- (27) Roberts, M. F.; Redfield, A. G.; Mohanty, U. *Biophysical Journal* **2009**, *97*, 132-141.
- (28) Villalain, J. *European Journal of Biochemistry* **1996**, *241*, 586-593.

- (29) Segwick, M. A.; Trujillo, A. M.; Hendricks, N.; Levinger, N. E.; Crans, D. C. *Langmuir* **2010**, *27*, 948-954.
- (30) Johnson, M. D.; Lorenz, B. B.; Wilkins, P. C.; Lemons, B. G.; Baruah, B.; Lamborn, N.; Stahla, M.; Chatterjee, P. B.; Richens, D. T.; Crans, D. C. *Inorganic Chemistry* **2012**, *51*, 2757-2765.
- (31) Molina, P. G.; Silber, J. J.; Correa, N. M.; Sereno, L. *Journal of Physical Chemistry C* **2007**, *111*, 4269-4276.
- (32) Crans, D. C.; Levinger, N. E. *Accounts of Chemical Research* **2012**, *45*, 1637-1645.
- (33) Lemons, B. G.; Richens, D. T.; Anderson, A.; Sedgwick, M.; Crans, D. C.; Johnson, M. *D. New Journal of Chemistry* **2013**, *37*, 75-81.
- (34) Sostarecz, A. G.; McQuaw, C. M.; Ewing, A. G.; Winograd, N. *Journal of the American Chemical Society* **2004**, *126*, 13882-13883.
- (35) El-Sayed, M. Y.; Guion, T. A.; Fayer, M. D. *Biochemistry* **1986**, *25*, 4825-4832.
- (36) Gutierrez, J. A.; Falcone, R. D.; Silber, J. J.; Correa, N. M. *Dyes and Pigments* **2012**, *95*, 290-295.
- (37) Gaidamauskas, E.; Cleaver, D. P.; Chatterjee, P. B.; Crans, D. C. *Langmuir* **2010**, *26*, 13152-13161.
- (38) Baruah, B.; Roden, J. M.; Sedgwick, M.; Correa, N. M.; Crans, D. C.; Levinger, N. E. *Journal of the American Chemical Society* **2006**, *128*, 12758-12765.
- (39) Yoshikawa, S.; Muramoto, K.; Shinazawa-Itoh, K. *Annual Review of Biophysics* **2011**, *40*.
- (40) Ojemyr, L. N.; Von Ballmoos, C.; Faxen, K.; Svahn, E. *Biochemistry* **2012**, *51*, 1092-1100.

- (41) Wraight, C. A. *Biochemica et Biophysica Acta* **2006**, *1757*, 866-912.
- (42) Yamashita, T.; Voth, G. A. *Journal of Physical Chemistry B* **2010**, *114*, 592-603.
- (43) Piletic, I. R.; Moilanen, D. E.; Spry, D. B.; Levinger, N. E.; Fayer, M. D. *Journal of Physical Chemistry A* **2006**, *110*, 4985-4999.
- (44) Cai, K.; Kiefer, G. E.; Caruthers, S. D.; Wickline, S. A.; Lanza, G. M.; Winter, P. W. *NMR in Biomedicine* **2012**, *25*, 279-285.
- (45) Alberts, B.; Johnson, A.; Lewis, J.; M., R.; Roberts, K.; Walter, P. *Molecular Biology of The Cell*; Garland Science, Taylor & Francis Group LLC.: New York, 2008.
- (46) Kaiser, H. J.; Lingwood, D.; Levental, I.; Sampaio, J. L.; Kalvodoca, L.; Rejendran, L.; Simons, K. *Proceedings of the National Academy of Sciences* **2009**, *106*, 16645-16650.
- (47) Tai, W.; Yang, Y.; Lin, H.; Huang, C.; Cheng, Y.; Chen, M.; Yen, H.; Liau, I. *Journal of Physical Chemistry B* **2010**, *114*, 15642-15649.
- (48) Ivankin, A.; Kuzmenko, I.; Gidalevitz, D. *Physical Review Letters* **2012**, *108*, 238103 (238101-238105).
- (49) McConnell, H. M. *ACS Chemical Biology* **2008**, *3*, 265-267.
- (50) Roess, D. A.; Smith, S. M. L.; Winter, P.; Zhou, J.; Dou, P.; Baruah, B.; Trujillo, A. M.; Levinger, N. E.; Yang, X.; Barisas, B. G.; Crans, D. C. *Chemistry & Biodiversity* **2008**, *5*, 1558-1569.
- (51) Bukiya, A. N.; Belani, J. D.; Rychnovsky, S.; Dopico, A. M. *The Journal of General Physiology* **2011**, *137*.
- (52) Okamura, M. Y.; Paddock, M. L.; Graige, M. S.; Feher, G. *Biochemica et Biophysica Acta* **2000**, *1458*, 148-163.

- (53) Crans, D. C.; Baruah, B.; Ross, A.; Levinger, N. E. *Coordination Chemistry Reviews* **2009**, *253*, 2178-2185.
- (54) Halliday, N. A.; Peet, A. C.; Britton, M. M. *Journal of Physical Chemistry B* **2010**, *114*, 13745-13751.
- (55) Samara, N.; Borah, J. M.; Mahiuddin, S. *Journal of Physical Chemistry B* **2001**, *115*, 9040-9049.
- (56) Yang, L. K.; Zhao, K. S. *Langmuir* **2007**, *23*, 8732-8739.
- (57) Liu, A. H.; Mao, S. Z.; Liu, M. L.; Du, Y. R. *Colloid and Polymer Science* **2008**, *286*, 1629-1636.
- (58) Rimal, V.; Stepankova, H.; Stepanek, J. *Concepts in Magnetic Resonance Part A* **2011**, *38A*, 117-127.
- (59) Klicova, L.; Sebej, P.; Stacko, P.; Filippov, S., K.; Bogomolova, A.; Padilla, M.; Klan, P. *Langmuir* **2012**, *28*, 15185 - 15192.
- (60) Giustini, M.; Palazzo, G.; Colafemmina, G.; Della Monica, M.; Giomini, M.; Ceglie, A. *Journal of Physical Chemistry* **1996**, *100*, 3190-3198.
- (61) Law, S. J.; Britton, M. M. *Langmuir* **2012**, *28*, 11699-11706.
- (62) Corbeil, E. M.; Levinger, N. E. *Langmuir* **2003**, *19*, 7264-7270.
- (63) Stahla, M. L.; Baruah, B.; James, D. M.; Johnson, M. D.; Levinger, N. E.; Crans, D. C. *Langmuir* **2008**, *24*, 6027-6035.
- (64) Einstein, A. *Annalen der Physik* **1905**, *17*, 549-560.
- (65) McConnell, H. M. *Journal of Physical Chemistry* **1958**, *28*, 430-431.
- (66) Bain, A. D. *Progress in Nuclear Resonance Spectroscopy* **2003**, *43*, 63-103.

- (67) Bolean, M.; Simao, A. M. S.; Favarin, B. Z.; Millan, J. L.; Ciancaglini, P. *Biophysical Chemistry* **2010**, *152*, 74-79.
- (68) Zundel, G. *Advances in Chemical Physics* **2000**, *111*, 1-217.
- (69) Rousseau, R.; Kleinschmidt, V.; Schmitt, U. W.; Marx, D. *Angewandte Chemie-International Edition* **2004**, *43*, 4804-4807.
- (70) Giordani, C.; Wakai, C.; Okamura, E.; Matubayasi, N.; Nakahara, M. *Journal of Physical Chemistry B* **2006**, *110*, 15205-15211.
- (71) Bloembergen, N.; Purcell, E. M.; Pound, R. V. *Physical Review* **1948**, *73*, 679-712.
- (72) Aramini, J. M.; Vogel, H. J. *Journal of Magnetic Resonance, Series B* **1996**, *110*, 182-187.
- (73) Holt, P. R.; Tamami, B. *Polymer* **1973**, *14*, 645-648.
- (74) Bogardus, J. B. *Journal of Pharmaceutical Sciences* **1984**, *73*, 906-910.
- (75) Bicknese, S.; Periasamy, N.; Shohet, S. B.; Verkman, S. A. *Biophysical Journal* **1993**, *65*, 1272-1282.

## CHAPTER 2: <sup>2</sup>Penetration of Negatively Charged Lipid Interfaces by the Doubly Deprotonated Dipicolinate

### SUMMARY

The possibility that a negatively charged organic molecule penetrates the lipid interface in a reverse micellar system is examined using UV-vis absorption and NMR spectroscopy. The hypothesis that deprotonated forms of dipicolinic acid, H<sub>2</sub>dipic, such as Hdipic<sup>-</sup> and dipic<sup>2-</sup>, can penetrate the lipid interface in a microemulsion is based on our previous finding that the insulin-enhancing anionic [VO<sub>2</sub>dipic]<sup>-</sup> complex was found to reside in the hydrophobic layer of the reverse micelle (Crans et al. *J. Am. Chem. Soc.* 2006, 128, 4437-4445). Penetration of a polar and charged compound, namely Hdipic or dipic<sup>2-</sup>, into a hydrophobic environment is perhaps unexpected given the established rules regarding the fundamental properties of compound solubility. As such, this work has broad implications in organic chemistry and other disciplines of science. These studies required a comprehensive investigation of the different dipic species and their association in aqueous solutions at varying pH values. Combining the aqueous studies using absorption and NMR spectroscopy with those in microemulsions defines the differences observed in the heterogeneous environment. Despite the expected repulsion between the surfactant head groups and the dianionic probe molecule, these studies demonstrate that dipic resides deep in the hydrophobic portion of the reverse micellar interface. In summary, these results provide evidence that ionic molecules can reside in nonpolar locations in microheterogeneous environments. This suggests that additional factors such as solvation are

---

<sup>2</sup> By: Debbie C. Crans\*, Alejandro M. Trujillo Sandra Bonetti, Christopher D. Rithner, Bharat Baruah and Nancy E. Levinger

Alejandro M. Trujillo performed all NMR experiments except figure 2.8  
*Manuscript published in: The Journal of Organic Chemistry, 2008, 73 (24) 9633-9640.*

important to molecule location. Documented ability to penetrate lipid surfaces of similar charge provides a rationale for why specific drugs with less than optimal hydrophobicity are successful even though they violate Lipinski's rules.

## *INTRODUCTION*

The nature of organic compounds defines their properties and reactions. For example, the rules of solubility, ergo that "like dissolves like", are taught to beginning chemistry students to explain why reactions such as those involving 2-oxazolines<sup>1</sup> take place in organic solvents. Solvents dictate how molecules react<sup>1-4</sup> and can be used to establish a chiral environment<sup>5</sup> such as exemplified in the work by the late Albert I. Meyers detailing approaches in enantiomeric synthesis. Solubility is also a critical consideration in the design of compounds targeted for use in alleviation of diseases. Ideally, potential drugs adhere to the few rules defined by Lipinski which state that cell penetration is optimal when compounds possess a low molecular weight, a small number of H-bonds as both an acceptor and donor, a reasonable partition coefficient in hydrophobic solvents, and overall neutral charge.<sup>6</sup> Many drugs currently on the market are known to violate these simple rules and, regardless of these tenets, penetrate membranes and enter cells with relative ease. We became interested in penetration of lipid interfaces because one of the vanadium compounds that we had demonstrated to be an effective antidiabetic agent, the negatively charged oxovanadium dipicolinate [ $\text{VO}_2\text{dipic}$ ]<sup>-</sup>, is found to reside deep into the interface of microemulsions.<sup>7</sup> Since related systems are currently in phase II clinical trials,<sup>8,9</sup> fundamental information regarding related systems is important. In this work, we investigate the solubility of an aromatic carboxylic acid, dipicolinic acid (dipic). These studies relate to how the ligand of the [ $\text{VO}_2\text{dipic}$ ]<sup>-</sup> complex interacts with lipid interfaces, and we will specifically

investigate whether the dipic ligand, a doubly charged dianion at pH 7, can penetrate model lipid interfaces as recently suggested in the controversy regarding the ability of aromatic acids to partition in hydrophobic environments.<sup>10-12</sup> To test this hypothesis, the behavior of this ligand in aqueous solution is contrasted to its properties in the heterogeneous environment of the reverse micelles.

H<sub>2</sub>dipic is a polar aromatic acid that in the acidic form is soluble in organic and chlorinated solvents and thus can penetrate lipid interfaces<sup>10-14</sup> and be solubilized in hydrophobic environments.<sup>15</sup> In the mono- and dianionic form, the dipic is soluble in aqueous solution at a pH above the two pK<sub>a</sub> values 2.22 and 5.22, as shown in Scheme 2.1.<sup>16</sup> Depending on the pH, dipic assumes various forms. From left to right, we show the cationic dipic ligand, found only in highly acidic conditions at or below pK<sub>a</sub> -1.05,<sup>16</sup> the neutral H<sub>2</sub>dipic ligand that prevails near pH 4, then the monoprotonated form prevalent at pH 5.5, and finally, the fully deprotonated form at pH 7 and above. These forms and their properties are likely key to the transport of this and other simple acids and fatty acids that are known to cross cell membranes.

A range of methods has been employed to examine the structure of dipic in aqueous solutions.<sup>16-20</sup> UV-vis studies suggested that dipicolinates associate very strongly in aqueous solution from pH 3 to 5.<sup>16,17</sup> Both dimeric and polymeric forms are likely to exist, although there is some disagreement in the literature on which form predominates under specific conditions.<sup>16-20</sup> Associative processes of dipic<sup>16,17,21-23</sup> are favorable when fewer water molecules are present, contribute to the penetration of the dipic molecule in lipid interfaces, and can be observed by UV-vis spectroscopy.<sup>16-18,23-27</sup>

Biphasic systems and microemulsions are heterogeneous systems used to solubilize compounds and facilitate reactions that would not easily take place in conventional

homogeneous systems.<sup>28</sup> In microemulsions, multiple regimes exist with different polarities, and details of the interactions of the lipid layer constituents with water and the organic solvent can be investigated.<sup>24</sup> A common surfactant sodium bis(2-ethylhexyl) sulfosuccinate, abbreviated AOT, Figure 2.1, organizes into reverse micelles, that is, isolated aqueous droplets delineated from a continuous organic phase by a lipid interface. The reverse micelles illustrated in Figure 2.1b are described by a  $w_0 = [\text{H}_2\text{O}] / [\text{AOT}]$  that is proportional to their size.<sup>29-31</sup> The simplicity of these structures and their convenient preparation<sup>30,32</sup> makes them a desirable system for experimentation.

In this paper, we investigate the interactions between dipic ligand and AOT microemulsions. In this work, we characterize dipic both in aqueous solution and in microemulsions using UV-vis and <sup>1</sup>H NMR spectroscopy. Through <sup>1</sup>H NMR studies, including 1D and 2D NOESY experiments, we directly characterize the interactions between the dipic ligand and AOT molecules in microemulsions. These studies provide data clarifying the structure of dipic isomers in aqueous solution. Importantly, our observations were consistent with the dianionic form of dipic penetrating and residing deep in the AOT lipid interface. These studies confirm previous reports<sup>10-12</sup> that simple aromatic acids are capable of penetrating and existing in hydrophobic environments. This work thus has important consequences for organic reactions and drug penetration.

## *MATERIALS AND METHODS*

### *Materials.*

2,6-Pyridinedicarboxylic acid (H<sub>2</sub>dipic, 99.5% purity) and AOT (sodium bis(2-ethylhexyl)sulfosuccinate, 98% purity) were purchased from a commercial supplier. The AOT

was purified as described previously,<sup>30</sup> which includes dissolution of the surfactant in methanol and charcoal, filtration and rotary evaporation until flaky, followed by <sup>1</sup>H NMR analysis to check purity. Purified AOT was used for all the reverse micelle investigations and is hereafter referred to as highly purified or HP AOT. Deuterium oxide (D<sub>2</sub>O), 2,2,4-trimethylpentane (isooctane), and deuterated 2,2,4-trimethylpentane (isooctane-*d*<sub>18</sub>) were also purchased from a commercial supplier and were used as received. Manipulation of aqueous solution pH for NMR samples was performed using dilutions of 35% deuterium chloride in D<sub>2</sub>O (99% deuterium) and 30% sodium deuterioxide in D<sub>2</sub>O (99% deuterium). Fine-tuning of solution pH for UV-vis analyses used aqueous HCl and/or NaOH before adjusting to the desired final volume.

#### *Preparation of Reverse Micelles (RMs).*

RMs or microemulsions were prepared as described previously.<sup>30</sup> The 200 and 750 mM stock solutions of HP AOT were prepared by dissolving the surfactant in isooctane. Stock solutions of dipic were prepared by dissolution in water, and pH was adjusted to the desired value. A range of RMs was prepared with  $w_0$  ranging from 6 to 20. Upon mixing these solutions as prescribed, a cloudy solution resulted that cleared after vigorous vortexing. Verification of RM formation was performed using several methods including conductivity measurements<sup>24</sup> (Thermo Orion 150A+ meter with an attached Orion 0111020 cell, range of 10  $\mu$ s/cm to 200 ms/cm) and viscosity<sup>24</sup> (Cannon-Fenske routine viscometer). These measurements allowed comparison with previous samples of RMs prepared with water to confirm that micelle structure is not appreciably altered by addition of dipic.<sup>30-32</sup>

#### *UV-vis Spectroscopy.*

Samples for UV-vis spectroscopy were prepared from 200 mM HP AOT stock solution in isooctane at  $w_0$  sizes ranging from 6 to 20 and containing 0.10-0.16 mM dipic in H<sub>2</sub>O at the

desired pH values. Aqueous dipic stock solutions were prepared in volumetric flasks where pH, and then volumes were adjusted to the desired values. The RMs were prepared just prior to measurements; however, no changes were observed in the samples over the course of 24 h.

UV-vis spectroscopic measurements were carried out using a Perkin-Elmer Lambda 25 UV-vis spectrometer and UV Winlab software. Data was processed using OriginPro (version 7E, Origin Laboratories). Samples were contained in quartz cells with a 1 cm path length. Concentrations of dipic in the samples were generally from 1.5 to 1.0 mM and were adjusted so that the absorbances were less than 1.5 at  $\lambda = 271$  nm. Spectra were routinely recorded from 200 to 600 nm. Spectra of all samples were collected in duplicate unless deviations were observed, in which case additional scans were obtained.

#### *<sup>1</sup>H NMR Spectroscopy.*

RM samples for NMR spectroscopy were prepared from 750 mM HP AOT stock solutions in isooctane, and 5-25 mM dipic in D<sub>2</sub>O at the desired pH values were prepared. The dipic stock solutions were adjusted near the desired pH using DCl and NaOD before the final dilutions were made. The mixtures of AOT in isooctane microemulsion (1 mL volume) were vortexed in sample vials where they were stored before and after <sup>1</sup>H NMR spectra were recorded.

<sup>1</sup>H NMR spectra were recorded on a Varian 400 MHz NMR spectrometer or a Varian Inova-500 MHz spectrometer using the Varian supplied pulse sequence. The 1D spectra were recorded using routine parameters as described previously,<sup>33</sup> and the chemical shift was referenced against an external sample of 3-(trimethylsilyl)propanesulfonic acid (DSS).

<sup>1</sup>H-<sup>1</sup>H NOESY NMR experiments were performed on a 400 or 500 MHz Varian Inova NMR spectrometer. The NOESY data were acquired with a 7 kHz window for proton in  $t_2$  and  $t_1$ . The NOESY mixing time was varied from 0 to 500 ms. The total recycle time between transients

was 2.1 s. The data set consisted of 1000 complex points in  $t_2$  by 256 complex points in  $t_1$  using States-TPPI. Cosine-squared weighting functions were matched to the time domain in both  $t_1$  and  $t_2$ , and the time domains were zero-filled prior to the Fourier transform. The final resolution was 3.5 Hz/pt in  $F_2$  and 15 Hz/pt in  $F_1$ . Data processing was done using the Varian VNMRJ-1.1D software, both the Solaris and the Macintosh versions.

## RESULTS AND DISCUSSION

### *UV-vis Spectroscopy of Dipic in Aqueous Solution at Varying pH Values.*

Figure 2.2 shows the UV-vis spectra of a 0.10 mM aqueous dipic solution adjusted from pH 0.9 to 10.1. Since the concentration of dipic is maintained constant, the spectra illustrate the differences in spectrum shape and extinction coefficients,  $\epsilon$ , of dipic as the pH is varied and protonation states and association states changes. A hypsochromic shift in the UV-vis spectra of aqueous solutions of 0.10 mM dipic with pH varying from 0.9 to below 3.3 has previously been attributed to dipic dimerization and was confirmed in Figure 2.2.<sup>16</sup> Similar results were obtained with nicotinic acid.<sup>24,34,35</sup> Stacking of related pyridine-based systems has been studied in detail and has been observed in dipic and other heteroaromatic rings such as the nucleotide bases in RNA and DNA.<sup>26</sup> At pH values from 1.0 to 2.2 ( $pK_{a2}$ ), monobasic dipic exists as primarily the zwitterion 2 or the neutral species 5.<sup>16</sup> Between pH 2.2 and 3.3, dipic loses a second proton and may exist as the minus one dipic species 3 or 6.

The hyperchromic shift observed at pH 3.3 provides clear evidence that dipic exists in the colinear dimeric form shown in structure 7.<sup>16</sup> Dimerization of the dipic monoanion at pH 3.3-3.5 is supported by the large association constants,  $K_a = 2 \pm 1 \times 10^6$ , reported at this pH.<sup>16</sup> Our UV-vis results are in agreement with these results and conclusions.

From pH 4.3 to 6.2,  $\epsilon$  continues to decrease indicating conversion of the dipic dimer to the fully deprotonated dipic 4, in agreement with the results reported by Peral and co-workers, who concluded that dipic is undergoing base-stacking interactions in this pH range.<sup>16,23,24,26,36</sup> Polymerization is discounted because no secondary hypochromic effect is observed<sup>23,24</sup> in contrast to that reported for the monocarboxylic picolinic acid (pic). Indeed, pic exists as a monocation below pH 3, as the zwitterion from pH 3 to 7 and as a monoanion above pH 7 and at pHs approaching their isoelectric points, pic and other pyridinecarboxylic acids exist primarily as zwitterions with very low solubility.<sup>24</sup> For several pyridine-related systems, such as dipics,<sup>16-18</sup> the monocarboxylic pyridines picolinic, nicotinic and isonicotinic acids,<sup>24,34,35</sup> and pyridine,<sup>25,37</sup> the aqueous species have been characterized. While UV-vis spectroscopy provides a very sensitive tool for detection of changes in dipic speciation and association, the nature of dipic species are under some debate<sup>16,18,34</sup> and made further characterization of dipic especially compelling. Additional structural information obtained by high-field <sup>1</sup>H NMR studies allowed us to distinguish between similarly charged dipic isomeric species and to clarify existing questions regarding dipic structures in both aqueous solutions and reverse micelles.

#### *<sup>1</sup>H NMR Spectroscopy of Dipic at Varying pH Values in Aqueous Solutions.*

The <sup>1</sup>H NMR spectra of aqueous dipic solutions (at 20 or 25 mM depending on solubility) shown in Figure 2.3 demonstrate the effect that pH and the varying species has on the chemical shift of the pyridinyl methine proton signals. The observed chemical shift changes are the result of dynamic equilibria between major isomers of a particular charge and protonation state and the association equilibria that occur at a specific pH. In the interpretation of our data we refer to dipic structures 1-4 found in Scheme 2.1, structures 5-8 shown in Scheme 2.2, and structure 9 in Figure 2.3, which shows the designations H<sub>a</sub>, H<sub>b</sub>, and H<sub>c</sub> for the pyridinyl ring protons. In the

interpretation presented here, first the data is interpreted assuming that proton transfer and associative processes are slow and observable on the NMR time scale. However, an asymmetric isomer if undergoing a rapid equilibrium with an opposing asymmetric species will appear symmetric and must be considered.

In Figure 2.4 we have plotted the chemical shifts of  $H_a$  and  $H_b$  in aqueous solutions as a function of pH. Because the fully protonated, triprotic dipic species 1 has a  $pK_a$  of -1.05,<sup>16</sup> these NMR studies were performed outside of the pH region for this species. In 1D NMR studies of aqueous dipic solutions with pH values from 0.9 to 1.6 we observed an  $A_2X$  splitting pattern<sup>38</sup> containing signals for  $H_b$  near  $\delta$  8.2 ppm and upfield of the  $H_a$  protons near  $\delta$  8.3 ppm. The pattern is consistent with the symmetrical structure of the neutral dipic, 5, which contains a deprotonated pyridine nitrogen. The designations for  $H_a$ ,  $H_b$ , and potentially  $H_c$ , when the isomer is asymmetric, are shown in structure 9 in Figure 2.3 and will vary depending on the protonation and association state of the species. The asymmetrical neutral dipic structure, 2, containing one protonated carboxyl and a protonated ring nitrogen, contains three different protons  $H_a$ ,  $H_b$ , and  $H_c$  and is not consistent with the NMR data observed without invoking dynamic processes. However, a rapid interconversion on the NMR time scale between 2 and 2' shown in Scheme 2.3 is consistent with the observed  $^1H$  NMR spectra.

As the pH increases above 1.9, the  $H_b$  proton signals shift downfield and the first-order spectrum converts into a second order spectrum with a complex multiplet centered at 8.4 ppm that encompasses the signals for all of the methine protons on the ring. As the pH increases, the downfield shifts in the  $A_2X$  pattern resonances indicate that the dipic species is changing from the neutral structure into a minus one species. This conversion to a minus one charged dipic species is consistent with the second reported  $pK_a$  for dipic being 2.22. At pH 2.6, the  $A_2X$

splitting pattern changes when the  $H_b$  signals move further downfield than the  $H_a$  signals, Figure 2.4. At pH 3.20 when the  $H_b$  proton is near 8.65 ppm, the species in solution giving rise to the  $A_2X$  system splitting pattern are best described by a symmetric monoanionic structure such as 3. The asymmetric structure 6 or dimeric structure 7 are not consistent with the NMR data without invoking dynamic processes equilibrating two unsymmetrical species.

At pH values above 5.73, the doublet and triplet merge to form a complex multiplet that encompasses the methine protons in the  $A_2B$  system beginning around 7.9 ppm. At pH values above 7.50 the multiplet is centered at  $\delta$  8.0 ppm. This multiplet is ascribed to the completely deprotonated dipic species, structure 4. As pH increases from 5.7 to 7.0, the multiplet simplifies to a broad singlet at pH 7.0 and above. From pH 6.1 to 6.9 a slight downfield shift is observed. However, above pH 7.0 no further chemical shift and signal pattern changes are observed in Figures 2.3 and 2.4.

Our  $^1H$  NMR studies confirm the changes observed in the absorption spectra of dipic, and provide specific information regarding the structure of the dipic species in solution. Over the entire pH range, the NMR spectra show the presence of an  $A_2X$  or  $A_2B$  spin system consistent with a symmetric structure or proton symmetry achieved through a rapid equilibration of two asymmetric species. Although the NMR splitting pattern changes dramatically, the spin system remains the same while the chemical shifts of  $H_a$  and  $H_b$  change.<sup>38</sup> As the pH increases, the chemical shifts of the  $H_a$  and  $H_b$  protons merge and then separate. In the pH range from 2.6 to 4.8 the chemical shift of  $H_b$  is further downfield than the  $H_a$  in an  $A_2X$  spin system. This pH coincides with the large hyperchromic effect in the UV-vis spectra in Figure 2.2 and the formation of dimeric species.<sup>16</sup> The dimer structure has an increased electron density at the pyridine N. Hydrogen bonding moves both the  $H_a$  and  $H_b$  chemical shifts downfield. Since the

dimer structure, 7, is asymmetric, it must undergo equilibration on the time scale of the NMR experiment.

In the literature, the structure for Hdipic<sup>-</sup> is generally attributed to the zwitterion shown as structure 2 above. Since this zwitterion is not symmetrical, our results will require that rapid proton transfer reactions convert structure 2 to 2' as shown in Scheme 2.3 where H<sub>a</sub> and H<sub>c</sub> become equivalent as a result of the equilibrium.

The NMR data are consistent with both the zwitterionic structure 2 and the diprotonated dicarboxylpyridine shown in structure 5. The NMR spectra at high pH values above the third pK<sub>a</sub> of dipic reflect the formation of dianionic dipic, 4. This dianion is symmetrical and, therefore, is consistent with the observed A<sub>2</sub>B spin system. The UV-vis spectra in Figure 2.2 are also consistent with progressive disappearance of the dimer 7 and formation of dianion 4 because the extinction coefficient decreases from the maximum observed at pH 3.2 (3.5 in literature) as pH decreases.<sup>5</sup> At pH's above 6.9, little or no change is seen in both NMR and absorbance spectra indicating that the dianionic species 4 predominates.

In summary, the dipic species observed by NMR studies in aqueous solutions are represented in the Scheme 2.4 shown below. Although the existence of other monomeric and dimeric species cannot be disregarded, on the basis of our NMR and UV-vis results combined with those reported previously,<sup>17,23,26,27</sup> the species shown in Scheme 2.4 best explain all the available data.

#### *UV-vis Spectroscopy of Dipic at Varying pH Values in Microemulsions.*

We have also measured UV-vis absorption spectra of dipic in RMs. For these studies, aqueous dipic stock solutions similar to those shown in Figure 2.2 were prepared, albeit at a slightly higher concentration because these solutions were to be added to the microemulsions

(0.158 mM overall concentration in microemulsion). The spectra recorded, shown in Figure 2.5, differ from those obtained in aqueous solution, Figure 2.2. Here, we observe an increase in the extinction coefficients at pH 2.6, a lower value compared to the pH of 3.3 observed in the spectra of aqueous dipic. Furthermore, in the RM suspensions the spectra appear the same for all the samples at pH 4 and above. Several key differences exist between the spectra shown in Figures 2.2 and 2.5. First, in the RMs spectral variations occur over a much narrower pH range than in aqueous solutions. Second, the spectra of dipic in the RMs show three distinct maxima  $\lambda = 265$ , 271, and  $278 \pm 2$  nm which are only observed in aqueous solution at very low pH values ( $<1.1$ ) or at pH's equal to 6.27 and above. Third, the high baseline in the spectrum of the dipic sample at pH 0.8 in RMs indicates that nonhomogeneous RM preparations may form at very acidic pH. The extinction coefficients of sodium dipic (Figure 2.5) in microemulsions are smaller than those observed in aqueous solution (Figure 2.2).

A separate investigation in microemulsions examined the effect of RM size and, therefore, water pool size on the UV-vis absorption by dipic. The absorption spectra were recorded at different  $w_o$  values (6, 12, 16, and 20) for RMs containing 0.10 mM aqueous dipic at pH 2.6 and 3.3. As shown in Figure 2.6, at each pH value only small changes in the extinction coefficient were observed for RM sizes 12-20. At both pH values, however, we observed a change in the ratio of the peaks as the RM size decreases to  $w_o = 6$ . All spectra of dipic in RMs of any size display a hypochromic (also referred to as hypsochromic) shift compared to the spectra in aqueous solutions. Furthermore, the spectrum of dipic in the RMs shows a slightly larger extinction coefficient at pH 2.6 than at pH 3.5.

$^1\text{H}$  NMR spectra of dipic in 750 mM AOT/isooctane microemulsions were recorded for a series of solutions with pH values ranging from 0.9 to 12.3. The spectra are shown in Figure 2.7.

From pH 0.9 to 1.5, the  $A_2X$  splitting pattern was observed with the  $H_a$  doublet around 8.4 ppm and the  $H_b$  triplet near 8.0 ppm. At pH's from 1.9 to 4.8 a complex splitting pattern was observed until pH 6.9 and higher where a lone singlet at 8.1 ppm was observed. Studies were carried out by NMR spectroscopy at  $w_0 = 6$ . We anticipated that for small RM sizes if dipic remained in the water pool, some interaction with the interface would be observable since such effects are generally more pronounced at small  $w_0$  sizes.<sup>30</sup> The spectra recorded from dipic in the microemulsions (Figure 2.7) are very different than those observed for the aqueous samples (Figure 2.3). The spectra in microemulsions show no severe downfield shifts as observed from pH 3.2 to 4 in aqueous solutions. This observation provides evidence that no dimer species form in the microemulsion. Importantly, the NMR studies of dipic in the microemulsions show that it does not undergo the dimerization processes observed in aqueous solution.

$^1H$  NMR spectroscopy of the dipic solutions in the microemulsion show an  $A_2X$  or  $A_2B$  spin system and are consistent with the UV-vis results for dipic in RMs. Since the concentration of dipic was more than 10-fold higher than those recorded by UV-vis spectroscopy, dimerization would be favored more in the NMR studies than in the UV-vis studies. Under the conditions used for the NMR studies, the average number of dipic molecules per RMs ranged from 0.03 to 0.2 and were thus much below the 2 dipic molecules per RM needed to form a dimer.<sup>29,31,39</sup> Given the low concentration of dipic in the RM, dimerization is not favored under these conditions regardless of the high formation constant in aqueous solution.

#### *2D NOESY Spectroscopy of Dipic Ligand in Microemulsions.*

In order to investigate whether dipic can penetrate the negatively charged AOT interface, a 2D NOESY experiment was recorded of dipic in AOT/isooctane RMs. The spectrum of aqueous dipic (200 mM) at pH 6.1, in a microemulsion of 1 M AOT with  $w_0$  12, is shown in

Figure 2.8. The 1D spectrum of this solution results in only one signal at about 8.2 ppm that is consistent with fully deprotonated dipic with a minus two charge.

The 2D NOESY spectrum includes many cross signals arising from interactions between protons on AOT. To examine whether dipic can penetrate the AOT interface and traverse up into the hydrophobic chains of AOT, for simplicity, we show the portion of the 2D NOESY spectrum (Figure 2.8) containing the signal for the dianionic dipic around 8.2 ppm and on the opposing axis, the entire chemical shift range for AOT. In addition to the main signal at 8.2 ppm, we observe two small peaks attributed to  $^{13}\text{C}$  satellite signals for dipic. In the 2D spectrum, the major cross peaks to the dipic signal corresponded to signals for the methylene and methyl groups in the AOT. These signals indicate that the deprotonated dipic successfully penetrates the negatively charged AOT interface and resides deep in the AOT interface. Some additional minor cross signals are observed in Figure 2.8 with the other parts of the AOT molecule and provide support for the hypothesis that the dianionic dipic does indeed travel up into the surfactant interface.

The aqueous dipic solutions used for this study were at 200 mM, and AOT was at 1 M with a  $w_0 = 12$  in order to provide the sensitivity required for the 2D experiment. Our aqueous UV-vis studies suggested that dimerization should be a significant factor at this concentration. However, interactions of dipic with AOT may compete with hydrogen bonding between dipic molecules, thus making dimerization less likely. As observed in Figure 2.8, cross peaks between the dipic and AOT methyls and methylenes were observed. This result confirms that dipic resides deeply within the AOT interface and thus can penetrate the negatively charged AOT surface. Since it would be advantageous for dipic to protonate before penetration of the AOT layer, we examined the chemical shift of the dipic species that interacted with the AOT  $\text{CH}_2$  and

CH<sub>3</sub> groups. Because only one dipic signal was observed at a  $\delta = 8.2$  ppm, this is indeed consistent with the doubly deprotonated dipic species, structure 4, residing deep into the AOT interface layer. Attempts were made to prepare microemulsions as above using dipic solutions with a range of pH values. Microemulsions with high (200 mM) concentrations of dipic could only be successfully prepared at pH values above the second  $pK_a$  where the double-deprotonated dipic species predominates.

In the literature, several approaches have been used to examine Overton's rule and the ability of simple aromatic acids to penetrate membranes and lipid interfaces.<sup>10-12</sup> Classical electrostatic principles and some studies strongly favor protonation of these acids prior to penetration of the lipid interface and localization in a hydrophobic environment. The structural results obtained in our studies are unexpected. Our results suggest that not only dipic, but dipic in the dianionic form, is able to penetrate the surface. Why would a minus two charged molecule penetrate a negatively charged interface and reside in a hydrophobic environment deep inside the lipid layer? We propose the following explanations. The RMs are very dynamic structures that undergo forming and reforming processes on a millisecond time scale. It is possible that such events would allow dipic to associate sufficiently strongly with the AOT for penetration to take place. Alternatively, dipic could associate with cations and thus exist as an ion pair capable of lipid interface penetration. Evidence for such events has been reported<sup>40,41</sup> and ion pairs are commonly proposed in organic chemistry to explain effects in transition states or high energy intermediates. These considerations are important and will be investigated for our dipic system in the future. Our data suggest that the location of the highly charged dipic species is deep within the AOT interface. This finding goes against the existing dogma and contributes information regarding the unusual behavior of organic acids at lipid interfaces. Since  $[\text{VO}_2\text{dipic}]^-$  has

previously been found to penetrate the lipid interface and the free dipic<sup>2-</sup> ligand has been observed in those experiments,<sup>2</sup> our current finding shows that the vanadium is not necessary for penetration.

Studies with the dipic ligand are important to be able to elucidate what part of biological activity is due to the metal complex or the ligand. The dipic system is particularly suitable to probe the question of interface penetration, because the dipic ligand NMR spectrum is particularly sensitive to protonation state and, thus, provides information as to (1) what ion species is present, (2) whether it penetrates the reverse micelle hydrophobic interface, and (3) its potential to penetrate lipid bilayers in biological systems. Hydrogen bonding has been invoked in the specific structures that form in bacteria where dipic is part of the spore.<sup>36,42,43</sup> Undoubtedly, dipic's ability to associate and form isomers<sup>5</sup> in the presence and absence of Ca<sup>2+</sup> plays an important role in spore development. In the studies presented here, the finding that dianionic dipic is capable of penetrating the lipid interface goes beyond potential applications of the metal complexes as therapeutic agents. Previous studies with both mono- and dicarboxylic acids all point to membrane transport of only the neutral form.<sup>10-12,31,40,41,44</sup> However, our studies provide structural data that unequivocally show that dipic is in the dianionic form when associated with the hydrophobic part of AOT in location C depicted in Figure 2.1b. Our studies document that this simple charged aromatic carboxylate is stabilized sufficiently to exist in the hydrophobic environments. This work therefore provides an important contribution to the current debate examining the violations of the Overton and the Lipinski rules.

## *CONCLUSIONS*

As shown in Scheme 2.1, these studies reevaluated the speciation of dipic from acidic pH

to basic pH in aqueous solution. The structural information obtained by NMR spectroscopy shows that the species in solution is a symmetric species attainable by rapid equilibration of two asymmetric isomers. A summary of these results are shown in Scheme 2.4. Upon addition of these solutions to the microemulsions, the resulting NMR spectra resembled those in aqueous solution except for the pH region from 2.6 to 6. In this region, the spectra of ligand in microemulsions are very different from the aqueous dipic solutions. In addition, a 2D NOESY experiment was recorded and showed that the dipic molecules reside deep inside the lipid interface. Importantly, the penetrating form of dipic, as evidenced by the NMR chemical shifts, is the fully deprotonated  $H_2Dipic$  with a minus 2 charge. Thus, these results provide data that show a double negatively charged aromatic acid is capable of penetrating a lipid interface. Although we did not attempt to study the mechanism of the penetration, the fact remains that this polar and charged aromatic carboxylate is sufficiently stabilized in a very hydrophobic environment to overcome other seemingly attractive options. Future studies will explore the potential ion pairing of the acid and will determine the effects of electronic charges in the solubility of this multifaceted, dynamic molecule. Lastly, characterization of dipic behavior in mixed phase systems, such as microemulsions, is of special relevance to organic chemistry especially in reactions where heterogeneous catalysis or less conventional conditions are employed. Therefore, microemulsions serve as valuable model systems where solubility assumptions may be tested for charged organic molecules.

FIGURES AND SCHEMES

Scheme 2.1. Four Structures of H<sub>2</sub>dipic in Different Protonation States Are Shown along with Their Respective Equilibria with pK<sub>a</sub> Values<sup>16</sup>

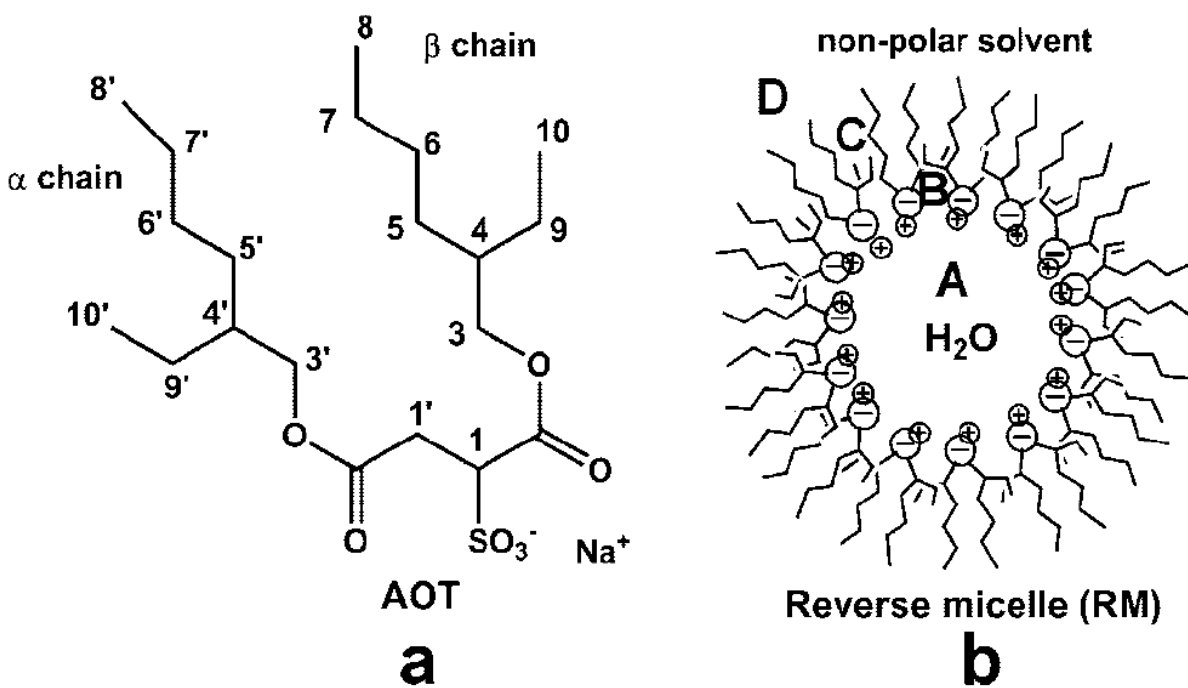
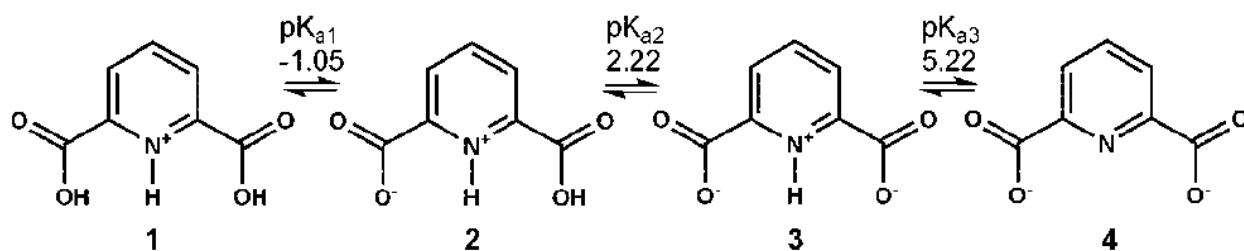


Figure 2.1. Illustrated structure of AOT (a) and an idealized reverse micelle (b) with labeled locations (A, B, C, and D) included. Labels are as follows: water pool interior (A), aqueous interface (B), surfactant tails (C), and the nonpolar solvent exterior (D).

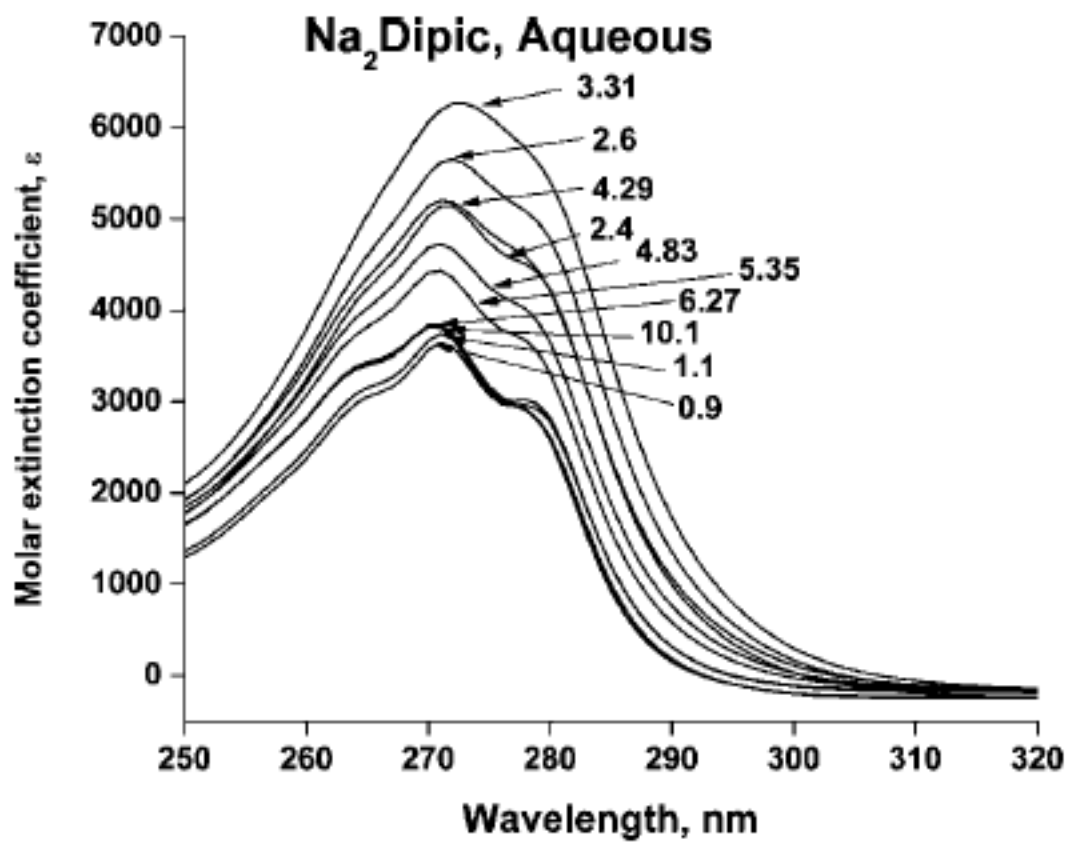


Figure 2.2. Molar extinction coefficient calculated from UV-vis absorption spectra measured in aqueous 0.10 mM dipic at different pH values from 0.9 to 10.1.

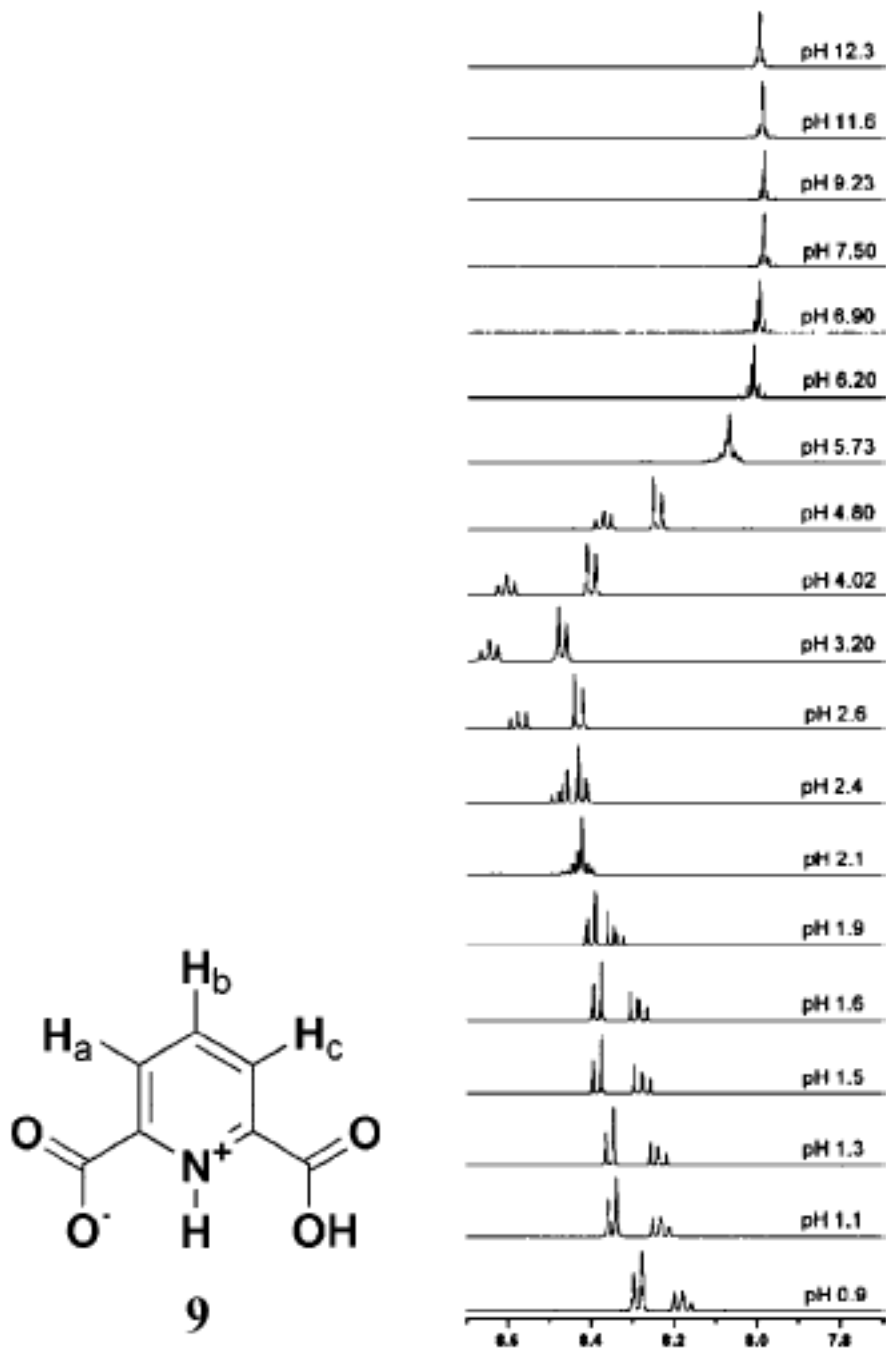
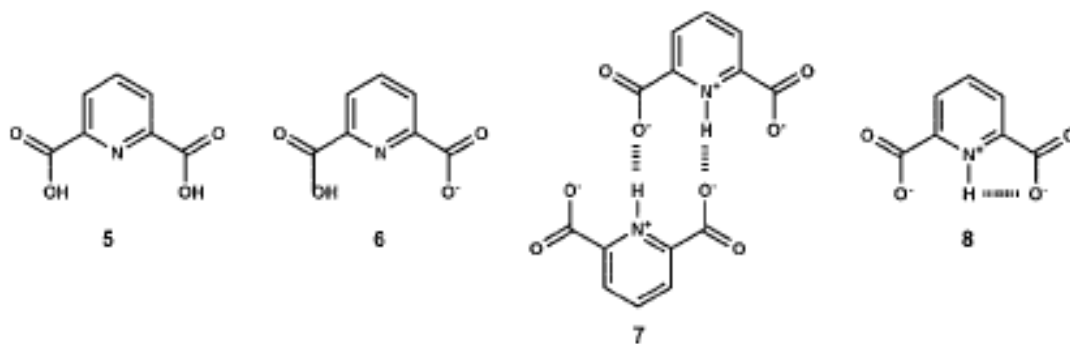
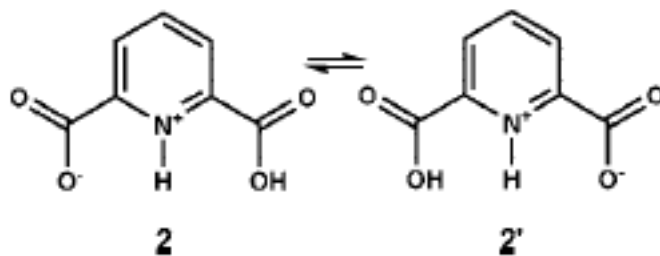


Figure 2.3. 400 MHz <sup>1</sup>H NMR spectra recorded in D<sub>2</sub>O of 20 mM dipic in aqueous solution at pH values 0.9-2.6, 9.23, and 11.6 and of 25 mM dipic in aqueous solution at pH values 3.20-7.50 and 12.3. Samples were referenced against an external DSS sample. In structure 9, the three different protons H<sub>a</sub>, H<sub>b</sub>, and H<sub>c</sub> are shown in an amphiphilic form of dipic

Scheme 2.2. Possible dipic Species at Varying pH Values Structures 5-8



Scheme 2.3. Monoprotonated Zwitterionic Structure of dipic (2) and the Corresponding Structure after Rapid Equilibrium (2')



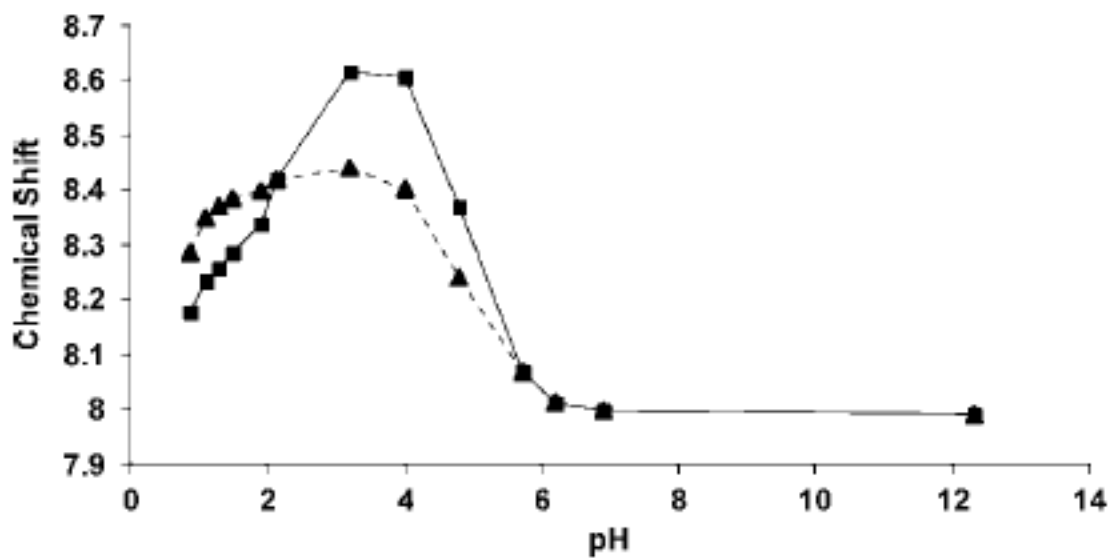
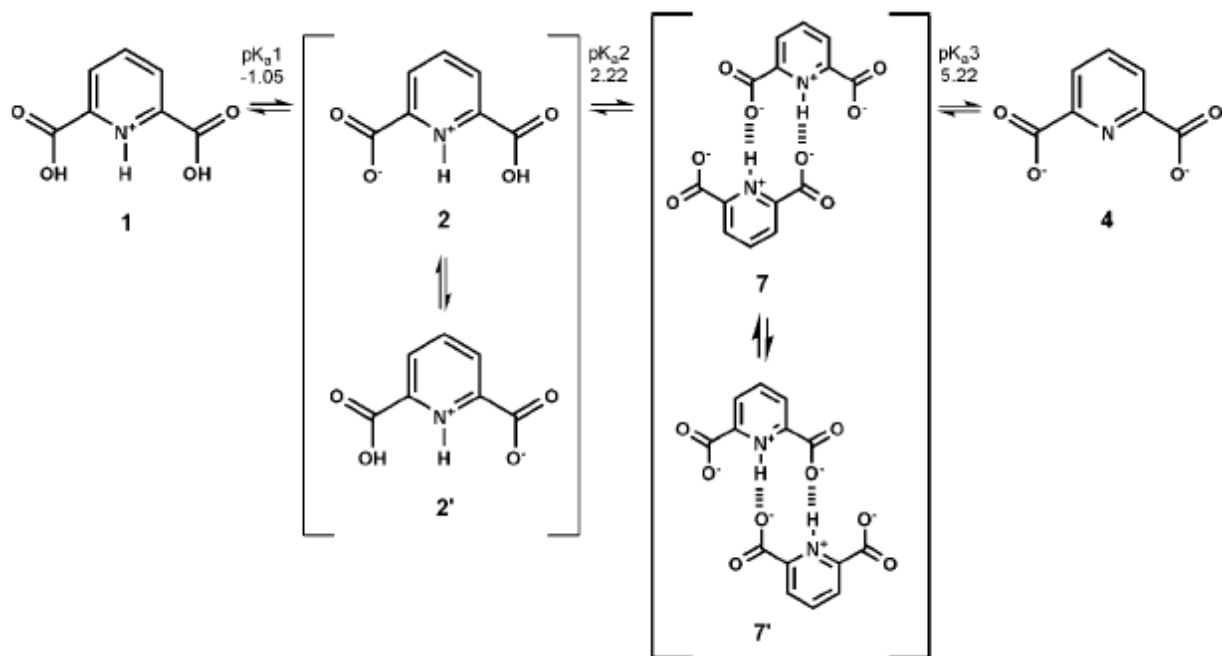


Figure 2.4. Chemical shifts of dipic protons H<sub>a</sub> (triangles) and H<sub>b</sub> protons (squares) plotted as a function of pH in aqueous solutions.

Scheme 2.4. Dipic Structures and Equilibria in Aqueous Solution with Corresponding pK<sub>a</sub> Values



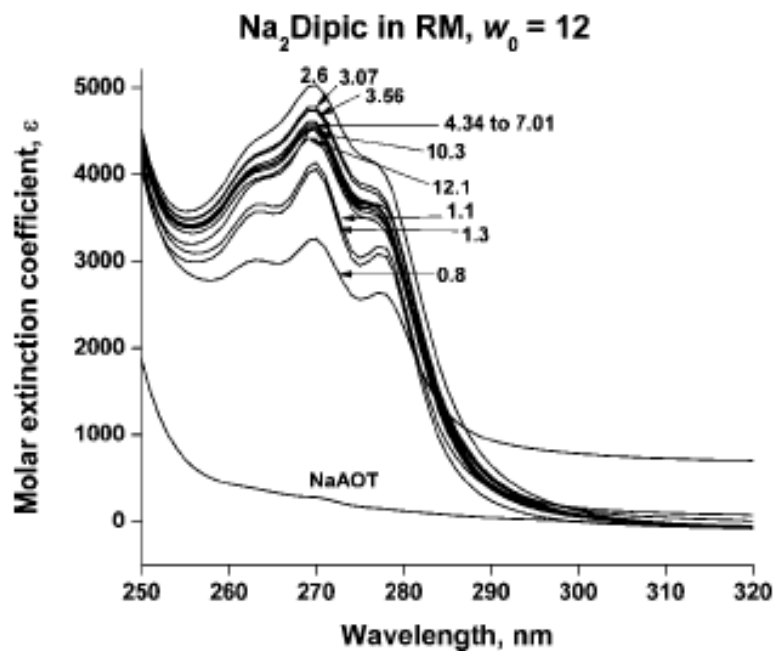


Figure 2.5. Absorption spectra of microemulsions containing 0.158 mM dipic in 200 mM AOT/isooctane. RMs ( $w_0 = 12$ ) were prepared from aqueous stock solutions at pH values from 0.8 to 12.1.

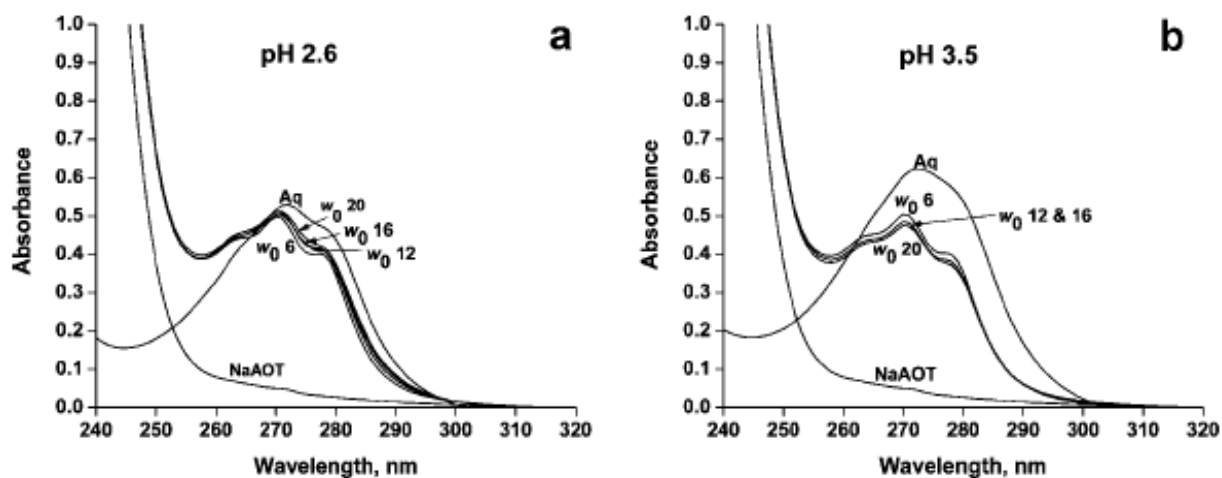


Figure 2.6. Absorption spectra of 0.10 mM dipic in 200 mM AOT/isooctane RMs. Aqueous dipic solutions at pH (a) 2.6 and (b) 3.5 were used to prepare microemulsions with  $w_0 = 6, 12, 16,$  and 20.

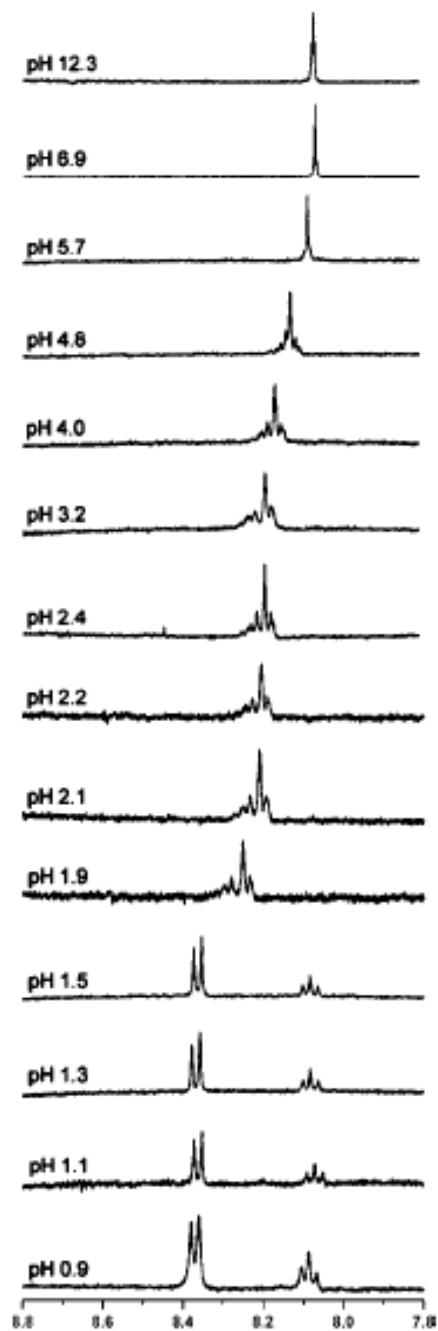


Figure 2.7. 400 MHz  $^1\text{H}$  NMR spectra of dipic in 750 mM AOT/ isooctane microemulsions with  $w_o = 6$ . Aqueous stock solutions of 20-25 mM dipic from pH 0.9 to 12.3 were used to prepare RMs with final dipic concentrations of 1.45-1.81 mM. Samples at pH 3.20-6.20 were prepared with the higher concentration stock solution; the rest were prepared with 20 mM dipic. Samples were referenced using isooctane.

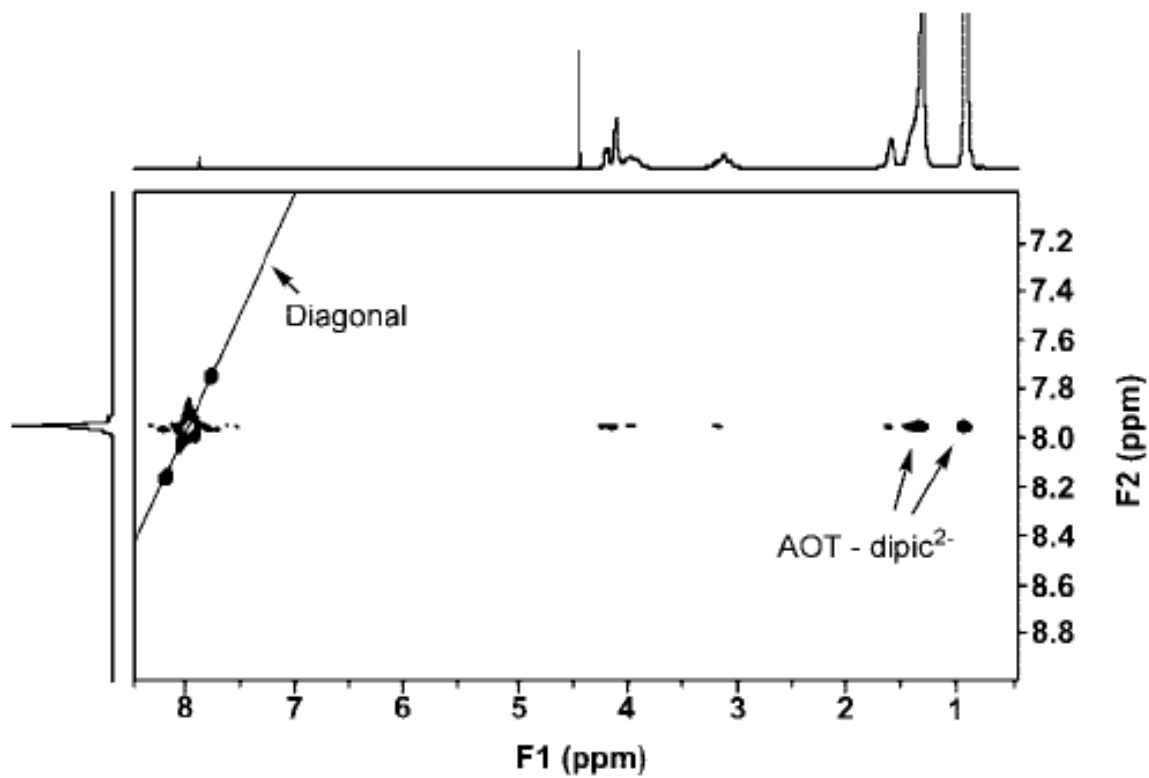


Figure 2.8. Section of the 2D NOESY of 200 mM dipic in 1 M AOT/ isooctane- $d_{18}$  in  $D_2O$ /pH 6.1.  $w_0 = 12$  adjusted to pH 6.1 with NaOD.

## REFERENCES

- (1) Gant, T. G.; Meyer, A. I. *Tetrahedron* **1994**, *50*, 2297–2360.
- (2) Meyers, A. I.; Rieker, W. F.; Fuentes, L. M. *Journal of the American Chemical Society* **1983**, *105*, 2082–2083.
- (3) Shimano, M.; Meyers, A. I. *Journal of Organic Chemistry* **1995**, *60*, 7445–7455.
- (4) Lemieux, R. M.; Meyers, A. I. *Journal of the American Chemical Society* **1998**, *22*, 5453–5457.
- (5) Elworthy, T. R.; Meyers, A. I. *Tetrahedron* **1992**, *48*, 2589–2612.
- (6) Lipinski, C. A.; Lombardo, F.; Dominy, B. W.; Feeney, P. J. *Advancement in Drug Delivery Reviews* **1997**, *23*, 3–25.
- (7) Crans, D. C.; Rithner, C. D.; Baruah, B.; Gourley, B. L.; Levinger, N. E. *Journal of the American Chemical Society* **2006**, *128*, 4437–4445.
- (8) Willsky, G. R.; Goldfine, A. B.; Kostyniak, P. J.; McNeil, J. H.; Yang, L. Q.; Khan, H. R.; Crans, D. C. *Journal of Inorganic Biochemistry* **2001**, *85*, 33–42.
- (9) McNeil, J. H.; Yuen, V. G.; Hoveyda, H. R.; Orvig, C. *Journal of Medicinal Chemistry* **1992**, *35*, 1489–1491.
- (10) Grime, J. M. A.; Edwards, M. A.; Rudd, N.; Umwin, P. R. *Proceedings of the National Academy of Sciences U.S.A.* **2008**, *105*, 14277–14282.
- (11) Saparov, S. M.; Antonenko, Y. N.; Pohl, P. *Biophysical Journal* **2006**, *90*, L86–L88.
- (12) Thomae, A. V.; Wunderli-Allenspach, H.; Kramer, S. D. *Biophysical Journal* **2005**, *89*, 1802–1811.
- (13) Overton, C. E. *Vierteljahsschr. Naturforsch. Ges. Zuerich* **1899**, *44*, 88–135.

- (14) Al-Awqati, Q. *Nature Cell Biology* **1999**, *1*, E201–E202.
- (15) Dupont-Leclercq, L.; Giroux, S.; Henry, B.; Rubini, P. *Langmuir* **2007**, *23*, 10463–10470.
- (16) Peral, F.; Gallego, E. *Spectrochimica Acta Part A* **2000**, *56*, 2149–2155.
- (17) Peral, F. *Journal of Molecular Structure* **1992**, *266*, 373–378.
- (18) Wasylina, L.; Kucharska, E.; Weglinski, Z.; Puszko, A. *Khimiya Geterotsiklicheskikh Soedinenii* **1999**, 210–218.
- (19) Edgecombe, K. E.; Weaver, D. F.; Smith, V. H. *Canadian Journal of Chemistry* **1994**, *72*, 1388–1403.
- (20) Xie, J. R. H.; Smith, V. H.; Allen, R. E. *Chemical Physics* **2006**, *322*, 254–268.
- (21) Morcillo, J.; Gallego, E.; Peral, F. *Journal of Molecular Structure* **1987**, *157*, 353–369.
- (22) Peral, F.; Gallego, E.; Morcillo, J. *Journal of Molecular Structure* **1990**, *219*, 251–256.
- (23) Tinoco, I. *Journal of the American Chemical Society* **1960**, *82*, 4785–4790.
- (24) Peral, F.; Gallego, E. *Journal of Molecular Structure* **1992**, *274*, 105–114.
- (25) Peral, F.; Gallego, E. *Journal of Molecular Structure* **1994**, *326*, 59–68.
- (26) Peral, F.; Gallego, E. *Biophysical Chemistry* **2000**, *85*, 79–92.
- (27) Peral, F.; Gallego, E. *Spectrochimica Acta Part A* **2000**, *56*, 747–759.
- (28) Branco, L. C.; Afonso, C. A. M. *Journal of Organic Chemistry* **2004**, *69*, 4381–4389.
- (29) Maitra, A. *Journal of Physical Chemistry* **1984**, *88*, 5122–5125.
- (30) Stahla, M. L.; Baruah, B.; James, D. M.; Johnson, M. D.; Levinger, N. E.; Crans, D. C. *Langmuir* **2008**, *24*, 6027–6035.
- (31) Baruah, B.; Roden, J. M.; Sedgwick, M.; Correa, N. M.; Crans, D. C.; Levinger, N. E. *Journal of the American Chemical Society* **2006**, *128*, 12758–12765.

- (32) Riter, R. E.; Willard, D. M.; Levinger, N. E. *Journal of Physical Chemistry B* **1998**, *102*, 2705–2714.
- (33) Crans, D. C.; Yang, L. Q.; Jakusch, T.; Kiss, T. *Inorganic Chemistry* **2000**, *39*, 4409–4416.
- (34) Green, R. W.; Tong, H. K. *Journal of the American Chemical Society* **1956**, *78*, 4896–4900.
- (35) Stephenson, H. P.; Sponer, H. *Journal of the American Chemical Society* **1957**, *79*, 2050–2056.
- (36) Lindsay, J. A.; Murrell, W. G. *Current Microbiology* **1986**, *13*, 255–259.
- (37) Tokuhiko, T.; Wilson, N. K.; Fraenkel, G. *Journal of the American Chemical Society* **1968**, *90*, 3622–3628.
- (38) *Organic Structure Analysis; 1 ed.*; Crews, P., Rodriguez, J., Jaspars, M. Ed.; Oxford University Press: New York, 1998.
- (39) Pal, T.; De, S.; Jana, N. R.; Pradhan, N.; Mandal, R.; Pal, A.; Beezer, A. E.; Mitchell, J. *C. Langmuir* **1998**, *14*, 4724–4730. 2003, *237*, 103–111.
- (41) Yang, X. G.; Yang, X. D.; Yuan, L.; Wang, K.; Crans, D. C. *Pharmaceutical Research* **2004**, *21*, 1026–1033.
- (42) Murrell, W. G. In *The Bacterial Spore*; Gould, G. W. H., A., Ed.; Academic Press, Inc.: New York, 1969; pp 215-273.
- (43) Hanson, R. S.; Halvorso, Ho; Curry, M. V.; Garner, J. V. *Canadian Journal of Microbiology* **1972**, *18*, 1139–1143.
- (44) Evtodienko, V. Y.; Bondarenko, D. I.; Antonenko, Y. N. *Biochimica et Biophysica Acta* **1999**, *1420*, 95–103.

## CHAPTER 3: <sup>3</sup>Correlating insulin enhancing properties with physical chemical properties of vanadium dipicolinate complexes

### *SUMMARY*

The effects of substituents on an anti-diabetic compounds,  $[\text{VO}_2(\text{dipic})]^-$ , was evaluated with regard to interactions with model membranes and molecular electronic properties. Several compounds in the series of were reported to have insulin-enhancing properties in STZ induced diabetic Wistar rats. The physical properties of the compounds series and their interactions with microemulsions of the Aerosol-OT reverse micelles were investigated. Specifically the ability of the drugs in reverse micelles associating with the water pool using differential FT-IR spectroscopy and the insulin enhancing drugs in the  $[\text{VO}_2(\text{dipic})]^-$  - series were all found to associate with the interface. The inherent electronic properties and environment of the complexes using <sup>51</sup>V NMR spectroscopy were found to correlate with the Hammett  $\sigma_{\text{para}}$  constants both in aqueous solution and in the microemulsion environment. These results show that although the environment of the vanadium compound may change, its inherent properties remain, which may be what cause the insulin enhancing effects.

### *INTRODUCTION*

A treatment of diabetes that has been considered for some time is transition metal complexes and salts. As a result a range of systems has been investigated for anti-diabetic properties.<sup>1-14</sup> Some of the most investigated systems are based on vanadium and chromium, and

---

<sup>3</sup> By: Alejandro M. Trujillo, Jerome A. Burke, Pabitra B. Chatterjee, Gail M. Willsky and Debbie C. Crans\*  
Alejandro M. Trujillo performed and assisted in all NMR and FT-IR experiments  
*Manuscript prepared for submission to ChemMedChem*

although their chemistry has many similarities their mode of actions are significantly different.<sup>8,15</sup> Both chromium and vanadium are available to the public as dietary supplements and in vitamins. However neither of the metal systems has yet survived clinical trials to be commercially available as drugs.<sup>11,16</sup> Considering the fact that vanadium compounds lower elevated blood glucose levels and do not cause the hypoglycemic episodes in normal subjects, these compounds have received much interest and attention. Mechanistic studies have been aiming to understand how such a small chemical entity can mimic or more recently enhance the effects of insulin.<sup>14,17-20</sup> Indeed, a range of different systems including simple salts such as vanadate, vanadyl and decavanadate and coordination complexes such as vanadium(III), vanadium(IV), and vanadium(V) complexes have been reported.<sup>14,21-26</sup> A few classes of vanadium compounds have undergone extensive structure activity studies, and the insulin-enhancing effects of the vanadium compounds on a range of *in vivo* and *in vitro* model systems have been reported.<sup>3,5,7 2,8,10-14,27,28</sup> In this work we will focus on *in vitro* studies of the dipicolinate systems with the objective of providing a further understanding of the possible role uptake and membrane interaction will have on the action of this class of drugs.

The two most well studied coordination complexes, the BMOV-BEOV system and the V-dipic systems both show that the parent and unsubstituted systems are the most effective, Figure 3.1.<sup>1,7,11,13</sup> That is Structure Activity Relationships (SAR) in which the ligands were modified with electron donating and withdrawing substituents resulted in a less active drug. These studies were carried out through intraperitoneal (IP) administration of V-maltolate derived compounds in STZ induced Wistar rats<sup>11</sup> and oral administration of V-dipicolinates in STZ induced Wistar rats.<sup>13</sup> In contrast Sakurai found a greater efficacy with electron donating groups examining primary cultures and measuring free fatty acid release by administration of the V-pic derived

complexes.<sup>4,9,10</sup> Since the oxidation state also has been found to be important, and for this series of compounds the vanadium(V)-dipic complexes were found to be most efficacious, further information on how the subtle differences in the chemical properties may be important to understand the mode of action of these compounds.

In the case of the V-dipic systems anti-diabetic studies have been accompanied by stability studies of the compounds investigated, and the parent V-dipic was found to be most stable than any of the substituted counterparts.<sup>13,25</sup> The series of compounds used herein are all stable in the acidic pH range with a pH maximum around 3.5 and little complex remaining at neutral pH.<sup>13,25,29</sup> However, it was found that complexation with simple ligands to form ternary complexes extended the pH stability to the neutral pH range,<sup>30</sup> and this fact combined with the observations reporting the chemistry of vanadium complexes with serum proteins and other metabolites, have led to the suggestions that at least initially the active species are complexes between the vanadium and cellular proteins, metabolites or other components.<sup>13</sup> A recent analysis of the vanadium uptake in a studies of orally administered vanadate however, that the insulin-enhancing properties did not correlate with the total vanadium level.<sup>31</sup> These studies proposed that the coordination chemistry was likely to play an important role in the distribution of the vanadium, and that chemistry involved many metabolites and enzymes for mode of action. Additionally the effects vanadium on membranes including those of the GI-tract may be critical for the mode of action of these drugs.<sup>24</sup> In this work we will investigate how different V-dipic complexes interact with interfaces, with the intention of understanding why these compounds have such similar effects as insulin enhancing agents.

In the following we will use interfaces formed in microemulsions to investigate the drugs association with a simple model system.<sup>32</sup> These systems are used to mimic the

microenvironments present in natural membranes. Specifically, we will use conditions placing the system in the section of the phase diagram where reverse micelles (RMs) form.<sup>33,34</sup> RM are self-assembled aggregations composed of amphiphilic molecules in an organic solvent surrounding a aqueous core, and this systems has been found to be a useful model system to determine surface-probe interactions experimentally.<sup>35-38</sup> The parameter  $w_0 = [\text{H}_2\text{O}]/[\text{AOT}]$  describes the size of the RMs in solution. In this work we will us sodium bis-2-ethylhexylsulfosuccinate (AOT), shown in Figure 3.2 which is well suited for these studies, because of the nature of the surfactant, the length of the surfactant and size of interface layer and how well it the interfaces form and mimic the a simplified lipid monolayer. These systems are dynamic, however, the thermodynamic stability governs the system, and compounds and water are known to penetrate the interface depending on molecular structure.

The parent chemical structure of  $[\text{VO}_2(\text{dipic})]^-$  is shown in Figure 3.3. The series of anti-diabetic vanadium compounds used will have replaced the H-group in the para- (position 4), Figure 3.1.  $[\text{VO}_2(\text{dipic-NH}_2)]^-$ ,<sup>28</sup>  $[\text{VO}_2(\text{dipic-Cl})]^-$ ,<sup>25</sup> and  $[\text{VO}_2(\text{dipic-OH})]^-$ <sup>39</sup> in addition to the parent complex have been investigated with regard to their insulin enhancing properties. In this work we will also investigate the  $-\text{NO}_2$  derivatives.<sup>30</sup> The chemistry of these complexes was investigated previously and the parent system was found to be most stable.<sup>13,25</sup> The electronic properties of these systems have been investigated using a range of techniques including electrochemistry and spectroscopies.<sup>40,41</sup> Specifically solid-state  $^{51}\text{V}$  NMR spectroscopy is a very sensitive tool for probing the electronic properties of the complexes.<sup>41-43</sup> Solid-state  $^{51}\text{V}$  NMR provides information on the electron structure and geometry of coordination complexes because  $^{51}\text{V}$  is a half integer quadrupolar nucleus ( $I = 7/2$ ) have electric field gradient and chemical shift anisotropy tensors generally sensitive to the complex electronic geometry and structure. For the

series of V-dipic complexes it has been shown that the solid-state  $^{51}\text{V}$  NMR chemical shifts correlate linearly with the  $^{51}\text{V}$  solution isotropic chemical shifts, and thus the latter can be used as a tool to investigate electronic changes in these compounds.<sup>40</sup>

In the following studies we will carry out two types of experiments probing the drug interacting with interfaces measured using first FT-IR spectroscopy and second  $^{51}\text{V}$  NMR spectroscopy. These studies will detail the interaction of the drugs with the interface, and the water pool in the microemulsion model system.

## *MATERIALS AND METHODS*

### *Materials.*

2,2,4-trimethylpentane (iso-octane), deuterium oxide ( $\text{D}_2\text{O}$  – 99% D), NaOH, NaOD (99% D), HCl and NaOD (99% D), were used as received from Sigma – Aldrich Laboratories without further purification. Sodium bis-2-ethylhexylsulfocuccinate (AOT) was purified in accordance with Chowdhury, et al., by dissolution of AOT in methanol with added activated charcoal<sup>44</sup> we tested the water content using  $^1\text{H}$  NMR spectroscopy. The vanadium compounds were prepared as described previously  $[\text{VO}_2(\text{dipic})]^-$ ,<sup>45</sup>  $[\text{VO}_2(\text{dipic-OH})]^-$ ,<sup>39</sup>  $[\text{VO}_2(\text{dipic-Cl})]^-$ ,<sup>25</sup>  $[\text{VO}_2(\text{dipic-NH}_2)]^-$ <sup>30</sup> and  $[\text{VO}_2(\text{dipic-NO}_2)]^-$ .<sup>30</sup>

### *NMR experimental procedures.*

The  $^{51}\text{V}$  NMR studies were performed on a 300 MHz NMR spectrometer using a  $90^\circ$  pulse angle with an 8kHz spectral window with a 0.096 s acquisition time. All  $^{51}\text{V}$  NMR spectra were referenced using  $\text{VOCl}_3$  as an external reference (0 ppm). All NMR files were worked up by referencing and phase correction on MestRec mNOVA software. The files were exported to Origin 7 where they were stack plotted and labeled.

### *Infrared (IR) experimental procedures.*

The IR spectral data were collected using a Magna 760 FT-IR at 25°C. The spectra collected used 32 scans with a 1 cm<sup>-1</sup> resolution. The IR apparatus required the samples to be added drop wise to the sample window for acquisition. The sample window was wiped clean with a methanol and dried with a chemwipe. The subtraction used a sample that contained an aqueous phase with 5% HOD (2.5 % D<sub>2</sub>O) in double deionized (DDI) H<sub>2</sub>O and a second identical sample with a water pool of DDI H<sub>2</sub>O. The two spectra were then subtracted and the remaining peak was the OD signal. The work up for the data was performed on Microsoft Excel and Origin 7.

### *Aqueous sample preparation for IR.*

The IR samples were prepared used double deionized (DDI) water and 5% D<sub>2</sub>O as the aqueous solution and the aqueous phase for the 750 mM AOT/isooctane RMs. The 50 mM dipicolinatooxovanadium(V) salts were used depending on the substituent used (H; OH; Cl; NH<sub>2</sub>; NO<sub>2</sub>) was stored at 0 °C in glass vials. The appropriate amounts of solid to form a 50 mM solutions of (VO<sub>2</sub>[dipic-X])<sup>-</sup> was added to an aqueous stock to create 2 mL samples. Two aqueous stock solutions (H<sub>2</sub>O or a 5% D<sub>2</sub>O / DDI H<sub>2</sub>O mix) were created for each complex. The solid was added to a sample vial and vortexed until all solid was dissolved. The pH of the solution was adjusted using DCl and stored in a glass vial.

### *Aqueous sample preparation for NMR.*

Preparation of the aqueous solutions for NMR studies was achieved by dissolving the appropriate amounts of the recrystallized solid to generate a 50 mM [VO<sub>2</sub>(dipic-H)]<sup>-</sup> solution (0.399 g) to form 3.0 mL in D<sub>2</sub>O. The solids used were [VO<sub>2</sub>(dipic-X)]<sup>-</sup> (X = H, OH, Cl, NH<sub>2</sub> or NO<sub>2</sub>) which were prepared using previously described methods.<sup>46,47</sup> The solutions were vortexed

until all solid was dissolved. The pH of the resulting solutions were measured using an Orion 420A pH meter and if necessary adjusted. The pH was corrected to pD according to the relationship  $\text{pH} + 0.4 = \text{pD}$ . The pD of the solution was adjusted using DCl and/or NaOD to achieve the  $\text{pD} \sim 3.5$  used in most of the results described in this manuscript.

#### *Reverse Micelle (RM) formulation.*

The formation of reverse micelle samples were generated by combining the appropriate amounts of AOT stock was combined with appropriate amounts of aqueous stock using glass syringes to obtain the desired  $w_0$  fitting the equation  $w_0 = [\text{H}_2\text{O}]/[\text{AOT}]$ . The aqueous phase was then added yielding a biphasic suspension. The samples were then vortexed until a homogenous and optically transparent.

## *RESULTS AND DISCUSSION*

### *FT-IR measurements on microemulsions containing $[\text{VO}_2(\text{dipic})]^-$ and $[\text{VO}_2(\text{dipic-X})]^-$ derivatives.*

Measurements were made on 750 mM AOT/isooctane microemulsion samples containing 50 mM  $[\text{VO}_2(\text{dipic})]^-$ ,  $[\text{VO}_2(\text{dipic-OH})]^-$ ,  $[\text{VO}_2(\text{dipic-Cl})]^-$  and  $[\text{VO}_2(\text{dipic-NO}_2)]^-$ . In the case of the  $[\text{VO}_2(\text{dipic-NH}_2)]^-$  the solubility was not 50 mM and the material did not completely dissolve. Samples were run containing 2.5%  $\text{D}_2\text{O}$  and corresponding samples were run with probe but without  $\text{D}_2\text{O}$  for background subtraction. This subtraction was made to avoid excitation transfer effects.<sup>48</sup> Several data series were investigated. First, series of data were done at varying  $w_0$  size, and second data were obtained at varying  $[\text{VO}_2(\text{dipic})]^-$  derivatives at constant  $w_0$  sizes 8 and 10. The drug samples were investigated at pH 3.5 near the pH optimum as well as at pH 5.5 where some of the complexes are already beginning to hydrolyze. The background

subtracted FT-IR data of the samples containing 5% HOD were compared with respect to peak position and linewidth to a sample containing the RMs with 5% HOD to document the effects the compound had on the H-bonding in the water pools of the RMs.

The series of  $[\text{VO}_2(\text{dipic-Cl})]^-$  as a function of different sizes of  $w_0$  compared to corresponding RMs series (data not show) illustrate that the changes varies depending on the size of the RMs. In the case of the  $[\text{VO}_2(\text{dipic-Cl})]^-$  we find that the changes from RMs to the  $[\text{VO}_2(\text{dipic-Cl})]^-$  is greater at larger  $w_0$  sizes. This observation suggests that in the case of this drug that as the size of the water pool increase the  $[\text{VO}_2(\text{dipic-Cl})]^-$  complex prefer to reside in the water pool. This observation underlines the importance of solvation. Indeed, we have recently reported significant changes in metal ion species at low solvation levels.<sup>49</sup>

In Figure 3.4 we show the differential FT-IR spectra of the series of  $[\text{VO}_2(\text{dipic-X})]^-$  at a  $w_0$  of 8. We chose this small size, because in general we find a great effect at small  $w_0$  sizes.<sup>50</sup> In addition, we record the peak position for these systems with standard deviation showing the error on 3 or 4 measurements, Table 3.1. The series show no probe and  $[\text{VO}_2(\text{dipic-H})]^-$  have experimentally indistinguishable peak maxima. In contrast  $[\text{VO}_2(\text{dipic-OH})]^-$  and  $[\text{VO}_2(\text{dipic-Cl})]^-$  are slightly blue-shifted. The  $[\text{VO}_2(\text{dipic-NH}_2)]^-$  complex if anything displays a slight red-shift. However, this derivative is very insoluble, and the samples were not completely transparent, so therefore the data is therefore not shown in Figure 3.4. The  $[\text{VO}_2(\text{dipic-NO}_2)]^-$  derivative shifts significantly and this suggest this derivative is found in the waterpool where it perturb the H-bonding more than any of the other complexes.

An additional series for  $[\text{VO}_2(\text{dipic-X})]^-$  was performed at pH  $\sim 3.5$  and the results are presented in Table 3.1. The series also confirm that no probe and  $[\text{VO}_2(\text{dipic-H})]^-$  have experimentally indistinguishable peak maxima while  $[\text{VO}_2(\text{dipic-OH})]^-$  and  $[\text{VO}_2(\text{dipic-Cl})]^-$  are

slightly blue-shifted. The  $[\text{VO}_2(\text{dipic-NH}_2)]^-$  complex if anything displays a slight red-shift. However, this derivative is very insoluble, and the samples sometimes were not completely transparent. The  $[\text{VO}_2(\text{dipic-NO}_2)]^-$  derivative shifts significantly and suggests this derivative is found in the waterpool where it perturbs the H-bonding more than the other complexes. Perhaps most importantly from this data it is clear that the greater shifts at pH 3.5 are observed at the larger  $w_o$  sizes; that is as the RMs and the waterpool becomes larger, the effect induced by the drug is larger.

We also recorded the spectra of  $[\text{VO}_2(\text{dipic})]^-$ , dipic ligand,  $[\text{VO}_2(\text{dipic-OH})]^-$ , and  $[\text{VO}_2(\text{dipic-Cl})]^-$  at higher pH values (data not shown). The pH of the aqueous phase was  $\sim 5.5$  at which point these complexes at least in part are beginning to hydrolyze. The  $\text{dipic}^{2-}$  and  $(\text{VO}_2[\text{dipic-H}])^-$  show maxima overlapping the sample without probe indicating that these probes do not interact with the water pool. However, the  $[\text{VO}_2(\text{dipic-OH})]^-$  and  $[\text{VO}_2(\text{dipic-Cl})]^-$  both blue-shifted in the OD stretching maxima that to a higher frequency indicating a change in the H-bonding in the aqueous phase of the AOT RMs at pH  $\sim 5.5$ .

Combined these studies showed that the  $[\text{VO}_2(\text{dipic})]^-$  complex does not impact the H-bonding in the water droplets in the RMs. The  $[\text{VO}_2(\text{dipic-NH}_2)]^-$  complex may also associate strongly with the interface and not the water pool. However, this interpretation is less certain, because this complex was less soluble and the samples were not always transparent. The  $[\text{VO}_2(\text{dipic-OH})]^-$  and  $[\text{VO}_2(\text{dipic-Cl})]^-$  complexes showed a small but definite shift, which is consistent with this complex being associated with the water pool. Finally the  $[\text{VO}_2(\text{dipic-NO}_2)]^-$  complex showed the largest shift of all the complexes. These results show that this series of complexes interacts with different affinities with the interface. Such disparity in properties suggests that may be some differences in the uptake of the compounds upon administration. Yet,

for the analogs that have been investigated the insulin enhancing effects have been observed ( $[\text{VO}_2(\text{dipic})]^-$ ,<sup>26</sup>  $[\text{VO}_2(\text{dipic-OH})]^-$ ,<sup>39</sup>  $[\text{VO}_2(\text{dipic-Cl})]^{51-}$  and  $[\text{VO}_2(\text{dipic-NH}_2)]^{-28}$ ) the difference in insulin-enhancing effect is modest and not as large as observed when the vanadium is modified by a ternary ligand.<sup>13</sup> Furthermore, the derivative that was found to be exclusively in the water pool  $[\text{VO}_2(\text{dipic-NO}_2)]^-$  and not likely associated with the interface, we do not have animal data on. It was recently demonstrated that the efficacy of the vanadium when administered in the form of vanadate to human diabetics did not correlate with the total vanadium absorbed.<sup>31</sup> Because of this finding it was proposed that some as of yet unidentified pool of active vanadium formed upon administration. Although it is possible that such a pool would form as a result of interaction with and traversing interfaces the studies here suggest that there may be a relatively wide range of properties of the insulin-enhancing agent that result in the same insulin-enhancing response. Because this series of compounds investigated suggests that all but the  $[\text{VO}_2(\text{dipic-NO}_2)]^-$  are associated to some degree with the interface, we sought additional information on the properties of this class of compounds.

*NMR Spectroscopic Studies of microemulsions containing  $[\text{VO}_2(\text{dipic-H})]^-$  and  $[\text{VO}_2(\text{dipic-Cl})]^-$ .*

Substituent effects of the vanadium complexes with 2,6-pyridinedicarboxylate ( $\text{dipic}^{2-}$ ) derivatives were evaluated measuring the  $^{51}\text{V}$  NMR chemical shifts in aqueous solution and in microemulsions. Previous studies have been carried out using  $^1\text{H}$  and  $^{13}\text{C}$  NMR chemical shifts to evaluate substituent effects.<sup>52-57</sup> The  $^{51}\text{V}$  nucleus is spin 7/2<sup>58</sup> and have been used to provide valuable information on coordination geometry as well as the electronic properties of the vanadium nuclei.<sup>25,40-43,59</sup> The aqueous stability of complexes was previously evaluated from acidic to neutral pH at a 1:1 ratio of ligand to vanadium. These studies were carried out at the pH stability optimum of the  $[\text{VO}_2(\text{dipic-X})]^-$  series. The parent complex,  $[\text{VO}_2(\text{dipic-H})]^-$  was found

to be the most stable with 95% intact.<sup>13,25,30</sup> The  $[\text{VO}_2(\text{dipic-OH})]^-$  and  $[\text{VO}_2(\text{dipic-NH}_2)]^-$  complexes were slightly less stable at ~80% while the  $[\text{VO}_2(\text{dipic-Cl})]^-$  and  $[\text{VO}_2(\text{dipic-NO}_2)]^-$  complexes were ~65% intact at pH 3.5. The  $^{51}\text{V}$  NMR spectra of the complexes where X is H, OH, Cl,  $\text{NH}_2$  and  $\text{NO}_2$  were measured in  $\text{D}_2\text{O}$  solutions as well as in AOT RM solutions and were referenced externally to a  $\text{VOCl}_3$  standard.

The chemical shifts for the  $[\text{VO}_2(\text{dipic})]^-$  complexes and derivatives measured in aqueous solution are listed in Table 3.3 The  $^{51}\text{V}$  NMR chemical shifts were found to shift upfield with electron withdrawing groups ( $\text{NO}_2$ ) and downfield with electron donating groups ( $\text{NH}_2$ , OH, Cl). This is consistent with the substituents induced shifts observed in  $^1\text{H}$  and  $^{13}\text{C}$  NMR spectroscopy.<sup>53-57</sup> Because the solid state  $^{51}\text{V}$  NMR chemical shifts have been found to describe the electronic properties of the vanadium<sup>40</sup> we were interested to expand the linear free energy relationships to this nucleus. The isotropic solution  $^{51}\text{V}$  NMR chemical shifts can show deviations with the solid-state  $^{51}\text{V}$  NMR chemical shifts.<sup>40,59</sup> When there are structural differences between the solution and the solid state, for the  $[\text{VO}_2(\text{dipic})]^-$  series of compounds the isotopic shift has been shown to correlate with the solid-state  $^{51}\text{V}$  NMR chemical shift.<sup>25,41</sup> In addition, limited correlation for a wide range of vanadium compounds have been reported documenting that when the solution structure is maintained the  $^{51}\text{V}$  nucleus is a valuable tool to probe ligand effects.<sup>60</sup>

The  $^1\text{H}$  and  $^{13}\text{C}$  NMR chemical shifts have been found to correlate with Hammett parameters for a range of V-compounds documenting that linear free relationships exist for vanadium coordination complexes.<sup>53,56,57,61</sup> Corresponding analyses have not previously been done with  $^{51}\text{V}$  NMR chemical shifts although the  $^{51}\text{V}$  NMR chemical shifts are known to describe the electronic properties at the vanadium atom. In this manuscript we undertook a linear free

energy analysis. First, the  $d_X - d_H (= rs)$  was calculated of the solution  $^{51}\text{V}$  NMR chemical shifts in analogy with the approaches previously found to be effective when correlating systems using  $^1\text{H}$  and  $^{13}\text{C}$  NMR shifts in plots against the Hammett  $s$  constants.<sup>62-64</sup> The linear fit to the data in Figure 3.5 shows a  $r = -6.7$  and an  $r^2 = 88\%$ . The high  $r^2$  indicates that  $^{51}\text{V}$  NMR parameters correlate with the substituent effects described by the Hammett  $s_{\text{para}}$  constant of the complexes in aqueous solution (pH 3.5).

The  $^{51}\text{V}$  NMR spectra were also recorded of AOT RM samples  $w_o = 12$  containing the  $[\text{VO}_2(\text{dipic})]^-$  complexes and derivatives. The chemical shifts for the  $[\text{VO}_2(\text{dipic-X})]^-$  complexes in this environment are also listed Table 3.2 and were also plotted against the Hammett  $s_{\text{para}}$  constants, Figure 3.6. The data was fitted to a linear regression with a  $r = -6.8$  and an  $r^2 = 92\%$ . The slight changes to the  $r$  (-6.7 to -6.8) and  $r^2$  (88% to 92%) from the plot of aqueous  $[\text{VO}_2(\text{dipic-X})]^-$  could be attributed to the fact one less point was included on this plot. The low solubility of the  $[\text{VO}_2(\text{dipic-NH}_2)]^-$  material rendered a sample that was not transparent and the data thus not used. The linear plot shown in Figure 3.6 demonstrates that the pattern observed in aqueous solution is upheld in the more hydrophobic environment of the RM system.

In order to use this data to examine the difference between the aqueous environment and the RMs environment we compared the chemical shifts in the aqueous and the reverse micelle solutions and the difference ( $\delta_{\text{RMX}} - \delta_{\text{aqX}}$ ) is listed in Table 3.2. Plotting  $\delta_{\text{RMX}} - \delta_{\text{aqX}}$  as a function of the Hammett  $\sigma_{\text{para}}$  also resulted in a linear relationship, Figure 3.7. As shown from this plot, a correlation of the  $\rho = -2.18$  and  $r^2 = 88\%$ . This correlation reflects the fact that all these derivatives show differences based on the electronic changes in the complexes and their response to the specific environment in the heterogeneous micelles. Thus, the complex located in the aqueous pool will respond differently than the compounds located at the interface. The fact that

the chemical shift for  $[\text{VO}_2(\text{dipic})]^-$  changes little as the compound is placed in the reverse micelle likely arise from counteracting effects that cancel each other out. Thus, the downfield shift observed by complex penetration is countered by the upfield effect found when placing the polar complex in a hydrophobic environment and requiring more electron donation from the pyridine nitrogen. The smaller  $\rho$  value than observed in the correlations shown in Figures 3.5 and 3.6 show that there is less substitution change when exploring the combined substituent and environments in reverse micelles. Reduced substituent effects in a less polar and more hydrophobic environment have been reported when comparing the basicity of pyridines in ionic liquids with basicity in aqueous solution.<sup>65,66</sup>

The plot shown in Figure 3.7 clearly separates out the  $-\text{NO}_2$  derivative from the others. The differences in the  $-\text{OH}$  and  $-\text{Cl}$  derivatives are interesting particularly in the light of the FT-IR data that suggests the compounds are located near the same interfacial locations. Together the data for the  $-\text{OH}$  and  $-\text{Cl}$  derivatives shows that although these compounds have very different electronic properties, when combined with their interaction with interfaces the overall net result is that these effects in part can cancel out. It is most likely to be the combined effects of the electronics and the location of the compounds that drives their specific the insulin enhancing properties can be inferred. Perhaps the most important observation for the compounds under investigation is that the modification of the dipic did not adversely impact their insulin enhancing properties.

In these studies with the V-dipic complexes we conclude that substituents do affect how the drugs interact with interfaces. Chen et al. also reached such conclusion in a series of studies probing pyridine and quinolone analogs and their membrane permeability using computational modeling.<sup>67</sup> Sakurai et al. evaluated substituent effects of vanadium(IV)(pic)<sub>2</sub> and noted that the

4 position of the pyridine ring had the greatest effect on  $\log P$ .<sup>10</sup> This series of vanadium complexes did exhibit a SAR relationship showing that the substitution with a halogen improved the insulin enhancing effects the most. In a very different venue, the substituent effects of vanadium(V) dipicolinate complexes have also been evaluated in association with their catalyst properties oxidizing lignin and analogs.<sup>68</sup> The studies shown in this work also demonstrate that Hammett correlation can predict the properties of the  $[\text{VO}_2(\text{dipic-X})]^-$  series of compounds.

The introduction of substituents modifies the complex properties as anticipated in both aqueous solution and in micellar environments. Hammett correlations were previously used to relate stability constants to  $\sigma$  values for a series of silver, copper and iron complexes.<sup>69</sup> We had previously examined the stability of these complexes in solution, and did not find a correlation with the complex stability.<sup>13</sup> This suggested that the counteracting factors for the stability of these complexes existed in aqueous solution. The studies reported here investigated the environments of the complexes near an interface and documented a linear free energy relationship with regard to the  $^{51}\text{V}$  NMR chemical shift in interfacial environment. However, insulin-enhancing properties is a complex parameter to measure. Such effects will vary with the biological system and what particular physical parameters are investigated. Thus, identifying simple parameters that are true predictors is non-trivial. We were interested in investigating the complex properties of the systems because changes in complex electronic properties could potentially affect their reactivity, processing and shift the mode of action and presumed insulin enhancing effects. Perhaps most significantly, this study resulted in the recognition that all the complexes that were found to have insulin-enhancing effects were also found to interact with the interface in some manner.

## CONCLUSIONS

In the above studies we investigated the properties of a series of insulin-enhancing compounds with regard to their physical properties and inherent ability to associate with interfaces to identify possible correlations. We selected a series of drugs that have previously been examined in animal studies and showed similar insulin-enhancing properties.<sup>13</sup> Specifically, we investigated the ability of the drugs in association with model membrane interfaces using differential FT-IR spectroscopy. These studies were based on monitoring the OD stretch in the water pool of the reverse micelle samples. The drugs that are associated with the interface will show little perturbation of the OD stretch, whereas drugs that are located in the water pool will interact strongly with the water molecules and change the H-bonding resulting in a large shift. We found that the insulin enhancing drugs in the [VO<sub>2</sub>dipic]<sup>-</sup> series that have been shown to be effective in animal studies were all associated with the interface to some degree.

To further investigate these systems we also examined their inherent electronic properties and environment of the complexes using <sup>51</sup>V NMR spectroscopy. These studies were carried out because the <sup>51</sup>V NMR nucleus is particularly sensitive to electronic changes, and the possibility that this system be used as a sensitive probe was evaluated. In these studies we found that the <sup>51</sup>V NMR chemical shifts of the [VO<sub>2</sub>dipic]<sup>-</sup> series correlate with the Hammett  $\sigma_{\text{para}}$  constants both in aqueous solution and in the microemulsion environments. In addition, when comparing the chemical shifts of the [VO<sub>2</sub>dipic]<sup>-</sup> series in aqueous solution with the more hydrophobic environment using the  $(\delta_{\text{RMX}} - \delta_{\text{aqX}})$  a correlation with the Hammett  $\sigma_{\text{para}}$  constants were also observed. These results show that although the environment of the vanadium compound may change, its inherent properties remain, which may be what cause the insulin enhancing effects. It is possible that the inherent reactivity and properties are important to formation of the as of yet

unidentified active pool of vanadium that was recently proposed based on pharmacokinetic studies in diabetic human beings.<sup>31</sup>

FIGURES AND TABLES

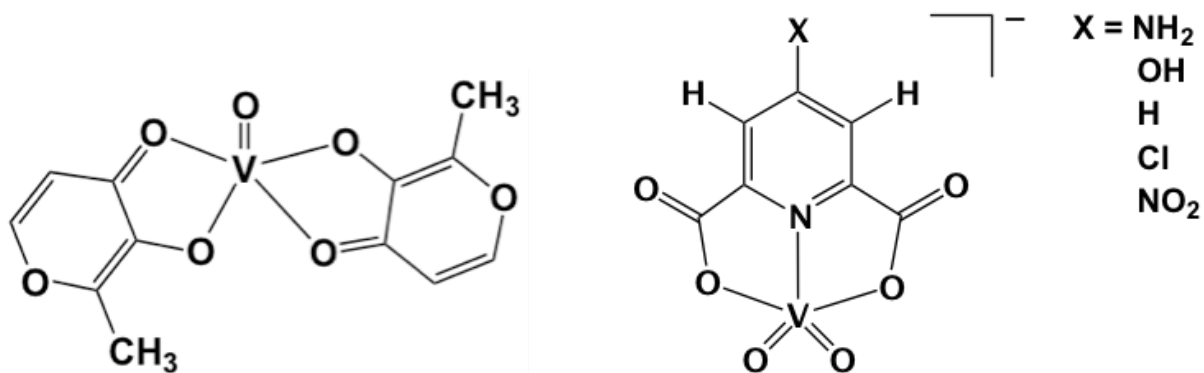


Figure 3.1. The structure of BMOV and [VO<sub>2</sub>(dipic-X)]<sup>-</sup>.

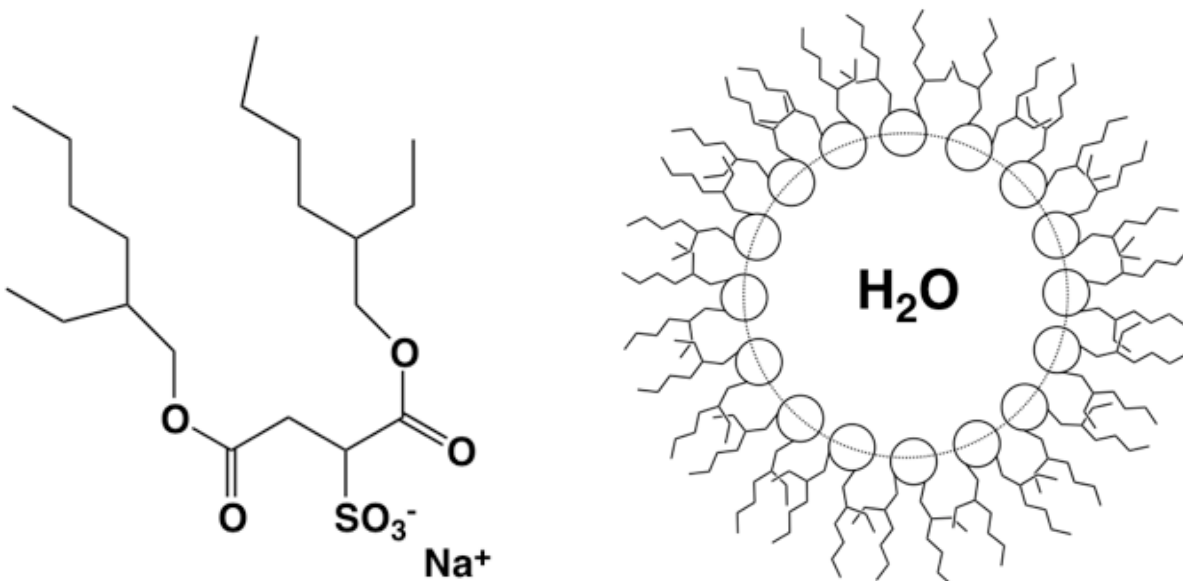


Figure 3.2. The structure of NaAOT and a reverse micelle (RMs).

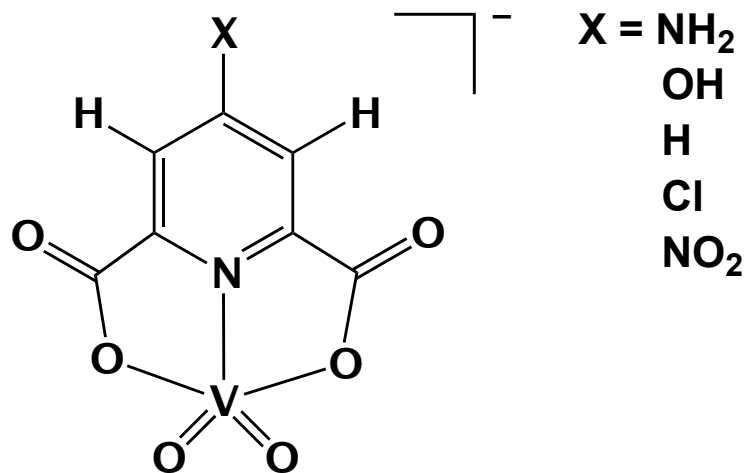


Figure 3.3. Substituents replacements on  $[\text{VO}_2\text{dipic}]^-$ .

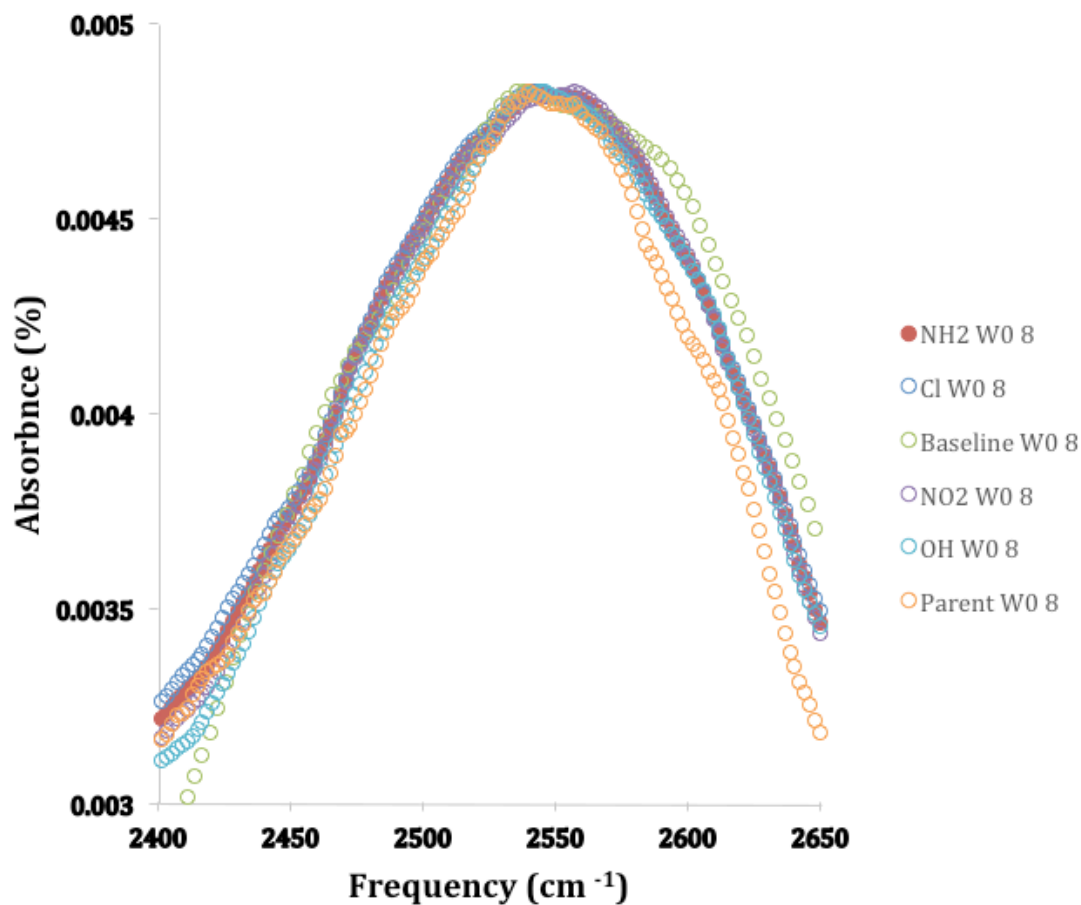


Figure 3.4. Background subtracted FT-IR spectra of the OD stretching frequency of 50 mM  $[\text{VO}_2(\text{dipic})]^-$ ,  $[\text{VO}_2(\text{dipic-OH})]^-$ ,  $[\text{VO}_2(\text{dipic-Cl})]^-$ ,  $[\text{VO}_2(\text{dipic-NH}_2)]^-$  or  $[\text{VO}_2(\text{dipic-NH}_2)]^-$ . The aqueous stock solutions were pH adjusted to  $\sim 3.5$ . The sample contained AOT RMs at  $w_o = 8$ . The concentrations for the stock solutions were 750mM AOT.

Table 3.1. Background subtracted FT-IR maxima for the OD stretching frequency. The samples were made twice (one 5% HOD and one H<sub>2</sub>O) and subtracted. The aqueous stock solutions were pH adjusted to ~3.5. The sample contained AOT RMs at  $w_0 = 6, 8, 10$  and 12. The concentrations for the stock solutions were 750mM AOT and 50 mM [VO<sub>2</sub>(dipic-Cl)]<sup>-</sup>.

$w_0$	No Probe (cm <sup>-1</sup> )	0.5 mM [VO <sub>2</sub> (dipic)] <sup>-</sup> (cm <sup>-1</sup> )	0.5mM [VO <sub>2</sub> (dipic-Cl)] <sup>-</sup> (cm <sup>-1</sup> )	0.5mM [VO <sub>2</sub> (dipic-OH)] <sup>-</sup> (cm <sup>-1</sup> )
6*	2546	2549	2547	Not Run
8	2541 ± 1.5	2541 ± 1.3	2551 ± 3.5	2546 ± 4
10	2528 ± 0.5	2553 ± 3	2538 ± 2	2539 ± 2
12*	2524	2526	2524	2528

\* Indicates only one run per sample, no statistical analysis was performed.

Table 3.2. Background subtracted FT-IR maxima for the OD stretching frequency. The samples were made twice (one 5% HOD and one H<sub>2</sub>O) and subtracted. The aqueous stock solutions were pH adjusted to ~3.5. The sample contained AOT RMs at  $w_0 = 8$ . The concentrations for the stock solutions were 750mM AOT and 50 mM [VO<sub>2</sub>(dipic-X)]<sup>-</sup> except for [VO<sub>2</sub>(dipic-Cl)]<sup>-</sup> and [VO<sub>2</sub>(dipic-NH<sub>2</sub>)]<sup>-</sup>.

Aqueous phase in $w_0 = 8$ AOT RM samples	Peak Avg. cm <sup>-1</sup>	St. Dev.
No Probe	2542	1.5
0.5 mM [VO <sub>2</sub> (dipic)] <sup>-</sup>	2542	1.3
0.5mM [VO <sub>2</sub> (dipic-Cl)] <sup>-</sup>	2551	3.5
0.5mM [VO <sub>2</sub> (dipic-OH)] <sup>-</sup>	2546	4.0
0.5mM [VO <sub>2</sub> (dipic- NO <sub>2</sub> )] <sup>-</sup>	2558	1.4
0.5mM [VO <sub>2</sub> (dipic- NH <sub>2</sub> )] <sup>-</sup>	2540	0.5

Table 3.3. The  $^{51}\text{V}$  NMR chemical shift resonances for aqueous  $[\text{VO}_2(\text{dipic-X})]^-$  and the  $[\text{VO}_2(\text{dipic-X})]^-$  complexes in AOT RM samples and the Hammett  $\sigma_{\text{para}}$  values for substituents.

$[\text{VO}_2(\text{dipic-X})]^-$	$^{51}\text{V } \delta_{\text{aq}}^{(a)}$	$^{51}\text{V } \delta_{\text{RM}}^{(a)}$	$^{51}\text{V } \delta_{\text{RM}} - \delta_{\text{aq}}^{(b)}$	$\sigma_{\text{para}}$
$\text{NH}_2$	-524.71	- <sup>(b)</sup>	- <sup>(b)</sup>	-0.66
$\text{OH}$	-529.40	-527.64	1.76	-0.37
$\text{H}$	-532.13	-532.04	0.09	0.00
$\text{Cl}$	-532.82	-532.74	0.08	0.23
$\text{NO}_2$	-534.76	-535.69	-0.93	0.78

- (a) The  $^{51}\text{V}$  NMR chemical shift values were referenced against an external  $\text{VOCl}_3$  standard.  
 (b) The  $[\text{VO}_2(\text{dipic-NH}_2)]^-$  AOT RM sample formed precipitates and the signal was extremely broadened.

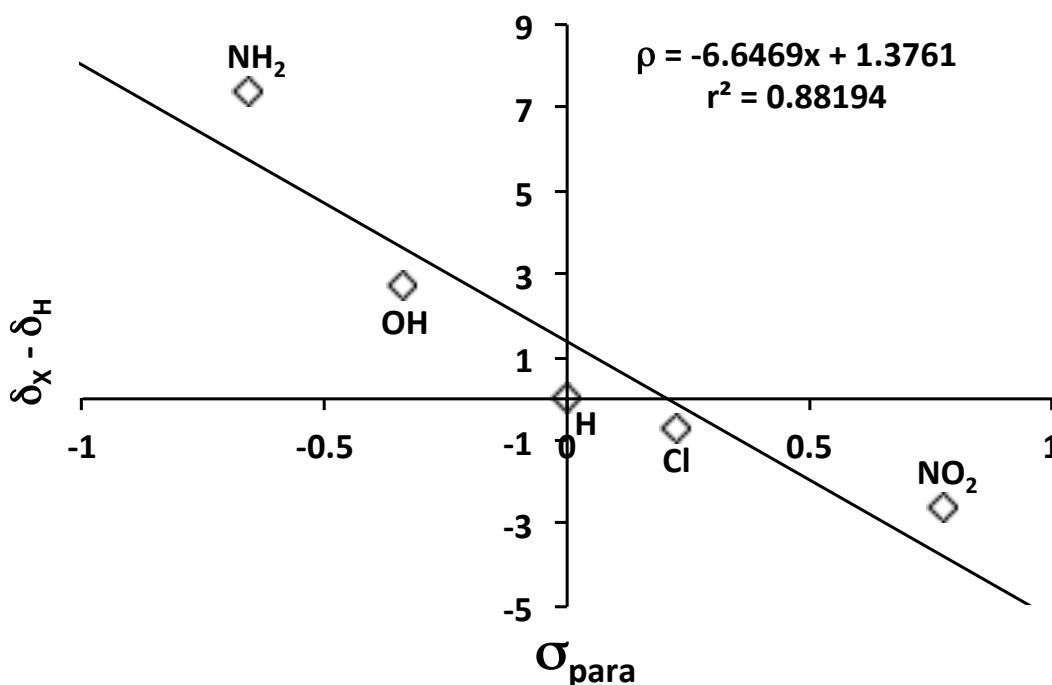


Figure 3.5. The  $^{51}\text{V}$  NMR chemical shifts difference of dipicolinatooxovanadium(V) complexes ( $\delta_{\text{X}} - \delta_{\text{H}}$ ) were plotted as a function of the Hammett  $\sigma_{\text{para}}$  constants. Samples contained 50 mM dipicolinatooxovanadium(V)  $[\text{VO}_2(\text{dipic-X})]^-$  in  $\text{D}_2\text{O}$  at  $\text{pH} \sim 3$ . The samples (X was OH, H, Cl,  $\text{NH}_2$  or  $\text{NO}_2$ ) were referenced to  $\text{VOCl}_3$  externally at 79 MHz ( $^1\text{H}$ -300 MHz spectrometer).

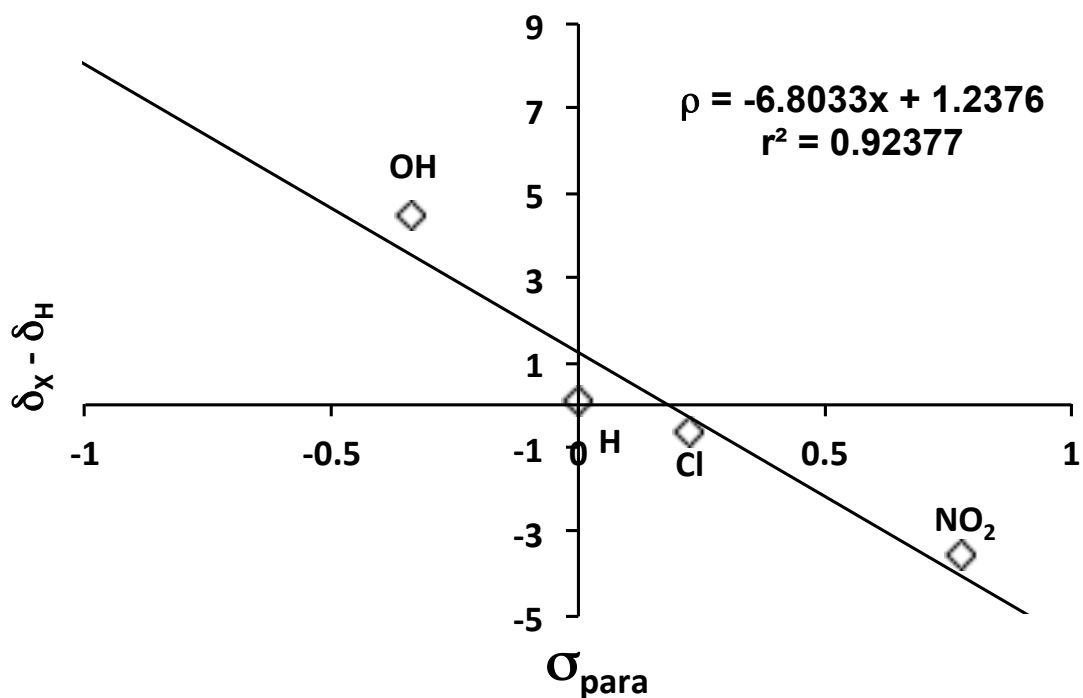


Figure 3.6. The  $^{51}\text{V}$  NMR chemical shifts difference of dipicolinatooxovanadium(V) complexes ( $\delta_{\text{RMX}} - \delta_{\text{RMH}}$ ) were plotted as a function of the Hammett  $\sigma_{\text{para}}$  constants. Samples contained 50 mM dipicolinatooxovanadium(V)  $[\text{VO}_2(\text{dipic-X})]^-$  in  $\text{D}_2\text{O}$  at pH  $\sim 3$  added to 750 mM AOT in isooctane with a  $w_o = 12$ . The samples (X was OH, H, Cl or  $\text{NO}_2$ ) were referenced to  $\text{VOCl}_3$  externally at 79 MHz ( $^1\text{H}$ -300 MHz spectrometer).

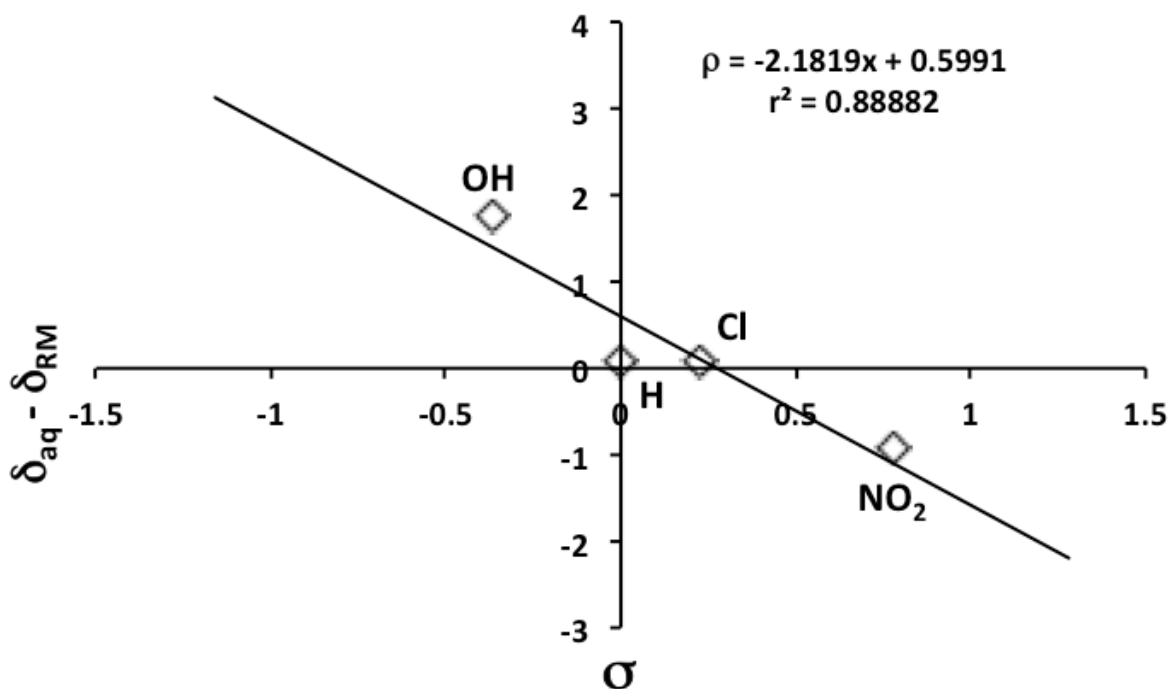


Figure 3.7. The  $^{51}\text{V}$  NMR chemical shifts difference of dipicolinatooxovanadium(V) complexes between the aqueous and micellar environment ( $\delta_{\text{RMX}} - \delta_{\text{RMH}}$ ) were plotted as a function of the Hammett  $\sigma_{\text{para}}$  constants. Aqueous samples contained 50 mM dipicolinatooxovanadium(V)  $[\text{VO}_2(\text{dipic-X})]^-$  in  $\text{D}_2\text{O}$  at pH  $\sim 3$ . Reverse micellar samples contained 50 mM dipicolinatooxovanadium(V)  $[\text{VO}_2(\text{dipic-X})]^-$  in  $\text{D}_2\text{O}$  at pH  $\sim 3$  added to 750 mM AOT in isooctane with a  $w_o = 12$ . The samples (X was OH, H, Cl or  $\text{NO}_2$ ) were referenced to  $\text{VOCl}_3$  externally at 79 MHz ( $^1\text{H}$ -300 MHz spectrometer).

SUPPLEMENTAL INFORMATION

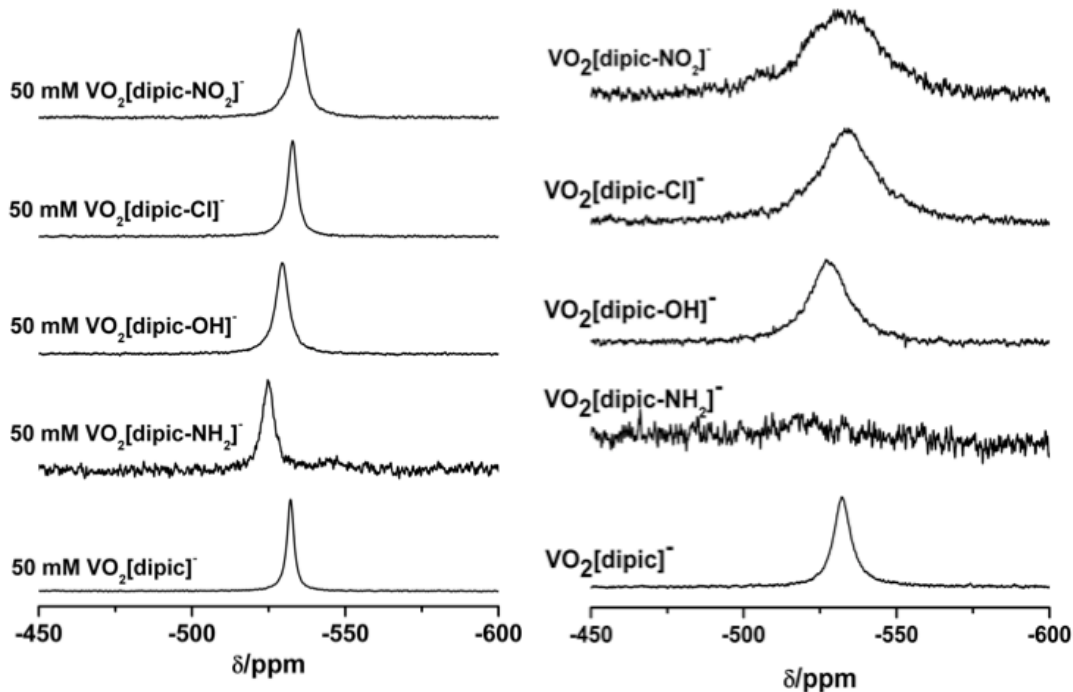


Figure S3.1. (right) A stacked plot of  $^{51}\text{V}$  NMR spectra acquired for vanadium(V) dipicolinate complexes with substituents, H,  $\text{NH}_2$ , OH, Cl,  $\text{NO}_2$ . 50 mM vanadium complex was added to  $\text{D}_2\text{O}$  solutions with a pH of  $\sim 3$ . (left) A similar  $^{51}\text{V}$  NMR stacked plot of RMs composed of 750 mM AOT in iso-octane. The aqueous phase was added to equal a  $w_o$  of 12 containing 50 mM vanadium(V) dipicolinate in  $\text{D}_2\text{O}$  at pH  $\sim 3$ .

## REFERENCES

- (1) McNeil, J. H.; Yuen, V. G.; Hoveyda, H. R.; C., O. *Journal of Medicinal Chemistry* **1992**, *35*, 1489-1491.
- (2) Reul, B. A.; Amin, S. S.; Buchet, J.-P.; N., O. L.; Crans, D. C.; Brichard, S. M. *British Journal of Pharmacology* **1999**, *126*, 467-477.
- (3) Anderson, R. A. *Diabetes & Metabolism* **2000**, *26*, 22-27.
- (4) Yasui, H.; Takechi, K.; Sakurai, H. *Journal of Inorganic Biochemistry* **2000**, *78*, 185-196.
- (5) Rehder, D.; Pessoa, J. C.; Geraldes, C.; Castro, M.; Kabanos, T.; Kiss, T.; Meier, B.; Micera, G.; Pettersson, L.; Rangel, M.; Salifoglou, A.; Turel, I.; Wang, D. R. *Journal of Biological Inorganic Chemistry* **2002**, *7*, 384-396.
- (6) Yang, L. Q.; Crans, D. C.; Miller, S. M.; la Cour, A.; Anderson, O. P.; Kaszynski, P. M.; Godzala, M. E.; Austin, L. D.; Willsky, G. R. *Inorganic Chemistry* **2002**, *41*, 4859-4871.
- (7) Crans, D. C. *Journal of Inorganic Biochemistry* **2000**, *80*, 123-131.
- (8) Thompson, K. H.; Chiles, J.; Yuen, V. G.; Tse, J.; McNeill, J. H.; Orvig, C. *Journal of Inorganic Biochemistry* **2004**, *98*, 683-690.
- (9) Adachi, Y.; Yoshikawa, Y.; Yoshida, J.; Kodera, Y.; Katoh, A.; Takada, J.; Sakurai, H. *Biochemical and Biophysical Research Communications* **2006**, *345*, 945-950.
- (10) Sakurai, H. *ACS Symposium Series* **2007**, *974*, 110-120.
- (11) Thompson, K. H.; Lichter, J.; LeBel, C.; Scaife, M. C.; McNeill, J. H.; Orvig, C. *Journal of Inorganic Biochemistry* **2009**, *103*, 554-558.

- (12) Jakusch, T.; Pessoa, J. C.; Kiss, T. *Coordination Chemistry Reviews* **2011**, *255*, 2218-2226.
- (13) Willsky, G. R.; Chi, L.; Godzala III, M.; Kostyniak, P. J.; Smee, J. J.; Trujillo, A. M.; Alfano, J. A.; Ding, W.; Hu, Z.; Crans, D. C. *Coordination Chemistry Reviews* **2011**, *255*, 2258-2262.
- (14) Pereira, M. J.; Carvalho, E.; Eriksson, J. W.; Crans, D. C.; Aureliano, M. *Journal of Inorganic Biochemistry* **2009**, *103*, 1687-1692.
- (15) Brautigan, D. L.; Kruszewski, A.; Wang, H. *Biochemical and Biophysical Research Communications* **2006**, *347*, 769-773.
- (16) Poucheret, P.; Verma, S.; Grynepas, M. D.; McNeill, J. H. *Molecular and Cellular Biochemistry* **1998**, *188*, 73-80.
- (17) Nakai, M.; Watanabe, H.; Fujiwara, C.; Kakegawa, H.; Satoh, T.; Takada, J.; Matsushita, R.; Sakurai, H. *Biological & Pharmaceutical Bulletin* **1995**, *18*, 719-725.
- (18) Lu, B.; Ennis, D.; Lai, R.; Bogdanovic, E.; Nikolov, R.; Salamon, L.; Fantus, C.; Le-Tien, H.; Fantus, I. G. *Journal of Biological Chemistry* **2001**, *276*, 35589-35598.
- (19) Mehdi, M. Z.; Srivastava, A. K. *Archives of Biochemistry and Biophysics* **2005**, *440*, 158-164.
- (20) Willsky, G. R.; Chi, L. H.; Liang, Y. L.; Gaile, D. P.; Hu, Z. H.; Crans, D. C. *Physiological Genomics* **2006**, *26*, 192-201.
- (21) Wei, D.; Li, M.; Ding, W. *Journal of Biological Inorganic Chemistry* **2007**, *12*, 1265-1273.
- (22) Cros, G. H.; Cam, M. C.; Serrano, J. J.; Ribes, G.; McNeill, J. H. *Molecular and Cellular Biochemistry* **1995**, *153*, 191-195.

- (23) Goldfine, A. B.; Patti, M. E.; Zuberi, L.; Goldstein, B. J.; LeBlanc, R.; Landaker, E. J.; Jiang, Z. Y.; Willsky, G. R.; Kahn, C. R. *Metabolism-Clinical and Experimental* **2000**, *49*, 400-410.
- (24) Zhang, Y.; Yang, X. D.; Wang, K.; Crans, D. C. *Journal of Inorganic Biochemistry* **2006**, *100*, 80-87.
- (25) Smee, J. J.; Epps, J. A.; Ooms, K.; Bolte, S. E.; Polenova, T.; Baruah, B.; Yang, L. Q.; Ding, W. J.; Li, M.; Willsky, G. R.; la Cour, A.; Anderson, O. P.; Crans, D. C. *Journal of Inorganic Biochemistry* **2009**, *103*, 575-584.
- (26) Buglyo, P.; Crans, D. C.; Nagy, E. M.; Lindo, R. L.; Yang, L. Q.; Smee, J. J.; Jin, W. Z.; Chi, L. H.; Godzala, M. E.; Willsky, G. R. *Inorganic Chemistry* **2005**, *44*, 5416-5427.
- (27) Yang, L. Q.; La Cour, A.; Anderson, O. P.; Crans, D. C. *Inorganic Chemistry* **2002**, *41*, 6322-6331.
- (28) Li, M.; Smee, J. J.; Ding, W. J.; Crans, D. C. *Journal of Inorganic Biochemistry* **2009**, *103*, 585-589.
- (29) Crans, D. C.; Trujillo, A. M.; Pharazyn, P. S.; Cohen, M. D. *Coordination Chemistry Reviews* **2011**, *255*, 2178-2192.
- (30) Smee, J. J.; Epps, J. A.; Teissedre, G.; Maes, M.; Harding, N.; Yang, L.; Baruah, B.; Miller, S. M.; Anderson, O. P.; Willsky, G. R.; Crans, D. C. *Inorganic Chemistry* **2007**, *46*, 9827-9840.
- (31) Willsky, G. R.; Halvorsen, K.; Godzala III, M.; Chi, L.; Most, M. J.; Kaszynki, P.; Crans, D. C.; Goldfine, A. B.; Kostyniak, P. J. *Metallomics* **2013**.
- (32) Warschawski, D. E.; Arnold, A. A.; Beaugrand, M.; Gravel, A.; A., C.; A., M. *Biochemica et Biophysica Acta* **2012**, *1808*, 1957-1974.

- (33) De, T.; Maitra, A. *Advancements in Colloid Interface Science* **1995**, *59*, 95-193.
- (34) Maitra, A. *Journal of Physical Chemistry* **1984**, *88*, 5122-5125.
- (35) Crans, D. C.; Rithner, C. D.; Baruah, B.; Gourley, B. L.; Leveinger, N. E. *Journal of the American Chemical Society* **2006**, *128*, 4437-4445.
- (36) Crans, D. C.; Trujillo, A. M.; Bonetti, S.; Rithner, C. D.; Baruah, B.; Levinger, N. E. *Journal of Organic Chemistry* **2008**, *73*, 9633-9640.
- (37) Johnson, M. D.; Lorenz, B. B.; Wilkins, P. C.; Lemons, B. G.; Baruah, B.; Lamborn, N.; Stahla, M.; Chatterjee, P. B.; Richens, D. T.; Crans, D. C. *Inorganic Chemistry* **2012**, *51*, 2757-2765.
- (38) Sedgwick, M.; Cole, R. L.; Rithner, C. D.; Crans, D. C.; Levinger, N. E. *Journal of the American Chemical Society* **2012**, *134*, 11904-11907.
- (39) Crans, D. C.; Yang, L. Q.; Alfano, J. A.; Chi, L. A. H.; Jin, W. Z.; Mahroof-Tahir, M.; Robbins, K.; Toloue, M. M.; Chan, L. K.; Plante, A. J.; Grayson, R. Z.; Willsky, G. R. *Coordination Chemistry Reviews* **2003**, *237*, 13-22.
- (40) Ooms, K. J.; Bolte, S. E.; Smee, J. J.; Baruah, B.; Crans, D. C.; Polenova, T. *Inorganic Chemistry* **2007**, *46*, 9285-9293.
- (41) Bolte, S. E.; Ooms, K. J.; Polenova, T.; Baruah, B.; Crans, D. C.; Smee, J. J. *Journal of Chemical Physics* **2008**, *128*.
- (42) Chatterjee, P. B.; Goncharov-Zapata, O.; Hou, G.; Polenova, T.; Crans, D. C. *European Journal of Inorganic Chemistry* **2012**, 4644-4651.
- (43) Chatterjee, P. B.; Goncharov-Zapata, O.; Quinn, L. L.; Hou, G.; Hamaed, H.; Schurko, R. W.; Polenova, T.; Crans, D. C. *Inorganic Chemistry* **2011**, *50*, 9794-9803.

- (44) Chowdhury, P. K.; Ashby, K. D.; Datta, A.; Petrich, J. W. *Photochemistry and Photobiology* **2000**, *72*, 612-618.
- (45) Wieghardt, K. *Inorganic Chemistry* **1978**, *17*, 57-64.
- (46) Wieghardt, K. *Inorganic Chemistry* **1978**, *17*, 57-64.
- (47) Crans, D. C.; Mahroof-Tahir, M.; Johnson, M. D.; Wilkins, P. C.; Yang, L. Q.; Robbins, K.; Johnson, A.; Alfano, J. A.; Godzala, M. E.; Austin, L. T.; Willsky, G. R. *Inorganica Chimica Acta* **2003**, *356*, 365-378.
- (48) Moilanen, D. E.; Fenn, E. E.; Wong, D.; Fayer, M. D. *The Journal of Chemical Physics* **2009**, *131*, 1-9.
- (49) Johnson, M. D.; Lorenz, B. B.; Wilkins, P. C.; Lemons, B. G.; Baruah, B.; Lamborn, N.; Stahla, M.; Chatterjee, P. B.; Richens, D. T.; Crans, D. C. *Inorganic Chemistry* **2012**, *51*, 2757-2765.
- (50) Crans, D. C.; Baruah, B.; Ross, A.; Levinger, N. E. *Coordination Chemistry Reviews* **2009**, *253*, 2178-2185.
- (51) Li, M.; Ding, W. J.; Smee, J. J.; Baruah, B.; Willsky, G. R.; Crans, D. C. *Biometals* **2009**, *22*, 895-905.
- (52) Hansch, C.; Leo, A.; Taft, R. W. *Chemical Review* **1991**, *91*, 165-195.
- (53) Hagen, H.; Barbon, A.; van Faassen, E. E.; Lutz, B. T. G.; Boersma, J.; Spek, A. L.; van Koten, G. *Inorganic Chemistry* **1999**, *38*, 4079-4086.
- (54) Mondal, B.; Ghosh, T.; Sutradhar, M.; Mukherjee, G.; Drew, M. G. B.; Ghosh, T. *Polyhedron* **2008**, *27*, 2193-2201.
- (55) Holmes, S.; Carrano, C. J. *Inorganic Chemistry* **1991**, *30*, 1231-1235.

- (56) Ghosh, T.; Mondal, B.; Ghosh, T.; Sutradhar, M.; Mukherjee, G.; Drew, M. G. B. *Inorganica Chimica Acta* **2007**, *360*, 1753-1761.
- (57) El-Sonbati, A. Z.; Belal, A. A. M.; El-Gharib, M. S.; Morgan, S. M. *Spectrochimica Acta Part A: Molecular and Biomolecular Spectroscopy* **2012**, *95*, 627-636.
- (58) Rehder, D. *Bulletin of Magnetic Resonance* **1982**, *4*, 33-83.
- (59) Goncharov-Zapata, O.; Chatterjee, P. B.; Hou, G.; Quinn, L. L.; Li, M.; Yehl, J.; Crans, D. C.; Polenova, T. *CrystEngComm* **2013**, ASAP.
- (60) Crans, D. C.; Shin, P. K. *Journal of the American Chemical Society* **1994**, *116*, 1305-1315.
- (61) Diab, M. A.; El-Bindary, A. A.; El-Sonbati, A. Z.; Salem, O. L. *Journal of Molecular Structure* **2012**, *1018*, 176-184.
- (62) Lynch, B. M. *Organic Magnetic Resonance* **1973**, *6*, 190-192.
- (63) Salmon, M.; Jimenez, A.; Salazar, I.; Zawadzki, R. *Journal of Chemical Education* **1973**, *50*, 370-371.
- (64) Bonesi, S. M.; Ponce, M. A.; Erra-Balsells, R. *Journal of Heterocyclic Chemistry* **2005**, *42*, 867-875.
- (65) Angelini, G.; De Maria, P.; Chiappe, C.; Fontana, A.; Pierini, M.; Siani, G. *Journal of Organic Chemistry* **2010**, *75*, 3912-3915.
- (66) Ebrahimi, A.; Habibi, M.; Masooodi, H. R.; Gholipour, A. R. *Chemical Physics* **2009**, *355*, 67-72.
- (67) Chen, I. J.; Taneja, R.; Yin, D.; Seo, P. R.; Young, D.; MacKerell, A. D.; Politi, M. J. *Molecular Pharmaceutics* **2005**, *3*, 745-755.

(68) Hanson, S. K.; Baker, R. T.; Gordon, J. C.; Scott, B. L.; Silks, L. A.; Thorn, D. L.

*Journal of the American Chemical Society* **2010**, *132*, 17804-17816.

(69) Frausto, J. J.; Goncalves Calado, J. *Journal of Inorganic Nuclear Chemistry* **1966**, *28*,

125-138.

## CONCLUSIONS

Experiments probing the passive uptake of  $[\text{VO}_2(\text{dipic})]^-$  and the effect of cholesterol in simplified systems were performed. Anti-diabetic agent,  $[\text{VO}_2(\text{dipic})]^-$  is absorbed through an unclear mechanism, however a passive mechanism is proposed <sup>1,2</sup>. RMs formed solution-state membrane mimics absent of protein transport machinery. Solution state spectroscopy probed the localization of  $\text{dipic}^{2-}$ .  $[\text{VO}_2(\text{dipic})]^-$  was evaluated for substituent effects altering permeation. Cholesterol incorporation into CTAB RMs developed an improved model containing the critical natural membrane component.

The small intestine contains  $\sim 120 \text{ m}^2$  of membrane surface area <sup>3</sup>. As a result, membrane interaction is a critical property for absorption.  $\text{Dipic}^{2-}$  permeated the AOT RM interface, playing a role in permeation, correlating with  $[\text{VO}_2(\text{dipic})]^-$  <sup>2</sup>.  $\text{Dipic}^{2-}$  permeated against intuition and established rules <sup>4</sup>. Substituent effects altered the properties of  $[\text{VO}_2(\text{dipic})]^-$ . However contrasting effects cancel each other out minimizing the observed effect. This conclusion is corroborated by the *in vivo* anti-diabetic properties <sup>5</sup> and *in vitro* uptake data <sup>6</sup>. Cholesterol altered CTAB RMs increasing interfacial packing and enhancing  $\text{H}^+$  transfer. Cholesterol samples provided data supporting a liquid disordered ( $L_d$ ) to liquid ordered ( $L_o$ ) effect and may produce a model system that closely mimics natural membranes.

After absorption  $[\text{VO}_2(\text{dipic})]^-$  may dissociate and bind ferritin <sup>7</sup>, reduce through glutathione <sup>8</sup> or ascorbic acid <sup>9</sup>, promote oxidative stress <sup>10,11</sup>, or remain intact forming stable complexes in the hydrocarbon tails <sup>12</sup>. All these routes are possible and could occur prior to distribution through human serum transferrin <sup>13</sup>. The complex chemistry of vanadium increases

the difficulty in determining the active form of the drug. However, it is clear that membrane permeation is key to the anti-diabetic action of  $[\text{VO}_2(\text{dipic})]^-$ .

### *Further Studies*

This work inspired experimentation on  $\text{dipic}^{2-}$  in CTAB Ms and RMs,<sup>14</sup> concentration dependence of  $\text{dipic}^{2-}$  permeation (*Chatterjee, unpublished*), permeation of  $(\text{dipic-OH})^{2-}$  (*Chatterjee, unpublished*) and 3,5-dipic. The effect of charge on the permeation of dipic has also been initiated, however further experimentation is needed. Further explorations using pyridine investigating the effects of carboxylate ( $\text{COO}^-$ ) groups would apply to drug absorption. Studying the localization of vanadate would provide data on the behavior of the dissociated product. Functional groups  $\text{OCH}_3$ ,  $\text{CH}_3$  and  $\text{C}_6\text{H}_5$  (methoxyl, methyl, benzyl) promoted permeability in modeling studies<sup>15,16</sup> and may increase permeability in  $[\text{VO}_2(\text{dipic})]^-$ .

Characterization determining the location of cholesterol in CTAB RMs is needed. Studies evaluating higher viscosity solvents by DLS and NMR may define the effect of cholesterol. NOE spectra acquired as part of this work should be re-analyzed after defining the location of 1-pentanol within the system. Determining if cholesterol concentration plays a role in the observed  $\text{H}^+$  transfer changes may apply to many biological systems. Concentration experiments were not been attempted in the CTAB system. However, a preliminary series using 6:1 to 2:1 AOT: cholesterol resulted in viscous gel-like substances at higher cholesterol concentrations. Cholesterol containing mixed surfactant gels were useful for drug targeting of lymphatic tissue<sup>17</sup>. Analysis of alcohol co-surfactants would be an important study as cholesterol is soluble in long chain alcohols<sup>18</sup>. The experiments of chapter 1 were performed at 25 °C, the affect of temperature on  $\text{H}^+$  transfer rates would increase biological relevancy, specifically experiments at

~37 °C. Lastly, combining the cholesterol containing model system with  $[\text{VO}_2(\text{dipic})]^-$  should be performed to probe the permeability and stability of  $[\text{VO}_2(\text{dipic})]^-$  in a cholesterol containing model system.

## REFERENCES

- (1) Zhang, Y.; Yang, X.; Wang, K. *Chinese Science Bulletin* **2005**, *50*, 1854-1859.
- (2) Crans, D. C.; Rithner, C. D.; Baruah, B.; Gourley, B. L.; Levinger, N. E. *Journal of the American Chemical Society* **2006**, *128*, 4437-4445.
- (3) Kararli, T. T. *Biopharmaceutics and Drug Disposition* **1995**, *16*, 351-380.
- (4) Abraham, M. H. *Journal of Pharmaceutical Sciences* **2011**, *100*, 1690-1701.
- (5) Willsky, G. R.; Chi, L.; Godzala III, M.; Kostyniak, P. J.; Smee, J. J.; Trujillo, A. M.; Alfano, J. A.; Ding, W.; Hu, Z.; Crans, D. C. *Coordination Chemistry Reviews* **2011**, *255*, 2258-2262.
- (6) Zhang, Y.; Yang, X. D.; Wang, K.; Crans, D. C. *Journal of Inorganic Biochemistry* **2006**, *100*, 80-87.
- (7) Chasteen, N. D.; Lord, E. M.; Thompson, H. J.; Grady, J. K. *Biochimica Et Biophysica Acta* **1986**, *884*, 84-92.
- (8) Dorneyi, A.; Marcao, S.; Pessoa, J. C.; Jakusch, T.; Kiss, T. *European Journal of Inorganic Chemistry* **2006**, 3614-3621.
- (9) Wilkins, P. C.; Johnson, M. D.; Holder, A. A.; Crans, D. C. *Inorganic Chemistry* **2006**, *45*, 1471-1479.
- (10) Crans, D. C.; Baruah, B.; Gaidamauska, E.; Lemons, B. G.; Lorenz, B. B.; Johnson, M. D. *Journal of Inorganic Biochemistry* **2008**, *102*, 1334-1347.
- (11) Yang, X. G.; Yang, X. D.; Yuan, L.; Wang, K.; Crans, D. C. *Pharmaceutical Research* **2004**, *21*, 1026-1033.

- (12) Crans, D. C.; Trujillo, A. M.; Pharazyn, P. S.; Cohen, M. D. *Coordination Chemistry Reviews* **2011**, *255*, 2178-2192.
- (13) Chasteen, N. D. *Vanadium-Protein Interactions*; Marcel Dekker: New York, 1995; Vol. 31.
- (14) Gaidamauskas, E.; Cleaver, D. P.; Chatterjee, P. B.; Crans, D. C. *Langmuir* **2010**, *26*, 13153-13161.
- (15) Acharya, C.; Seo, P. R.; Polli, J. E.; MacKerell, A. D. *Molecular Pharmaceutics* **2008**, *5*, 818-828.
- (16) Chen, I. J.; Taneja, R.; Yin, D.; Seo, P. R.; Young, D.; MacKerell, A. D.; Politi, M. J. *Molecular Pharmaceutics* **2005**, *3*, 745-755.
- (17) Woll, K. A.; Schuchardt, E. J.; Willis, C. R.; Ortengren, C. D.; Hendricks, N.; Johnson, M.; Gaidamauskas, E.; Baruah, B.; Sostarecz, A. G.; Worley, D. R.; Osborne, D. W.; Crans, D. C. *Chemistry & Biodiversity* **2011**, *8*, 2195-2210.
- (18) Giordani, C.; Wakai, C.; Okamura, E.; Matubayasi, N.; Nakahara, M. *Journal of Physical Chemistry B* **2006**, *110*, 15205-15211.

## APPENDIX

## APPENDIX ARTICLE 1<sup>4</sup>:

### Coexisting Aggregates in Mixed Aerosol OT and Cholesterol Microemulsions

Myles A. Sedgwick, Alejandro M. Trujillo, Noah Hendricks, Nancy E. Levinger,\* and Debbie C. Crans\*

Department of Chemistry, Colorado State University, Fort Collins, Colorado 80523, United States

Received September 27, 2010. Revised Manuscript Received November 19, 2010

Dynamic light scattering and NMR spectroscopic experimental evidence suggest the coexistence of two compositionally different self-assembled particles in solution. The self-assembled particles form in solutions containing water, Aerosol OT (AOT, sodium bis(2-ethylhexyl) sulfosuccinate) surfactant, and cholesterol in cyclohexane. In a similar series of studies carried out in 1-octanol only one aggregate type, that is, reverse micelles, is observed. Dynamic light scattering measurements reveal the presence of two different types of aggregates in the microemulsions formed in cyclohexane, demonstrating the coexistence of two compositionally distinct structures with very similar Gibbs energies. One particle type consists of standard AOT reverse micelles while the second type of particle consists of submicellar aggregates including cholesterol as well as small amounts of AOT and water. In microemulsions employing 1-octanol as the continuous medium, AOT reverse micelles form in a dispersed solution of cholesterol in 1-octanol. Although the size distribution of self-assembled particles is well-known for many different systems, evidence for simultaneous formation of two distinctly sized particles in solution that are chemically different is unprecedented. The ability to form microemulsion solutions that contain coexisting particles may have important applications in drug formulation and administration, particularly as applied to drug delivery using cholesterol as a targeting agent.

#### I. Introduction

Cholesterol is a key component of cellular membranes with crucial roles in metabolism and membrane fluidity of living systems. This molecule is tightly regulated in biological systems and a critical constituent of membrane microdomains serving as signal transduction platforms.<sup>1–5</sup> Cholesterol's interaction in membrane systems has been investigated both experimentally and theoretically.<sup>6–11</sup> Given the complex nature of cellular membranes, researchers often use simplified models to probe the molecular interactions of cholesterol. Recent applications also illustrate the utility of cholesterol as a targeting agent for administration of chemotherapeutics such as cisplatin (Lipoplatin)<sup>12–14</sup> and anti-inflammatory agents such as cyclosporin (Neoral) currently used in

clinical treatments of several cancers.<sup>15–17</sup> The systems discussed here provide fundamental experimental information on the types of structures that form in complex media, which remain very important and may impact the understanding of how cholesterol acts in many life-science-related systems.

Microemulsions, which form from mixtures of chemical components that often include fractions that are normally immiscible with each other, represent a simplified system often invoked for model studies of molecular interactions. Using a surfactant, a microemulsion can stabilize water in a nonpolar solvent.<sup>18,19</sup> Depending on the nature and the proportions of the components, various different phases can exist in the microemulsions,<sup>20,21</sup> such as bicontinuous sponge phases, hexagonal phases, micelles, and reverse micelles. The reverse micelle phase typically forms in ternary solutions of surfactants sequestering water from a nonpolar phase<sup>19,22–27</sup> but can also include a wide range of other components that enhance emulsification by adding to the polar phase, nonpolar phase, or the interface between the polar and nonpolar phases.<sup>25,26,28–34</sup> Microemulsions have been used in a wide range

\*Corresponding authors. E-mail: Nancy.Levinger@ColoState.edu (N.E.L.), Debbie.Crans@ColoState.edu (D.C.C.).

- (1) Lu, H.-Z.; Li, B.-Q. *Immunopharmacology* **2009**, *31*, 485–491.
- (2) Hao, M.; Mukherjee, S.; Maxfield, F. R. *Proc. Natl. Acad. Sci. U.S.A.* **2001**, *98*, 13072–13077.
- (3) Simons, K.; Toormre, D. *Nat. Rev. Mol. Cell Biol.* **2000**, *1*, 31–41.
- (4) Kucherak, O. A.; Oncul, S.; Darwich, Z.; Yushchenko, D.; Arntz, Y.; Didier, P.; Mely, Y.; Klymchenko, A. *J. Am. Chem. Soc.* **2010**, *132*, 4097–4916.
- (5) Zhang, Y.; Li, X.; Becker, K. A.; Gulbins, E. *Biochim. Biophys. Acta* **2009**, *1788*, 178–183.
- (6) Ivankin, A.; Kuzmenko, I.; Gidalevitz, D. *Phys. Rev. Lett.* **2010**, *104*.
- (7) Presti, F. T.; Pace, R. J.; Chan, S. I. *Biochemistry* **1982**, *21*, 3831–3835.
- (8) Ohvo-Rekila, H.; Ramstedt, B.; Leppimaki, P.; Slotte, J. P. *Prog. Lipid Res.* **2002**, *41*, 66–97.
- (9) Schubert, D.; Boss, K. *Fed. Eur. Biochem. Soc.* **1982**, *150*, 1–8.
- (10) Ramstedt, B.; Slotte, J. P. *Biophys. J.* **1999**, *76*, 908–915.
- (11) Mannock, D. A.; Lewis, R. N. A. H.; McMullen, T. P. W.; McElhaney, R. N. *Chem. Phys. Lipids* **2010**, *163*, 403–448.
- (12) Boulikas, T. *Expert Opin. Invest. Drugs* **2009**, *18*, 1197–1218.
- (13) Selvakumaran, M.; Pisarcik, D. A.; Bao, R.; Yeung, A. T.; Hamilton, T. C. *Cancer Res.* **2003**, *63*, 1311–1316.
- (14) Boulikas, T. *Cancer Ther.* **2007**, *5*, 351–376.
- (15) Dalmarco, E. M.; Frode, T. S.; Medeiros, Y. S. *Transpl. Immunol.* **2004**, *12*, 151–157.
- (16) Dong, X.; Shi, W.; Yuan, G.; Xie, L.; Wang, S.; Lin, P. *Graefes Arch. Clin. Exp. Ophthalmol.* **2006**, *244*, 492–497.
- (17) Dunn, C. J.; Wagstaff, A. J.; Perry, C. M.; Plosker, G. L.; Goa, K. L. *Drugs* **2001**, *61*, 1957–2016.

- (18) Kumar, C.; Balasubramanian, D. *J. Colloid Interface Sci.* **1979**, *69*, 271–279.
- (19) Zulauf, M.; Eicke, H. F. *J. Phys. Chem.* **1979**, *83*, 480–486.
- (20) Lang, J.; Jada, A.; Malliaris, A. *J. Phys. Chem.* **1988**, *92*, 1946–1953.
- (21) De, T. K.; Maitra, A. *Adv. Colloid Interface Sci.* **1995**, *59*, 95–193.
- (22) Maitra, A.; Dinesh; Patanjali, P. K.; Varshney, M. *Colloids Surf.* **1986**, *20*, 211–219.
- (23) Magid, L. J.; Konno, K.; Martin, C. A. *J. Phys. Chem.* **1981**, *85*, 1434–1439.
- (24) Levinger, N. E. *Science* **2002**, *298*, 1722–1723.
- (25) Baruah, B.; Roden, J. M.; Sedgwick, M.; Correa, N. M.; Crans, D. C.; Levinger, N. E. *J. Am. Chem. Soc.* **2006**, *128*, 12758–12765.
- (26) Crans, D. C.; Trujillo, A. M.; Bonetti, S.; Rithner, C. D.; Baruah, B.; Levinger, N. E. *J. Org. Chem.* **2008**, *73*, 9633–9640.
- (27) Giustini, M.; Palazzo, G.; Colafemmina, G.; DellaMonica, M.; Giomini, M.; Ceglie, A. *J. Phys. Chem.* **1996**, *100*, 3190–3198.
- (28) Umegak, T.; Yan, J.-M.; Zhang, X.-B.; Shioyama, H.; Kuriyama, N.; Xi, Q. *J. Power Sources* **2009**, *191*, 209–216.
- (29) Correa, N. M.; Biasutti, M. A.; Silber, J. J. *J. Colloid Interface Sci.* **1995**, *172*, 71–76.

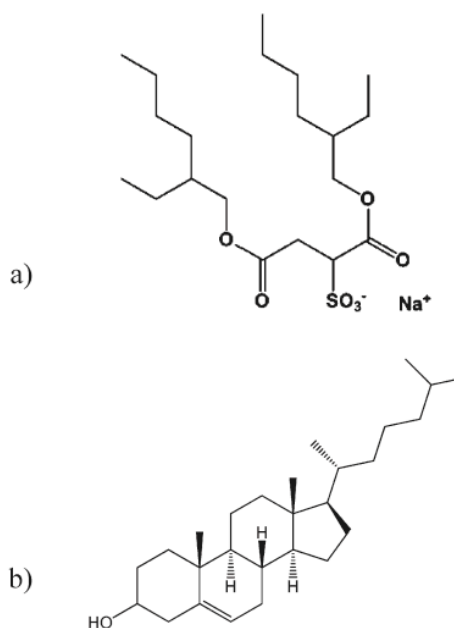
<sup>4</sup> Alejandro M. Trujillo contributed the preliminary work on the AOT/cholesterol RM system & figure 3.

of drug delivery applications,<sup>12,17,35–37</sup> recently including delivery of anticancer agents and anti-inflammatory agents.<sup>12,14,15,17</sup> Well-known drugs such as cisplatin have gained new life in novel microemulsion formulations.<sup>12</sup> Cholesterol has successfully been used as a targeting agent in microemulsions;<sup>38–40</sup> these applications, in addition to the fundamental action of cholesterol in signal transduction in membranes, underline the importance of understanding the types of structures formed in unconventional media.

The precise location of a particular molecule added to a microemulsion can sometimes be hard to predict and often is not determined. For example, many researchers expect ionic probes to remain solvated in the reverse micelle aqueous phase simply because of the molecule's net charge. We have recently shown that charged ionic probes that are very water-soluble can partition deeply into the interfacial region of reverse micelles.<sup>26,41</sup> The properties of these systems are sensitive to many components, including concentration of surfactant, pH, temperature, and amount of polar solvent added.<sup>21,42–44</sup> Adding other components can lead to changes in the microemulsion characteristics as the newly added component interacts with the self-assembled molecules that comprise the complex structure.<sup>45–47</sup> For example, in the phosphatidylcholine microemulsion systems described by Formariz et al., the addition of the solute, Doxorubicin, changes the size and shape of the structures formed.<sup>47</sup>

The surfactant AOT, sodium bis(2-ethylhexyl) sulfosuccinate (Scheme 1), has been used to form reverse micelles in a vast range of different systems, which have been characterized using many different techniques.<sup>19,21,22,25,26,48–57</sup> Generally, the size of these self-assembled reverse micelles follows a Poisson distribution centered around the thermodynamically favored compositionally distinct fundamental unit. At high surfactant concentrations,

Scheme 1. (a) Structure of Aerosol-OT (AOT); (b) Structure of Cholesterol



researchers observe flocculation, percolation, and aggregation of reverse micelles into larger structures.<sup>58</sup> However, even in these systems, research shows formation of single compositionally distinct fundamental units in these solutions. Solutions containing coexisting self-assembled particles with differing sizes were proposed by Rack et al. to explain experimental observations, but the authors provided no direct evidence supporting the existence of two differently sized particles in their solutions.<sup>59</sup> The possibility for two distinct self-assembled structures of similar energy to form in a single macroscopic phase in the same region of the phase diagram is rare, particularly considering the high propensity of AOT to self-aggregate and form highly stable reverse micelles. As a result, the potential number of molecules capable of competing with AOT to form structures of similar stability is very limited.

The importance of cholesterol interactions with lipids has encouraged researchers to explore its interactions in AOT microemulsions and controversy exists regarding its location.<sup>22,54,55,60</sup> Most of the data in the literature suggests that when cholesterol is added to a microemulsion solution, it associates with the AOT reverse micelles. Using <sup>13</sup>C NMR NOE experiments, Maitra found that cholesterol embeds in the interface of AOT reverse micelles.<sup>22</sup> Destree used AOT reverse micelles to make cholesterol nanoparticles, and these studies inferred that cholesterol is solubilized in the water pool.<sup>54</sup> Chattopadhyay and Kelker used a fluorescent probe and found that cholesterol was located in the interior of the interface in the AOT reverse micelle system.<sup>55</sup> Evidence has been reported showing changes in <sup>1</sup>H NMR chemical shifts of cholesterol in the AOT reverse micelle system,<sup>60</sup> although this was corrected upon subsequent in-depth studies.<sup>61</sup> Because the precise

- (30) Correa, N. M.; Silber, J. J. *J. Mol. Liq.* **1997**, *72*, 163–176.  
 (31) Sapp, S. A.; Elliot, C. M. *Chem. Mater.* **2003**, *15*, 1237–1241.  
 (32) Valentine, K. G.; Peterson, R. W.; Saad, J. S.; Summers, M. F.; Xu, X.; Ames, J. B.; Wand, A. J. *Structure* **2010**, *18*, 9–16.  
 (33) Levinger, N. E.; Swafford, L. A. *Annu. Rev. Phys. Chem.* **2009**, *60*, 385–406.  
 (34) Hazra, P.; Chakrabarty, D.; Sarkar, N. *Chem. Phys. Lett.* **2002**, *358*, 523–530.  
 (35) Lawrence, M. J.; Rees, G. D. *Adv. Drug Delivery Rev.* **2000**, *45*, 89–121.  
 (36) Gupta, S.; Moulik, S. P. *J. Pharm. Sci.* **2008**, *97*, 22–45.  
 (37) Kreilgaard, M. *Adv. Drug Delivery Rev.* **2002**, *54*, S77–S98.  
 (38) Beers, M. v.; Sauberborn, M.; Gilli, F.; Brinks, V.; Schellekens, H.; Jiskoot, W. *Pharm. Res.* **2010**, *27*, 1812–1824.  
 (39) Qin, Y.; Fan, W.; Chen, H.; Yao, N.; Tang, W.; Tang, J.; Kuai, R.; Zhang, Z.; Wu, Y.; He, Q. *J. Drug Targeting* **2010**, *18*, 536–549.  
 (40) Lee, S.-M.; Chen, H.; O'Halloran, T. V.; Nguyen, S. T. *J. Am. Chem. Soc.* **2009**, *131*, 9331–9320.  
 (41) Gaidamauskas, E.; Cleaver, D. P.; Chatterjee, P. B.; Crans, D. C. *Langmuir* **2010**, *26*, 13153–13161.  
 (42) Koper, G. J.; Sager, W. F. C.; Smeets, J.; Bedaux, D. *J. Phys. Chem.* **1995**, *99*, 13291–13300.  
 (43) Liu, Z.-T.; Erkey, C. *Langmuir* **2001**, *17*, 274–277.  
 (44) Luan, Y.; Xu, G.; Yuan, S.; Xiao, L.; Zhang, Z. *Langmuir* **2002**, *18*, 8700–8705.  
 (45) Kinugasa, T.; Kondo, A.; Nishimura, S.; Miyauchi, Y.; Nishii, Y.; Watanabe, K.; Takeuchi, H. *Colloids Surf., A* **2002**, *204*, 193–199.  
 (46) Stubenrauch, C.; Tessoroff, R.; Strey, R.; Lynch, I.; Dawson, K. A. *Langmuir* **2007**, *23*, 7730–7737.  
 (47) Formariz, T. P.; Sarmento, V. H. V.; Silva-Junior, A. A.; Scarpa, M. V.; Santilli, C. V.; Oliveira, A. G. *Colloids Surf., B* **2006**, *51*, 54–61.  
 (48) Piletic, I. R.; Moilanen, D. E.; Spry, D. B.; Levinger, N. E.; Fayer, M. D. *J. Phys. Chem. A* **2006**, *110*, 10369.  
 (49) Stahla, M. L.; Baruah, B.; James, D. M.; Johnson, M. D.; Levinger, N. E.; Crans, D. C. *Langmuir* **2008**, *24*, 6027–6035.  
 (50) Faeder, J.; Ladanyi, B. M. *J. Phys. Chem. B* **2000**, *104*, 1033–1046.  
 (51) Zhang, W.; Qiao, X.; Chen, J. *Colloids Surf., A* **2006**, *299*, 22–28.  
 (52) Pieniazek, P. A.; Lin, Y.-S.; Chowdhary, J.; Ladanyi, B. M.; Skinner, J. L. *J. Phys. Chem. B* **2009**, *113*, 15017–15028.  
 (53) Klymchenko, A. S.; Demchenko, A. P. *Langmuir* **2002**, *18*, 5637–5639.  
 (54) Destree, C.; Ghijssen, J.; Nagy, J. B. *Langmuir* **2007**, *23*, 1965–1973.  
 (55) Kelkar, D. A.; Chattopadhyay, A. J. *Phys. Chem. B* **2004**, *108*, 12151–12158.  
 (56) Li, M.; Mann, S. *Langmuir* **2000**, *16*.  
 (57) Spehr, T.; Frick, B.; Grillo, I.; Falus, P.; Muller, M.; Stuhn, B. *Phys. Rev.* **2009**, *79*.

- (58) Hasegawa, M.; Yamaaki, Y.; Sonta, N.; Shindo, Y.; Sugimura, T.; Kitahara, A. *J. Phys. Chem.* **1996**, *100*, 15575–15580.  
 (59) Rack, J. J.; McCleskey, M.; Birnbaum, E. R. *J. Phys. Chem. B* **2002**, *106*, 632–636.  
 (60) Roess, D. A.; Smith, S. M. L.; Holder, A. A.; Baruah, B.; Trujillo, A. M.; Gilsdorf, D.; Stahla, M. L.; Crans, D. C. *ACS Symp. Ser.* **2007**, *974*, 121–134.  
 (61) Roess, D.; Smith, S. M. L.; Winter, P.; Zhou, J.; Dou, P.; Baruah, B.; Trujillo, A. M.; Levinger, N. E.; Yang, X.; Barisac, B. G.; Crans, D. C. *Chem. Biodiversity* **2008**, *5*, 1558–1570.

location of cholesterol in the microemulsion varies with samples, given the diversity in the literature description of the AOT/cholesterol (AOT/cholesterol) system, direct evidence is needed for a fundamental understanding of how cholesterol interacts in AOT microemulsions.

In the research reported here, we have characterized the behavior of cholesterol added to various reverse micelle solutions formed with the commonly used surfactant, AOT. The experiments were designed to explore the interaction of cholesterol in a microemulsion system and probe the nature of the interaction between cholesterol and AOT using dynamic light scattering (DLS), NMR spectroscopy, and other routine characterization techniques for microemulsions. We have investigated the impact of a wide range of differing parameters on the particle size obtained from DLS measurements. In contrast to literature reports,<sup>22,54,55</sup> our results indicate that cholesterol does not add to AOT assemblies, forming a homogeneous membrane like structure. Instead, cholesterol forms submicellar aggregates in solution coexisting in solution with pure AOT reverse micelles. These findings represent a significant departure from previously reported structures. In addition, we present experimental proof-of-concept demonstrating the coexistence of two compositionally different self-assembled particles in solution.

## II. Experimental Methods

**II.A. Materials.** Sodium bis(2-ethylhexyl) sulfosuccinate (98%, Aerosol OT, AOT), cholesterol (98%, chol), isooctane (99%), cyclohexane (99%), DMSO (99%),  $d_{12}$ -cyclohexane (99%), and  $d_{12}$ -chloroform (99%,  $CDCl_3$ ) were all obtained from Sigma-Aldrich. All chemicals were used without further purification except AOT, which was purified using previously described techniques.<sup>49</sup> Dryness and purity of AOT were confirmed by  $^1H$  NMR analysis.<sup>49</sup> Doubly distilled water was used for all reverse micelle systems.

**II.B. Solution Preparation. Stock Solutions.** Stock solutions of AOT were prepared by dissolving purified AOT in cyclohexane to make a 100 mM solution. Studies were also performed with isooctane with similar results; however, the data presented here reflect samples prepared from cyclohexane. Aliquots of these stock solutions were used to make individual reverse micelle solutions. For cholesterol containing solutions, solid cholesterol and solid AOT were dissolved together in the nonpolar solvent simultaneously, before the addition of water.

**AOT/Cyclohexane/ $H_2O$  Reverse Micelles.** Samples were prepared with AOT concentrations ranging from  $10^{-4}$  to 1 M in cyclohexane. All samples used were optically transparent. Samples were prepared for various hydrations,  $w_0 = [water]/[AOT]$  values from 4 to 20, by dissolving the water, by mass, into each AOT solution and results are shown in Figure 1. These samples were used in DLS analysis to determine reverse micelle size and percolation effects and to compare to sizes reported in the literature.<sup>19</sup>

**AOT/Cholesterol/Cyclohexane/ $H_2O$  Reverse Micelle System.** Reverse micelles stock solutions were prepared in two different ways. One way was to prepare solutions from a stock solution of AOT and cholesterol solid, and the other way was to use co-dissolve solid AOT and solid cholesterol to volume by adding cyclohexane. Samples with AOT:cholesterol ratios of 6:1, 5:1, 4:1, 3:1, and 2:1 were prepared. All stock AOT solutions were made at 100 mM, and the appropriate amount of cholesterol was added to each solution, as a solid, to form the ratios listed above. Samples with ratios of AOT:cholesterol were attempted at 1:1, 1:2, and 1:3, but these samples were not homogeneous or optically transparent. Increasing/decreasing the overall AOT concentration did not alleviate the sample issues and thus was concluded the ratios in which there is more cholesterol than AOT are unachievable in this system. All samples used, for the data reported here, were homogeneous at all ratios and optically transparent. A range of reverse micelles with varying  $w_0$  sizes from  $w_0 = 4$  to 32 were made using

the 4:1 ratio of AOT:cholesterol. These systems were analyzed using both  $^1H$  NMR and DLS and generated sizes consistent with literature values.<sup>19,62</sup>

**II.C. Characterization: Dynamic Light Scattering.** Characteristics of the various solutions were measured using dynamic light scattering (DLS, Wyatt DynaPro Titan). To obtain effective data requires intensities of  $10^5$ – $10^6$  counts, we varied the instrument's GaAs laser power between 10 and 20 mW; scattered light was collected at  $90^\circ$ . Prior to data acquisition, samples were equilibrated in the DLS instrument for 10 min at  $25^\circ C$ . Each measurement consisted of a minimum of 10 runs, each of which is a set number of scans. Scans were performed at a rate of 10 acquisitions for 100 s.

To obtain valid results from DLS measurements requires knowledge of the system's refractive index,  $n_p$ , and viscosity,  $\eta$ , in addition to well-defined conditions. The refractive indices for the AOT RM solutions were assumed to be the same as neat organic solvent used.<sup>63,64</sup> Viscosities were measured for a range of AOT RM solutions and AOT stock solutions and determined to be about 1.04 cP. Figure 2 shows the size of the reverse micelles as a function of AOT concentration. All of these data were analyzed using this viscosity. Because the size of the RMs does not change as a function of concentration, and is consistent with the literature values, it was determined that the assertion to use the measured viscosity is appropriate. Cleanliness of the cuvettes used for measurements was of paramount importance for obtaining reliable and reproducible data. Cuvettes were cleaned in a 3:1 ratio of ammonium hydroxide:hydrogen peroxide base bath solution and rinsed with doubly distilled water and then dried with MeOH before use. Before introducing each sample to the cuvette, it was rinsed with pure isooctane twice, then with the 100 mM AOT stock solution, and finally with the sample to be analyzed. The sample was then filtered directly into the cuvette through a  $0.2 \mu m$  filter as needed. Prior to making measurements on a given day, the background signals from air, water, and a standard Triton X-100 solution<sup>65</sup> were collected to confirm cleanliness of the cuvettes. At the end of each day cuvettes were cleaned with a piranha solution and a "cuvette cleaner" (Stama Cells Inc.) solution.

The DLS instrument generated correlation functions from scattering of particles in solution. Typically, we use the DynaPro DYNAMICS software (ver. 6.7.3) assuming a spherical form for the particles to evaluate the light scattering data. The DYNAMICS ver. 6.7.3 analyzes the autocorrelation to regulated fits and a cumulant fit, which is an average of the regulated fits. We find that data extracted from the regulated fit and analyzed in Origin Pro v 8.1 provides more reliable sensitivity to correlation features associated with the particles in solution than using the DYNAMICS software. On the basis of our exponential fits to the data, we obtain reverse micelle size with a 10% instrument error. The reproducibilities of the experiments are reported with standard deviation.

**II.D. Characterization: NMR Spectroscopy and Other Supporting Methods.** Solutions were also characterized using  $^1H$  NMR spectroscopy. Water content in the AOT surfactant was determined by dispersing the surfactant in DMSO. Aggregation of AOT in protonated and deuterated cyclohexane was confirmed by  $^1H$  NMR as previously reported.<sup>49</sup> AOT concentrations ranged from submillimolar to 0.2 M. Spectra were obtained using a Varian 400 MHz NMR spectrometer or a Varian Inova500 MHz spectrometer using the Varian supplied pulse sequence at Colorado State University.

## III. Results

One effective method to measure the presence and properties of soft particles in solution enlists light scattering; we use this method

(62) Levanshov, A. V.; Khmel'nitsky, Y. L.; Klyachko, N. L.; Chernyak, V. Y.; Martinek, K. *J. Colloid Interface Sci.* **1982**, *88*, 444–457.

(63) Blitz, J. P.; Fulton, J. L.; Smith, R. D. *J. Phys. Chem.* **1988**, *92*, 2707–2710.

(64) Bohidar, H. B.; Behboudina, M. *Colloids Surf., A* **2001**, *178*, 313–323.

(65) *Surfactant Micelle Characterization Using Dynamic Light Scattering*; Malvern Instruments Ltd.: Worcestershire, U.K., 2006.

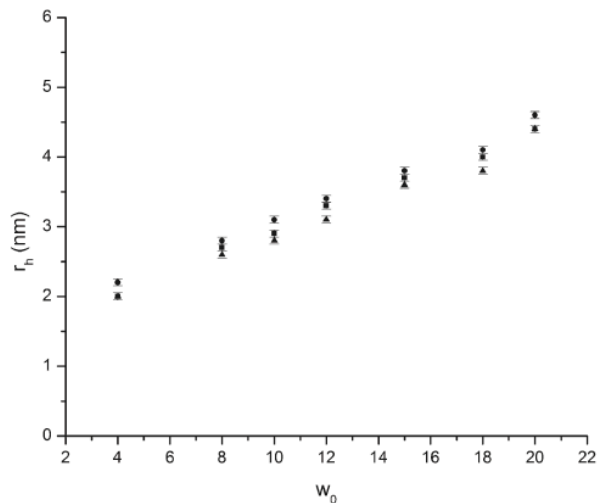


**Figure 1.** Hydrodynamic radius,  $r_h$ , of AOT reverse micelles as a function of  $w_0$  for various continuous bulk solvents, AOT (200 mM)/cyclohexane (circles), AOT (200 mM)/1-octanol (squares), AOT-(200 mM)/ $d_{12}$ -cyclohexane (triangles). Error bars represent standard deviation of the particle sizes measured by dynamic light scattering.

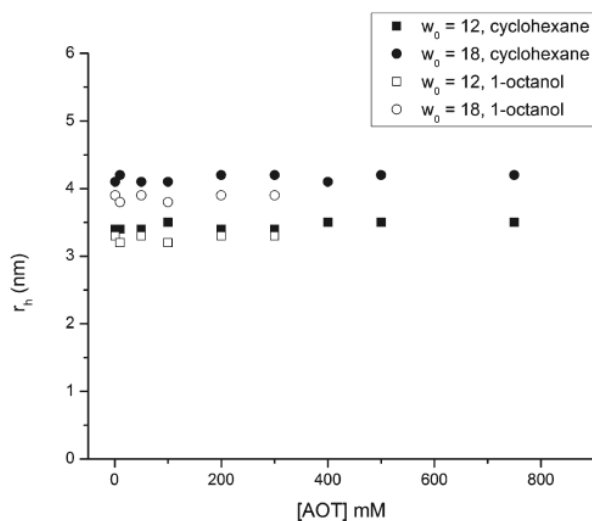


**Figure 2.** AOT reverse micelle [ $w_0 = 12$  (●, ○) and  $w_0 = 18$  (■, □)]; hydrodynamic radius,  $r_h$  (AOT), as a function of [AOT]. Filled symbols (■, ●) represent data for water/200 mM AOT/cyclohexane reverse micelles while hollow points (□, ○) are water/200 mM AOT/1-octanol reverse micelles. Error bars represent the standard deviation of the particle size and are covered by the symbol in all cases.

to explore the average size of particles in solution.<sup>19</sup> Our DLS measurements for AOT in cyclohexane,  $d_{12}$ -cyclohexane, and 1-octanol show the increasing size with increasing  $w_0$  in Figure 1, confirming that the size of the reverse micelles increased as the relative amount of water is increased in these microemulsions. The sizes we measure for the reverse micelles in cyclohexane are consistent with reports in the literature.<sup>62,66</sup> Normally reverse micelles form in nonpolar solvents,<sup>43</sup> but here we also present evidence of their formation in a somewhat polar solvent, 1-octanol. Figure 1 shows that for the same value of  $w_0$  reverse micelles

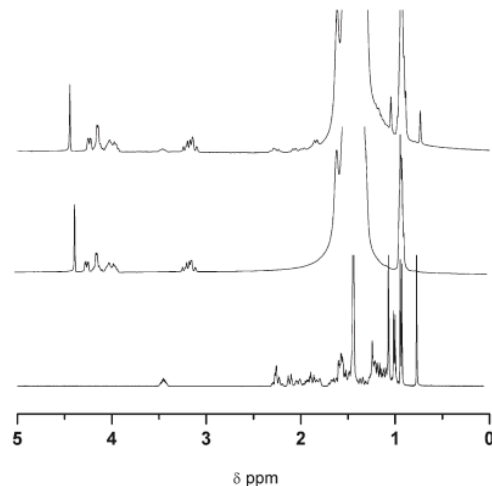


**Figure 3.**  $^1\text{H}$  NMR spectra of (bottom) cholesterol in chloroform, (middle) 100 mM AOT reverse micelles ( $w_0 = 8$ ) in  $d_{12}$ -cyclohexane, and (top) 100 mM AOT reverse micelles ( $w_0 = 8$ ) in  $d_{12}$ -cyclohexane with 25 mM cholesterol.

in each different solvent all have similar size and increase in size linearly with increasing  $w_0$ . Data in Figure 1 also show that particles formed in 1-octanol are slightly smaller than those formed in cyclohexane and that particle size is smaller in deuterated cyclohexane compared to protonated cyclohexane.

Reverse micelles can form over a range of AOT concentrations. Figure 2 shows the hydrodynamic radius of two differently sized (two different  $w_0$  values) reverse micelles formed in 1-octanol and in  $h_{12}$ -cyclohexane for a range of AOT concentrations, as measured by DLS. The data reveal insignificant variation in the hydrodynamic radius with concentration; the reverse micelle size does not depend on surfactant concentration. However, when the AOT concentration exceeds 0.2 M, secondary larger features appear in the DLS signals. These larger features are attributed to interactions between micelles, described by flocculation and/or percolation.<sup>67</sup> When collecting reverse micelle data, we avoid using concentrations that are above the flocculation and percolation point whenever possible.

In addition to observing the presence of particles in solutions by DLS, interactions between surfactants are evident in  $^1\text{H}$  NMR spectra. Figure 3 shows that the  $^1\text{H}$  NMR spectra of reverse micelles prepared using cyclohexane in both the absence and presence of cholesterol are similar, consistent with reverse micelle formation. The spectrum of pure cholesterol is presented at the bottom of the figure for comparison. The spectra show that cholesterol has little or no significant impact on the chemical shifts of the AOT in the spectrum. This suggests that AOT reverse micelles form in the presence of cholesterol without significant interaction. If there were an interaction between cholesterol and a significant fraction of the AOT reverse micelles, we would expect to see shifts in the AOT and the cholesterol peaks.<sup>49</sup> Attempts to characterize these interactions by 2D NOESY  $^1\text{H}$  NMR spectroscopy were inconclusive due to overlap of AOT and cholesterol peaks, size regime of the reverse micelles, and the time scale of the experiment. However, the 1D  $^1\text{H}$  NMR spectra in Figure 3 show that the environment of cholesterol in the AOT/cyclohexane solution is similar to that observed in chloroform. Because cholesterol

(66) Maitra, A. *J. Phys. Chem.* **1984**, *88*, 5122–5125.

(67) Goto, A.; Kuwahara, Y.; Suzuki, A.; Yoshioka, H.; Goto, R.; Iwamoto, T.; Imae, T. *J. Mol. Liq.* **1997**, *72*, 137–144.

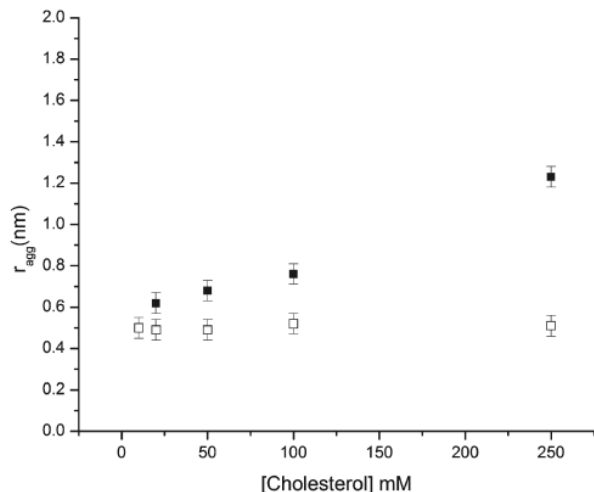


**Figure 4.** Cholesterol particle size,  $r_{\text{agg}}$ , as a function of [cholesterol] for cholesterol dissolved in cyclohexane (■) and 1-octanol (□). No AOT is present in these samples. Error bars represent the standard deviation in the particle size.

molecules self-aggregate in chloroform,<sup>68</sup> these spectra support the interpretation that self-aggregation takes place in cyclohexane as discussed further below.

Before considering mixed systems of AOT and cholesterol, we explored the solution behavior of cholesterol in cyclohexane and 1-octanol. Figure 4 shows the results from DLS experiments measuring the size of particles formed by cholesterol in cyclohexane and 1-octanol,  $r_{\text{agg}}$  the average radius of the cholesterol particles, as a function of cholesterol concentration. In the cyclohexane sample, as the concentration of cholesterol increases, the particle size increases. This suggests formation of cholesterol aggregates, in agreement with reports in the literature.<sup>69–74</sup> In contrast, the particle size does not change for cholesterol in 1-octanol as a function of concentration, consistent with the interpretation that cholesterol disperses as monomers in 1-octanol.<sup>70</sup>

With cholesterol's solution behavior in both cyclohexane and 1-octanol as reference points, we investigated the mixed AOT reverse micelle/cholesterol system. DLS measurements of solutions containing both AOT and cholesterol in either cyclohexane or 1-octanol generate two distinct diffusion times, indicating two types of particles coexist in the solutions. The bottom panel of Figure 5 shows the hydrodynamic radius for particles detected in DLS experiments probing AOT/cholesterol/mixed system in 1-octanol. The larger of the two aggregates is indistinguishable from the size observed for AOT reverse micelles described in Figure 1. The smaller of the two aggregates is the same as the particles observed when cholesterol is dispersed in 1-octanol, as shown in Figure 4. Neither the size of the large nor the small particle in 1-octanol depends on the cholesterol concentration. As shown in Figure 2, changing the AOT concentration has no impact on the reverse micelle size.

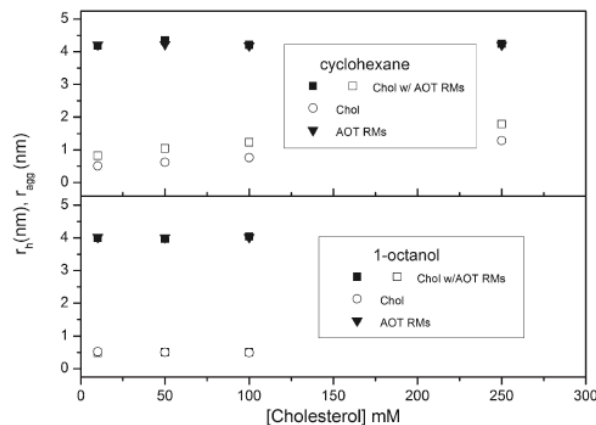


**Figure 5.** Particle size for AOT reverse micelles ( $r_h$ ) and cholesterol ( $r_{\text{agg}}$ ). Top panel: water/200 mM AOT/cyclohexane reverse micelles  $w_0 = 18$  (▼), cholesterol particles in cyclohexane with (200 mM) AOT reverse micelles  $w_0 = 18$  (■), and cholesterol in cyclohexane (●). Bottom panel: water/200 mM AOT/1-octanol reverse micelles  $w_0 = 18$  (▽), cholesterol particles in 1-octanol with (200 mM) AOT reverse micelles  $w_0 = 18$  (□), and cholesterol in 1-octanol (○).

Separately, we can make solutions of 0.1 M AOT in cyclohexane and 0.1 M cholesterol in cyclohexane. However, when attempting to make a solution including both 0.1 M AOT and 0.1 M cholesterol in the same cyclohexane solution, phase separation occurs. This fact alone demonstrates that AOT and cholesterol interact with each other. Because we found that certain ratios result in phase separation, the successful ratios targeted in this work generally did not contain less AOT than a 2:1 AOT:cholesterol. Because the solubility of cholesterol in these solutions depends on the AOT concentration, the data points used in this work require varying AOT concentrations to accommodate the increasing cholesterol concentrations. For example, when [cholesterol] = 50 mM, then we use [AOT] = 150 mM, but when [cholesterol] = 100 mM, we must increase to [AOT] = 250 mM; specific details about the concentrations used appear in the experimental section and the figure captions.

DLS data for AOT/cholesterol in cyclohexane, shown in the top panel in Figure 5, also reveal the presence of two distinct particle sizes coexisting in the solutions. The larger of the two aggregates is the same size as the AOT reverse micelles reported in Figure 1. However, the smaller of the two aggregates is much smaller than AOT reverse micelles reported in Figure 1 but is larger than the cholesterol-only aggregates shown in Figure 4. The data obtained for AOT RM samples,  $w_0 = 12$  and  $w_0 = 18$ , are reported here in Figure 5. These values for  $w_0$  were chosen out of the range of  $w_0$  from 4 to 32 for several reasons. First they were chosen due to the ability to resolve the size of the cholesterol aggregate from the AOT reverse micelle. Second,  $w_0 = 12$  and  $w_0 = 18$  are highly characterized and well understood in the literature with few issues of sample preparation and characterization.<sup>19,49,66</sup> For both the cyclohexane and the 1-octanol system, the size of the AOT reverse micelles does not change as a function of cholesterol concentration, indicating that the cholesterol is not associated with these particles. However, the smaller particles that form in cyclohexane depend distinctly on concentration; their size is larger than observed for cholesterol aggregates than in cyclohexane in the absence of AOT. This suggests that the AOT and water present in the microemulsion impact the size of the cholesterol particles. One likely interpretation of these observations is that these particles incorporate both cholesterol and AOT.

(68) Domanska, U.; Klotfutar, C.; Paljk, S. *Fluid Phase Equilib.* **1994**, *97*, 191–200.

(69) Cromie, S. R. T.; Ballone, P. *J. Chem. Phys.* **2009**, *131*.

(70) Giordani, C.; Wakai, C.; Okamura, E.; Matubayasi, N.; Nakahara, M. *J. Phys. Chem. B* **2006**, *110*, 15205–15211.

(71) Cromie, S. R. T.; Popolo, M. G.; Ballone, P. *J. Phys. Chem. B* **2009**, *113*, 4674–4687.

(72) Abendan, R. S.; Swift, J. A. *Langmuir* **2002**, *18*, 4847–4853.

(73) Goralski, P. *Fluid Phase Equilib.* **2000**, *167*, 207–221.

(74) Haberland, M. E.; Reynolds, J. A. *Proc. Natl. Acad. Sci. U.S.A.* **1973**, *70*, 2313–2316.

When the cholesterol aggregates are similar in size to the AOT reverse micelles, the signal from the aggregate and the signal from the reverse micelle appear as one broad peak and cannot be distinguished from each other. Having the cholesterol aggregate and reverse micelles similarly sized would make it difficult to resolve the peaks separately and are thus easily missed; as an example, this was done when we examined this system in AOT/isooctane.

#### IV. Discussion

On the basis of literature reports, the role of cholesterol in lipid bilayers suggests that cholesterol added to a solution containing self-assembled AOT reverse micelles would interact with AOT molecules and add to the interface of the reverse micelles.<sup>22,55,75</sup> Indeed, cholesterol and many other amphiphilic molecules interact with surfactants such as AOT.<sup>8,76</sup> However, cholesterol has a strong propensity to aggregate with itself both in polar and in nonpolar solvents,<sup>68,69,72–74,77</sup> which can substantially impact its behavior in microemulsions. Indeed, there are very few solvents in which cholesterol disperses in its monomeric state without forming aggregates.<sup>68,71,74,78–80</sup> The balance between polar and nonpolar nature found for 1-octanol provides an environment where cholesterol molecules exist without aggregation.<sup>70</sup> Here, we present a detailed study that explores the cholesterol in AOT reverse micelle systems in greater detail using DLS to determine the sizes of the particles forming. The data that we present here support the interpretation that cholesterol self-aggregation dominates its behavior in microemulsion solutions.

Our DLS measurements of the AOT reverse micelle/cholesterol mixed samples showed evidence for two aggregates coexisting in the solution. When we first analyze the DLS data of the cholesterol/AOT/cyclohexane system, we noticed that some of the reverse micelles formed were smaller than anticipated and that they had a larger polydispersity. Upon investigating the autocorrelation functions, we found substantially better fits to biexponential functions than the standard cumulant fit and regulated fit provided by the DYNAMICS software. Using a biexponential decay to fit the data reveals the presence of two aggregates in solution; one of the aggregates was exactly the size expected for the standard AOT reverse micelle aggregate,<sup>19,21</sup> but the other aggregate was much smaller. At the lowest cholesterol concentrations probed, 20 mM, the size of the smaller aggregate appears the same regardless of  $w_0$  or the presence of AOT, consistent with monomeric or possibly dimeric cholesterol.<sup>68</sup> We crudely estimate the long axis of monomeric cholesterol to be  $\sim 1.2$  nm, the size data measured by DLS shown in Figure 4, yielding a molecular diameter of 1.2 nm is consistent with the interpretation that the cholesterol in 1-octanol is monodisperse. However, trends for the hydrodynamic radius of the smaller peak differ depending on the organic solvent. In 1-octanol, the particle size remains constant as the cholesterol concentration varies, whereas in cyclohexane, the particles grow with increasing cholesterol concentration.

Cholesterol's aggregation has been widely characterized in aqueous solutions.<sup>74,78</sup> In contrast, cholesterol disperses without

aggregation in 1-octanol.<sup>70</sup> In nonpolar solvents such as cyclohexane and chloroform, Giordani et al. observed that cholesterol forms higher order aggregates.<sup>70</sup> Additionally, when water is present in the nonpolar solvent, they found larger cholesterol aggregates than when using dry solvents. These studies indicate that water incorporates into the cholesterol aggregates and provide precedent for cholesterol self-assembly occurring in multi-component solutions. We also find that water associates with the cholesterol–AOT aggregate. The DLS results show that the cholesterol containing aggregates present in the mixed systems had hydrodynamic radii about 0.5 nm larger on average than the pure cholesterol aggregates in neat solvent shown in Figure 3, consistent with AOT comprising a part of the cholesterol aggregates. Since the  $w_0$  size did not change significantly with changing cholesterol and AOT concentrations, water must accompany the AOT in the cholesterol aggregate. The fact that the amount of water in the cholesterol–AOT aggregate does not change significantly is because the water remains associated with the AOT in reverse micelles.

Cholesterol's solubility and aggregation in neat organic solvents is well-known.<sup>70,73,80,81</sup> However, when cholesterol is present in solution with AOT, the solubility of cholesterol changes. Cholesterol's solubility depends on the AOT:cholesterol ratio. In solutions with cholesterol at a ratio higher than 2:1 AOT:cholesterol, we observe precipitation, which we attribute to the cholesterol based on the absence of cholesterol peaks in the <sup>1</sup>H NMR spectra of the supernatant solution. For example, a solution containing 200 mM AOT in cyclohexane can only accommodate up to 100 mM cholesterol. Because the AOT reverse micelle size does not change as a function of AOT concentration, as shown in Figure 2, raising the AOT concentration should not significantly affect the self-assembled AOT reverse micelle structures that form. Thus, to achieve higher concentrations of cholesterol, we increased the AOT concentration accordingly.

Several previous studies have explored microemulsions containing both AOT and cholesterol.<sup>22,54,55,75</sup> We find that our interpretation of the state of the water/AOT/cholesterol solutions can account for the various results presented in the literature. In <sup>13</sup>C NMR nuclear Overhauser effect (NOE) studies, Maitra and co-workers presented evidence that cholesterol hydrogen bonds with AOT head groups.<sup>22</sup> They observed that as cholesterol was added, the negative NOE signal gradually increased to positive values, which they interpreted as the cholesterol interacting with the AOT headgroup inside the reverse micelle. This interpretation was based on the assumption that when cholesterol is added to solution, it incorporates into the AOT reverse micelles. However, the results by Maitra and co-workers can also be interpreted as cholesterol interacting with AOT in smaller aggregates as observed in our studies.

Destrée and co-workers report facilitation of AOT reverse micelles in heptanes in the formation of cholesterol nanoparticles.<sup>54</sup> They report that adding cholesterol dissolved in chloroform to a solution of water/AOT/heptanes provides stabilization in the form of cholesterol nanoparticles; they attribute the stabilization to the reverse micelles' ability to solubilize the cholesterol nanoparticle. In fact, it has been shown<sup>70</sup> that cholesterol forms aggregates in chloroform in the absence of AOT, especially if the chloroform contains water. By injecting a solution of cholesterol in chloroform to the AOT/heptanes/water solution, our observations support the suggestion that the cholesterol aggregates acquired some AOT and water from the system.

Chattopadhyay and Kelkar introduced fluorescently labeled cholesterol into solutions of water/AOT/isooctane.<sup>55</sup> They specifically

(75) Gupte, A.; Nagarajan, R.; Kilara, A. *Ind. Eng. Chem. Res.* **1995**, *34*, 2910–2922.

(76) Hao, M.; Mukkerjee, S.; Maxfield, F. R. *Proc. Natl. Acad. Sci. U.S.A.* **2001**, *98*, 13072–13077.

(77) Cromie, S. R.; Popolo, M. G. D.; Ballone, P. *J. Phys. Chem. B* **2009**, *113*, 4674–4687.

(78) Saad, H. Y.; Higuchi, W. I. *J. Pharm. Sci.* **1965**, *54*, 1205–1206.

(79) Randolph, T. W.; Clark, D. S.; Blanch, H. W.; Prausnitz, J. M. *Proc. Natl. Acad. Sci. U.S.A.* **1987**, *85*, 2979–2983.

(80) Jadzyn, J.; Hellemans, L. *Ber. Bunsen-Ges. Phys. Chem.* **1993**, *97*, 205–210.

(81) Goralski, P.; Tkaczyk, M.; Piekarski, H. *J. Solution Chem.* **1996**, *25*, 1227–1240.

employ this probe relying on cholesterol to drive the insertion of the probe into the interface. The fluorescent probe is polar and assumed to reside in the water pool.<sup>55</sup> Given the propensity for the fluorescent probe to be solubilized in water and cholesterol's low solubility in isooctane and water, this may drive the location of the labeled cholesterol. However, the low concentration of Chattopadhyay and Kelkar's study (below 8  $\mu\text{M}$ ) makes comparison of these studies with our results less straightforward.

Previously, we have studied the interactions of some vanadium containing antidiabetic drugs with AOT reverse micelles with and without cholesterol.<sup>60</sup> Following  $^1\text{H}$  NMR chemical shifts of cholesterol<sup>60,61</sup> and the drug, the chemical shifts we observed in the drugs and the surfactant signals suggested that the drug penetrated the interface. Recent studies demonstrated that most of the changes were observed in both self-assembled structures that contain cholesterol and those without cholesterol. These results are consistent with our observations reported here where a new AOT/cholesterol particle forms. The observed changes can be due to penetration of the drug in the interface of the AOT reverse micelles of the cholesterol containing particle.

Nagarajan and co-workers inferred that cholesterol assembles into the AOT reverse micelles because their experiments showing that cholesterol oxidase in solutions of AOT and cholesterol in isooctane. The reverse micelles not only continues to demonstrate the same enzymatic activity but actually enhances enzymatic activity.<sup>75</sup> They observed an increase in cholesterol oxidase enzymatic activity for solutions with small water content ( $\leq w_0 = 8$ ) but not for large ( $\leq w_0 = 30$ ) reverse micelles. However, given that AOT reverse micelles have dimensions smaller than the enzyme raises questions about the nature of the system and whether the enzyme is in solution.<sup>82</sup> This is particularly pertinent because in the large reverse micelles, when there is room for the enzyme, no enhancement in enzyme activity was observed. Whatever the nature of the AOT–enzyme particles that forms in these systems, the increased enzyme activity reflects some type of interaction favoring the process. Increased enzymatic activity could arise from the enzyme acting on the AOT–cholesterol aggregate that we observe in this work. The possibility exists that the AOT–cholesterol aggregate is a better substrate than aggregates composed only of cholesterol. This hypothesis could be tested by concentration-dependent dissolution of the enzyme and cholesterol in the organic solvent.

(82) Yue, Q. K.; Kass, I. J.; Sampson, N. S.; Vrieland, A. *Biochemistry* **1999**, *38*, 4277–4286.

## V. Conclusions

Through a series of careful measurements of cyclohexane solutions containing AOT reverse micelles and cholesterol, we have tested the hypothesis whether cholesterol incorporates into AOT reverse micelles. These experiments confirm the possibility that a complex media can support formation of two compositionally distinct self-assembled particles in solution. On the basis of our results, we conclude that cholesterol does not incorporate into the AOT reverse micelles in cyclohexane. Rather, cholesterol–AOT aggregates coexist in solution with the AOT reverse micelles. Our studies further suggest that cholesterol self-aggregates including some AOT and water in the adducts formed. The normal AOT reverse micelles form after the cholesterol has been used up. Studies with a dispersing solvent, 1-octanol, were also used for comparison to contrast these observations. We conclude that compositionally distinct self-assembled particles can form and coexist in the same complex solution. Importantly, such cases are only likely to be observed when the additional components readily self-assemble forming very stable structures.

The studies presented here show that cholesterol does not simply incorporate into AOT reverse micelles in cyclohexane as suggested in literature reports. Similar results were found when using isooctane as solvent, although the size of the cholesterol–AOT–water aggregate changed so that the resolution between the species was lower. Such systems may form aggregates consisting of cholesterol, AOT, and other surfactants and water. These findings are particularly important for administration of cholesterol for specific health purposes. Not only is cholesterol a metabolite, it is also used as a targeting agent for breast cancer drugs. Specific targeting of the lymph tissue is most likely related to the particular form of cholesterol administered. Because several drug formulations are based on the concept that cholesterol helps target the drug, fundamental information on possible nanostructures, should assist future applications of cholesterol. The fundamental studies described in this work are critically important for future understanding and applications of cholesterol in the life sciences.

**Acknowledgment.** We gratefully acknowledge assistance from Dr. Deborah Roess, Mr. Laurence Quinn, Dr. Bharat Baruah, and Ms. Michelle Romanishan. This material is based upon work supported by the National Science Foundation under Grant 0628260 (CRC). LQ and AMT performed research while supported NSF REU Grant 0649263. AMT was supported by a NSF Bridge to the Doctorate Fellowship, Grant NSF HRD 0832932.

## Effects of Vanadium-Containing Compounds on Membrane Lipids and on Microdomains Used in Receptor-Mediated Signaling

by Deborah A. Roess<sup>\*a</sup>), Steven M. L. Smith<sup>a</sup>), Peter Winter<sup>a</sup>), Jun Zhou<sup>a</sup>), Ping Dou<sup>a</sup>), Bharat Baruah<sup>b</sup>), Alejandro M. Trujillo<sup>b</sup>), Nancy E. Levinger<sup>b</sup>), Xioda Yang<sup>c</sup>), B. George Barisas<sup>b</sup>), and Debbie C. Crans<sup>\*b</sup>)

<sup>a</sup>) Department of Biomedical Sciences, Colorado State University, Fort Collins, CO 80523-1872, USA  
(e-mail: daroess@lamar.colostate.edu)

<sup>b</sup>) Department of Chemistry, Colorado State University, Fort Collins, CO 80523-1872, USA  
(e-mail: crans@lamar.colostate.edu)

<sup>c</sup>) Department of Chemical Biology, School of Pharmaceutical Sciences, Peking University, Beijing 100083, P. R. China

---

There is increasing evidence for the involvement of plasma membrane microdomains in insulin receptor function. Moreover, disruption of these structures, which are typically enriched in sphingomyelin and cholesterol, results in insulin resistance. Treatment strategies for insulin resistance include the use of vanadium (V) compounds which have been shown in animal models to enhance insulin responsiveness. One possible mechanism for insulin-enhancing effects might involve direct effects of V compounds on membrane lipid organization. These changes in lipid organization promote the partitioning of insulin receptors and other receptors into membrane microdomains where receptors are optimally functional. To explore this possibility, we have used several strategies involving V complexes such as  $[\text{VO}_2(\text{dipic})]^-$  (pyridin-2,6-dicarboxylatodioxovanadium(V)), decavanadate ( $\text{V}_{10}\text{O}_{28}^{6-}$ ,  $\text{V}_{10}$ ), BMOV (bis(maltolato)oxovanadium(IV)), and  $[\text{VO}(\text{saltris})]_2$  (2-salicylideniminato-2-(hydroxymethyl)-1,3-dihydroxypropane-oxovanadium(V)). Our strategies include an evaluation of interactions between V-containing compounds and model lipid systems, an evaluation of the effects of V compounds on lipid fluidity in erythrocyte membranes, and studies of the effects of V-containing compounds on signaling events initiated by receptors known to use membrane microdomains as signaling platforms.

---

**Introduction.** – Plasma membrane microdomains, typically small membrane regions characterized by detergent insolubility and enrichment in sphingomyelin and cholesterol [1], are increasingly associated with their ability to concentrate membrane proteins involved in transmembrane signaling. As an example of this, insulin receptors function optimally in membrane microdomains [2]. Exclusion of the insulin receptor from membrane microdomains, as seen under conditions where there is an excess of the ganglioside GM3 [3], or in *Neimann–Pick* disease where membrane microdomains are altered [4], produces an insulin-resistant state.

This role for membrane microdomains in insulin-mediated signaling suggests a pharmacologic strategy to increase insulin responsiveness. It has been known for many years that some vanadium (V) compounds can enhance insulin responsiveness [5–10]. Selected compounds can normalize both elevated blood glucose and lipid levels, and may have long-term benefits to cardiovascular health, which is a frequent complication

---

<sup>5</sup> Alejandro M. Trujillo contributed figure 4 & corrected figure 2.  
*Published in Chemistry & Biodiversity, 2008, (5) 1558-1570.*

of diabetes [11][12]. V Compounds are generally not believed to bind to the insulin receptor [13–15] and thus exert their insulin-enhancing effects downstream of the insulin receptor [10][16–19]. However, the likely effects on multiple pathways have recently been documented in, for example, the DNA microarray analysis of global gene expression levels documenting numerous changes in gene expression [16].

The possibility that V compounds interact directly with membranes or proteins closely associated with membranes seems high, particularly in light of the recent finding that the insulin-enhancing compound  $[\text{VO}_2(\text{dipic})]^-$  (Fig. 1,a) [20][21] penetrates the lipid interface and is located in the hydrophobic portion of the lipid layer of the microemulsion (Fig. 1,c) [22][23]. This result was unexpected considering the charge and polarity of this compound, but does support previous reports that some V compounds, such as naglivan [24], are able to penetrate membrane systems [6][25]. However, to date these studies have been carried out with different V complexes, and a more exhaustive study on this topic will be forthcoming. Several classes of V compounds are insulin-enhancing compounds, and this suggests that the specific ligand is less important than the presence of V within the complex. This observation is in agreement with existing literature showing that the effects of V compounds vary with different oxidation state of the metal [26][27], and that the various ligands exert a ‘fine-tuning’ effect [8][28].

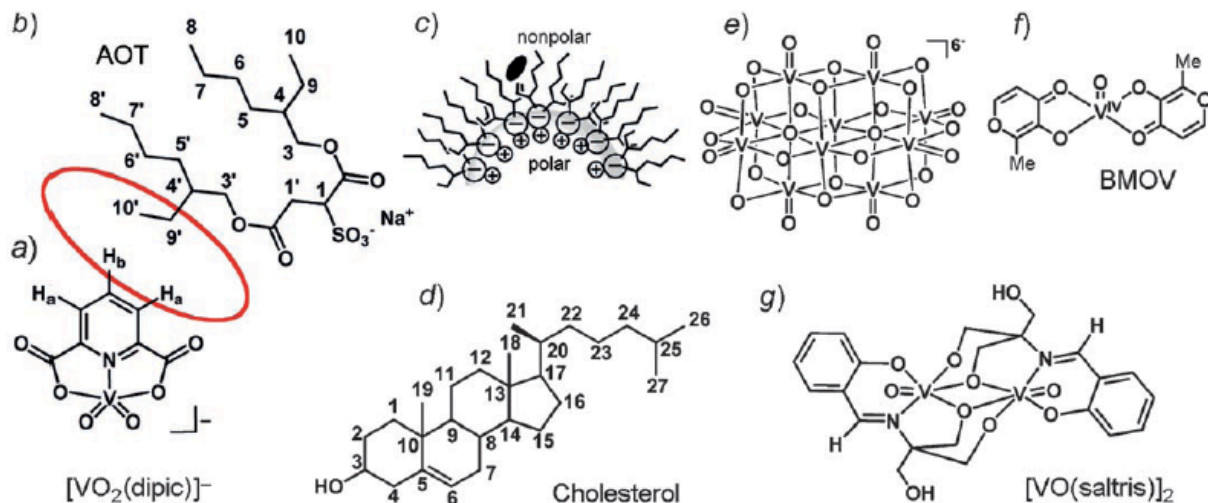


Fig. 1. a) The structure of  $[\text{VO}_2(\text{dipic})]^-$ . b) The structure of AOT. c) The schematic drawing of the location of  $[\text{VO}_2(\text{dipic})]^-$  in a AOT/isooctane/ $\text{H}_2\text{O}$  microemulsion and the proposed location in the more rigid cyclohexane system. The red circle between  $[\text{VO}_2(\text{dipic})]^-$  and AOT indicates the H-atoms seeing each other in the NOESY spectrum (see Fig. 2). d) The structures of cholesterol, e) decavanadate ( $\text{V}_{10}$ ), f) BMOV, and g)  $[\text{VO}(\text{saltris})]_2$ .

Here, we explore the hypothesis that V compounds facilitate insulin-enhancing effects through reorganization of plasma membrane lipids. These studies were motivated by the well-known insulin-enhancing properties of several lipophilic V compounds [5][6], and the fact that even a charged V compound can penetrate the lipid interfacial layer in a model system [22][23]. Although V compounds are generally believed to act downstream of the insulin receptor [10][16–19], some effects of these transition-metal compounds may be mediated through their actions on the plasma

membrane and the organization of proteins and lipids within the lipid bilayer. Thus, these insulin-enhancing V compounds might evoke some effects through direct interactions with the plasma membrane of cells expressing insulin receptors. These interactions could perturb the membrane lipid organization, and facilitate the translocation of insulin receptors or other signaling molecules into membrane microdomains that serve as signaling platforms and, in this fashion, enhance insulin-mediated cellular responses and reduce insulin resistance.

*V-Containing Compounds Affect the Packing of Lipids in Microemulsions.* The negatively charged V compound, pyridine-2,6-dicarboxylatodioxovanadium(V) ( $[\text{VO}_2(\text{dipic})]^-$ , *Fig. 1,a*), was reported to penetrate a model lipid interface. The nature of this interaction was examined in further detail in studies presented here in an AOT (*Fig. 1,b*)/cyclohexane system which also has a negatively charged head group as the AOT/isooctane/ $\text{H}_2\text{O}$  microemulsion (*Fig. 1,c*) system investigated previously [22]. The samples used in these studies and those reported previously were prepared by vortexing an aqueous-solution-containing compound, and an organic-phase-containing surfactant with or without cholesterol (*Fig. 1,d*) to yield an optically clear solution prior to  $^1\text{H}$ -NMR-spectroscopic measurements. Formation of reverse micelles was confirmed by dynamic light scattering (DLS) experiments, and the sizes obtained are similar to those reported in the literature [22][29]. Studies were carried out to demonstrate changes in lipid packing upon addition of V compounds and to examine the effect of membrane rigidity on compound penetration.

Our previous studies with the  $[\text{VO}_2(\text{dipic})]^-$  complex in an AOT/isooctane/ $\text{H}_2\text{O}$  system were conducted with a model system with a small ratio of  $\text{H}_2\text{O}$  to surfactant ( $w_o = [\text{H}_2\text{O}]/[\text{surfactant}]$ ). The data shown in *Fig. 2* of  $[\text{VO}_2(\text{dipic})]^-$  are in a AOT/isooctane/ $\text{H}_2\text{O}$  system with larger reverse micelles ( $w_o = 20$ ) at a size where the water pool is beginning to have bulk-like properties [30][31]. The 2D-NOESY experiment shown in *Fig. 2* for this system also showed cross-signals between the H-atom on complex and the  $\text{CH}_2$  and Me H-atoms on AOT. This observation show that these H-atoms are in vicinity of each other, and that the  $[\text{VO}_2(\text{dipic})]^-$  complex is likely to have penetrated the interface as was reported previously [22], albeit some differences in the specific location and orientation are observable.

The model system AOT/isooctane/ $\text{H}_2\text{O}$  is a well known system (*Fig. 1,c*) in which the organic solvent isooctane is known to penetrate the AOT chains in the reverse micelle. A closely related system in which less flexible surface movement takes place is comprised by the organic solvent cyclohexane in place of isooctane. Since membrane flexibility is likely to alter the response to agents, information is desirable in a system with less surface mobility. As a result, studies were undertaken in AOT/cyclohexane/ $\text{H}_2\text{O}$ . As shown in *Fig. 3,a*, the  $^{51}\text{V}$ -NMR spectra of solutions of  $[\text{VO}_2(\text{dipic})]^-$  complex added to the AOT/cyclohexane/ $\text{H}_2\text{O}$  system show some downfield shifting compared to the aqueous stock solution. This slight upfield shift of the complex signal is analogous to the shifting reported previously [22]. As shown in *Fig. 3,a*, the signal for this system has a much greater linewidth than stock solution, reflecting the lower mobility of the complex in the microemulsion environment.

The  $^1\text{H}$ -NMR spectra of these systems were also recorded, and are shown in *Fig. 3,b*. Interestingly, the modest upfield chemical shift of the  $^{51}\text{V}$ -NMR signal is contrasted to the significant downfield shift in the  $^1\text{H}$ -NMR spectra. In the past, an

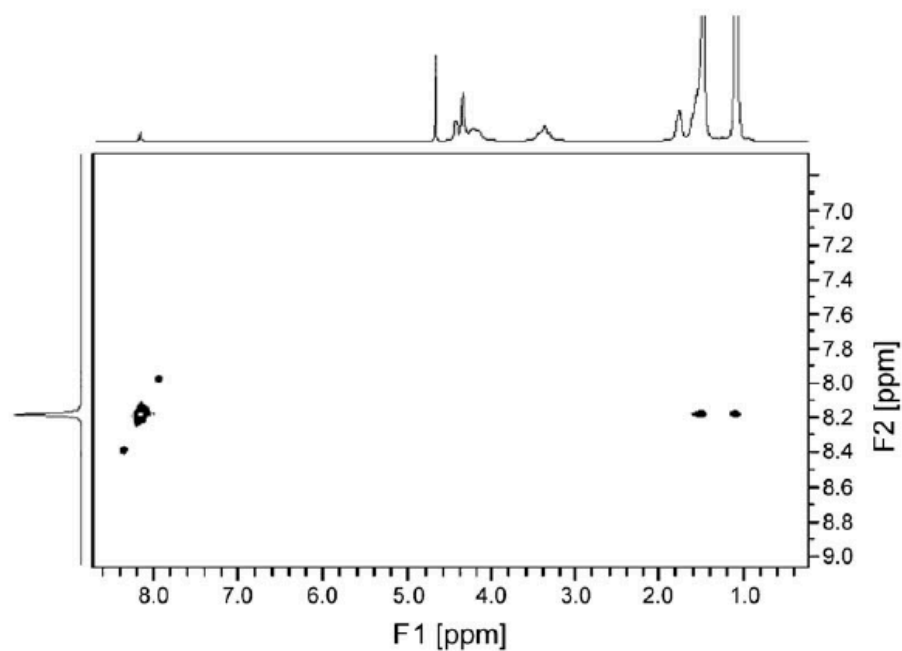


Fig. 2. 2D-NOESY Recorded of 100 mM  $[\text{VO}_2(\text{dipic})]^-$  complex in a 1M AOT/isoctane/ $\text{D}_2\text{O}$  (pH 4.5) microemulsion of  $w_o=20$

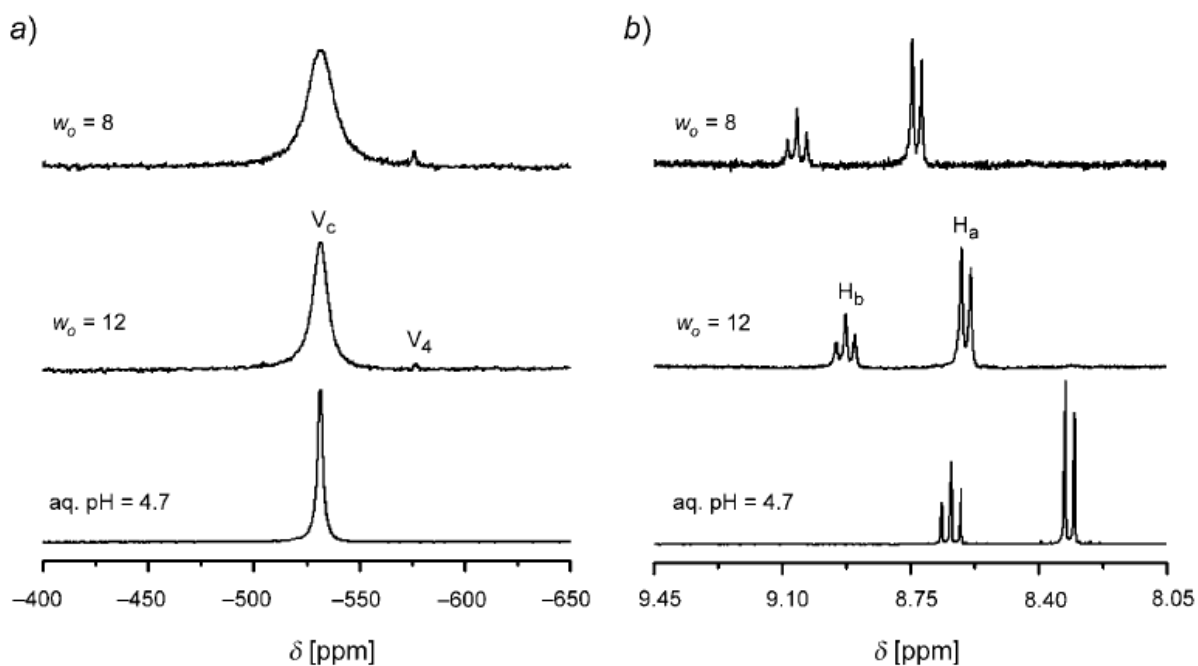


Fig. 3.  $^{51}\text{V}$ - (a) and  $^1\text{H}$ -NMR spectra (b) of  $[\text{VO}_2(\text{dipic})]^-$  complex in a 1M AOT/cyclohexane/ $\text{D}_2\text{O}$  (pH 4.7) microemulsion

upfield shift in the  $^1\text{H}$ -NMR spectra has been associated with interface interaction [32][33]. However, the 1D- $^1\text{H}$ -NMR results in the AOT/cyclohexane/ $\text{H}_2\text{O}$  system are similar to those observed previously with the AOT/isooctane/ $\text{H}_2\text{O}$  system, which, as shown in *Fig. 2*, show that the  $[\text{VO}_2(\text{dipic})]^-$  complex is in the vicinity of tail  $\text{CH}_2$  and Me groups of the AOT chains. The results shown in *Fig. 3* are consistent with the  $[\text{VO}_2(\text{dipic})]^-$  complex able to penetrate the surface and reside at least partly at the inner parts of the lipid interface. These studies are very different from those carried out in reverse micelles with positively charged surface, and where the complex is likely to be located near the interface [34].

Rafts are known to contain high concentrations of cholesterol (*Fig. 1,d*), and cholesterol is known to reduce membrane fluidity at physiological temperatures. Therefore, studies were carried out with microemulsions in the presence and absence of cholesterol [23]. Reverse micelles at a  $w_o$  of 8 were made containing a ratio of 1:4 (30 mM:120 mM) cholesterol/AOT using isooctane as the organic solvent. Reverse micelles were formed by the addition of aqueous solutions of preformed decavanadate ( $\text{V}_{10}$ ; in *Fig. 1,e*) (5.0, 10.0, and 20.0 mM  $\text{V}_{10}$ , resp.) for comparison with the reverse micelles in the absence of  $\text{V}_{10}$ . Previously, we reported that the chemical shifts for some of the H-atoms in the cholesterol molecule changed as the  $\text{V}_{10}$  compound was added to the water pool. The chemical shifts for the H-atoms at C(3), C(4), C(6), C(7), and C(12) changed slightly, whereas, a large shift was observed for the H-atoms at C(18). No or even less change was observed for the rest of the H-atoms on the cholesterol molecule. The variation in chemical shifts was interpreted as changes in environment, which is consistent with changes in lipid packing near these H-atoms upon addition of  $\text{V}_{10}$  probe to the reverse micelle. Upon further scrutiny, the referencing was found to be problematic given the complex nature of the system (manuscript in preparation). As shown in *Fig. 4*, no changes in chemical shifts were observed upon reinvestigation.

In comparison, we also examined the chemical shifts of the H-atoms on the AOT. Since there are many molecules of AOT for each  $\text{V}_{10}$ , a small change here would provide a strong indication that changes in the lipid packing are taking place. Some H-atoms have indistinguishable chemical shifts which is consistent with little change in their environment as would be anticipated from H-atoms further away from a cholesterol that was penetrating the lipid interface. As shown in *Fig. 4*, the H-atoms at C(1') and C(3') show no change in chemical shift, and no change is also observed for the H-atoms at C(1) and C(3). These data are inconsistent with penetration of cholesterol. Since  $\text{V}_{10}$  is believed to be located in the water pool in these microemulsions, any change in lipid packing by this solute probably indicate a significant change in the interface region of this system. When we recorded the  $^{51}\text{V}$ -NMR spectra, the data were inconclusive. The data combined support the possibility that cholesterol penetrate the lipid interface such that polar part of the molecule remains near the lipid interface associating more with the part of the AOT molecule that is further away from the charged  $\text{SO}_3^-$  group. Studies are now underway to probe the phenomena further.

*V-Containing Compounds Modulate Lipid Fluidity as Assessed by Changes in Polarization of a Lipid Probe.* Changes in lipid packing in reverse micelles in the presence of V-containing compounds suggest the possibility that membrane fluidity is influenced by these compounds. Although our previous studies have focused on membrane permeability of V-containing compounds [35–37], we have also observed

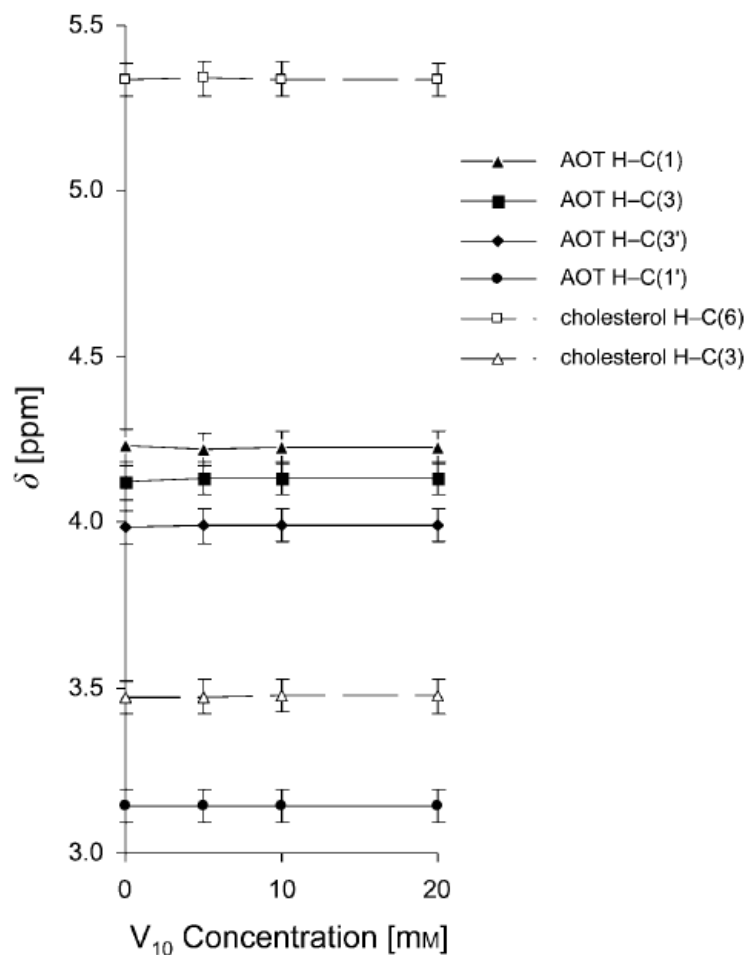


Fig. 4.  $^1\text{H-NMR}$  Chemical shifts of selected cholesterol H-atoms prepared from cholesterol (30 mM) and AOT (120 mM) based  $w_o=8$  reverse micelle is shown as increasing concentrations of  $V_{10}$  (in Fig. 1, e) is added to the water pool of the reverse micelle. The chemical shifts for H-atoms on C-atoms shown here are located as indicated in Fig. 1 on the structure.

that selected V-containing compounds can partition within plasma membrane lipids. We have evaluated lipid fluidity using erythrocyte membranes treated with various V-containing compounds. Using the lipid probe 1,6-diphenylhexa-1,3,5-triene (DPH) and fluorescence polarization methods [35], we have demonstrated that, to varying degrees, three compounds  $\text{NaVO}_3$ ,  $\text{VO}(\text{acac})_2$ , and BMOV (bis(maltolato)oxovanadium(IV)) (Fig. 1, f) decreased membrane fluidity and increased lipid order in erythrocyte membranes.

The results that three different V complexes are able to traverse the membrane are summarized in the Table. Since the NMR studies with  $[\text{VO}_2(\text{dipic})]^-$  suggest that a complex can penetrate the lipid interface, and the studies with  $V_{10}$  that the V complex can induce lipid reorganization, recent studies with the oxidized forms of BMOV (Fig. 1, f) in this simple model system suggest that these species also interact with the lipid interface [38]. These studies are thus also consistent with the studies listed in the Table with BMOV [35]. The possibility that BMOV affects lipid order in micro-

suspensions is currently under further investigation (manuscript in preparation). The results combined support the possibility that V-containing compounds with some hydrophobicity have the ability to intercalate within lipid layers and impact lipid organization.

Table. *Effects of V Compounds on the Lipid Fluidity of DPH-Labeled Human Erythrocyte Membranes* [35]

Concentration [mM]	Microviscosity <sup>a)</sup>		
	NaVO <sub>3</sub>	VO(acac) <sub>2</sub>	BMOV
1.0	1.90 ± 0.02	2.13 ± 0.02	2.13 ± 0.02
0.1	1.88 ± 0.02	2.00 ± 0.02	2.04 ± 0.02
0.0		1.83 ± 0.02	

<sup>a)</sup> Data represent the means ± S.D. ( $m=3$ );  $P < 0.05$  vs. control.

*Changes in Lipid Packing May Influence the Distribution of Receptors in Membrane Microdomains and Receptor Function.* One consequence of a change in lipid organization is to shift the distribution of membrane proteins, and the concentration and composition of membrane proteins in membrane microdomains. One of the most common methods to evaluate the preferential localization of membrane proteins into microdomains is simply to disrupt the integrity of these microdomains using methyl- $\beta$ -cyclodextran to extract cholesterol from membranes [1]. This approach demonstrates that cholesterol is critical to microdomain formation and stability, and to the localization of selected membrane proteins in membrane fractions with low buoyancy. We have shown that the V-containing compound [VO(saltris)]<sub>2</sub> (*Fig. 1, g*) can influence the distribution of the insulin receptor within membrane microdomains [23].

We evaluated the buoyancy of membrane fractions using discontinuous sucrose-gradient ultracentrifugation methods, and the results are shown in *Fig. 5*. Briefly,  $5 \times 10^6$  RBL-2H3 cells were obtained from cell culture and suspended in *Hank's* balanced salt solution (BSS). Cells were then treated with [VO(saltris)]<sub>2</sub> for 1 h prior to cell lysis. The cell lysate was mixed with an equal volume of 80% sucrose to obtain a sample consisting of cell membranes and their components in 40% sucrose. A discontinuous sucrose gradient from 10–80% sucrose was constructed with the cell fraction comprising the 40% sucrose fraction. Samples were then subjected to isopycnic ultracentrifugation using an overnight spin at *ca.* 180000 *g*. After centrifugation, 640- $\mu$ l fractions were carefully collected from the top down of the gradient downward. Aliquots from each fraction were probed for proteins of interest including the insulin receptor. The insulin receptor was identified on *Western* blots using an anti-insulin receptor antibody (*Sigma-Aldrich*, St. Louis, MO). As shown in *Fig. 5*, treatment of intact RBL-2H3 cells with [VO(saltris)]<sub>2</sub> resulted in movement of insulin receptor to membrane fractions with higher buoyancy.

The observed induced shift in membrane fractions containing insulin receptor was modest. However, both the Type-I Fc $\epsilon$  receptor [39–41] and the human luteinizing hormone receptors [40] have previously been shown to exhibit small shifts into higher

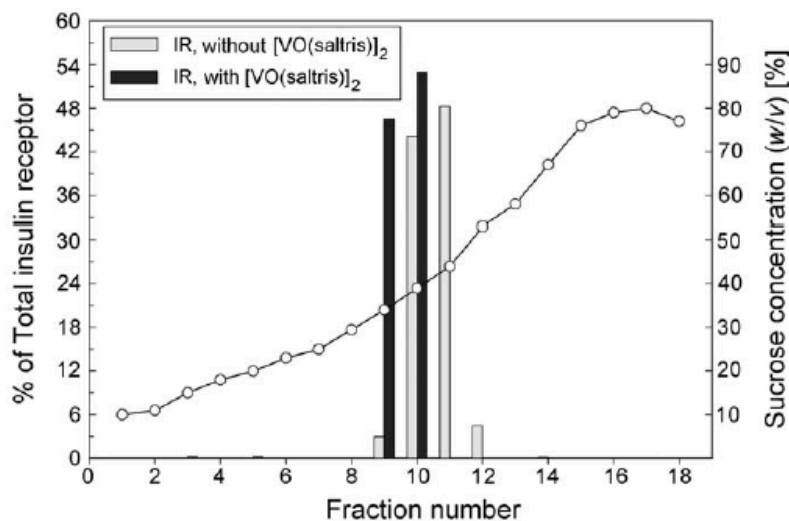


Fig. 5. Translocation of insulin receptor (IR) from higher-density sucrose fractions to lower-density sucrose fractions upon treatment with ca.  $30 \mu\text{M}$   $[\text{VO}(\text{saltris})]_2$ . The relative amount of IR in each fraction was measured from Western blots using a calibrated BioRad densitometer. Sucrose concentrations for each fraction were measured with a Bausch and Lomb refractometer (this figure is adapted with permission from [23]).

buoyancy membrane fractions under similar experimental conditions. Significantly, larger shifts in sucrose fractions were observed for ligand-treated rat LH receptors [42].

**BMOV Treatment Can Enhance Receptor-Mediated Responses.** The appearance of insulin receptors within membrane microdomains in the absence of a hormone signal raises a question as to whether receptor function is affected by the presence of V-containing compounds. To examine this, we have used cells expressing a well-characterized receptor, the Type-I  $\text{Fc}\epsilon\text{RI}$  (Fc $\epsilon$ RI), to determine whether presence of a V compound currently being evaluated in clinical trials phase II, BMOV [10][43][44], can enhance calcium flux in response to receptor cross-linking. Fc $\epsilon$ RI are expressed in RBL-2 H3 cells, a cell line derived from rat basophilic leukemia (RBL) cells, and were used in the studies presented here for several reasons. We have had considerable experience in evaluating the localization of RBL-2 H3 cell plasma membrane receptors in membrane rafts during cell signaling [45]. Furthermore, we have used biophysical methods for evaluating molecular dynamics of membrane lipids and proteins, and interactions between membrane molecules in this cell system [46]. Importantly, RBL-2 H3 cells have insulin receptors in addition to Fc $\epsilon$ RI, and are capable of downstream signaling in response to binding of these receptors' respective ligands. Moreover, vanadate has been reported to activate signaling in RBL-2 H3 cells including release of  $\text{Ca}^{2+}$  from intracellular stores and plasma membrane flux, although the mechanism is unclear [47]. Mast cells, which, like basophils, are derived from a  $\text{CD}34$  precursor in the bone marrow and have basophil-like activity in tissues, may also be involved in the development of heart disease [48], although their role remains controversial. Thus, signaling mechanisms utilized by RBL-2 H3 cells are, in and of themselves, of interest.

To establish conditions for cell treatment, RBL-2 H3 cells were treated with BMOV at concentrations that did not affect cell viability on the timescale of our experiments.

RBL-2H3 Cells were maintained in cell culture medium including Earle's Minimum Essential Medium (MEM), fetal bovine serum, and 5 mM L-glutamine, penicillin, ampicillin, and amphotericin B. Cells were harvested for experiments using 5 mM EDTA and washed in BSS, were plated in flat-bottom 96-well plates (Corning) at ca. 50000 cells/well and grown overnight. Media was removed and replaced with media containing indicated BMOV concentrations, and cells were incubated at 37° overnight. 3-(4,5-Dimethylthiazol-2-yl)-2,5-diphenyl-2H-tetrazolium hydrobromide (MTT) assay solution (Sigma) was then added to the culture medium at a volume equal to 10% of the culture volume (20 µl of MTT soln. added to 200 µl of culture medium). Cultures were then incubated for 4 h at 37°. After 4 h, culture medium was removed, and MTT solvent was added. Cultures were left in MTT solvent for 1 h on an oscillating shaker to assist in crystal dissolution, and were then read at 570 nm with a spectrophotometric plate reader. Media alone was also treated in the same manner to allow for background subtraction due to any colorimetric changes due to the phenol red-containing media. Treatment concentrations ranged from 0.1 nM to 100 µM BMOV. Data was analyzed by normalizing the data points (typically 3–5 time repeats at each concentration; symbol is covering error bars) to the media alone sample, taken as 100% viability (Fig. 6). Ten concentrations of 10 nM BMOV had no effect on cell viability.

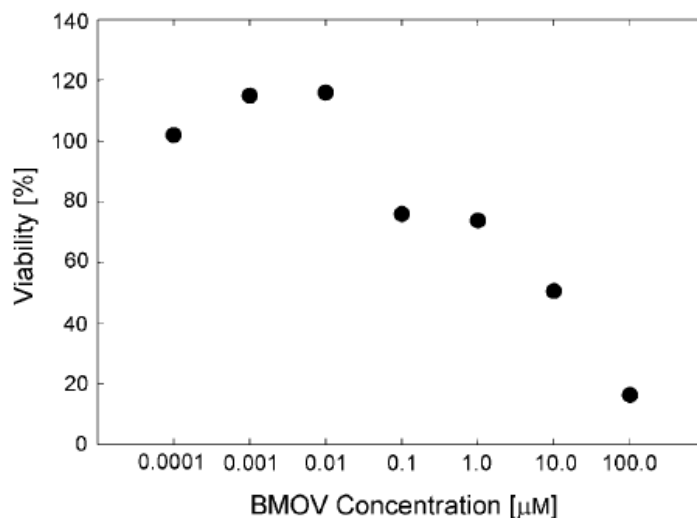


Fig. 6. Cell viability as measured by MTT assay following treatment with BMOV at increasing concentrations (each concentration point was repeated 3–5 times, but the error bars are covered by the symbols)

Pretreatment of RBL-2H3 cells with 10 nM BMOV affects calcium flux in response to cross-linking of FcεRI. Dinitrophenylated bovine serum albumin (DNP-BSA) cross-links FcεRI primed with DNP-specific IgE, and this cross-linking leads to both calcium flux and release of histamine-containing vesicles (data not shown). To evaluate calcium flux in response to FcεR1 receptor cross-linking, 2H3-RBL cells were labeled with Fura-2, a ratiometric dye sensitive to free calcium, using a stock solution of 50 ng of Fura-2 in 50 nl of DMSO. Cells were washed twice prior to the addition of Fura-2 at a final concentration of 5 or 10 nM. Prior to Fura-2 imaging, cells were incubated for 15–60 min at 37° or room temperature. In some experiments, cells were also preincubated

with 10 nM BMOV overnight before cross-linking of FcεRI with DNP-BSA, a treatment strategy which increased the magnitude and duration of calcium flux in response to DNP-BSA. In Fig. 7, we compare the Ca<sup>2+</sup> flux from untreated RBL-2 H3 cells with Ca<sup>2+</sup> flux from cells exposed to 10 nM BMOV following cross-linking of FcεRI with DNP-BSA. The larger Ca<sup>2+</sup> flux from the BMOV treated cells indicate that Ca<sup>2+</sup> homeostasis is affected by the presence of the V compound.

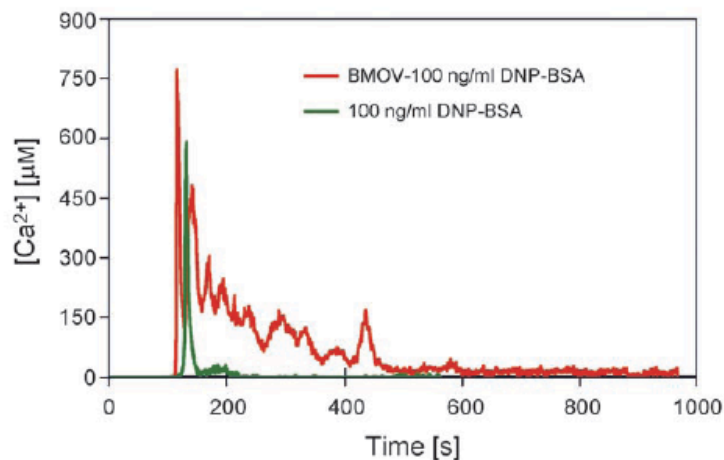


Fig. 7. Ca<sup>2+</sup> Flux from untreated RBL-2 H3 cells and cells exposed to 10 nM BMOV following cross-linking of FcεRI with DNP-BSA

We are currently using two additional approaches to more fully understand the role of membrane microdomains in insulin receptor function. In one series of ongoing studies, we are evaluating the effects of BMOV on GLUT4 insertion in the plasma membrane. Interestingly, both insulin-mediated signaling and the appearance of GLUT4 in the plasma membrane involve microdomains. To evaluate effects of BMOV on GLUT4 into the membranes of 2 H3-RBL cells, we have stably transfected RBL-2 H3 cells with a GFP-GLUT4 plasmid that was the generous gift of *Jeffrey Pessin* (SUNY at Stonybrook), and imaged this molecule either without or after treatment with 100 nM insulin for 30–60 min (Fig. 8). Following exposure to insulin, GFP-GLUT4 appears in the plasma membrane as has been described by *Pessin et al.* [49]. We are now evaluating whether overnight pretreatment with BMOV at concentrations that enhance calcium flux is also sufficient to increase insulin responsiveness of these cells.

A second approach to studies of insulin receptor-containing membrane microdomains is to directly image individual insulin receptors within these small membrane compartments. We have begun single-particle-tracking studies of the insulin receptor using a new strategy introduced by *Lidke et al.* at the University of New Mexico [50]. Our previous SPT studies have depended on epitope tagging of a membrane protein, usually using the FLAG epitope and the complementary anti-FLAG antibody from *Sigma*. However, it is also possible to identify endogenous insulin receptors with an insulin receptor-specific antibody from *Santa Cruz*. In its biotinylated form, this antibody can be conjugated to 605-nm quantum dots which are visualized on cell surfaces. The drawback to this approach is that quantum dots ‘blink’, they spontaneously turn on and off several times on the time scale of our experiments.

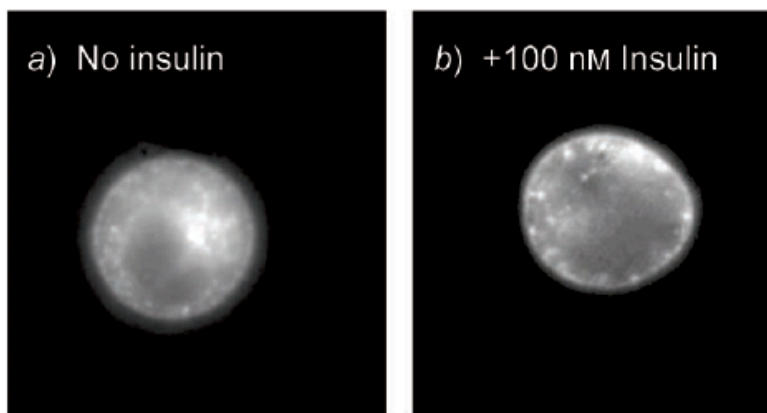


Fig. 8. a) *Insertion of GLUT4 (no insulin) in the plasma membrane.* b) *Membrane localization of GLUT4 in the plasma membrane following incubation of cells with 100 nM insulin.*

Owing to their dark ‘off’ periods, it has been previously impossible to obtain useful trajectories. *Lidke et al.* has developed particle-tracking software that projects a particle track for a quantum dot that has turned off and reacquires its track when the quantum dot turns on. We are now acquiring insulin receptor tracks on viable cells using this strategy which appears to have domain sizes of *ca.* 150 nm, comparable to those seen for luteinizing hormone receptors within the bulk membrane [40]. These experiments should visually demonstrate whether the insulin receptor, after treatment with lipophilic insulin-enhancing compounds, becomes trapped in small compartments.

**Conclusions.** – Together, these results provide preliminary evidence that ligand-mediated signaling can be enhanced by BMOV and other V-compound treatment of RBL-2H3 cells. Such a result may occur as the result of receptor translocation into plasma membrane microdomains where local concentrations of receptors are high and downstream signaling molecules are readily available. Evidence for the possibility that a V-containing probe would facilitate reorganization of the membrane organization, specifically involving cholesterol arrangement in a simple microemulsion model system is presented. Experiments show that membrane flexibility is an important factor, but that V compounds are able to penetrate lipid interfaces with variable flexibility. Effects of different V-containing probes were examined in cells and a very simple model system, cholesterol-doped AOT microemulsions. The results with the anionic and neutral V compounds are presented here, and  $^1\text{H-NMR}$  data is presented that  $\text{V}_{10}$  does not impact the packing of the reverse micelles containing cholesterol. These data are consistent with the model developed and the experiments reported in cells. Although the insulin-enhancing properties of V compounds generally are believed to occur further downstream, the studies shown here demonstrate that V compounds impact the signal transduction through the mechanisms such as  $\text{Ca}^{2+}$  flux.

Financial support for this work by the *American Heart Association* (0650081Z to DAR/DCC) and *National Science Foundation* (NSF; CHE 0244181 to DAR/DCC/NEL/GB) is gratefully acknowledged. We thank Dr. *Christopher D. Rithner* for technical assistance.

## REFERENCES

- [1] P. Schwille, J. Koralach, W. Webb, *Cytometry* **1999**, *36*, 176.
- [2] A. Saltiel, J. Pessin, *Traffic* **2003**, *4*, 711.
- [3] J. Inokuchi, *Yakugaku Zasshi* **2007**, *127*, 579.
- [4] S. Vainio, I. Bykov, M. Hermansson, E. Jokitalo, P. Somerharju, E. Ikonen, *Biochem. J.* **2005**, *391*, 465.
- [5] Y. Shechter, S. J. D. Karlish, *Nature* **1980**, *284*, 556.
- [6] Y. Shechter, J. Meyerovitch, Z. Farfel, J. Sack, R. Bruck, S. Bar-Meir, S. Amir, H. Degani, S. J. D. Karlish, in 'Vanadium in Biological Systems: Physiology and Biochemistry', Ed. N. D. Chasteen, Kluwer Academic Publishers, Boston, 1990, pp. 129–142.
- [7] H. Michibata, H. Sakurai, in 'Vanadium in Biological Systems: Physiology and Biochemistry', Ed. N. D. Chasteen, Kluwer Academic Publishers, Boston, 1990, pp. 153–172.
- [8] H. Sakurai, A. Tamura, J. Fugono, H. Yasui, T. Kiss, *Coord. Chem. Rev.* **2003**, *245*, 31.
- [9] D. C. Crans, J. J. Smee, E. Gaidamauskas, L. Yang, *Chem. Rev.* **2004**, *104*, 849.
- [10] K. H. Thompson, C. Orvig, *J. Chem. Soc., Dalton Trans.* **2006**, 761.
- [11] S. M. Haffner, *Diabetes Care* **2003**, *26*, S83.
- [12] T. Thom, N. Haase, W. Rosamond, V. J. Howard, J. Rumsfeld, T. Manolio, Z.-J. Zheng, K. Flegal, C. O'Donnell, S. Kittner, D. Lloyd-Jones, D. C. J. Goff, Y. Hong, R. Adams, G. Friday, K. Furie, P. Gorelick, B. Kissela, J. Marler, J. Meigs, V. Roger, S. Sidney, P. Sorlie, J. Steinberger, S. Wasserthiel-Smoller, M. Wilson, P. Wolf, *Circulation* **2006**, *113*, e85–e151.
- [13] G. Fantus, E. Tsiani, *Mol. Cell. Biochem.* **1998**, *182*, 109.
- [14] P. G. Drake, B. I. Posner, *Mol. Cell. Biochem.* **1998**, *182*, 79.
- [15] A. K. Srivastava, M. Z. Mehdi, *Diabetic Med.* **2005**, *22*, 2.
- [16] G. R. Willsky, L.-H. Chi, Y. Liang, D. P. Gaile, Z. Hu, D. C. Crans, *Physiol. Genomics* **2006**, *26*, 192.
- [17] W. Basuki, M. Hiromura, Y. Adachi, K. Tayama, M. Hattori, H. Sakurai, *Biochem. Biophys. Res. Commun.* **2006**, *349*, 1163.
- [18] Y. Shechter, I. Goldwasser, M. Mironchik, M. Fridkin, D. Gefel, *Coord. Chem. Rev.* **2003**, *237*, 3.
- [19] B. D. Liboiron, K. H. Thompson, G. R. Hanson, E. Lam, N. Aebischer, C. Orvig, *J. Am. Chem. Soc.* **2005**, *127*, 5104.
- [20] K. Wieghardt, *Inorg. Chem.* **1978**, *17*, 57.
- [21] D. C. Crans, L. Yang, T. Jakusch, T. Kiss, *Inorg. Chem.* **2000**, *39*, 4409.
- [22] D. C. Crans, C. D. Rithner, B. Baruah, B. L. Gourley, N. E. Levinger, *J. Am. Chem. Soc.* **2006**, *128*, 4437.
- [23] D. A. Roess, S. M. L. Smith, A. A. Holder, B. Baruah, A. M. Trujillo, D. Gilsdorf, M. L. Stahla, D. C. Crans, *ACS Symposium Series* **2007**, *974*, 121.
- [24] M. C. Cam, G. H. Cros, J. J. Serrano, R. Lazaro, J. H. McNeill, *Diabetes Res. Clin. Pract.* **1993**, *20*, 111.
- [25] I. Goldwasser, J. P. Li, E. Gershonov, M. Armoni, E. Karnieli, M. Fridkin, Y. Shechter, *J. Biol. Chem.* **1999**, *274*, 26617.
- [26] P. Buglyo, D. C. Crans, E. M. Nagy, R. L. Lindo, L. Yang, J. J. Smee, W. Jin, L.-H. Chi, M. E. Godzala, G. R. Willsky, *Inorg. Chem.* **2005**, *44*, 5416.
- [27] V. Monga, K. H. Thompson, V. G. Yuen, V. Sharma, B. O. Patrick, J. H. McNeill, C. Orvig, *Inorg. Chem.* **2005**, *44*, 2678.
- [28] H. Sakurai, K. Kawabe, H. Yasui, Y. Kojima, Y. Yoshikawa, *J. Inorg. Biochem.* **2001**, *86*, 94.
- [29] A. Maitra, *J. Phys. Chem.* **1984**, *88*, 5122.
- [30] A. Maitra, Dinesh, P. Patanjali, M. Varshney, *Colloids Surf* **1986**, *20*, 211.
- [31] A. Maitra, P. K. Patanjali, *Colloids Surf* **1987**, *27*, 271.
- [32] M. Vermathen, E. A. Louie, A. B. Chodosh, S. Ried, U. Simonis, *Langmuir* **2000**, *16*, 210.
- [33] M. Vermathen, P. Stiles, S. J. Bachofer, U. Simonis, *Langmuir* **2002**, *18*, 1030.
- [34] J. Stover, C. D. Rithner, R. A. Inafuku, D. C. Crans, N. E. Levinger, *Langmuir* **2005**, *21*, 6250.
- [35] X. Yang, K. Wang, J. Lu, D. C. Crans, *Coord. Chem. Rev.* **2003**, *237*, 103.
- [36] X.-G. Yang, X.-D. Yang, L. Yuan, K. Wang, D. C. Crans, *Pharm. Res.* **2004**, *21*, 1026.

- [37] Y. Zhang, X. Yang, K. Wang, D. C. Crans, *J. Inorg. Biochem.* **2006**, *100*, 80.
- [38] M. Aureliano, F. Henao, T. Tiago, R. O. Duarte, J. J. G. Moura, B. Baruah, D. C. Crans, *Inorg. Chem.* **2008**, submitted.
- [39] Y. Lei, G. M. Hagen, S. M. L. Smith, B. G. Barisas, D. A. Roess, *Biochem. Biophys. Res. Commun.* **2005**, *337*, 430.
- [40] Y. Lei, G. M. Hagen, S. M. Smith, J. Liu, G. Barisas, D. A. Roess, *Mol. Cell. Endocrinol.* **2007**, *65*, 260–262.
- [41] E. D. Sheets, D. Holowka, B. Baird, *Curr. Opin. Chem. Biol.* **1999**, *3*, 95.
- [42] S. M. L. Smith, Y. Lei, J. Liu, M. E. Cahill, G. M. Hagen, B. G. Barisas, D. A. Roess, *Endocrinology* **2006**, *147*, 1789.
- [43] J. H. McNeill, V. G. Yuen, H. R. Hoveyda, C. Orvig, *J. Med. Chem.* **1992**, *35*, 1489.
- [44] D. C. Crans, B. Baruah, E. Gaidamauskas, B. G. Lemons, B. B. Lorenz, M. D. Johnson, *J. Inorg. Biochem.* **2008**, *102*, 1334.
- [45] J. Song, G. M. Hagen, D. A. Roess, I. Pecht, B. G. Barisas, *Biochemistry* **2002**, *41*, 881.
- [46] D. A. Roess, S. M. L. Smith, *Biol. Reprod.* **2003**, *69*, 1765.
- [47] G. Ehring, H. Kerschbaum, C. Fanger, C. Eder, H. Rauer, M. Cahalan, *J. Immunol.* **2000**, *164*, 679.
- [48] G. Palladini, R. Tozzi, S. J. Perlini, *Hypertension* **2003**, *21*, 1823.
- [49] J. E. Pessin, D. C. Thurmond, J. S. Elmendorf, K. J. Coker, S. Okada, *J. Biol. Chem.* **1999**, *274*, 2593.
- [50] K. A. Lidke, N. L. Andrews, D. S. Lidke, J. R. Pfeiffer, B. S. Wilson, J. M. Oliver, A. R. Burns, *Biophys. J.* **2007**, 418A.

Corrected figure 2.

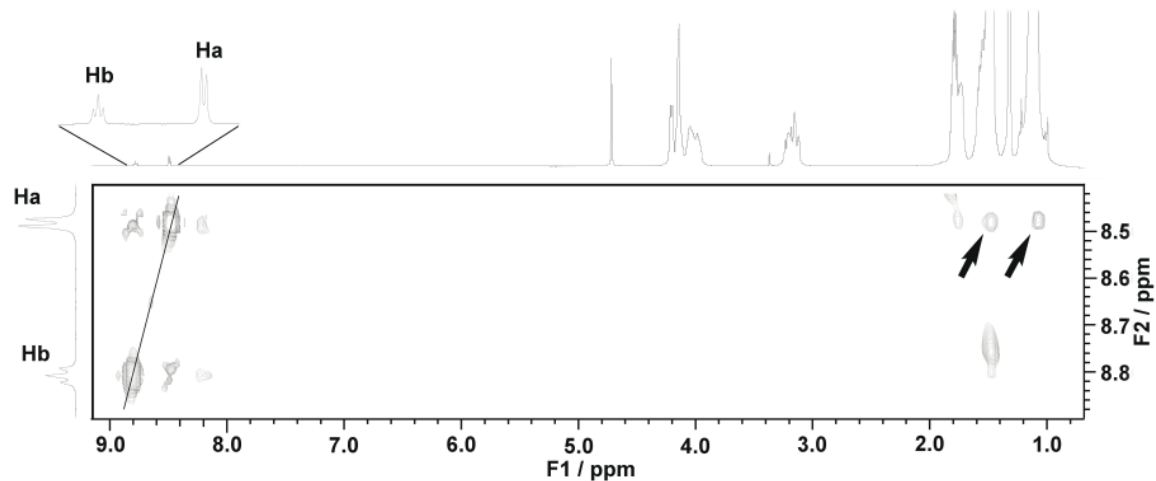


Fig. 2. 2D-NOESY Recorded of 100 mM  $[\text{VO}_2(\text{dipic})]$  complex in a 1M AOT / iso-octane- $d_{18}$  /  $\text{D}_2\text{O}$  (pH 4.5) microemulsion of  $w_0 = 20$ .

## **Do Vanadium Compounds Drive Reorganization of the Plasma Membrane and Activation of Insulin Receptors with Lipid Rafts?**

**Deborah A. Roess<sup>\*</sup>, Steven M. L. Smith, Alvin A. Holder, Bharat Baruah, Alejandro M. Trujillo, Daniel Gilsdorf, Michelle L. Stahla, and Debbie C. Crans<sup>\*</sup>**

**Departments of Biomedical Sciences and Chemistry, Colorado State University, Fort Collins, CO 80523–1872**

The enhancement by vanadium compounds of insulin-mediated signaling in RBL-2H3 cells was investigated. The studies were based on preliminary studies in which a hydrophobic vanadium compound facilitated the translocation of the insulin receptor into plasma membrane rafts. Such results led to the studies of a vanadium compound known to be insulin-enhancing in animal model studies. The proof of concept, namely that vanadium compounds could interact directly with lipid bilayers made up of amphipathic lipids, was supported by results in a very simple model system based on cholesterol-doped AOT reverse micelles. Studies adding vanadium compound to this simple model system demonstrated that the presence of the vanadium compound resulted in lipid reorganization.

---

<sup>6</sup>Alejandro M. Trujillo contributed figure 6 & 7  
*Published in ACS Symposium Series, 2007, (974) 121-134.*

## Introduction

The possibility for vanadium compounds facilitating any insulin-enhancing effects through reorganization of plasma membrane lipids was investigated in a cell line derived from rat basophilic leukemia (RBL) cells and a simple model system. The rationale for these studies was based on the well-known insulin-enhancing properties of several lipophilic vanadium compounds (1, 2) and the recent report of a vanadium compound penetrating the lipid layer in a model system (3). Effects of vanadium-containing compounds are of interest because they can normalize both elevated blood glucose and lipid levels and may have long-term benefits to cardiovascular health, which is a frequent complication of diabetes (4, 5). The mechanism of insulin action on its target cells involves binding of insulin to its plasma membrane receptor (6-9). Evidence for translocation of the receptor to specialized lipid microdomains (rafts) in the plasma membrane has led to the suggestion, that these rafts may serve as platforms for insulin receptor-mediated signal transduction (10, 11). Although vanadium compounds are generally believed to act downstream of the insulin receptor (12-16), some effects of transition metal compounds such as vanadium compounds may be mediated through their actions on the plasma membrane and the organization of proteins and lipids within the lipid bilayer. Here we investigate whether insulin-enhancing vanadium compounds may evoke their effects through direct interactions with the plasma membrane of cells expressing insulin receptors. Such direct interactions could result in the perturbation of membrane lipid organization and facilitate the movement of insulin receptors or other signaling molecules into membrane rafts in the absence of an insulin signal. Thus, insulin-enhancing vanadium compounds may concentrate these molecules in rafts where they have ready access to other molecules involved in downstream signaling events and, in this fashion, enhance insulin-mediated cellular responses.

Insulin-enhancing lipophilic vanadium compounds were found to be more readily absorbed *in vivo*, and less toxic than the vanadium salts (1, 2). Since these compounds might interact with cell membrane lipids, we tested the effects of one highly lipophilic vanadium compound prepared from salicylaldehyde and tris(hydroxymethyl)aminoethane to form an adduct with  $\text{VO}(\text{acac})_2$  referred to as  $[\text{VO}(\text{saltris})]_2$ , 1 here (17, 18). While these studies were underway vanadium-containing probes in reverse micelles (3, 19-21) e.g.  $\text{NH}_4[\text{VO}_2(\text{dipic})]$ , 2 and  $\text{V}_{10}\text{O}_{28}^{6-}$  ( $\text{V}_{10}$ ), 3 were reported to be excellent probes of the water pool (20, 21) and the interfacial region (3) in the reverse micelle, respectively. The fact that one vanadium compound was found to intercalate in the interfacial layer of the AOT-based reverse micelle (19) further supported the concept that vanadium compounds could exert some of their actions at the plasma membrane of cells *in vivo*. Given the complexities of studies involving plasma membranes or micelles formed from plasma membrane components, reverse micelles provide an

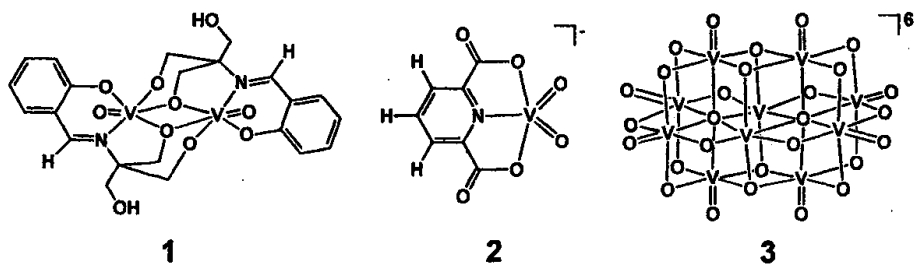


Figure 1. Structures of  $[VO(\text{saltris})]_2$ , 1;  $[VO(\text{dipic})]^-$ , 2 and  $V_{10}O_{28}^{6-}$ , 3.

attractive simple model system in which to evaluate vanadium compound interactions with lipids.

A cell line derived from RBL cells were used in the studies presented here for several reasons. We have had considerable experience in evaluating the localization of RBL-2H3 cell plasma membrane receptors in membrane rafts during cell signaling (22-24). Furthermore, we have used biophysical methods for evaluating molecular dynamics of membrane lipids and proteins and interactions between membrane molecules in this cell system (22). Importantly, RBL-2H3 cells have insulin receptors in addition to the Type I Fcε receptor (FcεRI), and are capable of downstream signaling in response to binding of these receptors' respective ligands. Moreover, vanadate has been reported to activate signaling in RBL-2H3 cells including release of  $Ca^{2+}$  from intracellular stores and plasma membrane flux although the mechanism is unclear (25). Mast cells, which like basophils are derived from a  $CD34^+$  precursor in the bone marrow and have basophil-like activity in tissues, may also be involved in the development of heart disease (26) although their role remains controversial. Thus, signaling mechanisms utilized by RBL-2H3 cells, a mast cell model, are, in and of themselves, of interest.

## Materials and Methods

**Chemicals.** Sodium metavanadate,  $NaVO_3$  (99.9%), salicylaldehyde (98%), tris(hydroxymethyl)aminoethane (99%), 2,6-pyridinedicarboxylic acid (99%), bis(acetylacetonato)oxovanadium(IV) (98%), AOT (sodium bis(2-ethylhexyl) sulfosuccinate (99%), cholesterol(98%), isooctane (99%) and carbon tetrachloride ( $CCl_4$ ) (99.9%) were purchased from Aldrich and used without purification unless noted otherwise. The  $[VO(\text{saltris})]_2$  was prepared by condensation of salicylaldehyde and tris in methanol and reacting the product, 2-salicylideneimino-2-(hydroxymethyl)-1,3-dihydroxy-propane ( $H_4\text{saltris}$ ) with  $VO(\text{acac})_2$  as reported previously (17, 18). Ammonium 2,6-dipicolinatodioxovanadium(V),  $NH_4[VO_2(\text{dipic})]$  was synthesized as described

previously (27-29). Decavanadate ( $V_{10}$ ) solutions were prepared from solid metavanadate, which upon dissolution were acidified to pH 4 and thus converted completely to  $V_{10}$ . The compounds were characterized by routine methods including NMR and IR spectroscopy and elementary analysis. AOT was purified by dissolution in methanol and stirring overnight in the presence of activated charcoal. Subsequent filtration and removal of methanol by distillation under vacuum yielded AOT suitable for use. Cyclohexane- $d_{12}$  ( $C_6D_{12}$ ) and  $D_2O$  (Cambridge Isotope Laboratories Inc.) were used without further purification.

*Stock Solution Preparation.* The low solubility of  $[VO(\text{saltris})]_2$  in aqueous solution led to preparation of stock solutions in dmsO. Aqueous stock solutions of  $NH_4[VO_2(\text{dipic})]$  were prepared by dissolution in  $D_2O$  in a volumetric flask. All the freshly prepared stock solutions were of 50, 25 and 15 mM at pH 4.5. Decavanadate ( $V_{10}$ ) solutions were prepared by dissolving  $NaVO_3$  (50, 100 and 200 mM) in  $D_2O$  and reducing the pH to 4.0 to ensure complete conversion to  $V_{10}$ . The pH values of the aqueous  $V_{10}$  stock solutions were measured at 25°C using an Orion 420A pH meter calibrated with three buffers of pH 4, 7 and 10. The pH of the vanadate aqueous solutions was adjusted using  $NaOD/DCI$ .

*Cell culture.* RBL-2H3 cells were maintained in cell culture medium including Earle's Minimum Essential Medium (MEM), fetal bovine serum, and 5mM L-glutamine, penicillin, ampicillin and amphotericin B. Cells were harvested for experiments using 5 mM EDTA and washed in Hank's balanced salt solution (BSS).

*Cell viability assay.* Initial experiments characterized the effects of various concentrations of  $[VO(\text{saltris})]_2$  or  $[VO_2(\text{dipic})]$  on cell viability. RBL-2H3 cells were plated in petri dishes and grown to 80% confluence and then washed with BSS. Cells were then incubated with various concentrations of either  $[VO(\text{saltris})]_2$  or  $[VO_2(\text{dipic})]$  overnight. Cell aliquots were withdrawn from each culture, mixed with an equal volume of trypan blue, and examined microscopically. Both the dead cells stained by trypan blue and unstained living cells were scored.

*Raft protocol.* To examine the distribution of insulin receptors within membrane fractions exhibiting either low or high buoyancy, sucrose gradient ultracentrifugation methods were used. Briefly,  $5 \times 10^6$  RBL-2H3 cells were obtained from cell culture and suspended in BSS. Cells were then treated with  $[VO(\text{saltris})]_2$  for one hour prior to cell lysis. The cell lysate was mixed with an equal volume of 80% sucrose to obtain a sample consisting of cell membranes and their components in 40% sucrose. A discontinuous sucrose gradient from 10-80% sucrose was constructed with the cell fraction comprising the 40% sucrose fraction. Samples were then subjected to isopycnic ultracentrifugation using an overnight spin at approximately 180,000 g. After centrifugation, 640  $\mu L$  fractions are carefully collected from the top down of the gradient downward. Aliquots from each fraction were probed for proteins of interest including the insulin receptor. The insulin receptor was identified using on Western blots using an anti-insulin receptor antibody (Sigma-Aldrich, St. Louis, MO).

*Effects of vanadium compounds of RBL-2H3 degranulation.* RBL-2H3 cells were grown in petri dishes and harvested as for other experiments. These cells, upon receiving signals via selected membrane receptors, can release the contents of their granules, which contain histamine and tryptase. The magnitude of a degranulation response was measured in RBL-2H3 cells by quantifying the amount of tryptase that is released using a mast cell degranulation assay kit from Chemicon (Temecula, CA) using Manufacturers' instructions.

*Reverse Micelle Preparation.* A 120 mM AOT stock solution was prepared by dissolving NaAOT in isooctane with a cholesterol concentration of 30 mM. Aliquots of aqueous stock solutions of concentration 5.0, 10 and 20 mM  $V_{10}$  were added to the AOT/cholesterol/isooctane stock solution to yield reverse micelle solution of  $w_0 = 8$ . A 50 mM AOT stock solution was prepared by dissolving AOT in cyclohexane- $d_{12}$  ( $C_6D_{12}$ ) under ambient conditions with a cholesterol concentration of 12.5 mM. Aliquots of aqueous stock solutions of concentration 50, 25 and 15 mM  $NH_4[VO_2(dipic)]$  were added to the AOT/cholesterol/ $C_6D_{12}$  stock solution to yield reverse micelle solution of  $w_0 = 8$ . All samples were mixed by vortexing to yield an optically clear solution prior to  $^1H$  NMR spectroscopic measurements. Formation of reverse micelles were confirmed by dynamic light scattering (DLS) experiments.

*NMR spectroscopy.* The samples were subjected to multinuclear NMR spectroscopy. The  $^1H$  NMR results described in this manuscript were obtained using a Varian Inova-500 spectrometer at 500 MHz. Routine parameters were used for the 1D  $^1H$  NMR experiments.  $^1H$  NMR chemical shifts were referenced against a 3-(trimethylsilyl)propane sulfonic acid sodium salt (DSS) as an external reference.

## Results

The rationale for compound selection of three different vanadium compounds  $[VO(saltris)]_2$ ,  $[VO_2(dipic)]^-$  and  $V_{10}$  was based on lipophilicity, insulin-enhancing effects (29) and previous studies carried out in reverse micelles (3). Together the results demonstrate that vanadium compounds have the potential to act through changes in lipid packing in cells and in simple model systems. The initial cellular experiments were carried out using the lipophilic vanadium compound ( $[VO(saltris)]_2$ ) and provided results showing translocation of insulin receptors into high buoyancy membrane fractions in the absence of insulin. The recent report documenting intercalation of a vanadium compound ( $[VO_2(dipic)]^-$ ) in the lipid interface (3) motivated additional studies with this compound that had already been demonstrated to have insulin-enhancing effects in an animal model system (29). The studies in the RBL-2H3 cells were supported by investigations in reverse micelles which showed that the vanadium-containing probe,  $V_{10}$  was able to impact the chemical shifts of some of the cholesterol H-atoms in the lipid interface. These effects can be interpreted as changes in lipid packing.

To examine effects of a hydrophobic vanadium compound on membrane localization of the insulin receptor in the absence of the insulin ligand, we treated RBL-2H3 cells for 1 hr with 30  $\mu$ M [VO(saltris)]<sub>2</sub> (17, 18). This compound is non-toxic at the concentrations used in these experiments (data not shown). As shown in Figure 2, the addition of [VO(saltris)]<sub>2</sub> to RBL-2H3 cells, resulted in movement of insulin receptor to higher buoyancy membrane fractions in the absence of insulin. Prior to [VO(saltris)]<sub>2</sub> treatment, 97% of IR was localized in sucrose fractions containing 39-52% sucrose. Following [VO(saltris)]<sub>2</sub> treatment, 97% of the receptor was localized in 34-39% sucrose. We believe that these structures are rafts based on previous reports showing that FcεRI on RBL-2H3 cells appearing in sucrose fractions containing less than 40% sucrose (30) following crosslinking of the receptor with antigen and similar results with the luteinizing hormone receptor in our laboratory (31). Furthermore, [VO(saltris)]<sub>2</sub> treatment caused degranulation of RBL-2H3 cells in a dose-dependant fashion, as demonstrated in Figure 3.

Given the problems associated with working with lipophilic compounds and to explore if insulin-enhancing vanadium compounds also exert similar effects, studies were continued using [VO<sub>2</sub>(dipic)]. Interestingly, treatment of cells with a vanadium compound that is much less lipophilic also enhanced the insulin-mediated effects on RBL-2H3 degranulation. Degranulation were measured

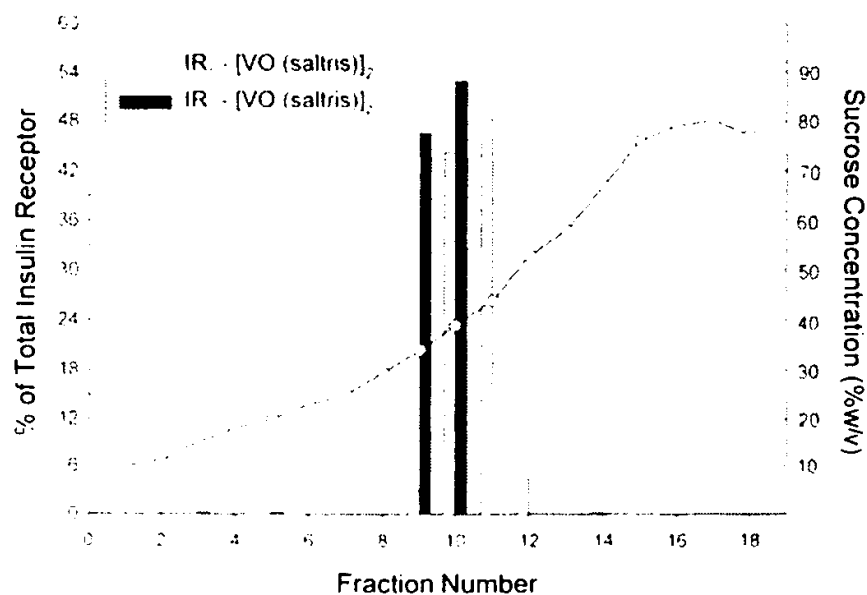


*Figure 2. Translocation of IR from higher density sucrose fractions to lower density sucrose fractions upon treatment with approximately 30  $\mu$ M [VO(saltris)]<sub>2</sub>. The relative amount of IR in each fraction was measured from western blots using a Biorad calibrated densitometer. Sucrose concentrations (%) for each fraction were measured using a Bausch and Lomb refractometer.*

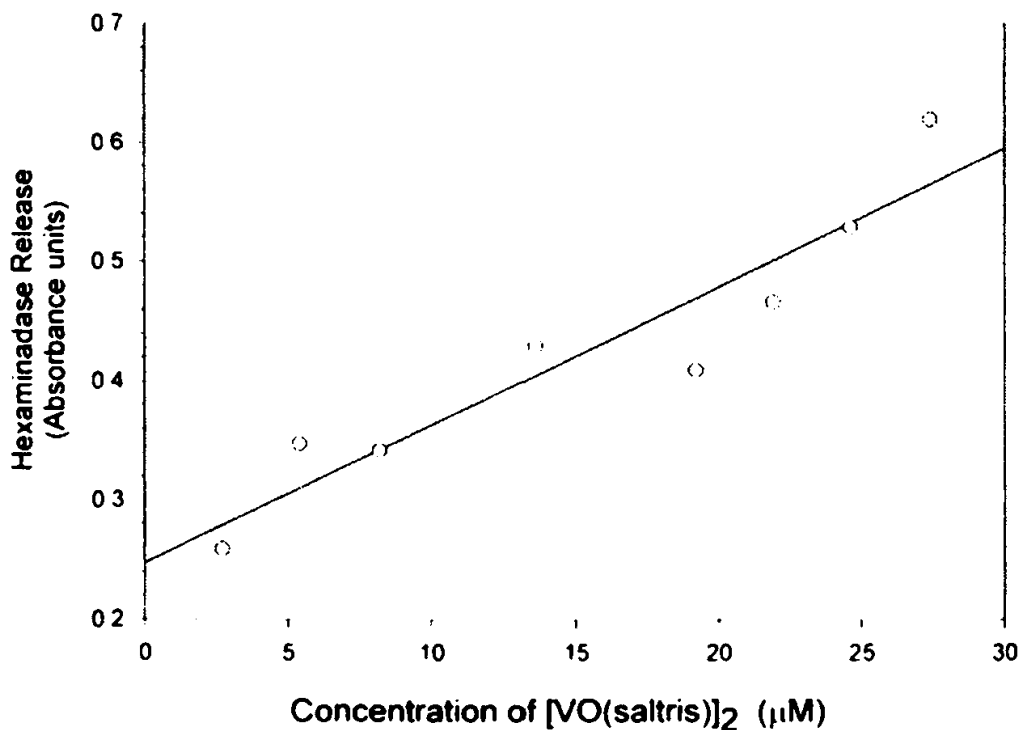


**Figure 3.** Degranulation of RBL-2H3 cells as measured by hexaminadase release from histamine-containing granules following incubation with increasing concentrations of [VO(saltris)]<sub>2</sub>.

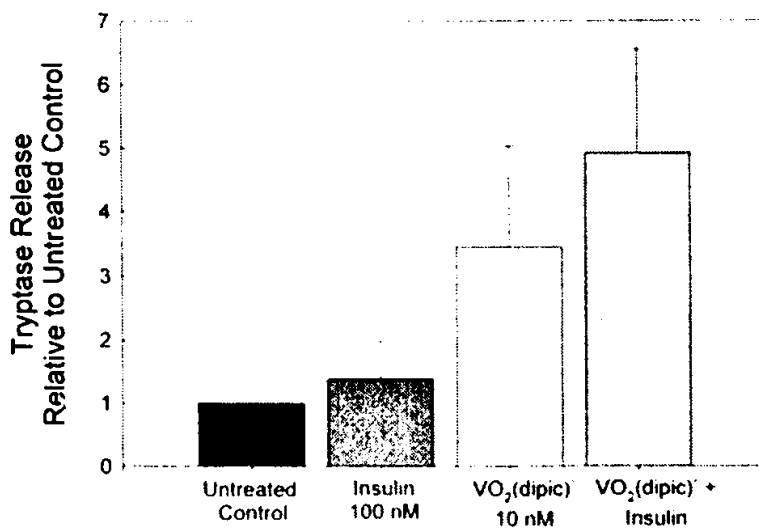


**Figure 4.** Degranulation of RBL-2H3 treated with [VO<sub>2</sub>(dipic)] alone or with insulin. [VO<sub>2</sub>(dipic)] caused increased degranulation of RBL-2H3 and enhanced insulin-mediated degranulation. Results shown are the mean and S.E.M. from three experiments performed in triplicate.

using hexamidase and tryptase release, respectively. There was a 3-fold increase in degranulation by RBL-2H3 cells compared to untreated cells following treatment with 10 nM  $[\text{VO}_2(\text{dipic})]^-$  alone (Figure 4). This concentration of  $[\text{VO}_2(\text{dipic})]^-$  was not toxic to cells on this timescale of these experiments (Figure 5). The extent of degranulation was 5-fold over untreated levels in response to 100 nM insulin and 10 nM  $[\text{VO}_2(\text{dipic})]^-$ . Surprisingly, insulin alone had comparatively little effect on degranulation. These results suggest that  $[\text{VO}_2(\text{dipic})]^-$  enhances the activity of insulin which, by itself, has comparatively little effect on these cells.

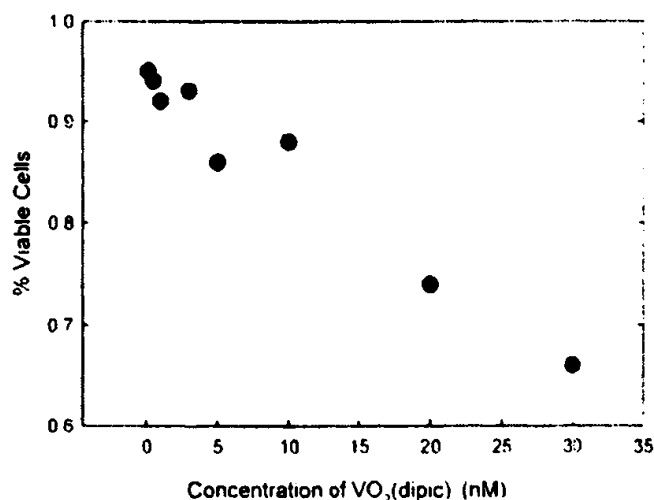


*Figure 5. Cell viability as measured by trypan blue dye exclusion following treatment with  $[\text{VO}_2(\text{dipic})]^-$  at increasing concentrations.*

Demonstration that two classes of vanadium compounds in the RBL-2H3 cells were able to facilitate insulin-mediated signal transduction led us to seek proof of concept in the simple cholesterol-containing AOT reverse micelles model system. Considering the stability of  $\text{V}_{10}$  in aqueous solution, and the recent studies with this probe (21) led us to first carry out studies with this compound.

### **Cholesterol Environment Change in the Presence of a Vanadium-Containing Probe ( $\text{V}_{10}$ )**

The  $^1\text{H}$  NMR chemical shifts of cholesterol were followed when cholesterol was interchelated into reverse micelles and dispersed in solution. The structure and numbering system used is shown in Figure 6. Spectra recorded of cholesterol and AOT dispersed in  $\text{CCl}_4$  were used as reference spectra for comparison.

Reverse micelles at a  $w_o = 8$  were made containing a ratio of 1: 4 (30 mM : 120 mM) cholesterol:AOT using isoctane as the organic solvent. The nature of the interaction between cholesterol and AOT was investigated using 2D NOESY spectroscopy and will be detailed elsewhere; suffice to summarize here, that cholesterol appears to be deeply entrenched into the lipid interface (32, 33) as reported for membrane systems (34, 35).

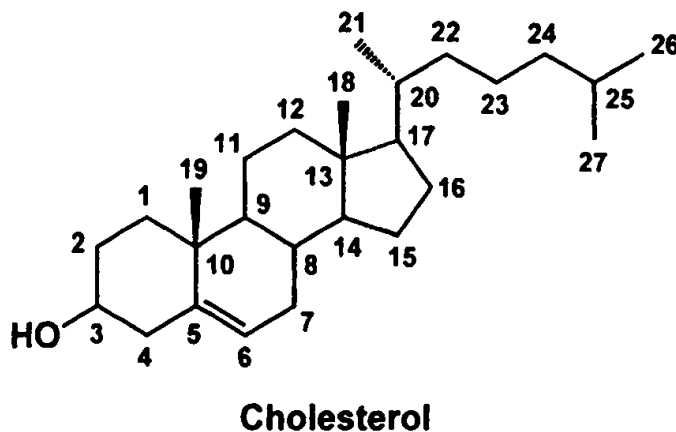


Figure 6. Structure of cholesterol.

Reverse micelles were formed by the addition of aqueous solutions of preformed  $V_{10}$  (50 mM, 100 mM and 200 mM) for comparison with the reverse micelles in the absence of  $V_{10}$ . The chemical shifts for some of the  $^1H$  in the cholesterol molecule changed as the  $V_{10}$  compound was added to the water pool and selected signals are shown in Fig. 6. The chemical shifts for the H-atoms on  $C_4$ ,  $C_7$  and  $C_{12}$  changed little, whereas, a large shift was observed for the H-atoms on  $C_3$ ,  $C_6$  and  $C_{18}$ .

The changes in chemical shifts reflect changes in environment and is consistent with changes in lipid packing near these H-atoms upon addition of  $V_{10}$  probe to the reverse micelle. However, other H-atoms change little indicating that their environments change little. Combined, these data support the possibility that the environment on one side (the one with the  $CH_3$ - group on  $C_{12}$ ) of the cholesterol molecule is changed more than the side with the  $CH_3$  group ( $C_{19}$ ) on  $C_{10}$ . Future studies will explore in greater detail these effects, as well as studies in which different vanadium compounds have been investigated.

## Discussion

The addition of  $[VO(\text{saltris})]_2$  to RBL-2H3 cells, resulted in movement of insulin receptor to slightly higher buoyancy membrane fractions. Although the shift in in location of the insulin receptor is modest, both the Fc receptor (23, 24,

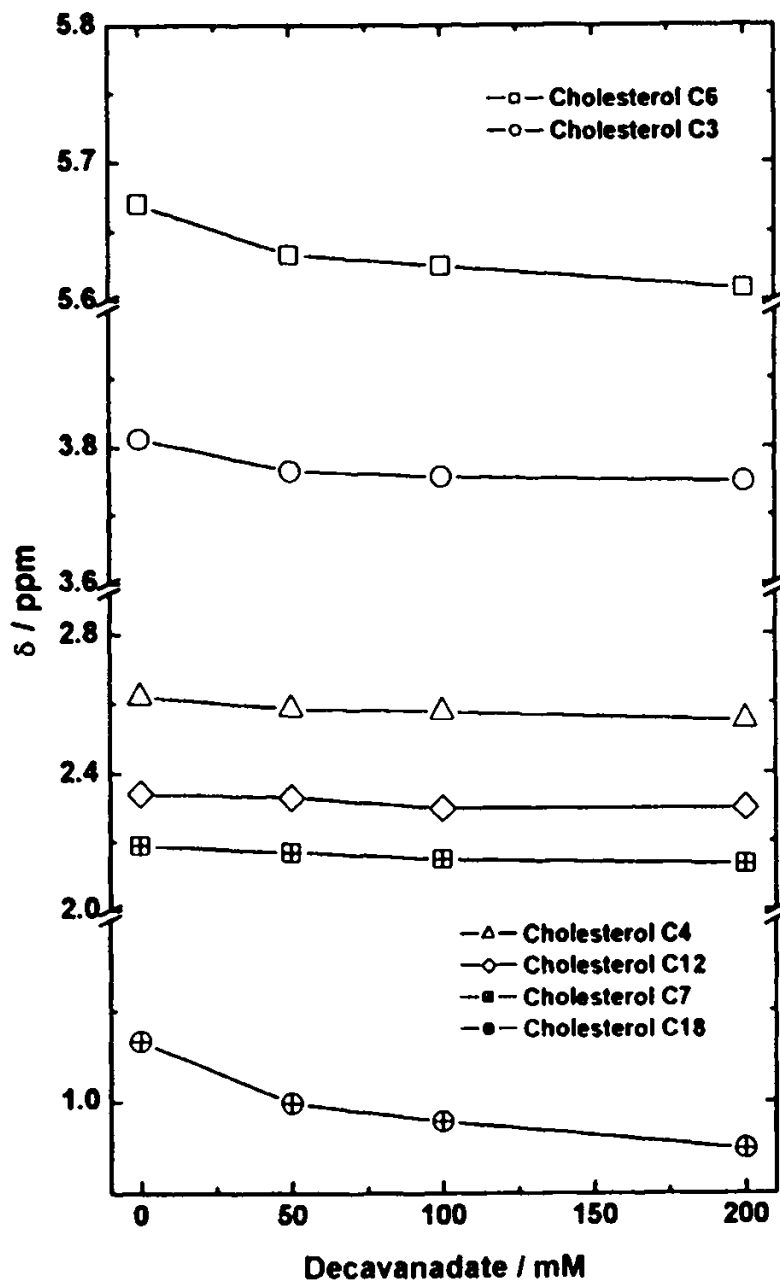


Figure 7. The  $^1\text{H}$  NMR chemical shift of selected cholesterol protons prepared from cholesterol (30 mM) and AOT (120 mM) based  $w_o = 8$  reverse micelles is shown as increasing concentrations of  $V_{10}$  is added to the water-pool of the reverse micelle. The chemical shifts for protons on carbons shown here are located as indicated in Figure 6 on the structure.

30) and the human luteinizing hormone receptor (24) have previously been shown to shift into higher buoyancy membrane fractions. Larger shifts were observed with the rat LH receptor (31). Additional work will document whether this modest shift is a characteristic of vanadium compounds effects on membranes in general and whether other compounds show greater shifts. We are continuing this work using a vanadium compound for which the insulin-enhancing effects have been documented in an animal model to determine if there is more pronounced movement to higher buoyancy membrane fractions.

The demonstration that  $[\text{VO}_2(\text{dipic})]^-$  facilitated increase in degranulation of RBL-2H3 cells is important and does imply that also vanadium compounds that are less lipophilic can exert these effects. The increase in insulin-mediated degranulation in the presence of  $[\text{VO}_2(\text{dipic})]^-$  could be the most significant result observed in these studies. However, verification using other treatment doses to confirm this interpretation of these observations with this complex and others are underway. Furthermore, experimentation to investigate whether the enhanced insulin response by  $[\text{VO}_2(\text{dipic})]^-$  treated cells is due to the translocation of the insulin receptor into rafts *prior to* binding of insulin is underway.

Vanadium compounds are generally not believed to bind to the insulin receptor (36-38) and are believed to exert their insulin-enhancing effects downstream of the insulin receptor (12-16). However, the likely effects on multiple pathways have recently been documented in, for example, the DNA microarray analysis of global gene expression levels documenting numerous changes in gene expression (12). The possibility that vanadium compounds interact directly with membranes or proteins closely associated with membranes seems high, particularly in light of the recent finding that the insulin-enhancing compound  $[\text{VO}_2(\text{dipic})]^-$  is located in the lipid layer of reverse micelles (19). This finding was particularly surprising considering the charge and polarity of this compound, but provide the precedent for other vanadium compounds partitioning in a similar manner similarly in the cell membranes. However, the evidence presented needs substantiation in terms of a more exhaustive study. The observation that several classes of vanadium-compounds exert these responses may imply that the specific ligand is less important than anticipated (39, 40). This observation is in agreement with existing literature that show although effects of vanadium compounds vary with different oxidation state of the metal (41, 42), ligand really exert a more fine-tuning type effect.

## Conclusions

Together these results suggest that insulin-mediated signaling in RBL-2H3 cells is enhanced by  $[\text{VO}(\text{saltris})_2]$  and  $[\text{VO}_2(\text{dipic})]^-$ . Such a result may occur as the result of insulin receptor translocation into plasma membrane rafts where

local concentrations of insulin receptors are high and downstream signaling molecules are readily available. Evidence for the possibility that a vanadium-containing probe would facilitate reorganization of the cholesterol arrangement in a model system is presented. Three different vanadium-containing probes were examined in this initial series of cells and a very simple model system, cholesterol-doped AOT reverse micelles. The results with the anionic probe V<sub>10</sub> are presented here, and suggest that the presence of the vanadium-containing probe impacts the packing of the AOT-based reverse micelles containing cholesterol. Although the biological investigations have been carried out with vanadium-compounds capable of associating in lipid-environments, the studies in the model system show that even a strongly charged vanadium-containing probe affect the arrangements of the surfactant with respect to the cholesterol.

### Acknowledgment

Financial support for this work by the American Heart Association (0650081Z to D.A.R.) and NSF 0314719 (DCC) is gratefully acknowledged. We thank Gabriel R. Harewood for providing some samples of [VO(saltris)]<sub>2</sub>. We thank Dr. Christopher D. Rithner for technical assistance and Dr. Nancy E. Levinger for stimulating discussions regarding the AOT-reverse system used in these studies.

### References

1. Shechter, Y.; Karlsh, S. J. D. *Nature* **1980**, *284*, 556-558.
2. Shechter, Y.; Meyerovitch, J.; Farfel, Z.; Sack, J.; Bruck, R.; Bar-Meir, S.; Amir, S.; Degani, H.; Karlsh, S. J. D. In *Vanadium in Biological Systems: Physiology and Biochemistry*; Chasteen, N. D., Ed.; Kluwer Academic Publishers: Boston, 1990, pp 129-142.
3. Stover, J.; Rithner, C. D.; Inafuku, R. A.; Crans, D. C.; Levinger, N. E. *Langmuir* **2005**, *21*, 6250-6258.
4. Haffner, S. M. *Diabetes Care* **2003**, *26*, S83-S86.
5. Thom, T.; Haase, N.; Rosamond, W.; Howard, V. J.; Rumsfeld, J.; Manolio, T.; Zheng, Z.-J.; Flegal, K.; O'Donnell, C.; Kittner, S.; Lloyd-Jones, D.; Goff, D. C. J.; Hong, Y.; Adams, R.; Friday, G.; Furie, K.; Gorelick, P.; Kissela, B.; Marler, J.; Meigs, J.; Roger, V.; Sidney, S.; Sorlie, P.; Steinberger, J.; Wasserthiel-Smoller, S.; Wilson, M.; Wolf, P. *Circulation* **2006**, *113*, e85-e151.
6. Saltiel, A. R.; Kahn, C. R. *Nature* **2001**, *414*, 799-806.
7. Koricanac, G.; Isenovic, E.; Stojanovic-Susulic, V.; Miskovic, D.; Zakula, Z.; Ribarac-Stepic, N. *Gen. Physiol. Biophys.* **2006**, *25*, 11-24.

8. Dey, D.; Mukherjee, M.; Basu, D.; Datta, M.; Roy, S. S.; Bandyopadhyay, A.; Bhattacharya, S. *Cell. Physiol. Biochem.* **2005**, *16*, 217-228
9. Hegarty, B. D.; Bobard, A.; Hainault, I.; Ferre, P.; Bossard, P.; Fougelle, F. *P. Natl. Acad. Sci.* **2005**, *102*, 791-796.
10. Vainio, S.; Heino, S.; Mansson, J.-E. *EMBO reports* **2002**, *31*, 95-100.
11. Bickel, P. E. *Am. J. Physiol.* **2002**, *282*, E1-E10.
12. Willsky, G. R.; Chi, L.-H.; Liang, Y.; Gaile, D. P.; Hu, Z.; Crans, D. C. *Physiol. Genomics* **2006**, *26*, 192-201.
13. Basuki, W.; Hiromura, M.; Adachi, Y.; Tayama, K.; Hattori, M.; Sakurai, H. *Biochem. Bioph. Res. Co.* **2006**, *349*, 1163-1170.
14. Shechter, Y.; Goldwasser, I.; Mironchik, M.; Fridkin, M.; Gefel, D. *Coord. Chem. Rev.* **2003**, *237*, 3-11.
15. Thompson, K. H.; Orvig, C. *Dalton Trans.* **2006**, 761-764.
16. Liboiron, B. D.; Thompson, K. H.; Hanson, G. R.; Lam, E.; Aebischer, N.; Orvig, C. *J. Am. Chem. Soc.* **2005**, *127*, 5104-5115.
17. Asgedom, G.; Sreedhara, A.; Rao, C. P. *Polyhedron* **1995**, *13-14*, 1873-1879.
18. Asgedom, G.; Sreedhara, A.; Kivikoski, J.; Valkonen, J.; Kolehmainen, E.; Rao, C. P. *Inorg. Chem.* **1996**, *35*, 5674-5683.
19. Crans, D. C.; Rithner, C. D.; Baruah, B.; Gourley, B. L.; Levinger, N. E. *J. Am. Chem. Soc.* **2006**, *128*, 4437-4445.
20. Crans, D. C.; Baruah, B.; Levinger, N. E. *Biomed. Pharmacother.* **2006**, *60*, 174-181
21. Baruah, B.; Roden, J. M.; Sedgwick, M.; Correa, N. M.; Crans, D. C.; Levinger, N. E. *J. Am. Chem. Soc.* **2006**, *128*, 12758-12765
22. Roess, D. A.; Smith, S. M. L. *Biol. Reprod.* **2003**, *69*, 1765-1770.
23. Lei, Y.; Hagen, G. M.; Smith, S. M. L.; Barisas, B. G.; Roess, D. A. *Biochem. Bioph. Res. Co.* **2005**, *337*, 430-434.
24. Lei, Y.; Hagen, G. M.; Smith, S. M. L.; Barisas, B. G.; Roess, D. A. *Mol. Cell. Endocrinol.* **2006**, *in press*.
25. Ehring, G.; Kerschbaum, H.; Fanger, C.; Eder, C.; Rauer, H.; Cahalan, M. J. *Immunol.* **2000**, *164*, 679-687.
26. Palladini, G.; Tozzi, R.; Perlini, S. *J. Hypertens.* **2003**, *21*, 1823-1825.
27. Wieghardt, K. *Inorg. Chem.* **1978**, *17*, 57-64.
28. Nuber, B.; Weiss, J.; Wieghardt, K. *Z. Naturforsch.* **1978**, *33B*, 265-267.
29. Crans, D. C.; Yang, L.; Jakusch, T.; Kiss, T. *Inorg. Chem.* **2000**, *39*, 4409-4416.
30. Sheets, E. D.; Holowka, D.; Baird, B. *Curr. Opin. Chem. Biol.* **1999**, *3*, 95-99.
31. Smith, S. M. L.; Lei, Y.; Liu, J.; Cahill, M. E.; Hagen, G. M.; Barisas, B. G.; Roess, D. A. *Endocrinology* **2006**, *147*, 1789-1795.
32. Maitra, A.; Dinesh; Patanjali, P.; Varshney, M. *Colloids Surf.* **1986**, *20*, 211-219.

33. Maitra, A.; Patanjali, P. K. *Colloids Surf.* **1987**, *27*, 271-276.
34. Tenchov, B. G.; MacDonald, R. C.; Siegel, D. P. *Biophys. J.* **2006**, *91*, 2508-2516.
35. Crockett, E. L.; Hazel, J. R. *J. Exp. Zool.* **1995**, *271*, 190-195.
36. Fantus, G.; Tsiani, E. *Mol. Cell. Biochem.* **1998**, *182*, 109-119.
37. Drake, P. G.; Posner, B. I. *Mol. Cell. Biochem.* **1998**, *182*, 79-89.
38. Srivastava, A. K.; Mehdi, M. Z. *Diabetic Med.* **2005**, *22*, 2.
39. Sakurai, H.; Kawabe, K.; Yasui, H.; Kojima, Y.; Yoshikawa, Y. *J. Inorg. Biochem.* **2001**, *86*, 94-94.
40. Sakurai, H.; Tamura, A.; Fugono, J.; Yasui, H.; Kiss, T. *Coord. Chem. Rev.* **2003**, *245*, 31-37.
41. Buglyo, P.; Crans, D. C.; Nagy, E. M.; Lindo, R. L.; Yang, L.; Smee, J. J.; Jin, W.; Chi, L.-H.; Godzala, M. E.; Willsky, G. R. *Inorg. Chem.* **2005**, *44*, 5416-5427.
42. Monga, V.; Thompson, K. H.; Yuen, V. G.; Sharma, V.; Patrick, B. O.; McNeill, J. H.; Orvig, C. *Inorg. Chem.* **2005**, *44*, 2678-2688.

## APPENDIX ARTICLE 4<sup>7</sup>:

Review

# How environment affects drug activity: Localization, compartmentalization and reactions of a vanadium insulin-enhancing compound, dipicolinatooxovanadium(V)

Debbie C. Crans<sup>a,b,\*</sup>, Alejandro M. Trujillo<sup>a,b</sup>, Philip S. Pharazyn<sup>a</sup>, Mitchell D. Cohen<sup>c</sup>

<sup>a</sup> Dept. of Chemistry, Colorado State University, Fort Collins, CO 80523, United States

<sup>b</sup> Dept. of Cell and Molecular Biology, Colorado State University, Fort Collins, CO 80523, United States

<sup>c</sup> Dept. of Environmental Medicine, NYU School of Medicine, Tuxedo, NY 10987, United States

### Contents

1. The action of vanadium compounds can be beneficial and malicious; could chemical and biological transformation be related to function? ..	2179
2. Interactions of vanadium compounds and specifically [VO <sub>2</sub> dipic] <sup>-</sup> with proteins .....	2180
3. Uptake of vanadium compounds and specifically [VO <sub>2</sub> dipic] <sup>-</sup> .....	2182
4. Vanadium compounds and [VO <sub>2</sub> dipic] <sup>-</sup> as insulin-enhancing agents in animals and people .....	2183
5. Toxicity of vanadium compounds and [VO <sub>2</sub> dipic] <sup>-</sup> .....	2184
6. Chemistry of [VO <sub>2</sub> dipic] <sup>-</sup> in aqueous solution .....	2185
7. Compatible [VO <sub>2</sub> dipic] <sup>-</sup> complexes with organic and hydrophobic environments .....	2186
8. Reactions of dipicolinatooxovanadium(V) alkoxides .....	2188
9. How drug environment and compartmentalization might affect action of vanadium compounds .....	2190
10. Concluding remarks .....	2190
Acknowledgements .....	2191
References .....	2191

### ARTICLE INFO

#### Article history:

Received 3 November 2010

Accepted 19 January 2011

Available online 27 January 2011

#### Keywords:

Vanadium

Membrane interactions

Compartmentalization

Oxidation by vanadium complexes

Drug uptake

Insulin-enhancing

Toxicology

Mode of action

Intermembrane space

Chemical and biological transformations

Environmental effects

Hydrophobic environment

Oxovanadium(V) dipicolinate

Vanadate

Dipicolinic acid

2,6-Pyridinedicarboxylic acid

### ABSTRACT

The chemical and biological properties of a simple and traditional V(5+) coordination complex, dipicolinatooxovanadium(V) (abbreviated [VO<sub>2</sub>dipic]<sup>-</sup>), are described in order to present a hypothesis for a novel mode of action wherein a hydrophobic membrane environment plays a key role. Specifically, we propose that the compartmentalization and both chemical and biological transformations of vanadium-complexes direct whether beneficial or toxic effects will be observed with this class of compounds. This concept is based on the formation of high levels of uncontrollable reactive oxygen species (ROS) from one-electron reactions or alternative events possibly initiated by a two-electron reaction which may be directly or indirectly beneficial by reducing the high levels of ROS. The properties of dipicolinatooxovanadium(V) compounds in aqueous solution (D.C. Crans, et al., *Inorg. Chem.* 39 (2000) 4409–4416) are very different from those in organic solvents (S.K. Hanson, et al., *J. Am. Chem. Soc.* 131 (2009) 428–429) and these differences may be key for their mode of action. Since other vanadium complexes are known to hydrolyze upon administration, the low stability of the aqueous complex requires entrapment in hydrophobic environments for such a complex to exist sufficiently long to have an effect. The suggestion that the environment changes the reactivity of the compounds is consistent with the very different modes of action by which one complex act. In short, a novel hypothesis is presented for a mode of action of vanadium compounds based on differences in properties resulting from environmental conditions. These considerations are supported by recent evidence supporting a role for membranes and signal transduction events (D.A. Roess, et al. *Chem. Biodivers.* 5 (2008) 1558–1570) of the insulin-enhancing properties of these compounds.

© 2011 Elsevier B.V. All rights reserved.

\* Corresponding author at: Dept. of Chemistry, Colorado State University, 1301 Center Av., Fort Collins, CO 80523, United States. Tel.: +1 970 491 7635;

fax: +1 970 491 1801.

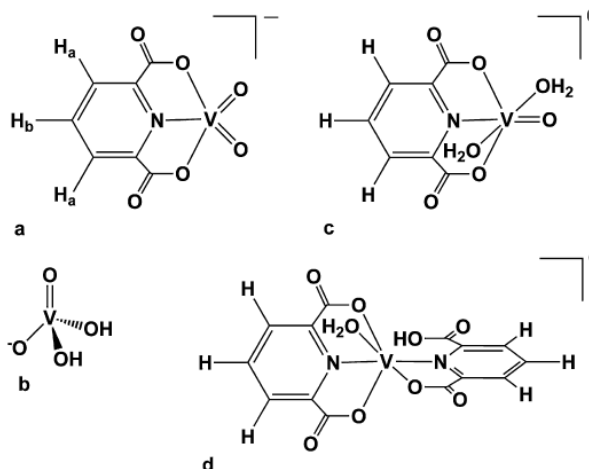
E-mail address: crans@lamar.colostate.edu (D.C. Crans).

<sup>7</sup> Alejandro M. Trujillo contributed to the writing and original figures 1, 2 & 12  
Published in *Coordination Chemistry Reviews*, 2011, (255) 2178-2192.

**1. The action of vanadium compounds can be beneficial and malicious; could chemical and biological transformation be related to function?**

Design, efficacy, and mode of action are defining properties of all drugs, including metal-containing drugs [1,2]. Drug efficacy is dependent on absorption, distribution, metabolism and excretion, properties that are disease- and organism-specific, and ultimately dictate mechanism of action. The action of a drug generally describes how the product impacts cellular function resulting in the reduction of a disease state. Drug design is often linked to its function and cellular uptake mechanism to facilitate efficacy. Pharmacokinetic studies characterize distribution and transformations that occur during drug function. Since the success of a drug is often a balance between beneficial and toxic concentrations, the greater the difference between therapeutic and toxic levels, the better. Targeting improves the benefit of a drug due to the inherent reduction in risk of toxicities in a host (i.e. by lowering potential systemic levels and the attainment of toxic levels) while still achieving therapeutic results. Therefore, for the successful development and administration of any drug, detailed information on its transformation and localization *in situ* is critical. Herein, we review available evidence regarding the biotransformation [3–9], localization [4,5,8,10–15], and toxicity [8,16,17] of one vanadium(V)-containing insulin-enhancing agent, 2,6-pyridinedicarboxylato-oxovanadium(V) ([VO<sub>2</sub>dipic]<sup>-</sup>; Scheme 1) [3–7,9,12,18–23], reconciling its beneficial and malevolent effects in cells and in diabetic animals with its chemical properties.

Vanadium (abbreviated as V) compounds, where salts are considered charged complexes, are particularly sensitive to their



**Scheme 1.** The structures of the (a) oxovanadium(V) dipicolinate ([VO<sub>2</sub>dipic]<sup>-</sup>) (b) vanadate, the V(5+) salt diprotonated anion, H<sub>2</sub>VO<sub>4</sub><sup>-</sup> (c) oxovanadium(IV) dipicolinate [VOdipic(H<sub>2</sub>O)<sub>2</sub>] (d) hydrogen bis(dipicolinato)vanadium(III) H[V(dipic)<sub>2</sub>(H<sub>2</sub>O)].

environment [24–27]. Importantly, various forms of V exert different biological activities [24,28–31]. It is well known that V salts and compounds undergo biotransformations (summarized in Fig. 1). Undoubtedly, the degree to which pentavalent V(5+) is reduced to tetravalent V(4+) is an important factor influencing how much metal/agent is transported into/out of cells, the magnitude of detoxification reactions initiated, how extensively superoxide

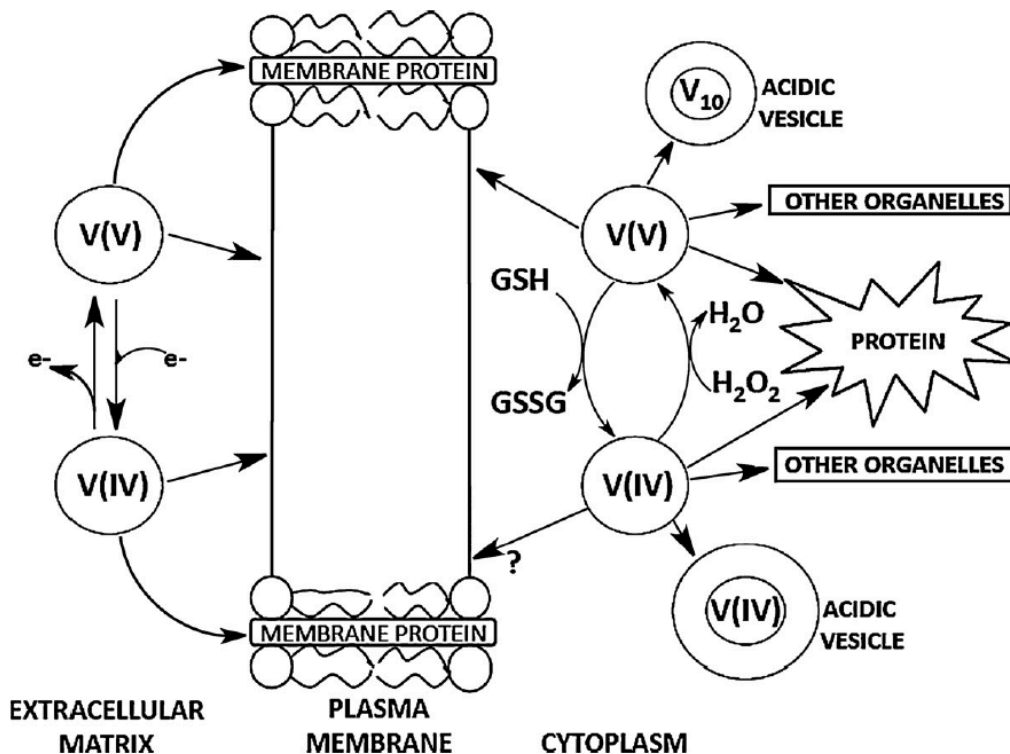


**Fig. 1.** An illustration of the current reported vanadium interactions in biological systems, with one electron V(4+/5+) redox chemistry occurring in the extracellular matrix (ECM). Membrane interactions are shown occurring via either passive diffusion of membrane protein interaction mechanisms. Upon entry into the cytoplasm V(4+) and (5+) affect cellular components in many ways.

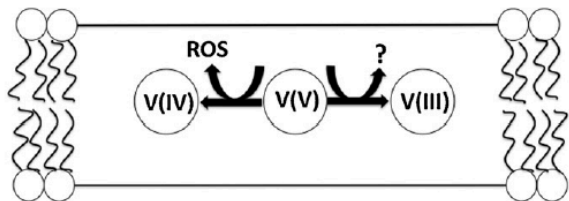


Fig. 2. Vanadium(3+), (4+) and (5+) salts and complexes enter by passive diffusion through the hydrophobic intermembrane space. The hydrophobic environment results in altered reactivity of the V complex. The formation of excessive amounts of reactive oxygen species (ROS) from V(5+/4+) redox results in toxic responses. Alternatively, the more controlled V(5+/3+) redox pathway result in unknown beneficial products.

anion ( $\text{O}_2^-$ ) and hydrogen peroxide ( $\text{H}_2\text{O}_2$ ) metabolism is affected (also referred to as reactive oxygen species formation), as well as the extent to which several key cellular processes are potentially impacted [14,16,32]. In this review, we evaluate the hypothesis that some novel chemistry that has recently been reported in organic solvents using catalytic V compounds [33–38] could apply to hydrophobic environments of the cell and as such, be relevant for the mode of action of vanadium compounds. Hydrophobic environments exist in the intermembrane spaces of bilayers and in various locations within folded proteins that are found throughout a cell. Fig. 2 illustrates two very different chemical events occurring in a hydrophobic membrane environment based on known chemistry in organic solvents. The one-electron process is accompanied by reactive oxygen species (ROS) and reactive oxygen nitrogen species (RONS) formation. The two-electron process, although much more rare, recent reports with the V-dipic system in organic solution suggest that this process may be possible [33–35]. An important consequence of this hypothesis is that the effects of V-based drugs may change depending on environment. Thus, more so than with carbon-based drugs, the location and compartmentalization of the V-containing drug are factors critical to the actions of these agents.

Vanadium compounds exert a range of biological/pharmacological effects. Both V(4+) and V(5+) compounds result in insulin-enhancing responses in both diabetic humans and animal models [22,24,39–44]. The insulin-enhancing effect of one particular V(5+) compound,  $[\text{VO}_2\text{dipic}]^-$ , is shown and compared to its corresponding free ligand and simple salt in Fig. 3 [3] and shows that the complex induces a statistically different response on Wistar rats with STZ-induced diabetes. This manuscript briefly reviews the insulin-enhancing effects of V-dipic compounds, [3,4,7–9,19,20,22] their effects reported on the cell membranes, [8,12,14,15] and aims to reconcile these effects with recently reported catalytic chemistry taking place in hydrophobic environments [33–35]. Based on known chemistry, we explain the biological activities of these compounds in the context of their fundamental physical and chemical properties in a hydrophobic membrane environment. Accordingly, we review the diverse properties of these compounds in aqueous and hydrophobic environments within the framework of the concepts of drug compartmentalization and localization.

Biological effects generally trace with the compartmentalization of a drug and are exemplified by cisplatin, where the anti-cancer effects arise after permeation into the nucleus forming irreparable adducts with DNA [45]. However, prior to reaching the nucleus, the primary cytotoxic effects are observed immediately after cell uptake and involve the hydrolyzed forms of cisplatin [45]. Although compartmentalization in biology generally refers to placement within specific cellular organelles, in chemistry, the definition is typically broader [46]. In this review, we use the term compartmentalization more broadly. Since we are primarily concerned with whether the drug is found in or at the membrane, the term

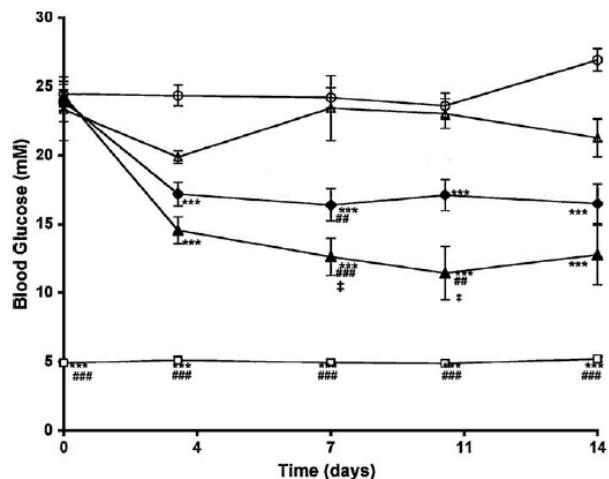


Fig. 3. The effect of vanadium-dipicolinate on hyperglycemia in Wistar rats with STZ-induced diabetes. Compounds were administered in drinking water, and blood glucose was measured for N ( $\square$ ,  $n=13$ ), untreated D ( $\circ$ ,  $n=25$ ),  $\text{H}_2\text{dipic}$ -treated D ( $\triangle$ ,  $n=6$ ),  $\text{VOSO}_4$ -treated D ( $\blacklozenge$ ,  $n=30$ ), and  $\text{NH}_4[\text{VO}_2\text{dipic}]$ -treated D ( $\blacktriangle$ ,  $n=5$ ) animals. Data are presented as the mean standard error of the mean (SEM). \*\*\* $p \leq 0.001$  vs. the D animals, \*\* $p < 0.05$  vs. the ligand-treated D animals, ### $p < 0.001$  vs. the ligand-treated D animals, † $p > 0.05$  vs. the N animals, which means it is statistically indistinguishable from normal. Adapted with permission from Ref. [3].

compartmentalization will also refer to placement of a drug in the membrane. Specifically, the term compartmentalization will describe placement of the V compounds in various environments. Regardless of the exact use of the term, compartmentalization undoubtedly has profound effects on V-based drug action. We hypothesize here that V compound compartmentalization – in the broad sense – can explain the diverse effects including beneficial and toxic effects exerted by V derivatives. We propose that the differences in the effects of V compounds may in part originate from the environment of the compound and that the membrane provides the framework from which the beneficial and malicious effects of V compounds resulted.

## 2. Interactions of vanadium compounds and specifically $[\text{VO}_2\text{dipic}]^-$ with proteins

Vanadium compounds interact with a range of diverse proteins [28,29,31,43,47–57]. Only few proteins have specific known functions involving binding of V [54,58–64]. One example is the recently discovered vanabins, abbreviated from *vanadium binding* proteins, have only been found in tunicates (sea squirts) so far [58]. These proteins bind multiple V ions, generally in oxidation state 4+. Vanabins are thought to be involved in transport of V through the cytoplasm to vacuoles; however, their role is not yet been firmly established [59,60]. V(4+) has also been found as a co-factor in V-containing nitrogenases found in free-living and symbiotic diazotrophs (bacteria), where V replaces molybdenum [61]. In red algae, V is found as a co-factor in haloperoxidases, and in the presence of the vanadate V(5+) co-factor act as a peroxidase [54,62,63]. The activity of these proteins in the absence of vanadate exhibits a dual activity from peroxidases to phosphatases [64]. These proteins have also not yet been found in mammals.

There are numerous effects of V on mammalian biological proteins. Most well-known is inhibition of many phosphorylases including, phosphatases, myosin, ribozymes and phosphodiesterases; for which representative enzymes are shown in Fig. 4 [65]. Vanadium is a potent inhibitor for these enzymes because it is able to form a transition state geometry that resembles the

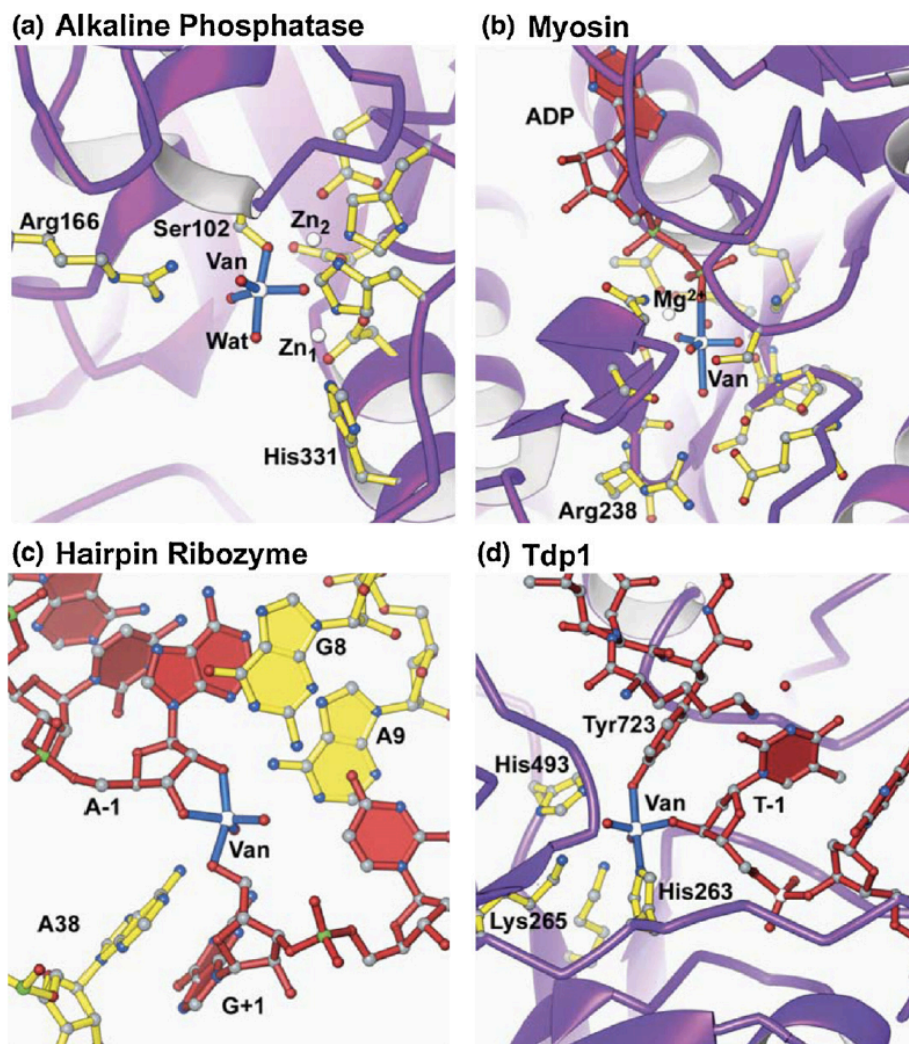


Fig. 4. Selected enzyme–vanadate complexes: (a) Alkaline phosphatase–vanadate complex from PDB ID 1B8J. The protein structure is displayed as a purple ribbon model with amino acid residues displayed as ball-and-stick structures with yellow bonds. The vanadate moiety (Van) is also displayed as a ball-and-stick structure with blue bonds. Carbon atoms are colored gray; nitrogen, blue; oxygen, red and metal atoms are white. Vanadate adopts distorted trigonal bipyramidal geometry with  $O_{\gamma}$  of the nucleophilic Ser102 residue comprising one apical ligand and a free oxygen atom representing the activated water molecule comprising the other apical ligand. (b) Myosin–ADP–Mg–vanadate structure from PDB ID 1VOM. Coloration for the protein, metal ion and vanadate moieties is the same as in (a) and ADP is displayed as a ball-and-stick structure with red bonds, and phosphate atoms colored green. (c) Hairpin ribozyme–vanadate structure from PDB ID 1M50. Atoms are colored as in (b), with bonds for the ribozyme RNA strand colored yellow and bonds for the substrate RNA strand in red. The vanadate moiety (blue bonds) adopts distorted trigonal bipyramidal geometry with the ribose of nucleotide A-1 contributing one apical and one equatorial ligand and the 5'OH of nucleotide G+1 contributing the other apical ligand. (d) The quaternary complex around vanadate that mimics the transition state for Tyrosyl-DNA phosphodiesterase from PDB ID 1NOP. Coloration of the enzyme and vanadate moieties is the same as (a) and (b), with the peptide and DNA portions of the substrate analog displayed with red bonds. Adapted with permission from Ref. [65].

transition state of phosphoester and phosphoanhydride hydrolysis [66,67]. Most recognized is inhibition of several protein tyrosine phosphatases, which is believed to have implication for the insulin enhancing effects of these compounds [55,56,68,56,70,71]. The proposed mechanism of action is formation of a high energy intermediate or transition state complex with these protein tyrosine phosphatases. Studies have shown that some V compounds such as peroxovanadium derivatives irreversibly inhibit protein tyrosine phosphatases forming a covalent intermediate that has been observed using mass spectroscopy [56]. Other V compounds such as vanadate form a reversible complex [55,68,71,72]. Specifically V(3+, 4+, and 5+) complexes inhibit several phosphatases including as alkaline, acid, and protein tyrosine phosphatase such as PTP-1b

[28,55,67,68,73]. Specifically,  $[VO_2dipic]^-$  is a potent phosphatase inhibitor as anticipated by the five-coordinate geometry [67,69,70].

Vanadium is known to compete with iron (Fe) in binding to transferrin (Tf) and another key carrier protein, lactoferrin (Lf), both *in vivo* and *in vitro* [74–78].  $VO_2^{2+}$  has an affinity for both human serum transferrin and albumin, although the binding to the latter is significantly weaker than the former [78–81]. *In vitro* studies demonstrate decreased Fe delivery to local macrophages in the presence of V [77]. Of the two possible metal binding sites Harris [75] showed that with Tf, most  $Fe^{3+}$  binds at “Site A” with high selectivity (~90%) and then at “Site B” during states of excess iron. Additionally, when V or Cr was present,  $Fe^{3+}$  and V preferentially bind at site A, while Cr does so at

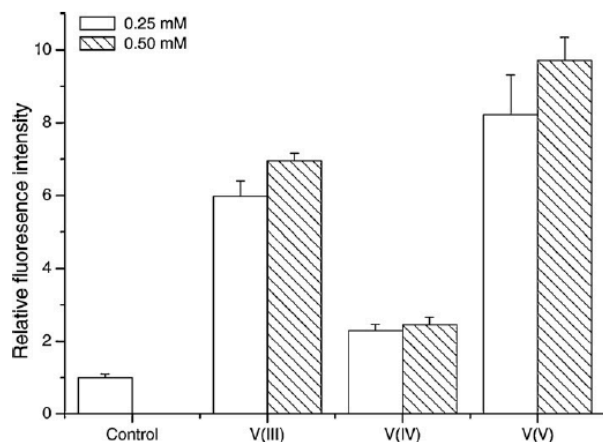


Fig. 5. Quantitation of RONS in Caco-2 cells induced by vanadium complexes using DCFH-DA fluorescent staining (DCFH-DA=2',7'-dichlorofluorescein diacetate). All data presented are means  $\pm$  SD of three measurements. Adapted with permission from Ref. [8].

site B. Thus, while V and Cr each could bind to Tf, V binds with higher affinity, effectively out competing, and thus, blocking  $\text{Fe}^{3+}$  binding at its preferential site [82]. Recent studies with V in oxidation states 3+, 4+, and 5+ demonstrated that V in all oxidation states can bind to Tf, but that the lower oxidation states bind tightest [80]. Some differences are therefore anticipated for interaction of these proteins with different V complexes. The available studies with bis(maltolato)oxovanadium(IV) BMOV, bis(ethylmaltolato)oxovanadium(IV) BEOV and other complexes, suggest that the metal ion is stripped from the compound upon complexation [44,83–88].

Redox cycling studies of V in cells and in animals are well documented [47]. Studies in animals have shown that both V in 4+ and 5+ forms are observed and continuously recycled, even though such studies are more difficult than corresponding *in vitro* studies [89]. In cells, V(5+) interaction with reductants such as NAD(P)H, glutathione, ascorbate, or catechols has resulted in V(4+) [24,90,91]. Subsequently, V(4+) interaction with oxygen ( $\text{O}_2$ ) or reactive oxygen species (ROS) results in oxidation back to V(5+) [92]. The presence of V(5+) and V(4+) in cells also affects critical enzymes and signal transduction pathways some of which lead to apoptotic cell death pathway [16,24,26,93]. The ability of V to continuously cycle has been suggested as a source of its toxicity [16], as well as its detoxification pathways [8,22]. Fig. 5 illustrates the sharp increase of RONS production in Caco-2 cells upon administration of V-containing compounds; as expected, differences are observed with oxidation state variations in the complex as shown in Fig. 5 [8]. While a constant shuffling of oxidation state for V in cells are anticipated, the fact that differences are observed is indicative that the biological transformations are important because each complex is likely to respond slightly differently. The stability of V is sensitive to environment because ligand coordination can stabilize V in both the V(4+) or V(5+) forms [24,94]. A prime example is the V(4+) stabilization by cellular phosphate anionic ligands which prevents the reduction of  $\text{O}_2$ /ROS [95] or the effects of redox active peptides [89]. How complexation effects the redox potential of the metal has recently been discussed in detail within the parameters of physiological conditions [96]. Most intracellular V is found complexed as (4+), while (5+) predominates as salt extracellularly [97–99]; this has led to the suggestions that V exits the cell through exocytosis both in the form of salt as V(5+) and complexed as V(4+).

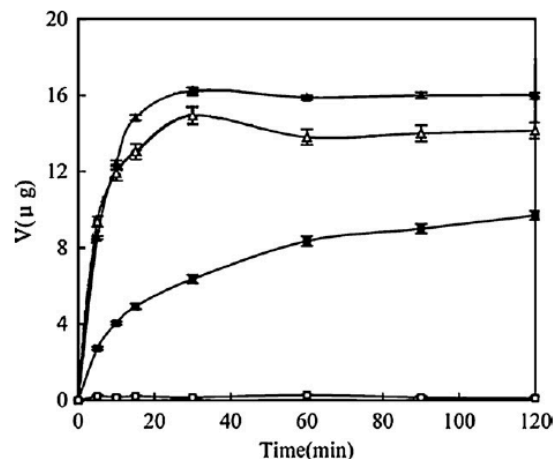


Fig. 6. Kinetic uptake and the DIDS inhibition of the uptake of various vanadium compounds (375 mM) by human erythrocytes. The x-axis represents the incubation time and the y-axis represents the amounts of vanadium in the cell ( $C_m$ ) at different times. ( $\blacktriangle$ ,  $\text{VO}(\text{ma})_2$ ;  $\triangle$ ,  $\text{VO}(\text{ma})_2 + \text{DIDS}$ ;  $\blacksquare$ ,  $\text{NaVO}_3$ ;  $\square$ ,  $\text{NaVO}_3 + \text{DIDS}$ ) (4,4'-diisothiocyano-2,2'-stilbenedisulfonic acid is abbreviated DIDS). Data represent the means  $\pm$  SD ( $n=3$ ). Adapted with permission from Ref. [15].

### 3. Uptake of vanadium compounds and specifically $[\text{VO}_2\text{dipic}]^-$

Vanadium is readily transported in the blood and high amounts (90–95%) of V in blood are in the plasma fraction, mostly in the form of vanadyl, i.e., V(4+). Salts and several V complexes including BEOV have been studied both *in vitro* and *in vivo* in serum [43,44,83–88,100,101]. Circulatory transport of V in biological systems occurs primarily in association with serum transferrin (Tf), with smaller amounts being associated with albumin and/or low molecular mass (i.e., citrate or lactate) components [22,79]. The degree of involvement of albumin in transport of V is less clear, possibly because some of the *in vitro* studies were done at high concentrations [79,84–86]. In the *in vivo* studies done at lower concentrations [84], no evidence for albumin involvement was found; albumin involvement is likely to vary with the amounts of doses administered. Vanadate has also been found in blood, though at far lower amounts than anticipated considering the reducing environment and significant presence of reductants (e.g., glutathione, ascorbate, and cysteine). Some evidence for V uptake into cells via Tf receptors (TfR) has been reported [102]. In general, Tf serves as the major Fe carrier protein *in situ*, facilitating Fe recycling by transporting Fe from destroyed erythrocytes to the bone marrow for re-use in developing erythrocytes. Administration of BMOV and BEOV resulted in increased amounts of V in bone marrow, consistent with transport and uptake of V through Fe uptake pathways [79]. In addition to protein assisted uptake mechanisms it has been proposed that less soluble V compounds may also use phago- or pinocytosis mechanisms [103].

In salts such as tetravalent ( $\text{VO}^{2+}$ ) or pentavalent ( $\text{VO}_2^+$ ) present in biological systems, transport of V typically takes place through protein ion carriers. V(4+) is transported quickly into cells and presumably takes advantage of the  $\text{Fe}^{2+}$ - $\text{VO}^{2+}$  analogy [47,104]. The low oxidation state V was also proposed to transport through a mechanism similar to Fe polysulfates [105]. Vanadium(5+), because of the vanadate-phosphate analogy, uses the same anion channels as phosphate for uptake [8,97]. The early studies were carried out in yeast [97] have more recently been confirmed in erythrocytes, along with other cell types, demonstrating that several anion transporters are used Fig. 6 [15]. However, both high oxidation state V

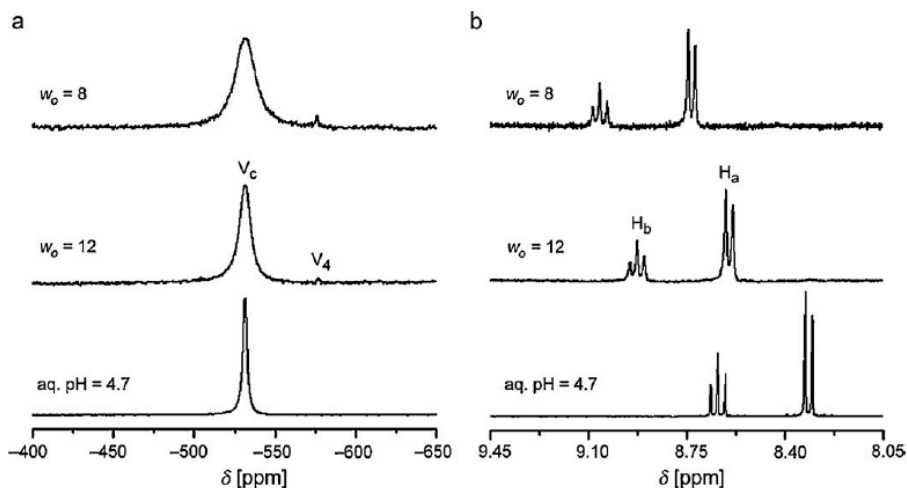


Fig. 7. Stackplot of  $^{51}\text{V}$  NMR spectra (a) and  $^1\text{H}$  NMR stackplot shown, (b) of  $100\text{ mM VO}_2[\text{dipic}]^-$  in a  $1\text{ M AOT/cyclohexane/D}_2\text{O}$  ( $\text{pH } 4.7$ ) reverse micelle microemulsion system. Adapted with permission from Ref. [12].

and low oxidation state V more readily enter cells upon complexation [105,106].

Caco-2 cells arranged in a monolayer in a permeability assay show uptake of neutral V coordination complexes through the passive diffusion mechanism [8,14]. Passive diffusion mechanisms of V compounds in cellular systems are consistent with the possibility that membranes play an important role for the action of these compounds. For example, diffusion of BMOV and  $\text{VO}(\text{acac})_2$  through human erythrocyte membranes was not inhibited by the anion channel inhibitor, 4,4'-diisothiocyanatostilbene-2,2'-disulfonate (DIDS), illustrated in Fig. 6 [15]. In contrast, as illustrated in Fig. 6, vanadate uptake was completely prohibited by anion channel inhibition [15]. These studies demonstrate that V compounds can employ several different mechanisms for entering cells.

It has been proposed, based on previous studies in cells, that V compounds have the potential to reside within the membrane [14,15]. Evidence exists supporting the interpretation that some V compounds affect signal transduction platforms and subsequent signalling events [12,106]. In one simple model membrane system, the  $^{51}\text{V}$  and  $^1\text{H}$  NMR spectra in Fig. 7 showing significant changes in linebroadening ( $^{51}\text{V}$ ) and changes in  $^1\text{H}$  chemical shift indicated an altered environment for  $[\text{VO}_2\text{dipic}]^-$  in this system [12]. These findings were further supported through 2D  $^1\text{H}$  NMR studies shown in Fig. 8 indicating that  $[\text{VO}_2\text{dipic}]^-$  is present in hydrophobic interfaces [107]. In recent studies, the dipic-ligand showed that a charged form of it is also stable in these environments [10]. This work was performed in the absence of proteins and other variables, and, as such, demonstrates that passive diffusion mechanisms are possible, regardless of the negative charge on the drug. These findings lend support to the possibility that this charged compound and other V compounds can exist in hydrophobic membranous spaces. Importantly, these studies provide precedence that charged V compounds can be thermodynamically favored in hydrophobic environments such as the intermembrane spaces of cells.

#### 4. Vanadium compounds and $[\text{VO}_2\text{dipic}]^-$ as insulin-enhancing agents in animals and people

Vanadium complexes are known to exert an insulin-enhancing effect in diabetic animals and humans [23,24,27,39–41,43,100,101,108–114]. Some of these compounds, including BEOV, as well as simple salts such as vanadyl

sulfate ( $\text{VOSO}_4$ ) and sodium vanadate ( $\text{NaVO}_3$ , also called sodium metavanadate), have been used to treat patients in Phase 2 clinical trials [24,40,44,114]. In addition, a wide range of V compounds are known to reduce elevated blood glucose, lipid levels, and in general, alleviate symptoms of diabetes, in streptozotocin (STZ)-induced diabetic Wistar rats [24]. These V-containing compounds lower elevated levels of glucose in diabetic animals as other anti-diabetic drugs. As a result, the symptoms of diabetes, such as increased liquid intake and decreased weight, begin to normalize. However, most remarkable is that these compounds do not lower normal glucose levels in normal animals and thus avoid the potential of

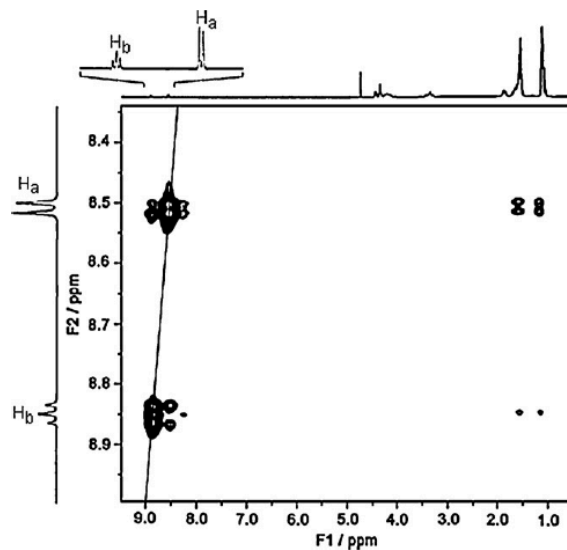


Fig. 8. NOESY spectrum of  $[\text{VO}_2\text{dipic}]^-$  complex in AOT microemulsions in the region showing the negative NOEs arising from interactions between the  $\text{CH}_2$  and  $\text{CH}_3$  groups in the AOT and  $[\text{VO}_2\text{dipic}]^-$  protons. The scale of F2 domain, showing only the dipic ligand protons are substantially expanded compared to F1, which shows the entire range from AOT methyl groups to  $[\text{VO}_2\text{dipic}]^-$  protons. Microemulsion samples prepared from  $1.0\text{ M AOT}$  stock solution in  $(^2\text{H}_{18})\text{isooctane}$  with the  $200\text{ mM NH}_4[\text{VO}_2\text{dipic}]^-$  in  $\text{D}_2\text{O}$ ,  $\text{pH}=4.5$  stock solution at  $w_0 = 12$ , resulting in an overall concentration of  $43\text{ mM } [\text{VO}_2\text{dipic}]^-$ . Adapted with permission from Ref. [107].

hypoglycemia [22,23,49]. Reports exist which show that the effects remain for some time after the patients are no longer taking the drug [115].

Vanadium salts and compounds exert many effects that, combined, result in the observation of insulin-enhancing properties. The most recognized mode of action is the effective inhibition of protein tyrosine phosphatases such as PTP-1B. Inhibition of PTP-1B results in reduced regulation of insulin receptor phosphorylation events leading to increased glucose uptake [116–118]. Recently, the effects of V salts have been characterized using DNA microarray where vanadyl sulfate and oxovanadium(V)4-hydroxydipicolinate normalize the expression of mRNAs [18,22,40]. These studies show that not only were the glucose and lipid metabolism affected, but that also proteins with roles in oxidative stress, the immune system, and iron metabolism were impacted. The increasing and continued need for treatment of diabetes speaks to the necessity for further investigation of the ability of potential chemotherapeutics to enhance insulin sensitivity [117,118].

Vanadium(4+) complexes represent the largest class of V compounds tested for insulin-enhancing activity [23,24,27,39–41,44,108–114]. Vanadium(4+) complexes such as BEOV have been used in Phase 2 clinical trials [44] although, because of patent protection, most literature exist on the closely related BMOV complex. These complexes have been used in both animal and cell studies showing a significant reduction in diabetic symptoms [3,23]. Studies have shown that reduction of diabetes-induced symptoms such as hyperglycemia and hyperlipidemia, in addition to diabetes-altered genetic effects are decreased with administration of these compounds. More recently, V(5+) and V(3+) complexes have also been found to have insulin-enhancing properties [3,5,8,18,19,119]. Because V(4+) complexes have no charge, they are perceived to be candidates for easy bio-absorption. This fact, combined with the perceived greater stability of these complexes at neutral pH, explains why the V(4+) complexes are popular V insulin-enhancing compounds. However, in the case of the V dipicolinates, for the two derivatives investigated (i.e., the parent and the 4-chloro substituted dipic derivative), the V(5+) complex was the most effective compound in the sense that it was the dipicolinate derivative that produced a statistically-different effect compared to STZ-induced diabetic rats [3,8,19]. Based on the hydrolytic and redox instability of  $[\text{VO}_2\text{dipic}]^-$ , the origin of effectiveness for the dipicolinate complexes is not clear, but suggests that some characteristics of these compounds support their biological activities. For this compound it seems likely that transformations are important to its insulin-enhancing action. Therefore, the dipicolinates are a class of compounds that should be particularly well suited for studies investigating compartmentalization of V compounds.

The V(5+) salt, vanadate, and peroxovanadium compounds [120–122] were found early on to be insulin-enhancing. These complexes were subsequently followed by simple coordination complexes of which the oxovanadium(V) dipicolinate was the first [5,18,20,108,123]. Since it was reported, additional V(5+) complexes have been studied including peroxovanadium compounds [122], decavanadate [21], L-glutamic acid gamma-monohydroxamate-vanadium [108,124] and 5-chlorosalicylaldehydeethylenediamineoxovanadium(V) [123]. In BMOV and many vanadium complexes investigated early on [24], the vanadium is in oxidation state 4+; however, the other oxidation states have now also been accepted as insulin-enhancing [8,19]. A few reports in the literature that suggest V compounds have no effects [125] can be attributed to a statistical abnormality with a heterogeneous population in which both responders and non-responders exist [22]. In contrast, amavadin was found to induce some toxic effects, but no insulin enhancing effects [49]. Since amavadin has reversible aqueous redox chemistry, it

has been suggested that the redox properties may be important for the compound's biological activities. Vanadium dipicolinate and chloro-dipicolinate complexes were the most effective with the metal in oxidation state 5+ ( $[\text{VO}_2\text{dipic}]^-$  and  $[\text{VO}_2\text{dipic-Cl}]^-$ ). Given recently reported chemistry with dipicolinate vanadium complexes in hydrophobic environments [33–35], we describe the known activities of the parent compound, ( $[\text{VO}_2\text{dipic}]^-$ ) and reconciling it with its fundamental physical and chemical properties. We propose here a framework in which both beneficial and toxic effects can result from the same vanadium compound based on its chemical and biological transformations.

## 5. Toxicity of vanadium compounds and $[\text{VO}_2\text{dipic}]^-$

The toxicology for different V(5+) and V(4+) agents, some of which are shown in Fig. 9, has been reported [16,126,127]. However, much less has been reported for the V-dipic complexes. Of the few studies in the literature on this system, most have dealt with clinical parameters affected by V-dipic complexes in diabetic hosts [92]. Though endpoints such as weight loss and renal function were monitored in many studies, these revealed little toxicity. In contrast, at both a cellular and an organ/organ-system level, V(3+), V(4+), or V(5+)-dipic agents are known to impart differential toxicities [8]. In studies with Caco-2 cells obtained from a human epithelial colorectal adenocarcinoma line, changes in viability over a 48-h treatment period showed trends in toxicity potentials with the 5+ changing most and the 4+ changing least (V(5+)>V(3+)>V(4+)), although absolute values of the reported endpoints (i.e.,  $\text{IC}_{50}$ s) did not statistically differ [8]. Specifically, the  $\text{IC}_{50}$  values reported for  $[\text{VO}_2\text{dipic}]^-$  were close to those of  $[\text{VO}(\text{ma})_2]$ , yet much higher (i.e., less cytotoxic) than for  $[\text{VO}(\text{acac})_2]$  or metavanadate [14,60]. A relatively greater toxicity from V(3+) compared to the V(4+)-dipic complex was also evident in rats that inhaled either complex 5 h/d for five consecutive days [16,17]. These effects were determined by examination of the animals's lungs and associated local immune responses [16,17]. As in the *in vitro* studies, in comparison to V(3+) and V(4+)-dipic complexes, vanadate again imparted the greater toxic effect *in vivo*.

Though precise mechanisms underlying toxicities of the various V-dipic agents are not known, several potential clues exist. For example, in the Caco-2 studies, treatment with  $[\text{VO}(\text{ma})_2]$ ,  $[\text{VO}(\text{acac})_2]$ , and vanadate each resulted in significant increases in formation and intra-cytoplasmic localization of ROS. It is reasonable that these same cells also displayed decrements in trans-epithelial electrical resistance (TEER) that paralleled ROS formation trend patterns among the three agents. In similar studies with dipic complexes in oxidation state 3+, 4+, and 5+, on production of RONS, the cytotoxicity potency patterns were followed. However, unlike with vanadate and the other agents, effects on TEER did not follow the same pattern; the weak RONS inducer V(4+)-dipic-derivative caused as strong a decrease in membrane integrity as its V(5+)-dipic counterpart. These unexpected outcomes with the V-dipic compounds – with respect to membrane integrity and/or cell survival – suggest that the relationship between capacity to induce reactive species and damage to the lipid bi-layer may not be the sole basis for toxicity.

Indeed, in assessing effects of  $[\text{VO}(\text{ma})_2]$ ,  $[\text{VO}(\text{acac})_2]$ , and vanadate on erythrocyte membrane fragility, it was suggested that the binding with biomolecules affect the action of the compounds and thereby their potency [15]. Alternatively, the ability of each V agent to impact on levels of cellular reductants not only would affect the cell ability to abrogate any ROS/RONS-induced damage to the inner membrane. However, this mechanism gives rise to the conundrum that the same lack of reductants would lead to mitigation of the

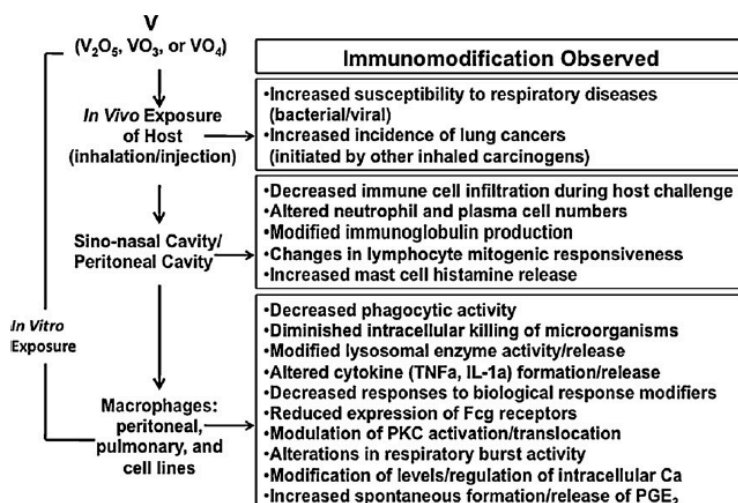


Fig. 9. Known toxic effects from exposure to vanadium compounds *in vivo* and *in vitro* and corresponding effects on the immune system.

activity of a key enzyme involved in initiating ROS/RONS formation in a cell, NADPH oxidase. Of course, many ROS/RONS can be formed non-enzymatically; thus, the mere presence of these metals that can redox shuttle V(5+)/V(4+) creates a scenario for formation of reactive species. This is, of course, particularly possible if the V(5+) or V(4+) is chelated by some unidentified cytoplasmic biomolecule or entrapped in a membrane environment.

Taken together, results of these Caco-2 studies clearly demonstrate that the ligand influences the toxicity of a V agent but, that for any given ligand, the oxidation state/redox behavior of the metal itself ultimately defines its toxic potential. Stated differently, ligand effects are reflected by variations in extent of permeability into (or out of) cells; with the complex redox potential, the amount of oxidative damage to critical cellular macromolecules (proteins, DNA, RNA, etc.) is defined. Thus, the localization of V compounds (in particular, the V-dipics) at the interface of a cell membrane and subsequent interactions with membrane-associated constituents prior to entry into the cytoplasm are potentially critical events in defining toxicity of the agent/drug. As such, the membrane should impact on the degree of interaction with a given V compound and so affect metal/agent penetrance. The particular location of the cell in the body and/or the cell type-associated composition of the membrane are also likely to be important variables to consider in defining the potential efficacy and toxicity of V-based drugs.

## 6. Chemistry of [VO<sub>2</sub>dipic]<sup>-</sup> in aqueous solution

The coordination complex [VO<sub>2</sub>dipic]<sup>-</sup> has been structurally characterized and the vanadium is five coordinate, in a distorted trigonal bipyramidal geometry [128]. The N-atom is in the plane with the cis-dioxo group with the V=O bonds lengths of about 1.6 Å and V-O bonds around 2.0 Å. The V-N bond length is around 2.08 Å, which is a normal V-N bond length even though V-atom coordinates to the pyridine-N atom. These parameters reflect the structural rigidity of this tridentate ligand. Structural characterization of several different salts and of different dipic-derivatives have been reported, with little difference in the anionic coordination complex [4,7,18,129,130].

The [VO<sub>2</sub>dipic]<sup>-</sup> forms from vanadate and H<sub>2</sub>dipic in aqueous solutions ranging from pH 2.0–6.5. Solutions prepared from solid complex or vanadate and ligand are identical within milliseconds

of dissolution of complex and ligand. The hydrolytic stability of the complex is highest from pH 3–5 as have been demonstrated both using <sup>51</sup>V NMR spectroscopy (Fig. 10a) and <sup>1</sup>H NMR spectroscopy (Fig. 10b) [4]. These studies have also been confirmed using potentiometry (Fig. 10c) [4]. Outside of this pH range, the complex hydrolyzes to form ligand and vanadate in an aqueous environment. The complex stability is sensitive to ionic strength and reduces in the reducing cellular environment. The cyclic voltammogram is irreversible in aqueous solution. The properties for a series of derivatives of this V(V) complex have been characterized and some differences and similarities have been identified; the reader is referred to the original publications for details [4,7,18,129].

Although the complex is stable from pH 2.0–6.5, the complex undergoes chemical exchange because the ligand comes on and off in aqueous solution (Fig. 11). The complex reacts with hydrogen peroxide and then its lability decreases and stability increases [131]. The lability of the parent complex is least near pH 3 and it was considered as an important factor in the compound's mode of action [4]. Other derivatives have been prepared and their chemistries described [4,7,18,129,130]. Several of these compounds have also been tested in animals, and all were found to be insulin-enhancing [3,5,6,18–20]. Nevertheless, none of these novel agents was significantly better than the original parent complex.

The question which species exist after the [VO<sub>2</sub>dipic]<sup>-</sup> complex is administered is important and key to speculations regarding the mode of action of the complex. In the absence of experimental data, we attempt to answer this question based on properties of the complex and that of others for which pharmacokinetic information is available [44,84–88]. Studies with BMOV and/or have shown that this complex, which is significantly less labile than [VO<sub>2</sub>dipic]<sup>-</sup>, results in the dissociation of the complex [44]. Accordingly, the consensus in the literature would be that the metal and the ligand part ways. However, some of the biological studies have shown that there are statistically significant differences in the results depending on the specific V-dipic complex used [3,6,8,19]. If such differences exist, some form of stabilization must be in effect or differences would not be observed. One possible solution is that the [VO<sub>2</sub>dipic]<sup>-</sup> complex is trapped, possibly by some form of compartmentalization, which could involve a protein and/or a membrane. Since proteins and membranes are much more hydrophobic environments, it becomes important to consider the properties of these complexes in hydrophobic environments.

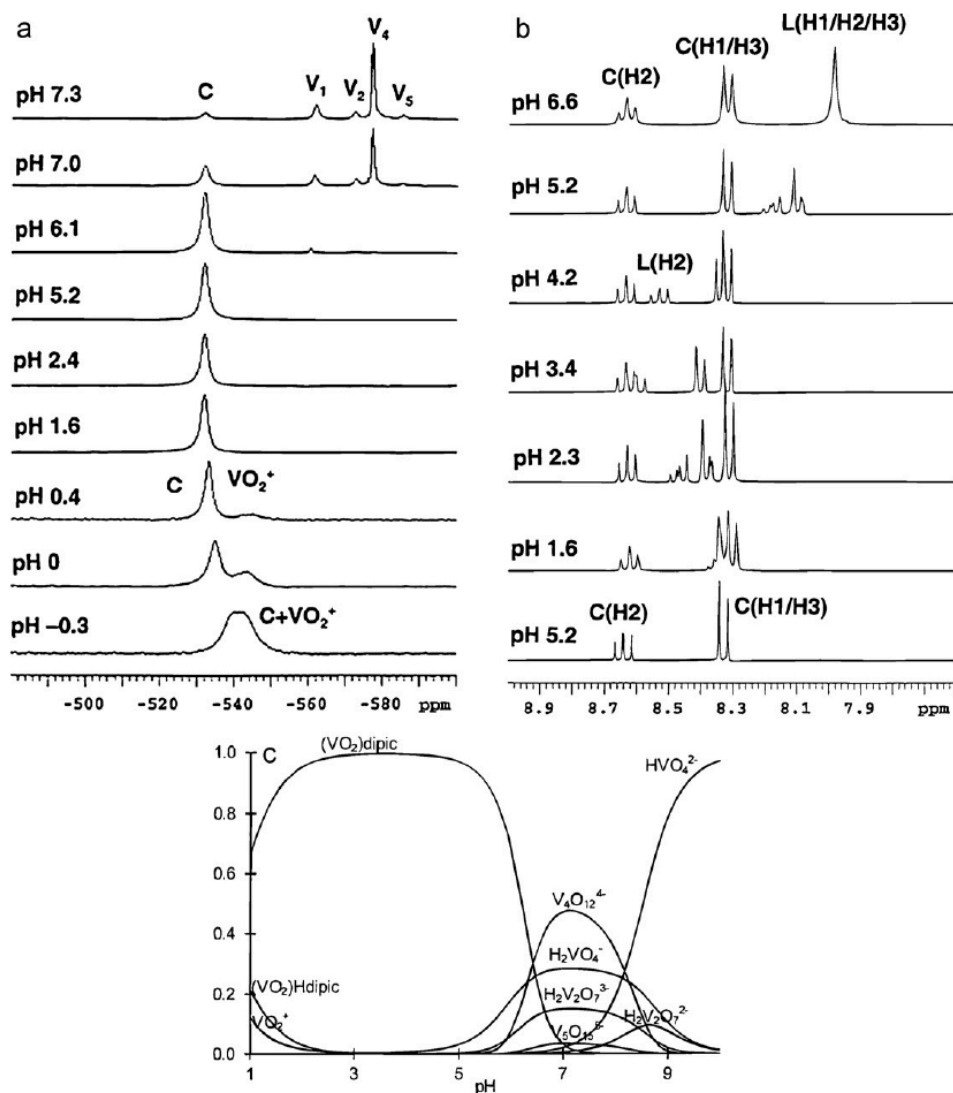


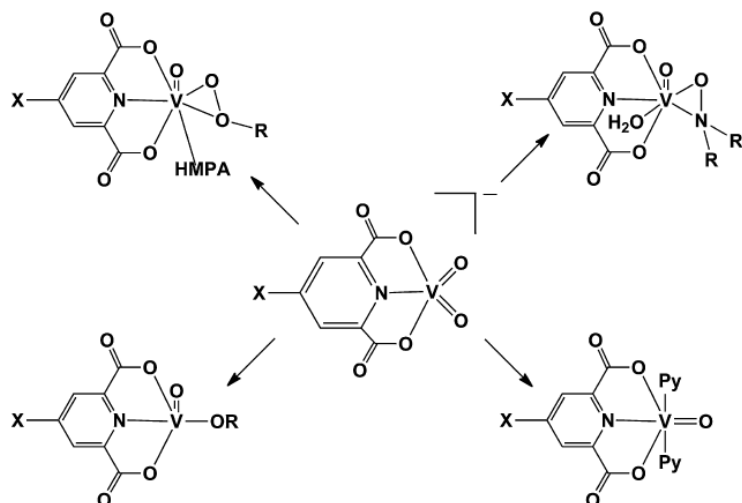
Fig. 10. The  $^{51}\text{V}$  NMR spectra of 10 mM  $\text{NH}_3[\text{VO}_2\text{dipic}]$  at varying pH (a),  $^1\text{H}$  NMR spectra of 37 mM  $\text{NH}_3[\text{VO}_2\text{dipic}]$  and 31 mM free  $\text{H}_2\text{dipic}$  at varying pH; bottom spectrum is from crystalline  $\text{NH}_3[\text{VO}_2\text{dipic}]$  (b) and speciation diagram of 2.00 mM  $[\text{VO}_2\text{dipic}]^-$  in 0.40M KCl at 25 °C (c). Adapted with permission from Ref. [4].

### 7. Compatible $[\text{VO}_2\text{dipic}]^-$ complexes with organic and hydrophobic environments

A number of  $\text{VO}_3^{3+}$ -dipic derivatives reported in organic solvents, including peroxy, hydroxylamido, and alkoxovanadium compounds, are shown in Scheme 2. Despite the polarity of the  $\text{VOdipic}$  unit, these reports demonstrate that derivatives can form in hydrophobic environments even when beginning with the parent  $[\text{VO}_2\text{dipic}]^-$  complex. The first characterized system is the peroxovanadium-derivative, of which the asymmetric peroxovanadium-derivative has the seven coordinate vanadium in a distorted pentagonal bi-pyramidal coordination geometry. This system provides the structural evidence for an asymmetric peroxovanadium compound [131]. Reaction of  $\text{VO}(\text{O}i\text{Pr})_3$  with aqueous *tert*-BuOOH and  $\text{H}_2\text{dipic}$  in  $\text{CH}_2\text{Cl}_2$  resulted in a complex containing a coordinated water or hexamethylphosphoramide (HMPA) molecule depending on the presence of HMPA [131], Schemes 3 and 4. The HMPA adduct is soluble in organic solvents

and the water adduct was only soluble in acetonitrile, acetone or water. The water adduct could be converted to the HMPA peroxovanadium derivative demonstrating that the water is exchangeable and that the HMPA adduct is very stable.

The hydroxylamidovanadium complex is a similar system to the peroxovanadium; a range of dipicolinate complexes have been reported, Scheme 5 [129,130,132]. Structural characterization also shows this class of complexes expand the coordination sphere from six to seven by coordination of a  $\text{H}_2\text{O}$  molecule. The stability of this class of complexes has been characterized in detail both in aqueous and organic solutions. The complexes have been prepared by a high yielding two-step synthesis through the  $[\text{VO}_2\text{dipic}]^-$  complex first or a lower yielding one-step pH sensitive process from vanadate, dipic, and hydroxylamine at ambient or lower temperature as illustrated in Scheme 5. The electronic properties of the complexes are very sensitive to the substitution on the hydroxylamines and less so to the substitution on the dipic [129,130]. In aqueous solution, the systems are more stable than the parent complex once formed both



Scheme 2. The types of compounds that have been reported in hydrophobic environment derived from  $[\text{VO}_2\text{dipic}]^-$  complexes.

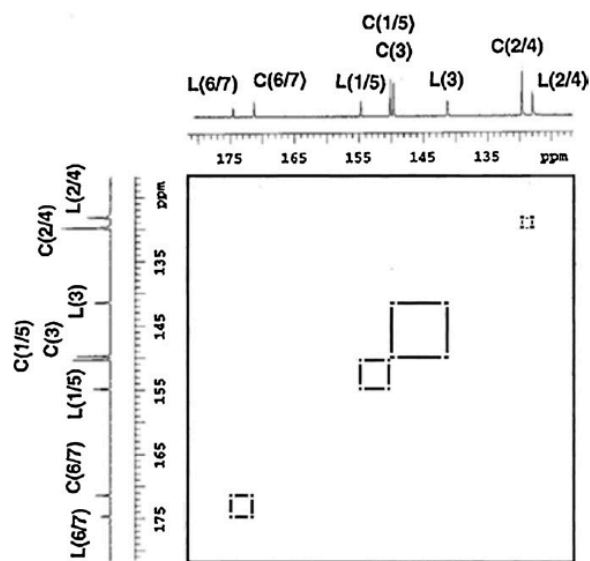
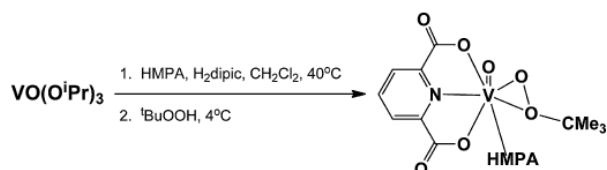


Fig. 11. The  $^{13}\text{C}$  EXSY spectrum of the  $[\text{VO}_2\text{dipic}]^-$  complex (687 mM) in the presence of free ligand (581 mM) at pH 6.6 ( $\pm 0.1$ ). Adapted with permission from Ref. [4].

with regard to hydrolysis and with regard to redox chemistry. Less information is available regarding the reactions of these complexes in organic solution, although related systems have been studied and found to undergo hydroxylamine exchange in acetonitrile [132]. Formation of these complexes from the basic components and their

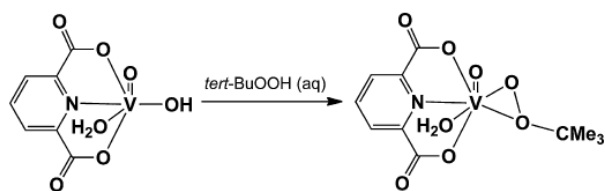


Scheme 3. Reaction of  $\text{VO}(\text{O}^i\text{Pr})_3$  with aqueous *tert*-BuOOH,  $\text{H}_2\text{dipic}$  and HMPA in  $\text{CH}_2\text{Cl}_2$  afforded the peroxovanadium compound in a 75% yield [131].

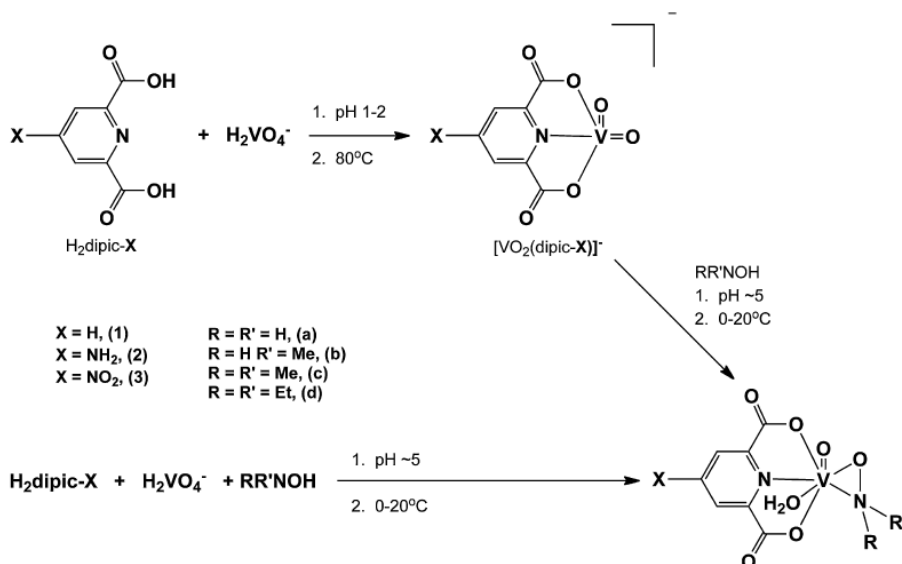
resulting stability are important because they document that such complexes can form from the parent  $[\text{VO}_2\text{dipic}]^-$  complex, and once formed, can exist in a hydrophobic environment.

Recently, alkoxide derivatives of the parent  $[\text{VO}_2\text{dipic}]^-$  complex have been reported to form and react in hydrophobic environments. Oxovanadium trialkoxides are well known, including the methyl, ethyl, isopropyl, *t*-butyl, benzyl, norbornyl and adamantyl derivatives [133–136]. The simplest of these derivatives are prepared from  $\text{VOCl}_3$  or  $\text{V}_2\text{O}_5$  through azeotropic distillation. Generally, these complexes associate in organic solvents which can be readily seen by  $^{51}\text{V}$  NMR spectroscopy. The most dramatic example is observed for  $\text{VO}(\text{OCH}_3)_3$ , where the shifts at sub-millimolar concentration is 100 ppm downfield from more concentrated solutions [133,134,137]. The most commonly used alkoxide derivative, oxovanadium triisopropoxide, is a convenient starting material for preparation of a range of  $\text{V}(5+)$  compounds and is commercially available. With exception of the alkoxides of the larger alkyl derivatives, such as norbornyl and adamantyl derivatives, these complexes hydrolyze in the presence of water [136]. A wide range of chloroxovanadium mono and dialkoxides have been prepared and studied [133–144]. Some of these exhibit the same association tendencies as found for the oxovanadium trialkoxides. Many of these alkoxides have been used as synthetic catalysts in organic syntheses.

Dipicolinatooxovanadium monoalkoxides such as the ethoxide have been reported, Scheme 6 [145]. Additional complexes are readily formed by alcohol exchange reactions. The literature is in disagreement with regard to the exact nature of these compounds. The original report by Wiegardt [128] described the compound as a protonated  $[\text{VO}_2\text{dipic}]^-$ -complex with a coordinated



Scheme 4. Reaction of  $\text{H}[\text{VO}_2(\text{dipic})]\cdot\text{H}_2\text{O}$  (concentrated aqueous solution) with excess aqueous 70% *tert*-BuOOH at  $5^\circ\text{C}$  in 75% yield. Structure was confirmed by elemental analysis [131].



**Scheme 5.** Two possible routes for preparation of hydroxylamido dipicolinatooxovanadium complexes. The higher yielding two-step reaction (top) or a more sensitive lower yielding one-pot reaction in which redox side-products are more prevalent (bottom), Ref. [129].

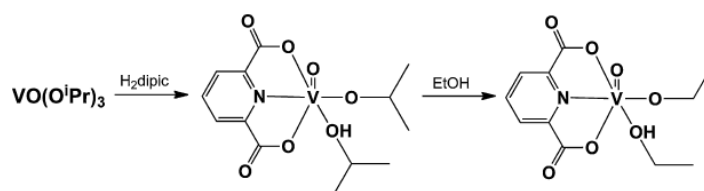
alcohol,  $\text{H}[\text{VO}_2\text{dipic}]\cdot\text{C}_2\text{H}_5\text{OH}$ . This was formed when attempting to recrystallize  $\text{H}[\text{VO}_2\text{dipic}]\cdot 2\text{H}_2\text{O}$  from ethanol. Upon heating at atmospheric pressure and under a nitrogen atmosphere, this complex releases ethanol. The corresponding peroxovanadium complex is sufficiently stable that an X-ray structure could be obtained demonstrating that this complex could withstand the radiation source [145]. The Thorn group represent the oxovanadium(V)dipicolinate complexes as five coordinate oxovanadium(V) alkoxides, in part, because they report that the solvent (alcohol) adduct does not impact the properties of the complex [33–35]. The formation of pinacolate complexes of oxovanadium(V)dipicolinate was achieved by reacting either of the aforementioned  $\text{V}(5+)$  species  $[(\text{dipic})\text{VO}(\text{OEt})]\cdot\text{EtOH}$  or  $[(\text{dipic})\text{VO}(\text{O}^i\text{Pr})]\cdot^i\text{PrOH}$  with the pinacol in acetonitrile [33]. The structure of this hexacoordinate dipicolinatooxovanadium(V) complex was confirmed by X-ray crystallography. Acetonitrile is a weakly coordinating solvent, and during the crystallization the complex dimerizes. One of the V-atoms remains coordinated with an alcohol whereas the other V-atom has the sixth coordination site occupied by the carboxylate oxygen of the dipic group. These two V-atoms are distinct and should result in two different  $^{51}\text{V}$  NMR chemical shifts. Only one chemical shift of  $-518$  ppm was observed suggesting rapid exchange between the vanadium atoms or accidental overlap between the signals [34,35]. This structure is different than a previously-reported dimer prepared from methanol by the Parajon-Costa group. In this complex the two six-coordinate V-atoms are identical and is formed by a diamond core structure by

dimerization of the  $[\text{VO}_2]$  unit [146]. Regardless of the nature of these complexes, these studies demonstrate that a rich redox chemistry is observed in a hydrophobic environment. If a  $[\text{VO}_2\text{dipic}]^-$  complex associates with a membranous environment, such reactions could take place and it becomes important to understand these reactions further.

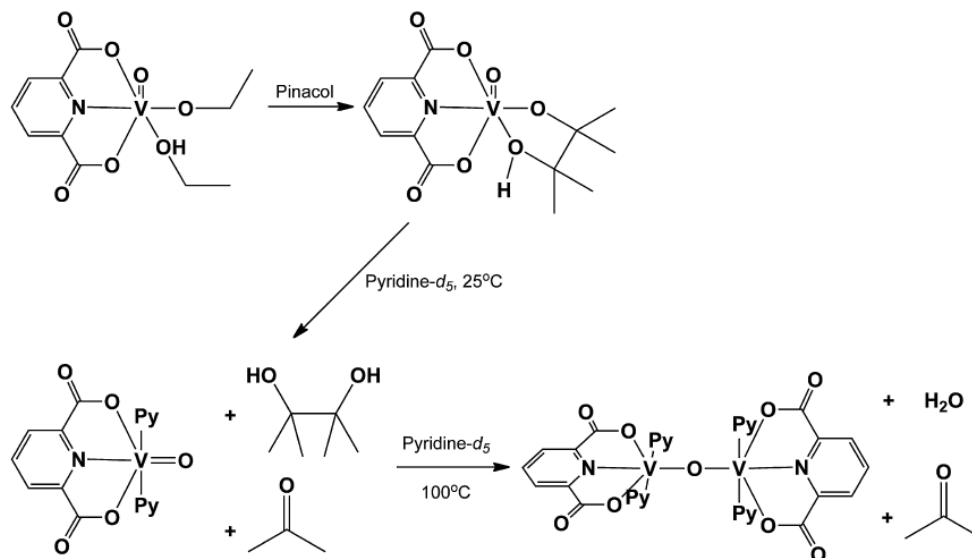
## 8. Reactions of dipicolinatooxovanadium(V) alkoxides

Dipicolinatooxovanadium(V) alkoxides catalyze the oxidation of lignin via C–C bond cleavage [34,147,148], a particularly hard synthetic challenge. The dissolution of dipicolinatooxovanadium(V) alkoxides in pyridine resulted in adducts that are sufficiently stable to have been isolated and characterized by X-ray crystallography (Scheme 7). The isolation of pyridine coordination adducts provide sufficient support that several V complexes form and can facilitate further reaction. In fact, absence of pyridine coordination was found to significantly decrease similar oxidation reactions.

One of these dipicolinatooxovanadium(V) alkoxides formed from pinacol undergoes redox chemistry, resulting in C–C bond cleavage of the coordinated pinacol [33]. Specifically, by heating the pinacolate complex of oxovanadium dipicolinate in pyridine, a mixture of starting material, C–C bond cleavage products of the pinacol and a bis(pyridine) adduct of oxovanadium(V) dipicolinate were isolated [33]. At ambient temperature, the same reactants formed the bis(pyridine) adduct and corresponding starting mate-



**Scheme 6.** Formation and alcohol exchange of a dipicolinatooxovanadium alkoxide.  $\text{VO}(\text{O}^i\text{Pr})_3$  was combined with  $\text{H}_2\text{dipic}$  in acetonitrile forming the dipicolinatooxovanadium isopropoxide which was confirmed by X-ray crystallography. The isopropoxide was converted to the ethoxide by adding either ethanol or ethanol/acetonitrile solutions, Ref. [145].

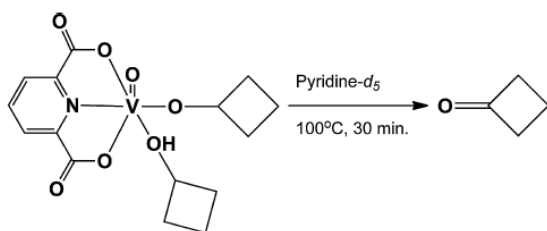


**Scheme 7.** Dipicolinatooxovanadium ethoxide ( $\text{VO}(\text{OCH}_2\text{CH}_3)(\text{dipic})\text{-HOCH}_2\text{CH}_3$ ) reacts in the absence of water as a catalyst in oxidation reactions such as lignin oxidation. The  $\text{VO}(\text{OCH}_2\text{CH}_3)(\text{dipic})\text{-HOCH}_2\text{CH}_3$  complex was reacted with pinacol in pyridine forming a bis(pyridine) adduct at low temperature and a dinuclear complex at high temperature  $\text{V}_2\text{O}(\text{pyr})_2(\text{dipic})_2$  complex, Ref. [33].

rial, but also resulted in oxidation of the pinacol, to the ketone [33–35]. Perhaps the particular reactivity of this complex is due to the coordination of both the alkoxide and an alcohol adduct to the V-atom.

Dipicolinatooxovanadium alkoxides also convert to the  $[\text{VO}_2\text{dipic}]^-$  coordination complex, with loss of both the alkoxide and alcohol. Reaction of either  $[(\text{dipic})\text{VO}(\text{O}^i\text{Pr})]\cdot\text{PrOH}$  or  $[(\text{dipic})\text{VO}(\text{Hpinacol})]\cdot\text{solvent}$  with water and pyridine resulted in formation of  $[\text{VO}_2\text{dipic}]^-$  as the pyridinium salt and the alcohol [33]. The coordination of the pyridine to the  $[\text{VO}_2\text{dipic}]^-$  is likely, although as discussed above, only peroxide and hydroxylamine derivatives were observed. Also, the electronic perturbation of the dipic-functionality did result in reorganization of the orbital arrangement of these complexes [130].  $^{51}\text{V}$  NMR studies as a function of pyridine concentration should confirm if such association takes place and was recently reported by the Thorn group [35].

Studies investigating the mechanism of these reactions, specifically regarding whether these reaction take place through a one-electron ( $\text{V}(5+/4+)$ ) or two-electron ( $\text{V}(5+/3+)$ ) redox process, were performed. The Thorn group used the reaction of cyclobutanol [149,150] as diagnostic for this investigation (illustrated in Scheme 8). As described previously, the result of the reaction using cyclobutoxide would indicate a two-electron process if the cyclobu-



**Scheme 8.** A two-electron reduction of  $\text{VO}(\text{dipic})(\text{OR})\text{-ROH}$  ( $\text{R} = \text{cyclobutoxide}$ ) alkoxide was observed after reaction  $100^\circ\text{C}$ . An average yield of 93% of cyclobutanone with  $(\text{dipic})\text{VO}(\text{pyr})_2$  as co-product was determined by  $^1\text{H}$  NMR spectroscopy, Ref. [33].

tanone resulted and a one-electron process should aliphatic chain product(s) result [151]. The dipicolinatooxovanadium(V) cyclobutoxide produces the cyclobutanone as predicted if a two-electron process were taking place and thus suggests that the V-atom is able to undergo a two-electron transfer reaction under these conditions. Indeed, reactions explored by the pinacol substituted monoethers yielded analogous products [34] suggesting that corresponding chemistry takes place with both protonated and alkylated oxygen. This result is remarkable considering that there is very little precedent for two-electron  $\text{V}(5+/3+)$  reactions [24,152]. However, the Espenson group questioned the choice of cyclobutanol as it may not be as good a representative alcohol as commonly believed [153] because variations in the product distribution are observed with minor changes in the vanadium complex giving support to alternative explanations. More mechanistic studies on this system have recently been reported [35].

Recent applications of vanadium catalysts have demonstrated that the studies described above are not unique to dipicolinatooxovanadium(V) complexes [33,34,154–158]. For example, glycine and sarcosine derivatives react in  $\text{CH}_2\text{Cl}_2$  with  $\text{VO}(\text{iOPr})_3$  and form, but in the presence of methanol forms a different complex, both of which are effective catalysts for chiral sulfoxide oxidation [154]. Slight modification in ligand or the addition of Lewis base changes the reaction course significantly [155,156]. A second example of how the environment and fine-tuning of a complex allow for improved catalytic effect is reported for the oxovanadium(V) triethanolamine in combination with pyrazine-2-carboxylic acid [157,158]. This system activates C–H bonds through a water-assisted H-transfer mechanism. The formation of  $\text{HO}^\bullet$  occurs via the addition of  $\text{H}_2\text{O}_2$  to the  $\text{V}(4+)$  complex with pyrazine-2-carboxylate [159], but minor changes in this component can significantly change the outcome of the reaction.

In summary, these studies demonstrate the versatility observed in these systems, and support the proposal that hydrophobic environments will dramatically change the reactions of the V–dipicolinate complexes. Thus, should the V–dipic complexes chelate a ligand and be able to interact and penetrate the lipid interface, a different reactivity of the complexes will result. As we

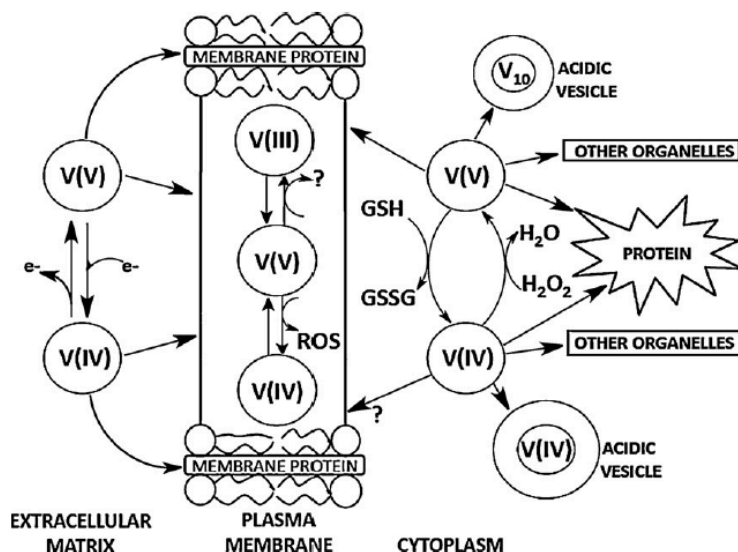


Fig. 12. A proposed pathway for toxic and beneficial responses to vanadium compounds after passive diffusion into the membrane where the hydrophobic membrane environment result in one electron  $V(4+/5+)$  redox chemistry and two electron  $V(3+/5+)$  redox chemistry. The presence of  $V(4+)$  and  $(5+)$  in the cytoplasm result in interaction with cellular components in many ways.

present in this manuscript, the biological effects observed by the  $V$ -complexes may be a result from the chemical and biochemical transformation that these compounds undergo in the environment in which they are found.

### 9. How drug environment and compartmentalization might affect action of vanadium compounds

In this manuscript, we suggest that the distribution of vanadium compounds within a cell is critical to their modes of action. Specifically, we propose that a change from a hydrophilic aqueous environment (i.e., as in cytoplasm) to a hydrophobic environment (i.e., as in/near membranes or microenvironments of proteins) governs how any given vanadium compound acts (i.e., beneficial or toxic). Chemistry in organic environments support both one-electron (Figs. 1, 2 and 12) and two-electron processes (Scheme 8 and Figs. 2 and 12) [24,35,152] and thus expands the reactivity of the compound observed in aqueous solution. The compartmentalization is important, because a compound that is less thermodynamically stable in aqueous environments could extend its lifetime by entrapment through compartmentalization in the hydrophobic environment in the membrane. In this review we link the chemistry in both hydrophilic and hydrophobic environments with biological effects of  $[VO_2dipic]^-$ .

It is generally accepted that vanadium compounds localized in the cytoplasm react with one or more reducing agent constituents, e.g., glutathione, cysteine, and ascorbate (Fig. 12) [24,95,159]. The accumulation of  $V(5+)$  in acidic vesicles resulted in decavanadate formation, which has been observed in yeast and other cellular systems [31,97]. The redox of  $V(5+)$  has been associated with transportation of the vanadium into acidic vesicles and with detoxification processes.

Importantly, we have shown that  $[VO_2dipic]^-$  and the charged free ligand readily penetrates a membranous surfactant interface residing in a hydrophobic environment [10,107]. Interface penetration takes place despite the high solubility of the complex in aqueous environments and the negatively charged interface. Why this complex is stabilized in this hydrophobic environment is surprising and suggests that some stabilizing forces exist for this

system. The recognition that a charged polar compound such as  $[VO_2dipic]^-$  has a great affinity for hydrophobic environments is critical for the alternative considerations suggested in this review. Lipid compatibility is not only important for this specific compound, but also demonstrates the concept that charged  $V$  derivative and ligands are compatible with hydrophobic membrane environments. As a consequence, the possibility that action of  $V$  compounds may involve hydrophobic membrane environments has experimental precedent.

The chemical precedence for conversion of  $[VO_2dipic]^-$  to a range of different compounds in organic solvents, Schemes 3–8, show that this compound can form derivatives in hydrophobic environments regardless of its charged precursor. These studies thus support the possibility that the polar  $[VO_2dipic]^-$  complex can convert to derivatives that are known to exert very different types of chemistry as described in Schemes 3–8. We propose that  $V$ -complexes can form in the membrane environment akin to the reactions taking place in organic solvents. Accordingly, in the presence of as of yet unidentified ligand substitution reactions will lead to controlled two-electron chemistry as is observed for a range of different alcohols. Alternatively, formation of other derivatives that undergo one-electron chemistry is likely to take place, thus result in various radicals and possible formation of ROS and RONS (Figs. 1, 2 and 12). High levels of ROS are likely to result in the deleterious radical chemistry that could signal toxic responses. However, low levels of ROS and RONS have been reported as beneficial, so it is possible that alternative ligands can change the amount of the one-electron reactions or that a two-electron pathway simply serves to reduce the amounts of radicals formed. In both cases the net result could reduce toxicity. Although, it is premature to assign a toxic and a beneficial route for the proposed pathways shown in Figs. 2 and 12; the proposed mechanism does provide alternative modes of action in which membrane interaction are critical to action of vanadium compounds.

### 10. Concluding remarks

In this review, we have described the chemical and biological properties of a simple and traditional  $V(5+)$  coordination complex,  $[VO_2dipic]^-$  [128]. The compound is stable in aqueous solution at

acidic pH, but hydrolyzes to form vanadate at neutral and alkaline pHs. At low pHs, the complex forms  $\text{VO}_2^+$  and the protonated  $\text{H}_2\text{dipic}$ . The complex is stable in the presence of oxygen, but the vanadium reduces in any reducing cellular environment. The complex is subject to ligand exchange; this occurs both in aqueous hydrophilic as well as a nonaqueous hydrophobic environments and as such result in changes in complex stability and properties [5]. Although we currently do not know the active species, based on the chemical properties of the complex and the different biological activities exerted by this complex, we propose that entrapment of the complex is responsible for the observations. Indeed, compartmentalization of the complex would affect its properties, and provide a rationale for the observations.

Vanadium dipicolinate complexes have been investigated for insulin-enhancing properties; in diabetic animal models, the  $\text{V}(5+)$  complex generates a statistically different response in treated hosts compared to in untreated controls or diabetic animals [5]. Neither the  $\text{V}(3+)$  or  $\text{V}(4+)$  dipicolinate complexes induce a similarly significant response among the diabetic animals. In contrast, the  $\text{V}(4+)$  in the BMOV complex induced the best response compared to the  $\text{V}(3+)$  and  $\text{V}(5+)$  complexes [3]. Since the  $\text{V}(5+)$  dipicolinate is both unstable hydrolytically and with respect to redox, it is particularly surprising that the  $[\text{VO}_2\text{dipic}]^-$  is so effective. Accordingly, the specific properties of the vanadium dipicolinate complexes are likely important underpinnings to the biological outcomes. We propose that these observations are a result of the compatibility of the  $[\text{VO}_2\text{dipic}]^-$  complex with the membrane environment and its reactivity in hydrophobic environments.

Here, we summarize the known chemistry of  $[\text{VO}_2\text{dipic}]^-$  in organic solvents. Both two-electron and one-electron redox chemistry have been reported [33–35]. We propose that these reactions can take place in analogous hydrophobic environments such as the lipid bi-layers in membranes and in protein interiors. We propose that controlling the chemistry in these environments may induce the observed beneficial effects of vanadium complexes, whereas the less controlled reactions giving rise to high levels of ROS may result in malicious effects of V compounds. At this time, details of the proposed mechanism are ill-defined. We do not know what ligand(s) undergo ligand exchange reaction with the dipicolinate complex to form “the active species”. We do not know if the two-electron process is the beneficial process, or simply serves to reduce the ROS levels. However, the hypothesis does provide a more defined alternative mechanistic possibility giving the membrane a role and thus provide explanations to observations not previously explained. Thus, in addition to the inhibition of protein tyrosine phosphatases, changes in redox state of the cell, and interaction with the transport proteins, a testable mechanism has now been proposed in which the membrane plays a key role. Importantly, this proposal (illustrated in Figs. 2 and 12) provides a simple model that explains how the identical complex in some cases induce beneficial effects, and other cases is toxic.

## Acknowledgements

DCC thank NSF CHE-0628260 for funding this work. AMT was supported by NSF Bridge to the Doctorate fellowship, grant NSF HRD 0832932. PSP was supported by NIH 1U19CA105010. MDC was supported, in part, by NIEHS Center Grant ES00260 and CDC/NIOSH Grant OH008280-01A2.

## References

- [1] C. Lipinski, F. Lombardo, B. Dominy, P. Feeney, *Adv. Drug Deliv. Rev.* 23 (1997) 3.
- [2] H. Gronemeyer, J.A. Gustafsson, V. Laudet, *Nat. Rev. Drug Discov.* 3 (2004) 950.
- [3] P. Buglyo, D.C. Crans, E.M. Nagy, R.L. Lindo, L.Q. Yang, J.J. Smee, W.Z. Jin, L.H. Chi, M.E. Godzala, G.R. Willsky, *Inorg. Chem.* 44 (2005) 5416.
- [4] D.C. Crans, L.Q. Yang, T. Jakusch, T. Kiss, *Inorg. Chem.* 39 (2000) 4409.
- [5] D.C. Crans, *J. Inorg. Biochem.* 80 (2000) 123.
- [6] D.C. Crans, L.Q. Yang, J.A. Alfano, L.A.H. Chi, W.Z. Jin, M. Mahroof-Tahir, K. Robbins, M.M. Toloue, L.K. Chan, A.J. Plante, R.Z. Grayson, G.R. Willsky, *Coord. Chem. Rev.* 237 (2003) 13.
- [7] J.J. Smee, J.A. Epps, K. Ooms, S.E. Bolte, T. Polenova, B. Baruah, L. Yang, W. Ding, M. Li, G.R. Willsky, A.I. Cour, O.P. Anderson, D.C. Crans, *J. Inorg. Biochem.* 103 (2009) 575.
- [8] Y. Zhang, X.D. Yang, K. Wang, D.C. Crans, *J. Inorg. Biochem.* 100 (2006) 80.
- [9] G.R. Willsky, M. Godzala, P.J. Kostyniak, L. Chi, J.J. Smee, D.C. Crans, *The 7th International Symposium on the Chemistry and Biological Chemistry of Vanadium*, 2010.
- [10] D.C. Crans, A.M. Trujillo, S. Bonetti, C.D. Rithner, B. Baruah, N.E. Levinger, *J. Org. Chem.* 73 (2008) 9633.
- [11] E. Gaidamauskas, D.P. Cleaver, P.B. Chatterjee, D.C. Crans, *Langmuir* 26 (2010) 13153.
- [12] D.A. Roess, S.M.L. Smith, P. Winter, J. Zhou, P. Dou, B. Baruah, A.M. Trujillo, N.E. Levinger, X.D. Yang, B.G. Barisas, D.C. Crans, *Chem. Biodivers.* 5 (2008) 1558.
- [13] J. Stover, C.D. Rithner, R.A. Inafuku, D.C. Crans, N.E. Levinger, *Langmuir* 21 (2005) 6250.
- [14] X.G. Yang, X.D. Yang, L. Yuan, K. Wang, D.C. Crans, *Pharm. Res.* 21 (2004) 1026.
- [15] X.G. Yang, K. Wang, J.F. Lu, D.C. Crans, *Coord. Chem. Rev.* 237 (2003) 103.
- [16] M.D. Cohen, M. Sisco, C. Prophete, L.C. Chen, J.T. Zelikoff, A.J. Ghio, J.D. Stonehauer, J.J. Smee, A.A. Holder, D.C. Crans, *J. Immunotoxicol.* 4 (2007) 49.
- [17] M.D. Cohen, M. Sisco, C. Prophete, K. Yoshida, L.C. Chen, J.T. Zelikoff, J. Smee, A.A. Holder, J. Stonehauer, D.C. Crans, A.J. Ghio, *Inhal. Toxicol.* 22 (2010) 169.
- [18] D.C. Crans, M. Mahroof-Tahir, M.D. Johnson, P.C. Wilkins, L.Q. Yang, K. Robbins, A. Johnson, J.A. Alfano, M.E. Godzala, L.T. Austin, G.R. Willsky, *Inorg. Chim. Acta* 356 (2003) 365.
- [19] M. Li, W.J. Ding, J.J. Smee, B. Baruah, G.R. Willsky, D.C. Crans, *Biometals* 22 (2009) 895.
- [20] M. Li, J.J. Smee, W.J. Ding, D.C. Crans, *J. Inorg. Biochem.* 103 (2009) 585.
- [21] M.J. Pereira, E. Carvalho, J.W. Eriksson, D.C. Crans, M. Aureliano, *J. Inorg. Biochem.* 103 (2009) 1687.
- [22] G.R. Willsky, L.H. Chi, Y.L. Liang, D.P. Gaile, Z.H. Hu, D.C. Crans, *Physiol. Genomics* 26 (2006) 192.
- [23] G.R. Willsky, A.B. Goldfine, P.J. Kostyniak, J.H. McNeill, L.Q. Yang, H.R. Khan, D.C. Crans, *J. Inorg. Biochem.* 85 (2001) 33.
- [24] D.C. Crans, J.J. Smee, E. Gaidamauskas, L.Q. Yang, *Chem. Rev.* 104 (2004) 849.
- [25] D. Rehder, *Inorg. Chem. Commun.* 6 (2003) 604.
- [26] A.S. Tracey, G.R. Willsky, E.S. Takeuchi, *Vanadium: Chemistry, Biochemistry, Pharmacology and Practical Applications*, CRC Press, Boca Raton, 2007.
- [27] K.H. Thompson, C. Orvig, *J. Inorg. Biochem.* 100 (2006) 1925.
- [28] D.C. Crans, E.M. Willging, S.R. Butler, *J. Am. Chem. Soc.* 112 (1990) 427.
- [29] D.C. Crans, C.M. Simone, A.K. Saha, R.H. Glew, *Biochem. Biophys. Res. Commun.* 165 (1989) 246.
- [30] M. Aureliano, F. Henao, T. Tiago, R.O. Duarte, J.J.G. Moura, B. Baruah, D.C. Crans, *Inorg. Chem.* 47 (2008) 5677.
- [31] M. Aureliano, D.C. Crans, *J. Inorg. Biochem.* 103 (2009) 536.
- [32] M.D. Cohen, in: K. Kustin, J.C. Pessoa, D.C. Crans (Eds.), *Vanadium: The Versatile Metal*, American Chemical Society, Washington, DC, 2007, p. 217.
- [33] S.K. Hanson, R.T. Baker, J.C. Gordon, B.L. Scott, A.D. Sutton, D.L. Thorn, *J. Am. Chem. Soc.* 131 (2009) 428.
- [34] S.K. Hanson, R.T. Baker, J.C. Gordon, B.L. Scott, D.L. Thorn, *Inorg. Chem.* 49 (2010) 5611.
- [35] S.K. Hanson, R.T. Baker, J.C. Gordon, B.L. Scott, L.A. Silks, D.L. Thorn, *J. Am. Chem. Soc.* 132 (2010) 17804.
- [36] S. Sunghee, R. Dean Toste, *Angew. Chem.* 49 (2010) 3791.
- [37] C. Limberg, *Angew. Chem.* 42 (2003) 5932.
- [38] V. Conte, B. Floris, *Inorg. Chim. Acta* 363 (2010) 1935.
- [39] S.M. Brichard, *Mol. Cell. Biochem.* 153 (1995) 121.
- [40] A.B. Goldfine, M.E. Patti, L. Zuberi, B.J. Goldstein, R. LeBlanc, E.J. Landaker, Z.Y. Jiang, G.R. Willsky, C.R. Kahn, *Metab. Clin. Exp.* 49 (2000) 400.
- [41] D. Rehder, J.C. Pessoa, C. Galdes, M. Castro, T. Kabanos, T. Kiss, B. Meier, G. Micera, L. Pettersson, M. Rangel, A. Salifoglou, I. Turel, D.R. Wang, *J. Biol. Inorg. Chem.* 7 (2002) 384.
- [42] K.H. Thompson, C. Orvig, *Coord. Chem. Rev.* 219 (2001) 1033.
- [43] H. Sakurai, in: K. Kustin, J.C. Pessoa, D.C. Crans (Eds.), *Vanadium: The Versatile Metal*, American Chemical Society, Washington, DC, 2007, p. 110.
- [44] K.H. Thompson, J. Lichter, C. LeBel, M.C. Scaife, J.H. McNeill, C. Orvig, *J. Inorg. Biochem.* 103 (2009) 554.
- [45] R.C. Todd, S.J. Lippard, *Metallomics* 1 (2009) 280.
- [46] D.P. Jones, Y.M. Go, *Diabetes Obes. Metab.* 12 (2010) 116.
- [47] N.D. Chasteen, in: H. Sigel, A. Sigel (Eds.), *Metal Ions in Biological Systems*, Vol. 31: Vanadium and Its Role in Life, Marcel Dekker, New York, 1995, p. 231.
- [48] M. Aureliano, R.M.C. Gandara, *J. Inorg. Biochem.* 99 (2005) 979.
- [49] D.C. Crans, *Pure Appl. Chem.* 77 (2005) 1497.
- [50] A.M. Evangelou, *Crit. Rev. Oncol. Hematol.* 42 (2002) 249.
- [51] I.G. Fantus, G. Deragon, R. Lai, S. Tang, *Mol. Cell. Biochem.* 153 (1995) 103.
- [52] I.G. Fantus, E. Tsiani, *Mol. Cell. Biochem.* 182 (1998) 109.
- [53] A. Messerschmidt, R. Wever, *Inorg. Chim. Acta* 273 (1998) 160.
- [54] A. Butler, *Curr. Opin. Chem. Biol.* 2 (1998) 279.
- [55] M. Li, W.J. Ding, B. Baruah, D.C. Crans, R.L. Wang, *J. Inorg. Biochem.* 102 (2008) 1846.

- [56] G. Huyer, S. Liu, J. Kelly, J. Moffat, P. Payette, B. Kennedy, G. Tsaprailis, M.J. Gresser, C. Ramachandran, *J. Biol. Chem.* 272 (1997) 843.
- [57] D.A. Barrio, P.A.M. Williams, A.M. Cortizo, S.B. Etcheverry, *J. Biol. Inorg. Chem.* 8 (2003) 459.
- [58] T. Hamada, M. Asanuma, T. Ueki, F. Hayashi, N. Kobayashi, S. Yokoyama, H. Michibata, H. Hirota, *J. Am. Chem. Soc.* 127 (2005) 4216.
- [59] H. Michibata, M. Yoshinaga, M. Yoshihara, N. Kawakami, N. Yamaguchi, T. Ueki, in: K. Kustin, J.C. Pessoa, D.C. Crans (Eds.), *Vanadium: The Versatile Metal*, American Chemical Society, Washington, DC, 2007, p. 264.
- [60] T. Ueki, M. Satake, K. Kamino, H. Michibata, *Biochim. Biophys. Acta, Gen. Subj.* 1780 (2008) 1010.
- [61] J.P. Bellenger, T. Wichard, A.B. Kustka, A.M.L. Kraepiel, *Nat. Geosci.* 1 (2008) 243.
- [62] J. Littlechild, E. Garcia-Rodriguez, E. Coupe, A. Watts, M. Isupov, in: K. Kustin, J.C. Pessoa, D.C. Crans (Eds.), *Vanadium: The Versatile Metal*, American Chemical Society, Washington, DC, 2007, p. 136.
- [63] A. Messerschmidt, R. Wever, *Proc. Natl. Acad. Sci. U.S.A.* 93 (1996) 392.
- [64] W. Hemrika, R. Renirie, H.L. Dekker, P. Barnett, R. Wever, *Proc. Natl. Acad. Sci. U.S.A.* 94 (1997) 2145.
- [65] D.R. Davies, W.G.J. Hol, *FEBS Lett.* 577 (2004) 315.
- [66] J.C. Borden, D.C. Crans, J. Florian, *J. Phys. Chem. B* 10 (2006) 14988.
- [67] D.C. Crans, A.D. Keramidias, C. Drouza, *Phosphorus Sulfur Silicon Relat. Elem.* 109–110 (1996) 245.
- [68] X.L. Gao, L.P. Lu, M.L. Zhu, C.X. Yuan, J.F. Ma, X.Q. Fu, *Acta Chim. Sin.* 67 (2009) 929.
- [69] C.C. McLaughlan, J.D. Hooker, M.A. Jones, Z. Dymon, E.A. Backhus, M.A. Youkhana, L.M. Manus, *J. Inorg. Biochem.* 104 (2010) 274.
- [70] C.X. Yuan, L.P. Lu, X.L. Gao, Y.B. Wu, M.L. Guo, L. Li, X.Q. Fu, M.L. Zhu, *J. Biol. Inorg. Chem.* 14 (2009) 841.
- [71] C. Cuncic, S. Desmarais, N. Detich, A.S. Tracey, M.J. Gresser, C. Ramachandran, *Biochem. Pharmacol.* 58 (1999) 1859.
- [72] E. Tsiani, I.G. Fantus, *Trends Endocrinol. Metab.* 8 (1997) 51.
- [73] C.C. McLaughlan, J.D. Hooker, M.A. Jones, Z. Dymon, E.A. Backhus, B.A. Greiner, N.A. Dornier, M.A. Youkhana, L.M. Manus, *J. Inorg. Biochem.* 104 (2010) 274.
- [74] J.P. Harrington, *Int. J. Biochem.* 24 (1992) 275.
- [75] D.C. Harris, *Biochemistry* 16 (1977) 560.
- [76] M.H. Nagaoka, H. Akiyama, T. Maitani, in: M.A. Cser, I.S. Laszlo, J.C. Etienne, Y. Maynard, J.A. Centeno, L. Khassanova, P. Coltery (Eds.), *Metal Ions in Biology and Medicine*, vol. 8, John Libbey Eurotext, Montrouge, 2004, p. 63.
- [77] S.P. Doherty, C. Prophete, P. Maciejczyk, K. Salnikow, T. Gould, T. Larson, J. Koenig, P. Jaques, C. Sioutas, J.T. Zelikoff, M. Lippmann, M.D. Cohen, *Inhal. Toxicol.* 19 (2007) 553.
- [78] J.C. Pessoa, I. Tomaz, *Chim. Med. Chem.* 110 (2010) 3701.
- [79] B.D. Liboiron, K.H. Thompson, G.R. Hanson, E. Lam, N. Aebischer, C. Orvig, *J. Am. Chem. Soc.* 127 (2005) 5104.
- [80] D. Sanna, E. Garribba, G. Micera, *J. Inorg. Biochem.* 103 (2009) 648.
- [81] D.C. Crans, R.L. Bunch, L.A. Theisen, *J. Am. Chem. Soc.* 111 (1989) 7597.
- [82] H.P. Monteiro, C.C. Winterbourn, A. Stern, *Free Radic. Res. Commun.* 12–13 (1991) 125.
- [83] T. Kiss, T. Jakusch, D. Hollender, A. Dornyei, E.A. Enyedy, J.C. Pessoa, H. Sakurai, A. Sanz-Medel, *Coord. Chem. Rev.* 252 (2008) 1153.
- [84] H. Yasui, A. Tamura, T. Takino, H. Sakurai, *J. Inorg. Biochem.* 91 (2002) 327.
- [85] D. Sanna, E. Garribba, G. Micera, *J. Inorg. Biochem.* 103 (2009) 648.
- [86] D. Sanna, P. Buglyo, G. Micera, E. Garribba, *J. Inorg. Biochem.* 15 (2010) 825.
- [87] H. Esbak, E.A. Enyedy, T. Kiss, Y. Yoshikawa, H. Sakurai, E. Garribba, D. Rehder, *J. Inorg. Biochem.* 103 (2009) 590.
- [88] T. Jakusch, D. Hollender, E.A. Enyedy, C.S. Gonzalez, M. Montes-Bayon, A. Sanz-Medel, J. Costa-Pessoa, I. Tomaz, T. Kiss, *Dalton Trans.* 13 (2009) 2428.
- [89] D.C. Crans, H. Holst, A.D. Keramidias, D. Rehder, *Inorg. Chem.* 34 (1995) 2524.
- [90] E.J. Baran, *Chem. Biodivers.* 5 (2008) 1475.
- [91] L.A. Minasi, G.R. Willsky, *J. Bacteriol.* 173 (1991) 834.
- [92] A. Stern, X.F. Yin, S.S. Tsang, A. Davison, J. Moon, *Biochem. Cell Biol.* 71 (1993) 103.
- [93] P.S. Chien, O.T. Mak, H.J. Huang, *Biochem. Biophys. Res. Commun.* 339 (2006) 562.
- [94] D.C. Crans, B. Zhang, E. Gaidamauskas, A.D. Keramidias, G.R. Willsky, C.R. Roberts, *Inorg. Chem.* 49 (2010) 4245.
- [95] B.R. Nechay, L.B. Nanninga, P.S.E. Nechay, *Arch. Biochem. Biophys.* 251 (1986) 128.
- [96] D.C. Crans, B. Zhang, E. Gaidamauskas, A.D. Keramidias, G.R. Willsky, C.R. Roberts, *Inorg. Chem.* 49 (2010) 4245.
- [97] G.R. Willsky, D.A. Preischel, B.C. McCabe, *Biophys. J.* 45 (1984) A76.
- [98] M. Barac-Nieto, M. Alfred, A. Spitzer, *Exp. Biol. Med.* 227 (2002) 626.
- [99] S. Elmariha, R.B. Gunn, *Am. J. Physiol.: Cell Physiol.* 285 (2003) C446.
- [100] K. Kawabe, Y. Yoshikawa, Y. Adachi, H. Sakurai, *Life Sci.* 78 (2006) 2860.
- [101] M. Hiromura, A. Nakayama, Y. Adachi, M. Doi, H. Sakurai, *J. Biol. Inorg. Chem.* 12 (2007) 1275.
- [102] S. Tang, B. Lu, I.G. Fantus, *Metab. Clin. Exp.* 47 (1998) 630.
- [103] H. Zaporowska, A. Scibior, *Folia Histochem. Cytobiol.* 37 (1999) 113.
- [104] K. Wang, S. Afr, *J. Chem.* 50 (1997) 232.
- [105] R. Meier, M. Boddin, S. Mitzenheim, K. Kanamori, in: H. Sigel, A. Sigel (Eds.), *Metal Ions in Biological Systems*, Vol. 31: Vanadium and Its Role in Life, Marcel Dekker, New York, 1995, p. 45.
- [106] D.A. Roess, S.M.L. Smith, A.A. Holder, B. Baruah, A.M. Trujillo, D. Gilsdorf, M.L. Stahla, D.C. Crans, *ACS Symp. Ser.* 974 (2007) 121.
- [107] D.C. Crans, C.D. Rithner, B. Baruah, B.L. Gourley, N.E. Levinger, *J. Am. Chem. Soc.* 128 (2006) 4437.
- [108] Y. Shechter, I. Goldwaser, M. Mironchik, M. Fridkin, D. Gefel, *Coord. Chem. Rev.* 237 (2003) 3.
- [109] K.H. Thompson, C. Orvig, in: A. Sigel, H. Sigel (Eds.), *Metal Ions in Biological Systems*, Vol. 41: Metal Ions and Their Complexes in Medication, Marcel Dekker, New York, 2004, p. 221.
- [110] K.H. Thompson, C. Orvig, *Dalton Trans.* 17 (2000) 2885.
- [111] M. Melchior, S.J. Rettig, B.D. Liboiron, K.H. Thompson, V.G. Yuen, J.H. McNeill, C. Orvig, *Inorg. Chem.* 40 (2001) 4686.
- [112] J.H. McNeill, V.G. Yuen, S.T. Dai, C. Orvig, *Mol. Cell. Biochem.* 153 (1995) 175.
- [113] Y. Fujisawa, H. Sakurai, *Chem. Pharm. Bull.* 47 (1999) 1668.
- [114] A.B. Goldfine, D.C. Simonson, F. Folli, E. Patti, C.R. Kahn, *Mol. Cell. Biochem.* 153 (1995) 217.
- [115] G.H. Cros, M.C. Cam, J.J. Serrano, G. Ribes, J.H. McNeill, *Mol. Cell. Biochem.* 153 (1995) 191.
- [116] A.P. Seale, L.A. De Jesus, S.Y. Kim, Y.H. Choi, H.B. Lim, C.S. Hwang, Y.S. Kim, *Biotechnol. Lett.* 27 (2005) 221.
- [117] B.P. Kennedy, *Biomed. Pharmacother.* 53 (1999) 466.
- [118] B. Kennedy, C. Ramachandran, *Biochem. Pharmacol.* 60 (2000) 877.
- [119] K.H. Thompson, Y. Tsukada, Z.M. Xu, M. Battell, J.H. McNeill, C. Orvig, *Biol. Trace Elem. Res.* 86 (2002) 31.
- [120] B.I. Posner, R. Faure, J.W. Burgess, A.P. Bevan, D. Lachance, G.Y. Zhangsun, I.G. Fantus, J.B. Ng, D.A. Hall, B.S. Lum, A. Shaver, *J. Biol. Chem.* 269 (1994) 4596.
- [121] A.P. Bevan, P.G. Drake, J.F. Yale, A. Shaver, B.I. Posner, *Mol. Cell. Biochem.* 153 (1995) 49.
- [122] D.C. Crans, A.D. Keramidias, H. Hoover-Litty, O.P. Anderson, M.M. Miller, L.M. Lemoine, S. Pleasic-Williams, M. Vandenberg, A.J. Rossomando, L. Sweet, *J. Am. Chem. Soc.* 119 (1997) 5447.
- [123] M.J. Xie, X.D. Yang, W.P. Liu, S.P. Yan, Z.H. Meng, *J. Inorg. Biochem.* 104 (2010) 851.
- [124] Y. Shechter, I. Goldwaser, M. Mironchik, H. Tsubery, M. Fridkin, *Pure Appl. Chem.* 77 (2005) 1617.
- [125] V.G. Yuen, P. Caravan, L. Gelmini, N. Glover, J.H. McNeill, I.A. Setyawati, Y. Zhou, C. Orvig, *J. Inorg. Biochem.* 68 (1997) 109.
- [126] F.L. Assem, L.S. Levy, J. Toxicol. Environ. Health, Part B 12 (2009) 289.
- [127] J.D. Domingo, M. Gomez, D.J. Sanchez, J.M. Llobet, C.L. Keen, *Mol. Cell. Biochem.* 153 (1995) 233.
- [128] B. Nuber, J. Weiss, K. Wiegardt, *Z. Naturforsch. (B)* 33 (1978) 265.
- [129] J.J. Smee, J.A. Epps, G. Teissedre, M. Maes, N. Harding, L. Yang, B. Baruah, S.M. Miller, O.P. Anderson, G.R. Willsky, D.C. Crans, *Inorg. Chem.* 46 (2007) 9827.
- [130] K.J. Ooms, S.E. Bolte, J.J. Smee, B. Baruah, D.C. Crans, T. Polenova, *Inorg. Chem.* 46 (2007) 9285.
- [131] H. Mimoun, P. Chaumette, M. Mignard, L. Saussine, J. Fischer, R. Weiss, *Nouv. J. Chim.* 7 (1983) 467.
- [132] A.D. Keramidias, S.M. Miller, O.P. Anderson, D.C. Crans, *J. Am. Chem. Soc.* 119 (1997) 8901.
- [133] R.K. Mittal, R.C. Mehrotra, *Z. Anorg. Allg. Chem.* 332 (1964) 189.
- [134] A. Lachowicz, K.-H. Thiele, *Z. Anorg. Allg. Chem.* 431 (1977) 88.
- [135] F. Hillerns, D. Rehder, *Chem. Ber.* 124 (1991) 2249.
- [136] D.C. Crans, H. Chen, R.A. Felty, *J. Am. Chem. Soc.* 114 (1992) 4543.
- [137] W. Priebsch, D. Rehder, *Inorg. Chem.* 29 (1990) 3013.
- [138] D.C. Bradley, M.L. Mehta, *Can. J. Chem.* 40 (1962) 1183.
- [139] D.C. Bradley, R.K. Multani, W. Wardlaw, *J. Chem. Soc.* (1958) 4647.
- [140] D.C. Crans, R.A. Felty, O.P. Anderson, M.M. Miller, *Inorg. Chem.* 32 (1993) 247.
- [141] D.C. Crans, R.A. Felty, M.M. Miller, *J. Am. Chem. Soc.* 113 (1991) 265.
- [142] F. Jiang, O.P. Anderson, S.M. Miller, J. Chen, M. Mahroof-Tahir, D.C. Crans, *Inorg. Chem.* 37 (1998) 5439.
- [143] S. Mondal, S. Prasad Rath, S. Dutta, A. Chakravorty, *J. Chem. Soc., Dalton Trans.* 1 (1996) 99.
- [144] J. Salta, J. Zubieta, *Inorg. Chim. Acta* 257 (1997) 83.
- [145] D.L. Thorn, R.L. Harlow, N. Herron, *Inorg. Chem.* 35 (1996) 547.
- [146] A.C. Gonzalez-Baro, E.E. Castellano, O.E. Piro, B.S. Parajon-Costa, *Polyhedron* 24 (2005) 49.
- [147] E.C.E. Rosenthal, H. Cui, K.C.H. Lange, S. Dechart, *Eur. J. Inorg. Chem.* 23 (2004) 4681.
- [148] H. Cui, M. Mummert, S. Dechart, E.C.E. Rosenthal, *Inorg. Chem. Commun.* 13 (2010) 769.
- [149] K. Meyer, J. Rocek, *J. Am. Chem. Soc.* 94 (1972) 1209.
- [150] W.D. Chandler, Z. Wang, D.G. Lee, *Can. J. Chem.* 83 (2005) 1212.
- [151] J. Rocek, D.E. Aylward, *J. Am. Chem. Soc.* 97 (1975) 5452.
- [152] T. Hirao, *Chem. Rev.* 97 (1997) 2707.
- [153] S.L. Scott, A. Bakac, J.H. Espenson, *J. Am. Chem. Soc.* 114 (1992) 4205.
- [154] C. Wikete, P.S. Wu, G. Zampella, L. De Gioia, G.L. Licini, D. Rehder, *Inorg. Chem.* 46 (2007) 196.
- [155] S. Lovat, M. Mba, H.C.L. Abbenhuis, D. Vogt, C. Zonta, G. Licini, *Inorg. Chem.* 48 (2009) 4724.
- [156] M. Mba, M. Pontini, S. Lovat, C. Zonta, G. Bernardinelli, P.E. Kundig, G. Licini, *Inorg. Chem.* 47 (2008) 8616.
- [157] M.V. Kirillova, M.L. Kuznetsov, V.B. Romakh, L.S. Shul'pina, J. da Silva, A.J.L. Pombeiro, G.B. Shul'pin, *J. Catal.* 267 (2009) 140.
- [158] G.B. Shul'pin, Y.N. Kozlov, G.V. Nizova, G. Suss-Frank, S. Stanislas, A. Kitaygorodskiy, V.S. Kulikova, *J. Chem. Soc., Perkin Trans. 2* (2001) 1351.
- [159] D.C. Crans, B. Baruah, E. Gaidamauskas, B.G. Lemons, B.B. Lorenz, M.D. Johnson, *J. Inorg. Biochem.* 102 (2008) 1334.

APPENDIX ARTICLE 5<sup>8</sup>:

Review

Anti-diabetic effects of a series of vanadium dipicolinate complexes in rats with streptozotocin-induced diabetes

Gail R. Willsky<sup>a,\*</sup>, Lai-Har Chi<sup>a</sup>, Michael Godzala III<sup>a</sup>, Paul J. Kostyniak<sup>a</sup>, Jason J. Smee<sup>d,1</sup>, Alejandro M. Trujillo<sup>d</sup>, Josephine A. Alfano<sup>a</sup>, Wenjin Ding<sup>b</sup>, Zihua Hu<sup>c</sup>, Debbie C. Crans<sup>d</sup>

<sup>a</sup> University at Buffalo, School of Medicine and Biomedical Sciences, Buffalo, NY, USA

<sup>b</sup> College of Life Sciences, Graduate University of Chinese Academy of Sciences, Beijing, China

<sup>c</sup> University at Buffalo, Center for Computational Research, Buffalo, NY, USA

<sup>d</sup> Department of Chemistry, Colorado State University, Fort Collins, CO, USA

Contents

1. Introduction .....	2259
1.1. Insulin-enhancing effects of V in rats with STZ-induced diabetes.....	2259
1.2. V dipicolinate complexes: rationale for use and introduction of complexes reviewed .....	2260
1.3. Effects of ligands and V5dipic on diabetic hyperglycemia, diabetic hyperlipidemia, and toxicity.....	2260
2. Effect of oxidation state modification of Vdipic and VdipicCl complexes on insulin-enhancing activity .....	2261
2.1. Effects of oxidation state modification of Vdipic on diabetic hyperglycemia, hyperlipidemia and absorption into serum.....	2261
2.2. Effects of mode of administration on the anti-diabetic effect of V3dipic, V4dipic, and V5dipic .....	2263
2.3. Effects of oxidation state modification of VdipicCl complexes on diabetic hyperglycemia, hyperlipidemia, and serum metabolites .....	2263
3. Insulin-enhancing effects of V5dipic with OH modification of ligand and amine coordination at the metal .....	2263
3.1. Effects on diabetic hyperglycemia, diabetic hyperlipidemia and absorption into serum when the V5dipic complex is modified with OH and hydroxylamine is coordinated to the V.....	2263
3.2. The effects on global gene expression of treatment with V5dipicOH and VS .....	2264
4. Interpretations of the observed effects of the Vdipic complexes used as treatment in STZ-induced diabetic rats .....	2266
4.1. Summary of the insulin-enhancing effects seen in administration of Vdipic complexes to diabetic rats and toxicity implications.....	2266
4.2. Chemical stability and electrochemistry/catalytic studies of the V5dipic complexes with anti-diabetic effects.....	2267
5. Conclusions .....	2268
Acknowledgements.....	2268
References .....	2268

ARTICLE INFO

Article history:

Received 1 March 2011

Accepted 20 June 2011

Available online 26 June 2011

Keywords:

Vanadium

Dipicolinic acid

ABSTRACT

The effects of oral treatment of rats with streptozotocin-induced diabetes with a range of vanadium dipicolinate complexes (Vdipic) and derivatives are reviewed. Structure–reactivity relationships are explored aiming to correlate properties such as stability, to their insulin-enhancing effects. Three types of modifications are investigated; first, substitutions on the aromatic ring, second, coordination of a hydroxylamido group to the vanadium, and third, changes in the oxidation state of the vanadium ion. These studies allowed us to address the importance of coordination chemistry, and redox chemistry, as modes of action. Dipicolinate was originally chosen as a ligand because the dipicolinatooxovanadium(V) complex (V5dipic), is a potent inhibitor of phosphatases. The effect of vanadium oxidation state (3, 4 or 5),

*Abbreviations:* ANOVA, analysis of variance is the standard way to statistically analyze biological results when 2 or more groups are being compared; AST, aspartate aminotransferase; ALP, alkaline phosphatase; BB, biobreeding; BG, blood glucose; BEOV, Bbis(ethylmaltolato)oxovanadium(IV); BMOV, bis(maltolato)oxovanadium(IV); chol, cholesterol; Dipic, dipicolinate or 2,6-pyridinedicarboxylate; DipicCl, 4-chlorodipicolinate or 4-chloro-2,6-pyridinedicarboxylate; DipicOH, 4-hydroxydipicolinate or 4-hydroxy-2,6-pyridinedicarboxylate; FFA, free fatty acids; HA, hydroxylamine; MeHA, methylhydroxylamine; N, normal; ROS, reactive oxygen species; RNS, reactive nitrogen species; STZ, streptozotocin; TG, triglyceride; V, vanadium; VS, vanadyl sulfate; Vdipic, refers to all the vanadium-containing dipicolinate complexes of oxidation states III, IV and V; VdipicCl, refers to all the vanadium-containing chlorodipicolinate complexes of oxidation states III, IV and V; V3dipic, bis(dipicolinato)oxovanadium(III); V4dipic, dipicolinatooxovanadium(IV); V5dipic, dipicolinatooxovanadium(V); V3dipicCl, bis(4-chlorodipicolinato)oxovanadium(III); V4dipicCl, 4-chlorodipicolinatooxovanadium(IV); V5dipicCl, 4-chlorodipicolinatooxovanadium(V); V5dipic(MeHA), dipicolinatooxovanadium(V)methylhydroxylamine; V5dipicNH2, 4-aminodipicolinatooxovanadium(V); V5dipicOH, 4-hydroxydipicolinatooxovanadium(V); V5dipicOH(HA), 4-hydroxydipicolinatooxovanadium(V) hydroxylamine.

\* Corresponding author at: University at Buffalo (SUNY), Department of Biochemistry, School of Medicine and Biomedical Sciences, 140 Farber Hall, Buffalo, NY 14214, USA. Tel.: +1 716 829 2969; fax: +1 716 829 2725.

E-mail address: gwillsky@buffalo.edu (G.R. Willsky).

<sup>1</sup> Present Address: Department of Chemistry, The University of Texas at Tyler, Tyler, TX, USA.

<sup>8</sup> Alejandro M. Trujillo contributed figure 1 & 10

Published in *Coordination Chemistry Reviews*, 2011, (255) 2258-2269.

Dipicolinate  
Dipicolinatooxovanadium(V)  
Diabetes  
Streptozotocin  
Redox  
Coordination number  
Cellular oxidation of vanadium  
Gene expression  
Signal transduction

on the insulin-enhancing properties was studied in both the Vdipic and VdipicCl series. Effects on blood glucose, body weight, serum lipids, alkaline phosphatase and aspartate transaminase were selectively monitored. Statistically distinct differences in activity were found, however, the trends observed were not the same in the Vdipic and VdipicCl series. Interperitoneal administration of the Vdipic series was used to compare the effect of administration mode. Correlations were observed for blood vanadium and plasma glucose levels after V5dipic treatment, but not after treatment with corresponding V4dipic and V3dipic complexes. Modifications of the aromatic ring structure with chloride, amine or hydroxyl groups had limited effects. Global gene expression was measured using Affymetrix oligonucleotide chips. All diabetic animals treated with hydroxyl substituted V5dipic (V5dipicOH) and some diabetic rats treated with vanadyl sulfate had normalized hyperlipidemia yet uncontrolled hyperglycemia and showed abnormal gene expression patterns. In contrast to the normal gene expression profiles previously reported for some diabetic rats treated with vanadyl sulfate, where both hyperlipidemia and hyperglycemia were normalized. Modification of the metal, changing the coordination chemistry to form a hydroxylamine ternary complex, had the most influence on the anti-diabetic action. Vanadium absorption into serum was determined by atomic absorption spectroscopy for selected vanadium complexes. Only diabetic rats treated with the ternary V5dipicOH hydroxylamine complex showed statistically significant increases in accumulation of vanadium into serum compared to diabetic rats treated with vanadyl sulfate. The chemistry and physical properties of the Vdipic complexes correlated with their anti-diabetic properties. Here, we propose that compound stability and ability to interact with cellular redox reactions are key components for the insulin-enhancing activity of vanadium compounds. Specifically, we found that the most overall effective anti-diabetic Vdipic compounds were obtained when the compound administered had an increased coordination number in the vanadium complex.

© 2011 Elsevier B.V. All rights reserved.

## 1. Introduction

### 1.1. Insulin-enhancing effects of V in rats with STZ-induced diabetes

The modern era of studying the anti-diabetic properties of vanadium (abbreviated here as V) was initiated in 1985 by John McNeill, who monitored the cardiac function of rats with streptozotocin (STZ)-induced diabetes after treatment with vanadyl sulfate [1]. Previously insulin-like effects of V salts in cell systems such as adipocytes had been reported [2]. The STZ diabetic rat model is widely used to study the *in vivo* effects of vanadium (abbreviated here as V) compounds. STZ-induced diabetes is considered a type 1 diabetic model since it arises from destruction of some, but not all, of the insulin-producing pancreatic  $\beta$  cells [3]. Rats with STZ-induced diabetes are not dependent upon insulin, and can survive for many months, even years, without any treatment. Interestingly many of the anti-diabetes effects of V treatment have been reported to last at least 3 months after the treatment has stopped [4]. In the biobreeding (BB) rat, an inbred rat strain that spontaneously develops type 1 diabetes, treatment with V lowers the amount of insulin needed for treatment, although it cannot completely substitute for insulin [5]. In a similar way, serum insulin levels lower after administration of V-containing compounds to normal rats. Therefore, the anti-diabetic effect of V compounds on STZ-diabetic rats, is believed to be that of an "insulin-enhancer" [6].

The effects of treatment with a wide variety of V compounds, including simple salts, have been studied in rats with STZ-induced diabetes. McNeill and co-workers have extensively studied the effects of many V complexes, focusing on BMOV and its derivatives [7,8]. These studies are of particular interest because BEOV, a close derivative, was selected for phase 1 and 2 clinical trials [7–9]. This selection was put forth once clinical studies using V-containing simple salts suggested the potential for success for using V in the treatment of diabetes [10–13]. The Sakurai group has also reported on a number of V picolinate complexes [14] and many other V(4)-containing complexes in multiple animal systems, including the STZ-diabetic rat [15]. Studies in the STZ-induced diabetic rat have been done using the dipicolinate series of V complexes by the Willsky and Ding groups [16–23]. The dipicolinate ligand is a tridentate ligand (Fig. 1), and thus, different than the bidentate ligands

(picolinate and malto) listed above. This series distinguishes itself from other V-containing systems because the most effective compounds have the vanadium in oxidation state 5. In contrast, the other V compounds are generally most effective with the V in oxidation state 4. This fundamental difference suggests that studies on compounds within this class could be informative when the focus is compound optimization. This review focuses on work by Willsky, Crans, Ding and their collaborators investigating the effects of Vdipic complexes in rats with STZ-induced diabetes. The reader is referred elsewhere for animal studies using other V compounds [9,14,24–27].

The STZ-induced diabetic outbred Wistar rat was chosen as the diabetic animal model by Willsky and co-workers due to its prevalent use in studies with V as described above. In the outbred Wistar rat model of STZ induced diabetes, there is variability in the response of the animals with respect to blood glucose (BG) [6,18]. The use of the Wistar outbred rat model, in part, accounts for the large deviations seen in the error bars for determination of blood and serum parameters in these experiments. In an effort to get a more uniform response, the Willsky lab has tried to study STZ-induced diabetes in various inbred rat models without finding a response to V to equal that of the outbred Wistar Rat. In addition to the published results with the inbred Wistar Kyoto and Wistar Furth strains [18], we have also looked at the Dahl, ACI, PVG, Buffalo, Lewis, Brown Norway, and F344 inbred rat strains (Willsky unpublished results).

The exact mechanism of the insulin-enhancing activity exerted by V compounds is not completely understood. These compounds are coordination complexes, and are inherently susceptible to hydrolysis (that is loss of metal also described as demetalation), such that the specific active species remains unclear. Administration of these V complexes is likely to result in loss of ligand, and extensive work has been carried out aimed at determining the active species [17,19,28–36]. Studies using BMOV and BEOV demonstrate that upon administration of the complex, the malto ligand separates from the metal ion, and transport proteins such as transferrin are likely to play key roles in the distribution of vanadium intracellularly [8,31,36–40]. Due to transmetalation reactions and cellular compartmentation it is likely that other ligands in addition to transferrin are involved in the biological effects of V compounds. Transmetalation reactions are commonly seen

with coordinated metal complexes where the tightly bound metal is transferred to other ligands, for example, as documented for gadolinium chelates [41]. Some studies have been performed using other vanadium complexes, such as in vivo observation of vanadium in the blood of an animal that had received the vanadium picolinate complex [24,29,42]. In summary, all these studies document that at some point, the vanadium complex decomposes after administration and that other complexes can form with cellular components.

Various mechanisms of action have been implicated in the anti-diabetic effects of V [7,8,12,43]. The most widely accepted mode of action for V compounds thus far is attributed to the inhibition of protein tyrosine phosphatases [44–48]. Some V compounds are reversible inhibitors, whereas others are irreversible by modifying the protein through redox processes [46]. Our group has proposed that interactions of V complexes with cellular oxidation–reduction processes is important in the anti-diabetic effects of V compounds [19]. V causes increases in ROS and RNS via multiple mechanisms [49,50]. Systematic studies such as those reviewed here are therefore important, allowing for evaluation of the observed effects when altering coordination geometry, ligand and oxidation state of the vanadium.

### 1.2. V dipicolinate complexes: rationale for use and introduction of complexes reviewed

The insulin-enhancing effects of V were examined using a range of different dipicolinate complexes. In these studies alterations to the coordination chemistry around the V, the ligand, and the oxidation state were made. The common feature in this work was to maintain the dipic ligand coordinated to the V. These studies have investigated V compounds with diverse chemical properties, oxidation state, stability, redox potential, and lipophilicity. The dipicolinate ligand was originally chosen because Vdipic complexes are potent inhibitors of phosphatases [51]. At that time, this was considered the primary mode of action for the anti-diabetic effects observed with these compounds. Furthermore, the chemistry of the V(5) complex was not well characterized [16,52,53]. Several Vdipic complexes have been reported, including the V(5) complex with one dipic ligand. Vdipic also forms with V(4) however, two complexes can be present in solution; one that possesses a single dipic ligand and another that contains two [19,54–56]. The crystalline material that has been structurally characterized and used for most studies is the 1:1 complex. Only trace amounts of the 1:2 complex forms under physiological conditions. As a result, it is not necessary to consider the 1:2 complex for use in biological studies. The V(3) complex, on the other hand, forms mainly a complex that has two dipic ligands coordinated to the V [19,54–56].

The dipic ligand is a potent metal chelator, but structural modification changes the effectiveness of the chelator, as evidenced from studies with different dipicolinate ligands [23,52,55,57,58]. In particular, the dipic ligand forms ternary complexes. Ternary complexes significantly change the electronic properties of the V complex [59,60]. In addition, it is a natural metabolite in humans, making it a very promising system for the study of the anti-diabetic effects.

The chemistry of V-picolinate derivatives and their insulin-enhancing effects in cells and animals had been described [61–63]. Sakurai and co-workers have studied ‘insulin-like’ effects in V complexes by extensive structure–function experiments [14] in part employing a cell model in which the release of free fatty acids (FFA) from adipocytes is monitored and also utilizing real time monitoring of V in the blood of living rats [62].

Redox properties of these V dipic complexes are irreversible in aqueous media [64] and (Crans et al. unpublished). Recently, studies using the parent complex have demonstrated, that this class of

compounds are readily dissolved in interfaces [65,66]. Additionally, it has been found that the dipic ligand itself follows this trend, which may be important to the action of these compounds [67].

The V dipic and dipicCl complexes and ligands used in the studies that are reviewed here are shown in Fig. 1. V5dipic is the parent complex, and was one of the most effective compounds examined [16,19]. The aromatic moiety of the dipic ligand was perturbed and resulted in studies with dipicOH [58], dipicCl [21,22], and dipicNH<sub>2</sub> [20]. The coordination chemistry of V was perturbed by addition of a hydroxylamine (HA) group to the metal. This modification with the dipicolinate derivatives was studied [20,59,60] and some of these compounds were selected for testing in animals. Specifically the complexes used were V5dipic(MeHA) and V5dipicOH(HA). The chemistry and pharmacology of a range of V compounds including Vdipic complexes have been described in recent books [68,69].

The animal work reviewed here was conducted by Willsky and Ding in separate, parallel, repeated experimental studies, in collaboration with Crans and McNeill [17–19,32,53,70]. In addition, previously unpublished results are included from the Willsky laboratory involving the anti-diabetic effects of treatment with the V5dipicOH complex with hydroxylamine modifications and the effects of treatment with V5dipicOH on global gene expression. These studies were carried out as part of a larger study and were presented at the V7 Conference in Toyama Japan in October of 2010.

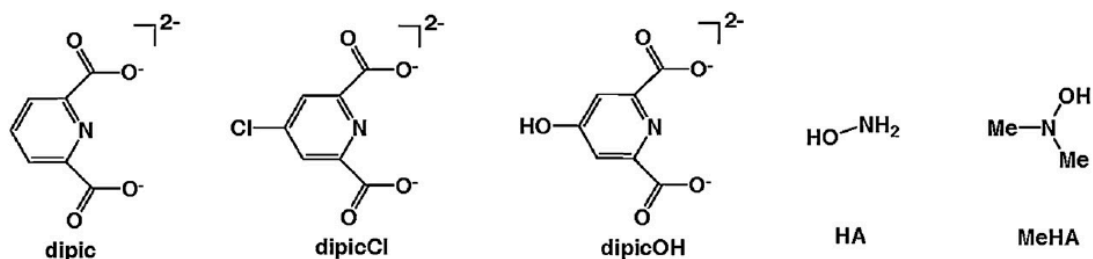
### 1.3. Effects of ligands and V5dipic on diabetic hyperglycemia, diabetic hyperlipidemia, and toxicity

The effect of treatment with V5dipic on BG in rats with STZ-induced diabetes has been previously reported [19] and is shown in Fig. 2. These results are compared with the effect of treatment with the simple salt VS, and treatment with the dipic and dipicOH ligands [18,19,32]. Lowering of BG upon V5dipic treatment yielded similar effects when compared to treatment with VS. Administration of the ligands (dipic and dipicOH) to diabetic rats did not cause a statistically significant difference in BG levels when compared to untreated diabetic animals. Lower BG levels were seen after treatment with dipic, while dipicOH treatment showed a tendency to raise BG. Treatment with another ligand, dipicCl, also raised BG levels (Fig. 5).

The effects of treatment with ligands and Vdipic complexes on diabetic hyperlipidemia was previously reported by Willsky and co-workers [19,58,71] and results are shown in Table 1. Treatment with dipic did not significantly lower serum lipid levels in diabetic animals, while treatment with dipicOH lowered diabetic hyperlipidemia. Note, treatment with the specific ligand showing a tendency to lower diabetic hyperglycemia did not lower diabetic hyperlipidemia, and vice versa. Administration of both the parent Vdipic complex (V5dipic) or simple salt (VS) significantly lowered diabetic hyperlipidemia. In another study, administration of another modified version of the dipic ligand, dipicCl [21,22], statistically lowered serum cholesterol (chol) with no effect on serum triglyceride TG (see below).

The toxicity of the ligands on the diabetic animals has been examined using weight loss, need for rehydration, elevated serum parameters such as alkaline phosphatase (ALP) and aspartate aminotransferase (AST) that are signs of liver dysfunction, and survival in various studies [21,22]. Animals treated with the ligand alone did not show any significant differences in the parameters observed in the diabetic animals. Treatment with most of the Vdipic complexes reported in these studies show some toxic effects while monitoring the parameters, and a few deaths did occur in a limited number of groups.

## LIGANDS:



## V-COMPLEXES:

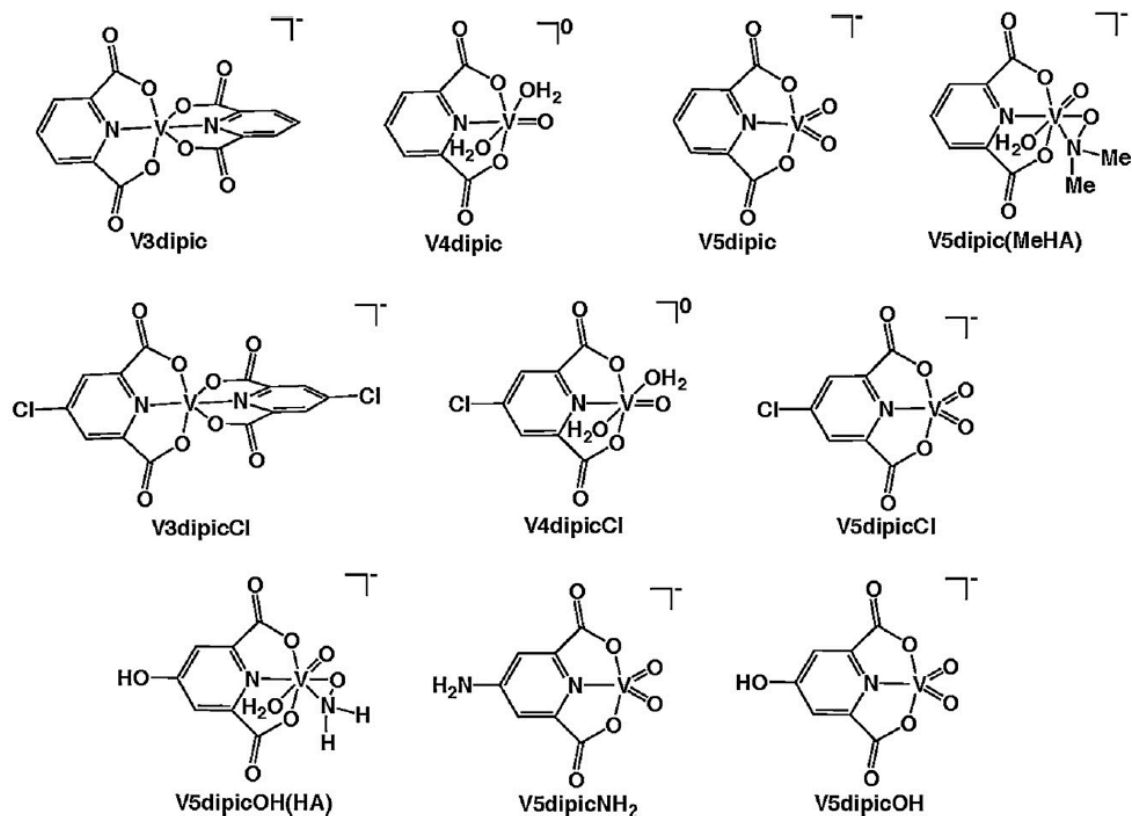


Fig. 1. Structures of compounds used.

## 2. Effect of oxidation state modification of Vdipic and VdipicCl complexes on insulin-enhancing activity

### 2.1. Effects of oxidation state modification of Vdipic on diabetic hyperglycemia, hyperlipidemia and absorption into serum.

Treatment of the diabetic rats with Vdipic complexes in the 3, 4 or 5 oxidation states lowered BG significantly after day 3 [19] and results are shown in Fig. 3. The BG lowering effect of administration of the Vdipic complexes may be additive with the non-statistically significant trend of treatment with dipic alone to lower BG (Fig. 2). Of the Vdipic complexes, only treatment with the V5dipic complex lowered BG significantly compared to treatment with the dipic ligand alone by ANOVA analysis. These results show that there are

oxidation state differences in the effect of treatment with Vdipic complexes in rats with STZ-induced diabetes.

The effects of varying the oxidation state on diabetic hyperlipidemia of the Vdipic complexes are seen in Table 1 [32]. Treatment with V3dipic, V4dipic, or V5dipic significantly lowered elevated TG, chol and FFA in the diabetic animals. Interestingly, the serum lipid levels for most of the treated diabetic rats were not statistically different from lipid levels observed in normal animals.

The effect of oxidation state on V absorption into serum was examined by comparing the dose ingested to the amount of V found in serum by atomic absorption (Table 2) [19]. In this analysis, only the animals treated with V4dipic showed a correlation of dose ingested to serum V using Spearman correlation analysis. Although the animals treated with VS and V3dipic showed Spear-

**Table 1**  
Effect of treatment with VS and V dipicolinic acid complexes on serum lipids in rats with STZ-induced diabetes.<sup>b</sup>

Treatment	n	TG (mg/dl)	Chol (mg/dl)	FFA (mg/dl)
Normal (N) <sup>a</sup>	18	134 ± 15.3***	78 ± 3.8***	78 ± 3.8***
N-VS <sup>a</sup>	15	111 ± 11.8***	80 ± 4.2***	80 ± 4.2***
Diabetic (D) <sup>a</sup>	32	1427 ± 124.2###	219 ± 15.0###	219 ± 15.0###
D-oral VS R <sup>a</sup>	5	173 ± 12.9***	79 ± 6.0***	79 ± 6.0***
D-oral VS NR	7	239 ± 51 (3)*, #	91 ± 5.7 (3)*	91 ± 5.7 (3)*
D-VS	27	245 ± 33***	104 ± 8***	104 ± 8***
D-V3dipic <sup>a</sup>	8	154 ± 22***	114 ± 5***	114 ± 5***
D-V4dipic <sup>a</sup>	5	121 ± 12.7***	101 ± 5.8***	101 ± 5.8***
D-V5dipic <sup>a</sup>	5	161 ± 20.5***	92.5 ± 5.77***	92.5 ± 5.77***
D-V5dipicOH <sup>a</sup>	12	76.7 ± 20.5***	97.5 ± 4.31***	97.5 ± 4.31***
D-V5dipicOH(HA)	5	141 ± 20***	106 ± 4.3***	106 ± 4.3***
D-V5dipic(MeHA)	5	1755 ± 483###	195 ± 21.3###	195 ± 21.3###

<sup>a</sup> Data previously published [19,59].

<sup>b</sup> Symbols used: \* significance compared to D, # significance compared to N one symbol  $p < 0.05$ , two symbols  $p < 0.01$ , three symbols  $p < 0.001$ .

**Table 2**  
Effect of treatment with VS and V dipicolinate acid complexes on V absorption into serum.

Treatment group	n	Average dose <sup>a,b</sup> (mmolV/kg/day)	Average serum V <sup>a</sup> (nmol/ml)	Spearman correlation of average dose to serum V (p-value)	Ratio of serum V to average dose <sup>a,b</sup>
D-VS <sup>c</sup>	13	0.95 ± 0.14 <sup>#</sup>	11.5 ± 1.1	0.544 (p=0.055)	13.6 ± 1.3###
D-V3dipic <sup>c</sup>	8	1.25 ± 0.04###	11.3 ± 1.0	0.690 (p=0.058)	9.0 ± 0.7###
D-V4dipic <sup>c</sup>	7	0.60 ± 0.08	13.2 ± 0.9	0.821 (p=0.023)	23.0 ± 1.4
D-V5dipic <sup>c</sup>	4	0.51 ± 0.09	14.3 ± 3.4	0.800 (p=0.200)	26.4 ± 4.0
D-V5dipicOH	8	1.03 ± 0.03##	24.2 ± 1.5***###	0.262 (p=0.531)	23.6 ± 1.4
D-V5dipicOH(HA)	7	0.64 ± 0.08	18.4 ± 1.8**	0.714 (p=0.071)	31.0 ± 3.9***
D-V5dipic(MeHA)	7	0.54 ± 0.04	10.1 ± 0.4	-0.286 (p=0.535)	19.4 ± 1.8 <sup>#</sup>
N-VS	7	0.48 ± 0.05*	14.2 ± 1.0	-0.577 (p=0.175)	32.9 ± 5.3***

<sup>#</sup>  $p \leq 0.05$ , <sup>\*\*</sup>  $p \leq 0.01$ , <sup>\*\*\*</sup>  $p \leq 0.001$  compared to N-VS.

<sup>a</sup> Symbols \*  $p \leq 0.05$ , \*\*  $p \leq 0.01$ , and \*\*\*  $p \leq 0.001$  compared to D-VS.

<sup>b</sup> Average dose was calculated for end of the experiment from days 16 to 28.

<sup>c</sup> Data previously published [19].

man correlation values close to significance  $p = (0.055$  and  $0.058$  respectively), the relationship of serum V to dose ingested for animals taking V5dipic was clearly not correlated ( $p = 0.20$ ). Since the V complexes were present in the drinking water and all animals did not drink the same amount of V, the results for the amount of V in the serum was normalized to the dose ingested. Diabetic animals dosed with VS or V3dipic had significantly lowered ratios for serum

V to average dose ingested compared to that seen in the normal animal dosed with VS. Treatment of diabetic rats with VS, one of the well studied anti-diabetic V compounds, resulted in significantly less V per dose ingested to be found in serum compared to that seen in Normal animals treated with VS. This is another example of the differences in metabolism and response to V of normal and diabetic animals.

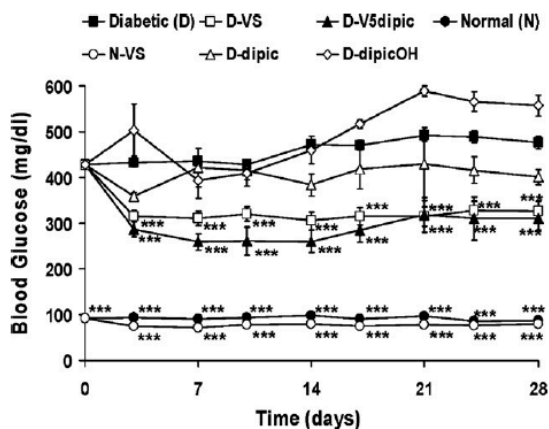


**Fig. 2.** Effect of oral chronic administration of V5dipic and dipic ligands on BG in rats with STZ-induced diabetes. Normal untreated (N, ●); Diabetic untreated (D, ■); N treated with VS (○), D treated with VS (□); D treated with dipic(△), D treated with dipicOH (◇), D treated with V5dipic (▲). Data redrawn from [18,19,32]. Data analyzed by one-way ANOVA with multiple means testing.\*\*\* represents  $p < .001$  vs diabetic rats.

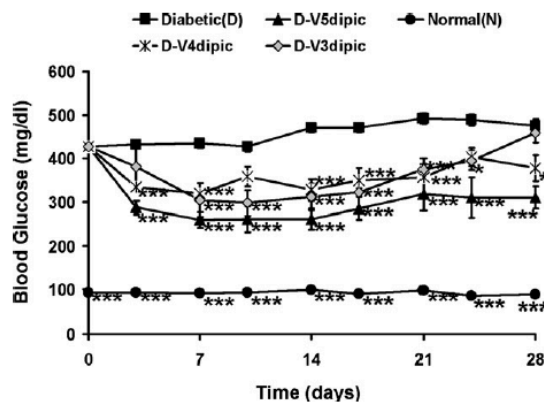


**Fig. 3.** Effect of oral chronic administration of V3dipic, V4dipic, or V5dipic on BG in rats with STZ-induced diabetes. Normal untreated (N, ●); Diabetic untreated (D, ■); D treated with V3dipic (◇); D treated with V4dipic (×); D treated with V5dipic (▲). The data for 14 days of treatment were previously published [19] and have been extended to 28 days. Data analyzed by one-way ANOVA with multiple means testing \*\*\* represents  $p < .001$  vs diabetic rats.

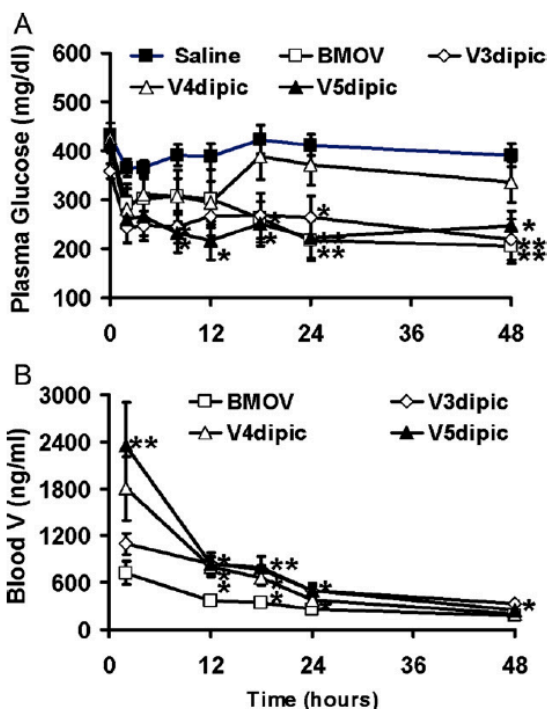


**Fig. 4.** Effect of acute interperitoneal administration of V3dipic, V4dipic, or V5dipic on plasma glucose in rats with STZ-induced diabetes. (A) Plasma glucose levels. Diabetic rats treated with saline (■), BMOV (□), V3dipic (◇), V4dipic (△), V5dipic (▲). (B) Blood Total V levels as determined by atomic absorption spectrometry. BMOV (□), V3dipic (◇), V4dipic (△), V5dipic (▲). Data redrawn from previous publication [32]. Data analyzed by one-way ANOVA with multiple means testing. \*\* represents  $p < .01$  vs diabetic rats.

## 2.2. Effects of mode of administration on the anti-diabetic effect of V3dipic, V4dipic, and V5dipic

When complexes are chronically administered orally they experience changing environments and pH before they enter the cells of the gastrointestinal tract and are distributed into serum and tissues. The effects of passage through the gastrointestinal system can be avoided if the therapeutic agent is administered either into the peritoneal cavity or intravenously. The effects of intraperitoneal administration of a single dose of V3dipic, V4dipic, or V5dipic were examined in the McNeill laboratory (Fig. 4) [32]. To differentiate this type of treatment from chronically administration in the drinking water; we are calling the one time ip injection mode of administration acute treatment. The oxidation state of the Vdipic complexes showed differential effects in this system with respect to lowering of diabetic hyperglycemia. In these acute treatment experiments, treatment with V3dipic and V5dipic maintained lowered diabetic hyperglycemia for 48 h, while treatment with V4dipic showed only a transient 12 h ability to slightly lower blood glucose (Fig. 4a).

The amount of V in the blood was determined as a function of time in an acute administration experiment (Fig. 4b). The concentration of V in blood over time was modeled using a one- or two-compartment model using the data shown in Fig. 4b. Data gathered for V4dipic, V5dipic and the control, BMOV, fit a two-compartment model. Data obtained after treatment with V3dipic fit to a one-compartment model. Correlations between blood V and plasma glucose levels were also obtained in this experiment [32]. A significant correlation ( $0.777 R^2$ ) was only seen for animals

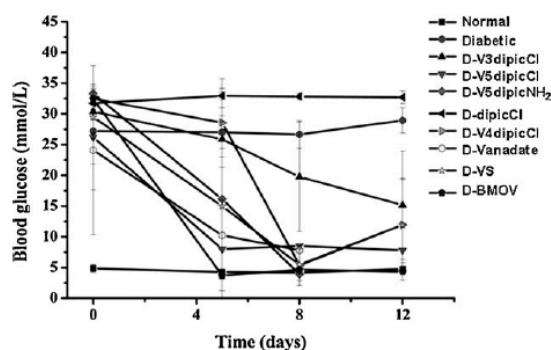


**Fig. 5.** Effect of oral chronic administration of V3dipicCl, V4dipicCl, V5dipicCl, V5dipicNH<sub>2</sub>, BMOV, VS, and vanadate on BG levels in normal rats and rats with STZ-induced diabetes. Data analyzed by one-way ANOVA with multiple means testing. Symbols for treatment group indicated in figure. Data redrawn from previous publications [21,22].

given V5dipic. However, both V3dipic and V5dipic were equally effective at lowering BG. The results reported here demonstrate that although different, there are oxidation state differences in the ability to lower diabetic hyperglycemia when the V3dipic, V4dipic or V5dipic complexes are administered either orally or intraperitoneally. These results would imply that there are significant changes to the V complex while it passes through the gastrointestinal tract affecting anti-diabetic efficacy.

## 2.3. Effects of oxidation state modification of VdipicCl complexes on diabetic hyperglycemia, hyperlipidemia, and serum metabolites

The effect of oxidation state in the Vdipic series was additionally examined using the dipicCl ligand. In this form of the ligand, the chlorine changes the electron density in the dipic ring. The dipicCl ligand alone showed a non-statistically significant trend to further raise diabetic hyperglycemia in rats [21,22] as shown in Fig. 5. Treatment with dipicCl did statistically significantly lower serum TG, but not serum cholesterol (Table 3), and did significantly lower the pathologically raised diabetic serum AST and ALP.

Treatment with the V3dipicCl, V4dipicCl or V5dipicCl complexes did show oxidation state differences. Administration of any of these three complexes caused lowered diabetic hyperglycemia by day 8. However, at day 5, significantly lowered BG was only seen after treatment with V5dipicCl (Fig. 5). Treatment with all three complexes lowered the elevated chol levels in the diabetic rats, while treatment with only V4dipicCl or V5dipicCl lowered the elevated TG levels (Table 3). Additionally, treatment with V4dipicCl or V5dipicCl significantly lowered AST from elevated diabetic levels in the animals. Treatment with all VdipicCl complexes lowered the elevated serum ALP. The oxidation state differences observed in the treatment of diabetic rats with the dipicCl series was different from those observed in treatment with the dipic series.

## 3. Insulin-enhancing effects of V5dipic with OH modification of ligand and amine coordination at the metal

### 3.1. Effects on diabetic hyperglycemia, diabetic hyperlipidemia and absorption into serum when the V5dipic complex is modified with OH and hydroxylamine is coordinated to the V

The aromatic ring of the V5dipic complex was first substituted with hydroxyl group in the para position altering the electronic properties of the complex. The effect of changing the coordination geometry around the V atom was done using the V5dipicOH com-

**Table 3**  
Effects of treatment with V3dipicCl, V4dipicCl, V5dipicCl, dipicCl ligand and V5dipicNH<sub>2</sub> on serum biochemical parameters in rats with STZ-induced diabetes.<sup>a</sup>

Group	Chol (mg/dl)	TG (mg/dl)	AST (U/l)	ALP (U/l)
Normal control	1.44 ± 0.29*	0.67 ± 0.21	216 ± 33	63 ± 7** ##
Diabetic	2.04 ± 0.42	0.94 ± 0.09	257 ± 133##	747 ± 326###
DipicCl	1.54 ± 0.12	0.90 ± 0.19	147 ± 14**	356 ± 146***
V3dipicCl	1.38 ± 0.36	0.75 ± 0.32	200 ± 46	358 ± 130**
V4dipicCl	1.25 ± 0.38*	0.54 ± 0.30* #	146 ± 17**	270 ± 84***
V5dipicCl	0.96 ± 0.36*	0.36 ± 0.3* #	170 ± 44*	212 ± 53***
V5dipicNH <sub>2</sub> <sup>b</sup>	1.10 ± 0.22*	0.47 ± 0.28	166 ± 27	223 ± 113

Values are expressed as the mean ± SD. N = 5–6, \**p* < 0.05, \*\**p* < 0.01 and \*\*\**p* < 0.001 vs diabetic. #*p* < 0.05, ##*p* < 0.01 and ###*p* < 0.001 vs dipicCl group.

<sup>a</sup> Parameters measured were total serum cholesterol (Chol), triglycerides (TG), aspartate aminotransferase (AST), and alkaline phosphatase (ASP).

<sup>b</sup> Data published separately [21] was not part of the statistical analysis of the rest of the data [22].

plex, which was the first V5dipic complex for which the details of the insulin-enhancing effects of the V5dipicOH complex were reported [18]. The coordination number of the V5dipic complex was increased to 7 by the addition of a dimethyl hydroxylamido group to the V complex [V5dipic(MeHA)]. The effects of coordinating the hydroxylamine to both parent complexes V5dipic and V5dipicOH has been described in detail [58].

The effect of administration of these hydroxylamine complexes on BG in Wistar rats with STZ-induced diabetes is shown in Fig. 6 (unpublished). The coordination of dimethyl hydroxylamine to the V5dipic interfered with the ability of the V5dipic complex to significantly lower BG when administered to diabetic rats. Previously it was shown that treatment with V5dipicOH was effective in lowering BG for the first two weeks of the experiment. However, BG values returned to those of the untreated diabetic control by the end of the experiment at 4 weeks. The effective time period for BG normalization in this animal model is very dependent upon the specific V compound used. In fact, treatment with BMOV showed that the BG lowering effect has been reported to continue for months after treatment was terminated [6]. In an attempt to lengthen the time of effectiveness of the dipic series, V5dipicOH was complexed to a hydroxylamine group, which improved the BG lowering effect at the end of the experimental time period. Treatment with V5dipicOH(HA) caused the lowered BG level to be maintained throughout the one month experiment. None of these modifications produced a complex that was more effective at lowering of BG than the parent, V5dipic. The effect of treatment with the complex with an addition of an amino group at the para position was also studied. In Fig. 5 it can be seen that the NH<sub>2</sub> substitution on the dipic ligand resulted in a V5dipicNH<sub>2</sub> complex that when adminis-

tered also significantly lowered diabetic hyperglycemia to similar levels as VS administration [22].

The effects of treatment with hydroxylamine modified V5dipic and V5dipicOH complexes on diabetic hyperlipidemia were monitored by measuring serum TG, chol and FFA (Table 1). All of the measured lipids were significantly lowered by administration of all of these V5dipic complexes. While V5dipicOH was the most effective complex at lowering the elevated TG levels associated with diabetes, administration of V5dipicNH<sub>2</sub> also significantly lowered serum chol and serum TG (Table 3)[22]. The V5dipic(MeHA) lowered serum TGs to normal levels, while the ternary complexes of V5dipic and V5dipicOH formed by addition of hydroxylamine were more effective at lowering FFAs than the five-coordinate complexes. The coordination of HA to the metal appears to have increased the ability of treatment with the V5dipic or V5dipicOH complexes to lower diabetic hyperlipidemia. Overall, the V5dipicOH(HA) was the best complex with respect to lowering serum lipids after treatment since it was the only complex that lowered both serum TG and FFA to normal levels.

The absorption into serum was measured and compared to the dose of V ingested by the animals treated with hydroxylamine modified Vdipic complexes. These results were compared to those seen in diabetic animals treated with VS or Vdipic complexes with differing oxidation states as described in Section 2.1 (Table 2). As discussed before the ratio of the serum V to the average ingested dose of V is the best measure of absorption into serum when the animals are dosed with vanadium complexes in the drinking water. Of the new complexes studied (V5dipicOH, V5dipicOH(HA) and V5dipic(MeHA)), animals treated with V5dipicOH accumulated the most V in serum of any in this study and significantly more than both the Normal animals and Diabetic animals treated with VS. However, these animals also ingested much more V, so the ratio of serum V to dose ingested was not significantly different from that seen with these two other groups. Animals dosed with V5dipicOH(HA) accumulated significantly more V into serum than the D animals treated with VS and the statistical significance of this was also observed when the ratio of serum V to dose is used as the metric. In the diabetic animals treated with V5dipic(MeHA) the ratio of serum V to average dose was significantly lower than that seen with normal animals treated with VS but not significantly higher than the ratio seen with diabetic animals treated with VS. Limiting the comparisons to the diabetic animals only the V5dipicOH(HA) significantly increased the absorption of V into serum with a 2.3 fold increase being observed in the ratio.

### 3.2. The effects on global gene expression of treatment with V5dipicOH and VS

Treating outbred Wistar rats with STZ-induced diabetes with the simple salt VS results in approximately 60% of the animals responding with both lowered diabetic hyperglycemia and hyperlipidemia. VS treated diabetic rats that responded to treatment with both low-

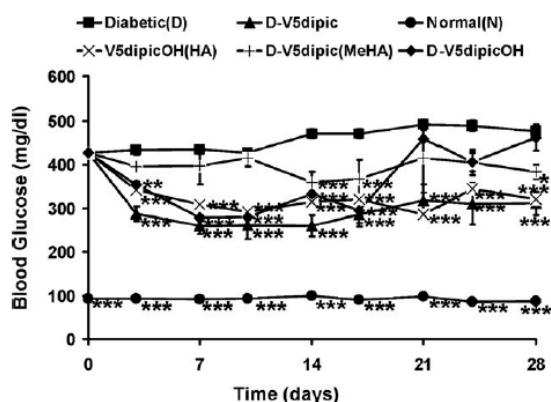


**Fig. 6.** Effect of oral chronic administration of hydroxylamine coordinated to V5dipic and V5dipicOH on BG levels in rats with STZ-induced diabetes. Data obtained as described in previous publications [18,19,32]. N (●), D (■), V5dipic (▲), V5dipic(MeHA) (+), V5dipicOH (◆), V5dipicOH(HA) (X). Data analyzed by one-way ANOVA with multiple means testing. \*\*\* represents *p* < 0.001 vs diabetic rats.

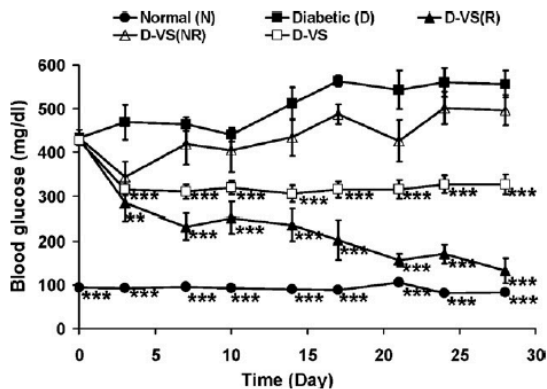


Fig. 7. Effect of oral chronic administration of VS on rats with STZ-induced diabetes. Parts of this figure has been previously published [71]. N (●), D (■), D-VS(R) responding with lowered BG and lowered Lipids (▲), D-VS not responding (NR) with lowered BG and but showing lowered Lipids (△), D-VS all responses of animals treated with VS (□). Data analyzed by one-way ANOVA with multiple means testing. \*\* represents  $p < 0.01$  and \*\*\* represents  $p < 0.001$  vs diabetic rats.

ered hyperlipidemia and hyperglycemia were originally selected for gene expression profiling studies. An Affymetrix rat chip with approximately 8000 probe sets was used to study gene expression in normal and diabetic animals in the presence and absence of VS treatment [71]. The Affymetrix probe sets used were sets of 16 short oligonucleotides specifically designed to monitor the expression of a single gene as monitored by various algorithms. An important conclusion of that earlier study was that in a two way ANOVA analysis (using diabetes and treatment as variables) of the 5100 probe sets that were expressed in any of our experimental conditions showed a statistically significant interaction. This result confirms what has been observed in individual assays that V treatment affects normal and diabetic animals differently. The response of the diabetic rats to VS when only hyperlipidemia and not hyperglycemia was controlled was similar to that observed for the diabetic rats treated with V5dipicOH (Fig. 6 and Table 1). In order to see the effect of the dipicOH ligand on global gene expression we extended our previous gene expression study to include data from these two new treatment groups which had not previously been published.

In our previous work 66 probe sets altered in diabetes and restored to normal levels in diabetic animals treated with VS in which both hyperlipidemia and hyperglycemia were controlled were identified. We now examined the expression of these same probe sets in the animals treated with VS with elevated BG levels and normalized hyperlipidemia (VS NR Table 1 and Fig. 7) and those treated with V5dipicOH as illustrated in Fig. 8. In this experiment each column represents data from one rat and there are five rats in each group. The expression data in each row are normalized to the median value seen in the normal control group. The pattern of gene expression obtained in Fig. 8 for the diabetic rats treated with VS who responded with lowered BG and lowered lipid levels resembles the expression pattern seen for the normal rats more than that of the diabetic rats. Interestingly the pattern of gene expression seen in the normal animals treated with VS shows a resemblance to that seen in diabetic animals, especially for the down regulated genes. The expression pattern seen with the rats treated with VS or V5dipicOH in which BG remained high and only the lipids were lowered resembled the diabetic gene expression pattern for this set of both up regulated and down regulated genes.

The number of probe sets differentially expressed when comparing the expression in three treated groups to that observed in the normal and diabetic animals was then examined (Table 4)

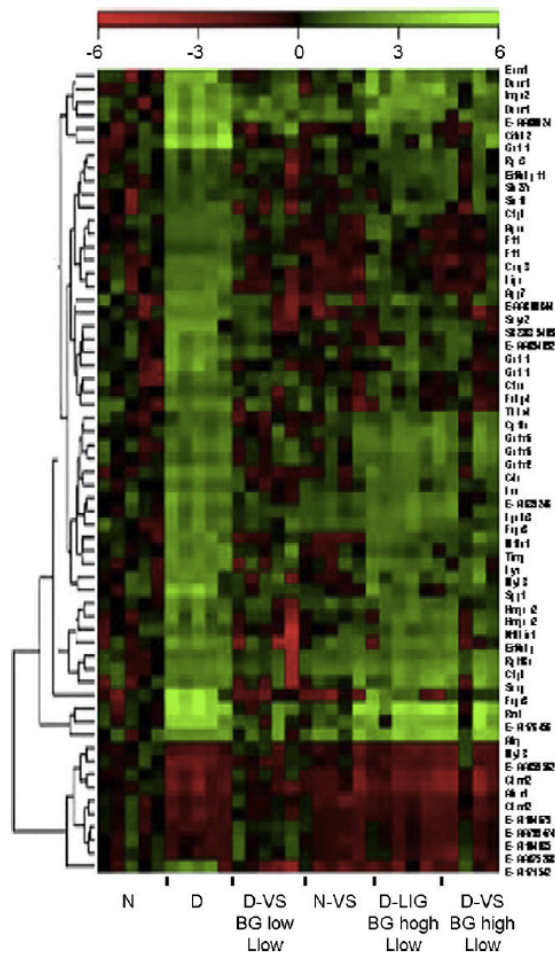


Fig. 8. Heatmap for the 62 probe sets selected as being both altered by diabetes and corrected by oral administration of VS. The expression of each individual gene is compared with that of the median of the N group, represented by black in the group of arrays for the N rats. The intensity of the color indicates the variability of the expression of that probe set in the group. Data from N and D untreated and treated with VS (where the treated rats showed lowered diabetic hyperlipidemia and hyperglycemia (D-VS BG low L low) have previously been published [71]. New data for D animals treated with VS in which only lipids were lowered (D-VS BG high, L low) and D animals treated with the liganded V5dipicOH (D-Lig BG high, L low).

for all of the 5100 genes showing some expression changes in the overall study. In comparisons of gene expression in diabetic animals with gene expression in VS treated diabetic groups and the V5dipicOH treated diabetic animals, hundreds of differentially

Table 4  
Comparisons of gene expression in diabetic rats treated with VS and V5dipicOH.<sup>a</sup>

Group	Number of probe sets expressed compared to untreated diabetic <sup>b</sup>	Number of probe sets expressed compared to untreated normal <sup>b</sup>
VS-BG low, lipid low <sup>b</sup>	523	33
VS-BG high, lipid low	476	516
V5dipic-BG high, lipid low	274	460

<sup>a</sup> Experimental methods for animal treatment, RNA extraction, and analysis with Affymetrix Rat Chip U34 described in Willisky et al. (2006) Physiological Genomics [71]. Probe sets identified by standard *t* test comparisons with False Discovery Rate of 0.05 using Affymetrix expression data.

<sup>b</sup> Data for this group previously published [71].

expressed probe sets were identified (first column, Table 4). Hundreds of differentially expressed genes were identified when gene expression in both the VS treated diabetics with high BG and low lipids and the V5dipicOH treated diabetic animals were compared to gene expression in normal animals (second column, Table 4). In contrast, when gene expression in the VS treated diabetics in which BG and serum lipids were lowered was compared to normal gene expression, only 33 differentially expressed probe sets were identified. Identification of 33 genes in this type of experiment is similar to a baseline measurement. These results imply that the changes in gene expression seen when diabetic hyperlipidemia and hyperglycemia are alleviated by V treatment returns gene expression to normal. However, the changes in gene expression when only diabetic hyperlipidemia is returned to normal are mediated via changes that do not involve a return to normal gene expression.

Gene expression data from Wistar rats classified as normal, diabetic, diabetic treated with vanadate, and diabetic treated with insulin have been obtained using the 96 genes on the GE Array for the insulin pathway [72]. Although the expression of most of the diabetes altered genes were returned to normal levels with VS and insulin treatment, expression patterns were not identical. This result is in agreement with data for mice with STZ-induced diabetes treated with VS or insulin using the Affymetrix array [73]. In addition, the identified probe sets with altered gene expression found in this mouse experiment using the Affymetrix chip [73] with VS treatment were very similar to those reported described above for the rat Affymetrix experiment using VS treatment [71].

#### 4. Interpretations of the observed effects of the Vdipic complexes used as treatment in STZ-induced diabetic rats

##### 4.1. Summary of the insulin-enhancing effects seen in administration of Vdipic complexes to diabetic rats and toxicity implications

Substitution to the 4-position of the dipic ligand in the Vdipic complexes screened had a limited effect on insulin-enhancement. When the OH or NH<sub>2</sub> functionalities perturbed the aromatic ring of the V5dipic complex, chronic administration did not significantly improve insulin-enhancement, as a matter of fact the BG lowering effect on diabetic hyperglycemia was reduced when V5dipicOH was used [18,22]. Administration of the ternary complex formed upon hydroxylamine coordination to the V improved the normalization effect on hyperlipidemia when compared to both V5dipic and V5dipicOH (Fig. 6. and Table 1). Complexation of the HA moiety to V5dipicOH extended the BG lowering effects on diabetic hyperglycemia to the end of the treatment period.

Differing results were also seen in the oxidation state series for both Vdipic [19] and VdipicCl [21]. Although there are significantly different changes after treatment of diabetic rats with Vdipic or VdipicCl complexes in oxidation states III, IV, or V; there is no statistically significant linear relationship of oxidation state and diabetic hyperglycemic (Figs. 3 and 5) or hyperlipidemic (Tables 1 and 3) effects. In the VdipicCl oxidation state series, treatment with V5dipicCl showed greater effectiveness than administration of V3dipicCl or V4dipicCl at normalizing diabetic hyperglycemia in the earlier timepoints, while all were equally effective after 12 days. A linear trend with oxidation state in the effectiveness at lowering diabetic hyperlipidemia was observed with the VdipicCl complexes. Treatment with V5dipicCl also was the most effective at normalizing elevated chol and TG levels in the diabetic animals.

In the chronic administration model [47] the Vdipic oxidation state series showed a trend in effectiveness (V5 > V4 > V3) for the treatment of diabetic hyperglycemia (Fig. 3). However, in the

acute model [32] V3dipic and V5dipic effectively lowered BG while V4dipic did not (Fig. 4). Since the administration routes of the complexes were different it is possible that the modification of efficacy is due to increased interactions with metabolites when the complex passes through the gastrointestinal tract. Interactions with other ligands, and possibly also with membranes within the animal, during the treatment process could also contribute to the results observed.

Of all the Vdipic complexes studied, treatment with V5dipic, V5dipicCl, V5dipicOH(HA) and V5dipicNH<sub>2</sub> appeared to alleviate most of the diabetic symptoms in our studies. V5dipic appears to normalize diabetic hyperglycemia to the greatest extent of the complexes examined. The hydroxylamine V complexes appeared to be most effective at normalizing diabetic hyperlipidemia. Currently we have only performed a two-week experiment with the V5dipicNH<sub>2</sub> and no data on absorption into serum is available for this complex. The V5dipicOH(HA) was the only Vdipic complex that accumulated more V into serum compared to VS after doses were normalized (Table 2). One could speculate that addition of HA to V5dipicNH<sub>2</sub> would further improve alleviation of diabetic symptoms.

It is encouraging to see a correlation between V in blood and dose for the complexes VS, V5dipic and V5dipicOH(HA) in chronic studies. However, corresponding studies are lacking for the other V complexes explored here. An inverse Spearman correlation of  $-0.488$  ( $p < 0.05$ ,  $n = 19$ ) was seen for BG and serum V when Vdipic in all oxidation states was administered using the data presented here in Fig. 3 and Table 2. An inverse Spearman correlation of  $-0.503$  ( $p < 0.05$ ,  $n = 22$ ) for serum V and cholesterol in animals treated with the V5dipic complexes described in Tables 1 and 2. Additional correlations are expected for V and metabolite markers in serum however such analyses would require additional animal samples. Treatment with V5dipic complex resulted in a correlation between V levels in blood, and BG levels in plasma using the acute administration protocol [32]. These results are consistent with the concept that the blood/serum compartment or another biological compartment in equilibrium with these is important in the anti-diabetic properties of the Vdipic complexes in this animal model.

The toxic effects of administration of the Vdipic complexes and their derivatives varied from minimal to significant morbidity and mortality (Section 1.3). Short term human clinical trials with vanadium salts have been completed with minimal toxicity observed [12,73]. Phase 1 and phase 2 clinical trials with BEOV [7,8], the first V coordination complex to be used in human studies, have concluded; and kidney toxicity has been reported in the phase 2 trial [74]. Therefore a brief discussion of how the results reported here relate to other rodent and human studies with V is warranted.

Worker exposure to excess vanadium has largely resulted from inhalation of vanadium pentoxide in workplace dust [75]. Respiratory effects predominate, but many organ systems can demonstrate adverse effects [76]. Non-occupational vanadium exposure is predominantly from the food supply and typical daily doses consumed by humans have been estimated at 0.01–0.03 mg V/day. Normal serum levels range from 0.02 to 0.9 ng V/ml [77]. Chronic one year oral exposure studies in rats indicate that doses as high as 19 mg V/kg/day as vanadyl sulfate in the drinking water caused no hematological or pathological effects, and a dose of 28 mg V/kg/day led to a small decrease in body weight gain [78–81]. Similarly, lifetime studies in rats and mice showed no adverse effects at doses of up to 4.1 mg V/kg/day [82,83].

One reason for the ability of animals to tolerate chronic exposures to high dose rates of vanadium is the poor absorption of vanadium salts in the GI tract. Less than 1% of the ingested vanadium is typically absorbed by this route of exposure. Although there may be higher absorption rates for various complexes of vanadium as indicated by the serum to dose rate ratios in Table 2, the mag-

nitude of the differences in absorption are within a factor of 2–3 when compared to VS. Dissociation of vanadium from the complex is likely necessary for both its toxicological and insulin-like effects. In addition, there may be compound specific differential distributions of vanadium to tissues, which may depend on the physico-chemical properties of each compound, and on the rate of release of V from each compound in body fluids and tissues. Additional studies are necessary to assess tissue specific pharmacokinetic parameters for individual vanadium complexes, and their role in producing adverse effects.

#### 4.2. Chemical stability and electrochemistry/catalytic studies of the V5dipic complexes with anti-diabetic effects

The chemistry and properties of a range of dipic-complexes have been studied in detail by our group [16–18,20–23,32,53,55,58–60,65,70,84–90]. Small changes in the properties of Vdipic complexes manifest themselves as changes in stability, redox properties and solubility. Our objective here was to associate these differences, with the observed effects of modified Vdipic complexes on insulin-enhancement. Formation of the V5dipic complexes can be determined using NMR spectroscopy, however, formation of V4 and V3dipic complexes must involve alternative methods, such as EPR and UV–vis spectroscopy. Although many excellent studies have been carried out on a range of V complexes with other ligands [16,25,26,68,69], less has been done with V4 and V3dipic complexes [17,19,54–56]. For V5dipic and the substituted complexes, the stability maximum is around pH 3.4. Because the  $pK_a$  for H<sub>2</sub>dipic is 4.49 [16,52,53] this observation is not due to the chemistry of the ligand, but due to the chemistry of V(5) in the aqueous solution. Below pH 3.4, complex formation is less pronounced because monomeric vanadate concentration is low. Above pH 3.4, less V5dipic complex is observed because of a combination of V(5) chemistry and dipic deprotonating, forming the dianion ligand species. Perturbation of the dipic ring with both electron donating and withdrawing substituents lowers complex stability. These changes trace with the trend of lowered effectiveness as insulin-enhancing agents. It is interesting that in the Vdipic complexes, as in the case of the BMOV–BEOV series, the parent and unsubstituted system is the most effective [7].

The stability of dipicolinate complexes are pH dependent as is illustrated in Fig. 9 for the [VO(dipic)(MeHNO)(H<sub>2</sub>O)]. A large and a small signal is shown from pH 2.2 to 5.2 reflect the two different isomers of this asymmetric hydroxylamine. Above pH 6.1 the complex is beginning to hydrolyze to form vanadates and the oxovanadium hydroxylamine complex. The effect of substituent perturbation is shown in Fig. 10 where the amount of intact V5dipicX is plotted as a function of pH [20,23,53,55,58]. As shown in Fig. 10 V5dipic, V5dipicOH, V5dipicNH<sub>2</sub>, V5dipicCl, and V5dipicNO<sub>2</sub> have stability maxima near pH 3.4. The V5dipic complex is the most stable over the tested pH range. Of particular interest to biology, V5dipic is also the most stable complex at physiological pH ranges. Interestingly, when X = OH, NH<sub>2</sub>, NO<sub>2</sub> or Cl, the resulting V complexes are less stable than V5dipic [20,23,55,58]. The higher relative stability of V5dipic presumably arises due to counteracting electronic effects created by the substituents reducing the chelating abilities of the modified ligands. Binding affinity reduction would result in the stability of monomeric vanadate becoming more favorable over complex formation. Since the parent version of the ligand creates the Vdipic complex possessing the greatest insulin-enhancement effect in animals, these properties correlate well with the chelating effect of the dipic ligand.

Coordination of the hydroxylamine (HA) ligand to the V atom forms a ternary complex which significantly changes the properties of the V complexes [20,60,91,92]. Although this ligand can rapidly

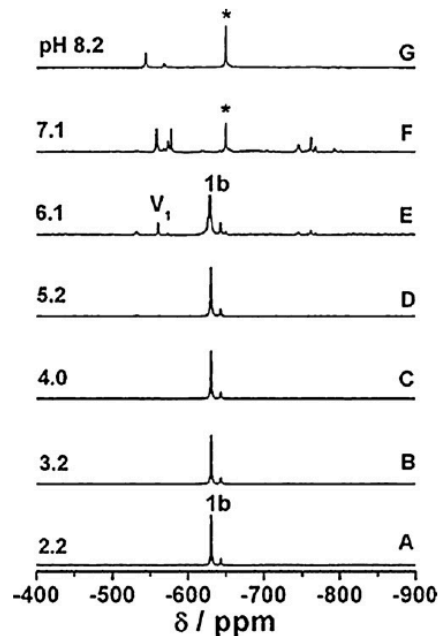


Fig. 9. The <sup>51</sup>V NMR spectra of [VO(dipic)(MeHNO)(H<sub>2</sub>O)] recorded as the pH was varied from 2 to 8 (A–G). Each spectrum was recorded from a separate sample with an initial concentration of 2 mM complex. Monomeric vanadate and the predominant hydroxylamido:V species are labeled as V1 and \*, respectively. Figure reproduced from Smee et al. [20] with permission.

dissociate in hydrophobic environments, the presence of HA significantly stabilizes the complex. However, reductions have been reported during Vdipic chelation to HA [20,23]. Subtle variations in the HA structure have a profound effect on the electronic properties exhibited by V and are readily observed by <sup>51</sup>V NMR chemical shifts. For the V5dipicOH complex a chemical shift of –534 ppm is observed, while –605 ppm is found for V5dipicOH(MeHA) and –671 ppm for V5dipicNO<sub>2</sub>(HA) [20]. For V5dipicCl(HA) a chemical shift of –679 ppm was observed, while –630 ppm is found for V5dipicCl(MeHA), –604 ppm for V5dipicCl(Me<sub>2</sub>HA) and –594 ppm for V5dipicCl(Et<sub>2</sub>HA), all of which are significantly further upfield compared to the parent complex V5dipicCl at –533 ppm [23]. The electronic changes in these systems have been characterized in detail [60].

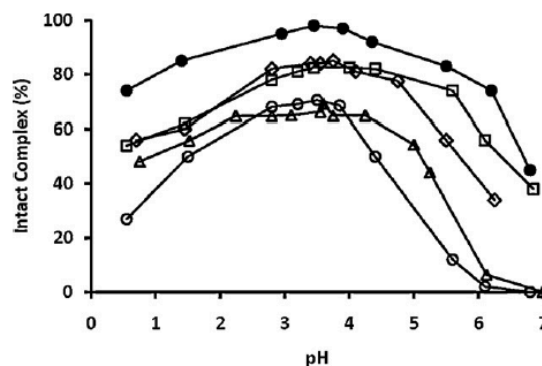


Fig. 10. Percentage of intact V5dipicX as a function of pH. <sup>51</sup>V NMR data obtained from previously published work by Smee et al. [20,23]. X = H (●); OH (○); NH<sub>2</sub> (□); NO<sub>2</sub> (△); Cl (◇).

Hydrolysis of these HA ternary complexes is more involved than the simple V5dipic system. Not only do the oxovanadates form, but the parent complexes (V5dipic and V5dipicCl) [23,53] as well as the Vdipic(HA) complexes form [91,93,94]. Indeed, the Vdipic(HA) complexes have been characterized in detail, showing an optimum pH near neutral pH with the existence of several species. These species include the oxovanadates, simple Vdipic(HA) complexes, as well as the ternary complexes [91,93,94]. Interestingly, the ternary HA ligands extend the stability of the ternary complexes by one to two pH units to the neutral pH range. As the Vdipic(HA) complex approaches neutral pH it begins to hydrolyze. However, the hydrolysis point is several pH units higher than the hydrolysis point of the parent complex, which occurs around pH 5 [23]. Combined, these studies show that the stabilization provided by the additional ligand on the V results in complexes that exist into the neutral pH range. These results suggest a mechanism for how the parent complexes are able to exert activities in biological systems. Interestingly, fine-tuning the properties of V5dipic could be important to rationalize the insulin-enhancing effects of these compounds [95].

V compounds undergo redox chemistry under physiological conditions [26,96]. Generally the redox cycling of V compounds under physiological conditions involves the transfer of one-electron. Recently evidence of two-electron transfer reactions with Vdipic complexes have been reported [97,98]. Redox cycling, involving a range of metabolites, forms reactive oxygen species (ROS) [99]. ROS are no longer considered toxic in all environments, and low concentrations have some beneficial effects [100]. In fact, insulin-induced ROS are believed to be involved in the insulin-signaling pathway [95]. Cell signaling processes involve receptor ligand interactions which are based on electrostatic potentials associated with the ions and dipoles in the receptor ligand complex [66]. These types of interactions take place with all types of ions including the many cations and phosphates in biological systems and shift the energetics associated with electron transfer processes [101]. Redox properties of V complexes can be tuned from favoring one-electron transfer reactions to two-electron transfer reactions, potentially decreasing the toxicity of these complexes [66].

Electronic properties of V complexes are altered upon substitution with electron withdrawing and donating groups [60]. It is well known that metal chelation will alter redox potential and was recently demonstrated for vanadate under physiological conditions [96]. Formation of ternary complexes under cellular conditions is likely, considering the increased stability of such complexes. Ternary Vdipic complexes are reported to form with peroxide, a series of hydroxylamines, pyridine, pinacol, and alcohols. These occur in hydrophobic environments and thus support the suggestion of membrane interaction being involved in the biological actions of V [66]. V5dipic readily penetrates lipid interfaces [65] residing in hydrophobic environments under near physiological conditions. Therefore, the potential exists that alteration of the insulin-enhancing and/or toxic actions of V complexes may be triggered by the movement of V complexes into membrane environments [66].

## 5. Conclusions

Structure-activity relationship studies were carried out using a range of Vdipic complexes. It was demonstrated that changes in coordination geometry caused the greatest improvement in the insulin-enhancing properties of these complexes. Changes in V oxidation state also impact the insulin-enhancing properties, however these effects were less pronounced. We conclude that with regard to improving the insulin-enhancing properties, dipic ligand substitution is less important when compared to the V oxidation state and ternary complex formation. We propose that the compound

stability and the ability to interact with cellular redox reactions are key components for the insulin-enhancing activity exerted by V compounds. Recently, the possibility that membrane interactions are influenced by the ligand was suggested, and such membrane effects may affect uptake and action of the V complexes [66]. Interestingly, the classes of compounds discussed here with the greatest insulin-enhancing effects are found for compounds that are most compatible with the lipid environment.

## Acknowledgements

DCC and GRW thank NIGMS Grant No. 40525 and the American Diabetes Association for funding this work. DCC also thanks NSF CHE-0628260 for funding. AMT was supported by NSF Bridge to the Doctorate fellowship, grant NSF HRD 0832932 and NSF CHE-0628260.

## References

- [1] C.E. Heyliger, A.G. Tahiliani, J.H. McNeill, *Science* 227 (1985) 1474.
- [2] H. Degani, M. Gochin, S.J.D. Karlish, Y. Shechter, *Biochemistry* 20 (1981) 5795.
- [3] J.H. McNeill (Ed.), *Experimental Models of Diabetes*, CRC Press, Boca Raton, FL, USA, 1999.
- [4] G.H. Cros, M.C. Cam, J.J. Serrano, G. Ribes, J.H. McNeill, *Mol. Cell. Biochem.* 153 (1995) 191.
- [5] M.L. Battell, V.G. Yuen, J.H. McNeill, *Pharmacol. Commun.* 1 (1992) 291.
- [6] M.C. Cam, R.W. Brownsey, J.H. McNeill, *Can. J. Phys. Pharmacol.* 78 (2000) 829.
- [7] K.H. Thompson, C. Orvig, *J. Inorg. Biochem.* 100 (2006) 1925.
- [8] K.H. Thompson, J. Lichter, C. Lebel, M.C. Scaife, J.H. McNeill, C. Orvig, *J. Inorg. Biochem.* 103 (2009) 554.
- [9] K.H. Thompson, C. Orvig, *Metal Ions in Biological Systems*, vol. 41: Metal Ions and Their Complexes in Medication, 2004, p. 221.
- [10] N. Cohen, M. Halberstam, P. Shlimovich, C.J. Chang, H. Shamoon, L. Rossetti, *J. Clin. Invest.* 95 (1995) 2501.
- [11] G. Boden, X. Chen, J. Ruiz, G.D.V. Van Rossum, S. Turco, *Metabolism* 45 (1996) 1130.
- [12] A.B. Goldfine, M.E. Patti, L. Zuberi, B.J. Goldstein, R. Leblanc, E.J. Landaker, Z.Y. Jiang, G.R. Willsky, C.R. Kahn, *Metabolism* 49 (2000) 400.
- [13] K. Cusi, S. Cukier, R.A. Defronzo, M. Torres, F.M. Puchulu, J.C.P. Redondo, *J. Clin. Endocrinol. Metabol.* 86 (2001) 1410.
- [14] H. Sakurai, H. Yasui, J. Trace Elem. Exp. Med. 16 (2003) 269.
- [15] M. Hiromura, Y. Adachi, M. Machida, M. Hattori, H. Sakurai, *Metallomics* 1 (2009) 92.
- [16] D.C. Crans, *J. Inorg. Biochem.* 80 (2000) 123.
- [17] D.C. Crans, M. Mahroof-Tahir, M.D. Johnson, P.C. Wilkins, L.Q. Yang, K. Robbins, A. Johnson, J.A. Alfano, M.E. Godzala, L.T. Austin, G.R. Willsky, *Inorg. Chim. Acta* 356 (2003) 365.
- [18] D.C. Crans, L.Q. Yang, J.A. Alfano, L.A.H. Chi, W.Z. Jin, M. Mahroof-Tahir, K. Robbins, M.M. Toloue, L.K. Chan, A.J. Plante, R.Z. Grayson, G.R. Willsky, *Coord. Chem. Rev.* 237 (2003) 13.
- [19] P. Buglyo, D.C. Crans, E.M. Nagy, R.L. Lindo, L.Q. Yang, J.J. Smee, W.Z. Jin, L.H. Chi, M.E. Godzala, G.R. Willsky, *Inorg. Chem.* 44 (2005) 5416.
- [20] J.J. Smee, J.A. Epps, G. Teissedre, M. Maes, N. Harding, L. Yang, B. Baruah, S.M. Miller, O.P. Anderson, G.R. Willsky, D.C. Crans, *Inorg. Chem.* 46 (2007) 9827.
- [21] M. Li, W. Ding, J.J. Smee, B. Baruah, G.R. Willsky, D.C. Crans, *Biomaterials* 103 (2009) 585.
- [22] M. Li, J.J. Smee, W.J. Ding, D.C. Crans, *J. Inorg. Biochem.* 103 (2009) 585.
- [23] J.J. Smee, J.A. Epps, K. Ooms, S.E. Bolte, T. Polenova, B. Baruah, L.Q. Yang, W.J. Ding, M. Li, G.R. Willsky, A. La Cour, O.P. Anderson, D.C. Crans, *J. Inorg. Biochem.* 103 (2009) 575.
- [24] D. Rehder, J.C. Pessoa, C. Galdes, M. Castro, T. Kabanos, T. Kiss, B. Meier, G. Micera, L. Petterson, M. Rangel, A. Salifoglou, I. Turel, D.R. Wang, *J. Biol. Inorg. Chem.* 7 (2002) 384.
- [25] D. Rehder, *Inorg. Chem. Commun.* 6 (2003) 604.
- [26] D.C. Crans, J.J. Smee, E. Gaidamauskas, L.Q. Yang, *Chem. Rev.* 104 (2004) 849.
- [27] T. Scior, A. Guevara-Garcia, P. Bernard, Q.-T. Do, D. Domeyer, S. Laufer, *Mini-Rev. Med. Chem.* 5 (2005) 995.
- [28] G.R. Hanson, Y. Sun, C. Orvig, *Inorg. Chem.* 35 (1996) 6507.
- [29] K. Fukui, Y. Fujisawa, H. Ohya-Nishiguchi, H. Kamada, H. Sakurai, *J. Inorg. Biochem.* 77 (1999) 215.
- [30] S.A. Dikanov, B.D. Liboiron, C. Orvig, *J. Am. Chem. Soc.* 124 (2002) 2969.
- [31] B.D. Liboiron, K.H. Thompson, G.R. Hanson, E. Lam, N. Aebischer, C. Orvig, *J. Am. Chem. Soc.* 127 (2005) 5104.
- [32] G.R. Willsky, M.E. Godzala, P.J. Kostyniak, L.H. Chi, R. Gupta, V.G. Yuen, J.H. McNeill, M. Mahroof-Tahir, J.J. Smee, L.Q. Yang, A. Lobernick, S. Watson, D.C. Crans, in: K. Kustin, J.C. Pessoa, D.C. Crans (Eds.), *ACS Symp. Ser.* 974 (2007) 93.
- [33] M. Hiromura, A. Nakayama, Y. Adachi, M. Doi, H. Sakurai, *J. Biol. Inorg. Chem.* 12 (2007) 1275.

- [34] H. Sakurai, in: K. Kustin, J.C. Pessoa, D.C. Crans (Eds.), Vanadium: The Versatile Metal, Am. Chem. Soc. (2007) 110.
- [35] K. Kawabe, Y. Yoshikawa, Y. Adachi, H. Sakurai, Life Sci. 78 (2006) 2860.
- [36] T. Kiss, T. Jakusch, D. Hollender, A. Dornyei, E.A. Enyedy, J.C. Pessoa, H. Sakurai, A. Sanz-Medel, Coord. Chem. Rev. 252 (2008) 1153.
- [37] W.R. Harris, Biochemistry 24 (1985) 7412.
- [38] A.-K. Bordbar, A.L. Creagh, F. Mohammadi, C.A. Haynes, C. Orvig, J. Inorg. Biochem. 103 (2009) 643.
- [39] D. Sanna, G. Micera, E. Garribba, Inorg. Chem. Inorg. Chem. 48 (2009) 5747.
- [40] J.C. Pessoa, I. Tomaz, Curr. Med. Chem. 17 (2010) 3701.
- [41] C. Corot, J.M. Idee, A.M. Hentsch, R. Santus, C. Mallet, V. Goulas, B. Bonnemain, D. Meyer, J. Magn. Reson. Imaging 8 (1998) 695.
- [42] M. Melchior, K.H. Thompson, J.M. Jong, S.J. Rettig, E. Shuter, V.G. Yuen, Y. Zhou, J.H. McNeill, C. Orvig, Inorg. Chem. 38 (1999) 2288.
- [43] M.Z. Mehdi, S.K. Pandey, J.F. Theberge, A.K. Srivastava, Cell Biochem. Biophys. 44 (2006) 73.
- [44] G. Huyer, S. Liu, J. Kelly, J. Moffat, P. Payette, B. Kennedy, G. Tsaprailis, M.J. Gresser, C. Ramachandran, J. Biol. Chem. 272 (1997) 843.
- [45] I.G. Fantus, E. Tsiani, Mol. Cell. Biochem. 182 (1998) 109.
- [46] A. Salmeeen, J.N. Andersen, M.P. Myers, T.C. Meng, J.A. Hinks, N.K. Tonks, D. Barford, Nature 423 (2003) 769.
- [47] M. Li, W.J. Ding, B. Baruah, D.C. Crans, J. Wang, J. Inorg. Biochem. 102 (2008) 1846.
- [48] C.C. Mclauchlan, J.D. Hooker, M.A. Jones, Z. Dymon, E.A. Backhus, M.A. Youkhana, L.M. Manus, J. Inorg. Biochem. 104 (2010) 274.
- [49] L.A. Minasi, G.R. Willsky, J. Bacteriol. 173 (1991) 834.
- [50] A.M. Cortizo, M. Caporossi, G. Lettieri, S.B. Etcheverry, Eur. J. Pharmacol. 400 (2000) 279.
- [51] D.C. Crans, A.D. Keramidias, C. Drouza, Phosphorus Sulfur Rel. Elem. 109 (1996) 245.
- [52] K. Wiegardt, Inorg. Chem. 17 (1978) 57.
- [53] D.C. Crans, L.Q. Yang, T. Jakusch, T. Kiss, Inorg. Chem. 39 (2000) 4409.
- [54] B.H. Bersted, R.L. Belford, I.C. Paul, Inorg. Chem. 7 (1968) 1557.
- [55] T. Jakusch, W.Z. Jin, L.Q. Yang, T. Kiss, D.C. Crans, J. Inorg. Biochem. 95 (2003) 1.
- [56] M. Chatterjee, M. Maji, S. Ghosh, T.C.W. Mak, Dalton Trans. (1998) 3641.
- [57] E. Norkus, I. Stalnioniene, D.C. Crans, Heteroatom Chem. 14 (2003) 625.
- [58] L.Q. Yang, A. La Cour, O.P. Anderson, D.C. Crans, Inorg. Chem. 41 (2002) 6322.
- [59] S.E. Bolte, K.J. Ooms, T. Polenova, B. Baruah, D.C. Crans, J.J. Smee, J. Phys. Chem. 128 (2008), 052317/1.
- [60] K.J. Ooms, S.E. Bolte, J.J. Smee, B. Baruah, D.C. Crans, T. Polenova, Inorg. Chem. 46 (2007) 9285.
- [61] H. Sakurai, K. Fujii, H. Watanabe, H. Tamura, Biochem. Biophys. Res. Commun. 214 (1995) 1095.
- [62] H. Sakurai, H. Sano, T. Takino, H. Yasui, J. Inorg. Biochem. 80 (2000) 99.
- [63] J. Gatjens, B. Meier, T. Kiss, E.M. Nagy, P. Buglyo, H. Sakurai, K. Kawabe, D. Rehder, Chem. Eur. J. 9 (2003) 4924.
- [64] D.C. Crans, M. Mahroof-Tahir, A.D. Keramidias, Mol. Cell. Biochem. 153 (1995) 17.
- [65] D.C. Crans, C.D. Rithner, B. Baruah, B.L. Gourley, N.E. Levinger, J. Am. Chem. Soc. 128 (2006) 4437.
- [66] D.C. Crans, A. Trujillo, P. Pharazyn, M. Cohen, Coord. Chem. Rev. 7 (2011), doi:10.1016/j.ccr.2011.01.032.
- [67] D.C. Crans, A.M. Trujillo, S. Bonetti, C.D. Rithner, B. Baruah, N.E. Levinger, J. Org. Chem. 73 (2008) 9633.
- [68] A.S. Tracey, G.R. Willsky, E.S. Takeuchi, VANADIUM Chemistry, Biochemistry, Pharmacology and Practical Applications, CRC Press, Boca Raton, FL, USA, 2007.
- [69] D. Rehder, Bioinorganic vanadium chemistry, John Wiley & Sons Ltd, West Sussex, England, 2008.
- [70] L. Yang, D.C. Crans, S.M. Miller, A.L. Cour, O. Anderson, P.M. Kaszynski, M.E. Godzala, L.D. Austin, G.R. Willsky, Inorg. Chem. 41 (2002) 4859.
- [71] G.R. Willsky, L.H. Chi, Y.L. Liang, D.P. Gaile, Z.H. Hu, D.C. Crans, Physiol. Genomics 26 (2006) 192.
- [72] D. Wei, M. Li, W. Ding, J. Biol. Inorg. Chem. 12 (2007) 1265.
- [73] V.K. Yehoor, M.E. Patti, R. Saccone, C.R. Kahn, Proc. Natl. Acad. Sci. U.S.A. 99 (2002) 10587.
- [74] Biospace, [http://www.biospace.com/news\\_story.aspx?NewsEntityId=123583](http://www.biospace.com/news_story.aspx?NewsEntityId=123583), 2009 (last checked May 25, 2011).
- [75] G.B. Irsigler, P.J. Visser, P.A. Spangenberg, Am. J. Ind. Med. 35 (1999) 366.
- [76] W.N. Rom, (Ed.), Environmental and Occupational Medicine Little, Brown and Co, Boston, MA, 1992.
- [77] R.U. Byerrum, in: E. Merian (Ed.), Metals and their Compounds in the Environment, VCH, Fed Rep Germany, Weinheim, 1991, p. 1289.
- [78] S. Dai, J.H. McNeill, Pharmacol. Toxicol. 74 (1994) 110.
- [79] S. Dai, K.H. Thompson, J.H. McNeill, Pharmacol. Toxicol. 74 (1994) 101.
- [80] S. Dai, K.H. Thompson, E. Vera, J.H. McNeill, Pharmacol. Toxicol. 75 (1994) 265.
- [81] S. Dai, E. Vera, J.H. McNeill, Pharmacol. Toxicol. 76 (1995) 263.
- [82] H.A. Schroeder, J.J. Balassa, J. Nutr. 92 (1967) 245.
- [83] H.A. Schroeder, M. Mitchener, A.P. Nason, J. Nutr. 100 (1970) 59.
- [84] D.C. Crans, L.Q. Yang, E. Gaidamauskas, A.R. Khan, W. Jin, U. Simonis, ACS Sym. Ser. 858 (2009) 304.
- [85] J. Stover, C.D. Rithner, R.A. Inafuku, D.C. Crans, N.E. Levinger, Langmuir 21 (2005) 6250.
- [86] Y. Zhang, X.D. Yang, K. Wang, D.C. Crans, J. Inorg. Biochem. 100 (2006) 80.
- [87] M. Aureliano, F. Henao, T. Tiago, R.O. Duarte, J.J.G. Moura, B. Baruah, D.C. Crans, Inorg. Chem. 47 (2008) 5677.
- [88] M.D. Cohen, M. Sisco, K. Yoshida, L.C. Chen, J.T. Zelikoff, J.J. Smee, A.A. Holder, J.D. Stonehuerner, D.C. Crans, A.J. Ghio, Inhal. Toxicol. 22 (2010) 169.
- [89] M.D. Cohen, M. Sisco, C. Prophete, L.C. Chen, J.T. Zelikoff, A.J. Ghio, J.D. Stonehuerner, J.J. Smee, A.A. Holder, D.C. Crans, J. Immunotoxicol. 4 (2007) 49.
- [90] X.G. Yang, X.D. Yang, L. Yuan, K. Wang, D.C. Crans, Pharm. Res. 21 (2004) 1026.
- [91] F. Nxumalo, A.S. Tracey, J. Biol. Inorg. Chem. 3 (1998) 527.
- [92] K. Wiegardt, Adv. Inorg. Bioinorg. Mech. 3 (1984) 213.
- [93] S.J. Angusdunne, P.C. Paul, A.S. Tracey, Can. J. Chem. 75 (1997) 1002.
- [94] P.C. Paul, S.J. Angus-Dunne, R.J. Batchelor, F.W.B. Einstein, A.S. Tracey, Can. J. Chem. 75 (1997) 429.
- [95] B.J. Goldstein, K. Mahadev, X. Wu, L. Zhu, H. Motoshima, Antioxid. Redox Signal. 7 (2005) 1021.
- [96] D.C. Crans, B. Zhang, E. Gaidamauskas, A.D. Keramidias, G.R. Willsky, C.R. Roberts, Inorg. Chem. 49 (2010) 4245.
- [97] S.K. Hanson, R.T. Baker, J.C. Gordon, B.L. Scott, A.D. Sutton, D.L. Thorn, J. Am. Chem. Soc. 131 (2009) 428.
- [98] S.K. Hanson, R.T. Baker, J.C. Gordon, B.L. Scott, D.L. Thorn, Inorg. Chem. 49 (2010) 5611.
- [99] N. Ardanaz, P.J. Pagano, Exp. Biol. Med. 231 (2006) 237.
- [100] S. Biswas, A.S. Chida, I. Rahman, Biochem. Pharmacol. 71 (2006) 551.
- [101] P. Kovacic, C.D. Draskovich, R.S. Pozos, J. Recept. Signal Transduct. Res. 27 (2007) 433.